

# **Germann Instruments**

*Test right - Sleep tight*



- ✓ **In-place strength & early loading**
- ✓ **Defect detection**
- ✓ **Corrosion evaluation**
- ✓ **Condition assessment**
- ✓ **Durability & Service life**
- ✓ **Repair quality**
- ✓ **Monitoring**
- ✓ **Mixture optimization**



**Training &  
International  
Workshops**

**Bridging NDT theory  
and practice**

**Catalog 2026**  
**[www.germanninstruments.com](http://www.germanninstruments.com)**

## **Concrete Testing Systems**

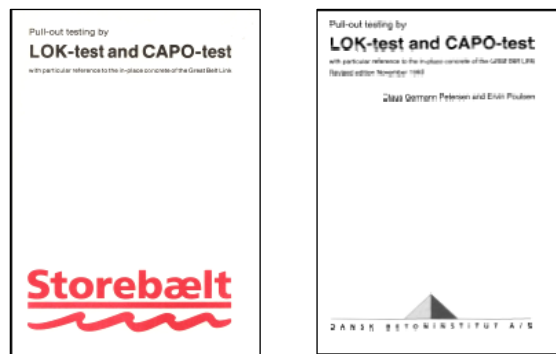
*This catalog is intended to be a comprehensive guide. Beyond the technical specifications of our test systems, it provides a clear understanding of the principles behind our proven instruments and offers practical examples of their typical applications. For further technical details or to place an order, please contact **Germann Instruments**.*

**On the cover:**

The East Bridge of the Great Belt Link in Denmark is a suspension bridge with a main span of 1,624 m, making it the second-longest in the world at the time of its opening. It serves as an example of modern engineering where **LOK & CAPO** test systems were used extensively.

An instructional booklet was published for the LOK-TEST and CAPO-TEST, which outlined the equipment, testing procedures, and the specific correlation between standard cylinders and pullout tests for the Great Belt Link structures. Detailed statistics were also included.

**“Great Belt Link: “LOK and CAPO Tests, The experience of pull-out testing during The Great Belt Link (Storebælt) project in Denmark, Storebæltsforbindelsen, Denmark, 1999”**



The project, which used 1.1 million m<sup>3</sup> of concrete, required a 100-year service life against chloride penetration. To ensure this requirement was met, the selected concrete was pre-tested in a laboratory. Large trial specimens were also cast and tested on-site for both chloride penetration and with the LOK-TEST / CAPO-TEST at various stages of maturity. This established acceptable pullout limits for testing the defect intensity of the concrete cover layer.

Approximately 40,000 pullout tests were conducted during the project. The general correlation was confirmed for the East Tunnel and East Bridge, while a separate correlation was used for the West Bridge. The relative strength of the cover layer, as measured by LOK-TEST / CAPO-TEST compared to the potential strength from laboratory cylinders, was found to be 0.78 for the East Tunnel, 0.98-0.99 for the East Bridge, and 0.90-0.93 for the West Bridge.

## ***Introduction***

---

For more than half a century, *Germann Instruments* has been the leader in the field of test systems for nondestructive testing (NDT) and on-site investigation of reinforced concrete structures.

*Germann Instruments* constantly develops, manufactures, and markets worldwide its innovative and cutting-edge product line through offices in Denmark, the United States, and Ecuador and through distributors in Europe, the Middle East, and Asia.

The test systems cover varied aspects of concrete construction and investigation, such as

**In-Place Strength**  
**Condition Assessment**  
**Defect Detection**  
**Corrosion Evaluation**  
**Durability and Service Life**  
**Repair Quality**  
**Concrete Mixture Optimization**  
**Monitoring**

The systems included in this catalog are used to perform totally nondestructive test methods or test methods that require limited near-to-surface specimen removal. If properly applied, these test systems allow rapid testing and provide immediate results on-site.

This catalog also includes some methods for testing fresh concrete. While they are not the traditional types of NDT tests, they are important methods for concrete mixture optimization, on-site quality control, and quality assurance.

For correct operation, the test systems have to be maintained properly and need to be calibrated according to the procedures outlined in the users' manuals and in accordance with applicable standards.

For optimal use of these systems, field engineers and consultants have to be trained and skilled in planing testing programs, using the test systems, and interpreting test results. Furthermore, an understanding of the fundamental deterioration mechanisms of reinforced concrete structures is essential for proper planing and execution of testing programs. *Germann Instruments* has, therefore, developed a comprehensive **Workshop Program** to provide basic knowledge on the underlying principles of the various tests systems included in this catalog. In addition, *Germann Instruments* has invested in the construction of three training facilities in Denmark, the United States, and Ecuador. These facilities include classrooms and testing facilities that incorporate full-scale concrete elements with various types of built-in defects. The testing facilities allow workshop participants to obtain hands-on training on the use of the different systems. The workshops are described on the following pages and workshop schedules may be found on the *Germann Instruments'* website:

**[www.germanninstruments.com](http://www.germanninstruments.com)**

*Germann Instruments* continues to affirm its commitment to serve the *in-situ* and nondestructive testing community by placing state-of-the-art, technically proven, diagnostic tools in the hands of field engineers and consultants.



## *Technical and Educational Support*

*Germann Instruments* believes that the key to promoting wider use and acceptance of the test systems described in this catalog is to enhance the knowledge of professionals involved in specifying test methods or performing tests and interpreting results. Furthermore, it is helpful for users to have an understanding of the fundamentals of concrete technology, including deterioration mechanisms of reinforced concrete structures, for proper planning and execution of testing programs. *Germann Instruments* has, therefore, committed its resources to provide world class technical and educational support to users of these test systems. This includes providing training facilities, workshop programs, and comprehensive system-specific training.

### **Training Facilities**

*Germann Instruments* has training facilities in Denmark, Ecuador, and the United States. These facilities include classrooms for presentations and testing sites for practical training with various systems. The testing sites incorporate full-scale concrete elements with various types of built-in defects and allow equipment purchasers to obtain hands-on training. Shown on the right is the training facility located outside of Quito, Ecuador. Contact *Germann Instruments* to arrange for in-depth training on any of the test systems described in this catalog.



*Outdoor facility in Copenhagen includes two 400 mm thick slabs with various simulated defects*



*The facility in Evanston, Illinois includes a 45-m<sup>2</sup> slab with varying thickness, embedded reinforcement, tendon ducts, and simulated defects*

### **Need for training**

The test systems described in this catalog vary in complexity from the simple dye methods for measuring depth of carbonation to the more complex methods for condition assessment based on stress-wave or electromagnetic wave propagation. The basic principles of these types of wave propagation are not covered in most college courses taken by civil engineers, who are the usual people performing condition assessments. Successful interpretation of the results from these indirect methods requires basic knowledge of the underlying principles and an understanding of the expected responses for different conditions. As an analogy, consider two x-ray images of the lower leg, just above the ankle. It is obvious in the image on the right that there are multiple fractures to the leg and ankle bones; but the following image on the left is not as easy to interpret. A trained person would recognize this as a





## Technical and Educational Support

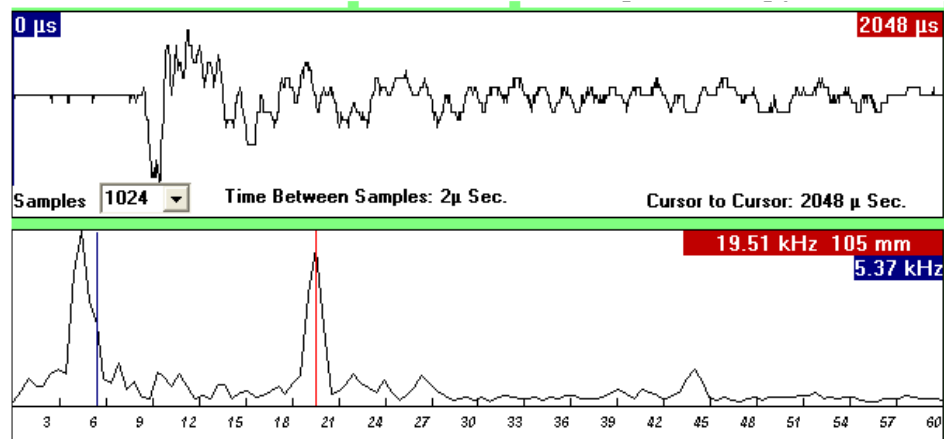
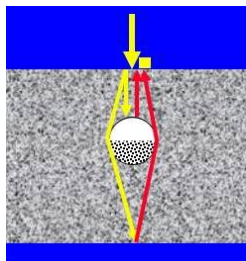


"Weber Type A lateral malleolar fracture," which is barely visible within the circled region. Recognition of this fracture requires an understanding of the expected image of a normal ankle and typical ankle fractures that are encountered.

The same idea applies to the interpretation of results based on complex wave propagation phenomena. Proper interpretation requires not only knowledge of the underlying principles of the method, but also the expected responses for an intact structure and for various types of defects. As an example, consider results from impact-echo testing. Two impact-echo test results are shown from tests over tendon ducts in the slab specimen at the Copenhagen training facility. This first result is for a test over a voided tendon duct. The upper waveform is the raw output of the receiver and the lower plot is the amplitude spectrum.

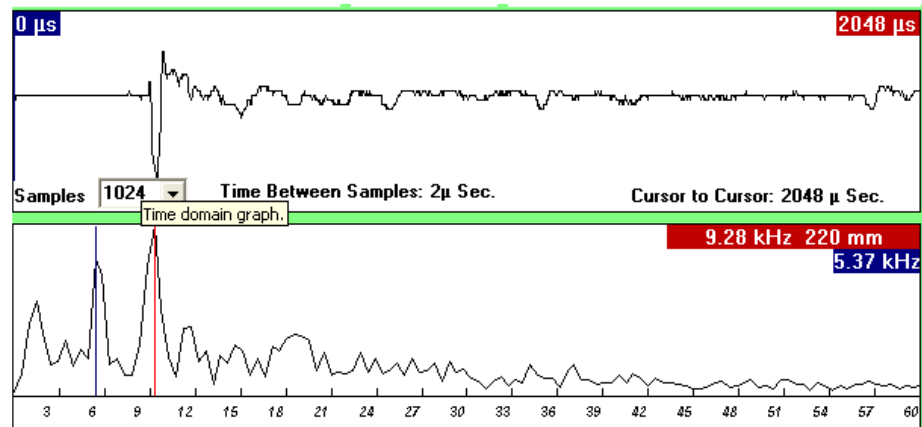
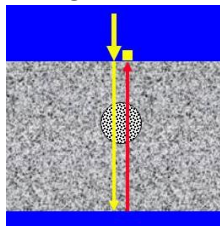
The presence of the void is indicated by two features: (1) the high frequency peak at 19.51 kHz (red

*Impact-echo result for test over a metal tendon duct at a nominal depth of 100 mm containing voids.*



line) and (2) the shift in the thickness frequency peak to a value less than the frequency for a solid slab (shown as the blue line in the spectrum). The combination of the high frequency peak and shifted thickness frequency peak are telltale indicators of a voided tendon duct. The second result shown below is for a test over a fully grouted duct containing pre-stressing strands.

*Impact-echo result for test over a fully grouted a metal tendon duct at a nominal depth of 100 mm containing pre-stressing strands.*



An untrained operator might conclude that the high amplitude peak at 9.28 kHz (red line) is due to an empty duct at a depth of 220 mm. In fact, the peak at 9.28 kHz is the result of multiple reflections from the steel in the duct. Correct interpretation requires that the operator understand the expected response for reflections from air voids at different locations and the difference between reflections from an air interface and from steel bars.

### Workshop Program

## *Technical and Educational Support*

A world-class workshop program has been developed to provide an introduction to modern, advanced nondestructive and other test methods for evaluation of concrete in structures and for evaluation of alternative concrete mixtures. The underlying principles and inherent advantages and limitations of the various techniques are presented. In addition, the operation of various instruments is demonstrated through hands-on exercises.

Workshops are conducted on a regular basis at the *Germann Instruments* training facilities in the United States, Denmark, and Ecuador. Workshops can also be organized worldwide in cooperation with professional societies, educational institutions, and local agencies. Workshop presentations and hand out materials are in English, but a simultaneous translation service can be arranged in cooperation with the host organization. Visit the *German Instruments*' website for current workshop announcements: [www.germanninstruments.com](http://www.germanninstruments.com)

Most of the workshops have been developed for a three-day format and organized around four principle themes, as follows:

### *Theme 1: Evaluation of in-place concrete strength*

The workshop begins with a presentation on testing drilled cores, with particular emphasis on the need to adhere strictly to standardized procedures. The rebound hammer is presented as a tool for assessing uniformity of concrete. The pullout test is summarized and the reason for its good reliability is explained along with interesting case studies. The purpose of the pull-off test is discussed. There is discussion of a major construction failure that could have been prevented if in-place strength had been measured. This leads to a comprehensive presentation of the maturity method. Presentations on the principles and use of covermeters and ground penetrating radar are included in this section.

### *Theme 2: Stress-wave methods for flaw detection*

The second theme begins with a review of the principles necessary to understand the basis of various methods based on stress-wave propagation. The application of the ultrasonic pulse velocity method is discussed. The underlying principles of the impact-echo method are explained and several typical applications are described. The impulse-response method for rapid initial screening of a structure is explained and typical applications are presented. The principles of the ultrasonic-echo method, which is the basis for the MIRA tomographic system, are discussed.

### *Theme 3: Durability related testing*

The third theme begins with an overview of concrete durability and discusses the key to obtaining durable concrete. Various fluid ingress mechanisms are presented, with emphasis on diffusion. A simple approach for in-place evaluation of water penetrability is presented. The principles of reinforcement corrosion are discussed along with the roles of chloride ions and carbonation. A practicable field method is described for obtaining the chloride ion distribution in the concrete cover layer. It is shown how the measured chloride ion profile can be used to make an approximate estimate of remaining service life. This portion of the workshop concludes the principles of the half-cell potential method, concrete resistivity, and corrosion rate measurements. It is explained how the rapid and simple measurement of concrete conductivity can be used to assess the resistance to chloride ion diffusion of alternative concrete mixtures.

### *Theme 4: Advanced test methods*

The workshop concludes with presentations of advanced test systems. The underlying cause of early-age autogenous shrinkage of concrete is presented and the test method for measuring this property is discussed. The objectives and components of a thermal control plan are discussed; and the applicable test systems and analytical tools are presented. The principles of freezing and thawing damage are explained, and the underlying basis of the Air Void Analyzer for fresh concrete is explained. The workshop concludes with discussion of the ICAR Rheometer for measurement of fundamental rheological properties of fresh concrete.

The following photographs were taken at previous workshops.



# *Technical and Educational Support*



*Quito, Ecuador*



*New Delhi, India*



*Hanoi, Vietnam*



*Dubai, UAE*



*Mexico City, Mexico*



*Ho Chi Minh City, Vietnam*



*Copenhagen, Denmark*



*Chicago, USA*



## ***Technical and Educational Support***

The most comprehensive NDT workshop is conveniently organized annually in Athens, Greece, taking advantage of its pleasant spring weather. One day a travel is organized to a facility at the foot of the world-famous multi-span cable-stayed Rio–Antirrio Bridge that crosses the Gulf of Corinth, where there are also full-scale specimens for training. A technical visit is usually available to learn more about the engineering behind the construction of this impressive bridge.



The workshop faculty comprises a unique combination of individuals with expertise in the science and theory behind the test systems, the development of testing instruments, on-site application of various test methods and systems, and standards development. They are members of the **NDTitans**, an international group of experts providing professional services in nondestructive testing (NDT) of concrete and are involved on a day-to-day basis with major consulting companies as well as educational and research institutions. The Team includes academics, consultants, and researchers, all with a practical background in testing.



[www.ndtitans.com](http://www.ndtitans.com)

Page No.	Product Name	Property or Parameter Measured	Relevant Standard/Document
1	<b>Auto-Shrink</b>	Autogenous shrinkage of specimens in special molds using sealed curing	ASTM C1698
3	<b>AVA-3000</b>	Spacing factor and specific surface of air-void system in air-entrained fresh concrete	AASHTO TP 75
12	<b>BOND-TEST</b>	Bond strength of overlay or tensile strength of substrate	BS 1881:207, ASTM C1583
17	<b>CAPO-TEST</b>	Concrete strength in existing structures	EN 12504-3, ASTM C900, BS 1881:207
25	<b>COMA-Meter</b>	Maturity of hardening concrete	ASTM C1074
28	<b>CORECASE</b>	Coring for strength and durability assessment	ASTM C42/C42M EN 12504-1
31	<b>CorroWatch</b>	Long-term monitoring of chloride penetration into concrete	
33	<b>CoverMaster</b>	Location, depth and size of reinforcement; plus half-cell potential	BS 1881:204, ACI 228.2R ASTM C876
36	<b>CrackScope</b>	Width of cracks	
37	<b>Deep Purple and Rainbow Indicators</b>	Carbonation depth indicators	BS EN 14630
39	<b>DOCter</b>	Thickness measurement and flaw detection, including depth of flaws by impact-echo	ASTM C1383
44	<b>ECHOLYST</b>	Advanced software for the Impact-Echo method	ASTM C1383
47	<b>ERE-Probe</b>	Long-term monitoring of half-cell potential of reinforcement using embedded probe	
48	<b>EyeCon</b>	Flaw detection and thickness measurement by ultrasonic pulse-echo	ACI 228.2R
54	<b>GalvaPulse</b>	Corrosion rate and half-cell potential of reinforcement; electrical resistance of concrete	ASTM C876 (half-cell potential)
58	<b>GWT</b>	Water penetrability	ISO/DIS 7031
62	<b>ICAR Plus Rheometer</b>	Measures yield strength and dynamic viscosity of fresh concrete	
67	<b>LOK-TEST</b>	Early-age strength of concrete	BS EN 12504-3, ASTM C900, BS 1881:207
72	<b>Merlin</b>	Bulk conductivity of saturated specimens, which can be related to the chloride ion diffusion coefficient	ASTM C1876
77	<b>Mini Great Dane</b>	Half-cell potential of reinforcement and electrical resistance of concrete	ASTM C876
80	<b>MIRA Classic</b>	Tomographic imaging of flaws and thickness measurement by ultrasonic pulse-echo	ACI 228.2R
87	<b>MIRA 3D &amp; MIRA 3D PRO</b>	Tomographic imaging of flaws and thickness measurement by ultrasonic pulse-echo with Full-Matrix-Capture (FMC) capabilities	ACI 228.2R

Page No.	Product Name	Property or Parameter Measured	Relevant Standard/Document
94	<b>MIRADOR</b>	Thickness measurement and flaw detection, including depth of flaws by impact-echo with the advanced Echolyst software	ASTM C1383
99	<b>Profile Grinder</b>	Chloride profiles on-site or after ponding of specimens in the laboratory; diffusion coefficient calculation	ASTM C1556, NT Build 443, ASTM C1543
103	<b>PROOVE`it</b>	Resistance to chloride ion penetration; electrical conductivity; and chloride migration coefficient	ASTM C1202, NT Build 492, ASTM C1760
109	<b>Pulsar</b>	Ultrasonic pulse velocity by through transmission	ASTM C597, BS EN 12504-4, BS 1881:203
112	<b>RapidAir</b>	Air content, spacing factor and specific surface of hardened, air-entrained concrete	ASTM C457, EN 480-11
115	<b>RAT</b>	Alkali content of fresh concrete	
118	<b>RCT and RCTW</b>	Chloride content of powder samples using acid or water to extract soluble chlorides	AASHTO T 260, ASTM C114, ASTM C1152, ASTM C1218
123	<b>s`MASH</b>	Rapid testing for flaws using impulse-response method	ASTM C1740
128	<b>Surfer</b>	Ultrasonic pulse velocity by surface measurement	ASTM C597, BS EN 12504-4, BS 1881:203
131	<b>VAKKA</b>	Wireless monitoring sensors to measure internal temperature for the maturity method and relative humidity	ASTM C1074, ASTM F2170

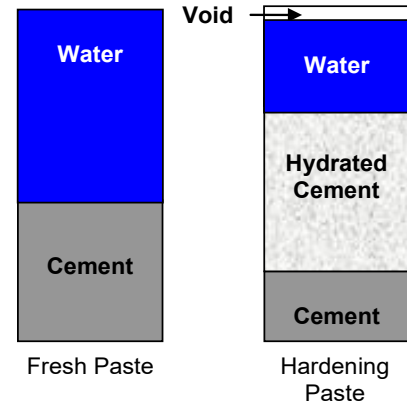


## Purpose

The **Auto-Shrink** system measures the unrestrained autogenous shrinkage of a specimen of cement paste or mortar cured under sealed conditions (ASTM C1698, Test Method for Autogenous Strain of Cement Paste and Mortar). **Auto-Shrink** permits evaluation of the relative autogenous shrinkage potential of different cementitious systems. Excessive autogenous shrinkage may lead to microcracking that increases the permeability of concrete.

## Principle

When cement hydrates through chemical reactions with water, the volume occupied by the products of hydration is less than the original volume of cement and water and thus internal voids are created. This phenomenon is known as “chemical shrinkage.” If concrete is cured under sealed conditions (no external source of water or moisture), the reduction in paste volume due to this hydration process can cause shrinkage and this in turn produces internal tensile stresses that may lead to microcracking. The microcracking reduces concrete’s resistance to penetration of water and deleterious substances.



If a specimen of paste or mortar is cured under sealed conditions and allowed to change in volume, the chemical shrinkage of the paste will cause **autogenous shrinkage** of the specimen. The **Auto-Shrink** digital dilatometer is designed for linear measurement of autogenous shrinkage in hardening cement-based materials. A special corrugated plastic mold is used to prevent moisture loss and allow the specimen to shrink freely. With **Auto-Shrink**, it is possible to measure the time dependent deformation of different specimens simultaneously over periods of weeks or even years. **Auto-Shrink** is intended primarily for measurements after setting of cement pastes or mortars with a maximum aggregate size of 4 mm (preferably 2 mm). To minimize the influence of temperature variations, the dilatometer should be used in a thermostatically controlled room. Background information on the measurement technique used in **Auto-Shrink** can be found in the following reference:

Mejlhede Jensen, O. and Freiesleben Hansen, P. “A Dilatometer for Measuring Autogenous Deformation in Hardening Portland Cement Paste,” *Materials and Structures*, 1995, 28 (181) 406-409

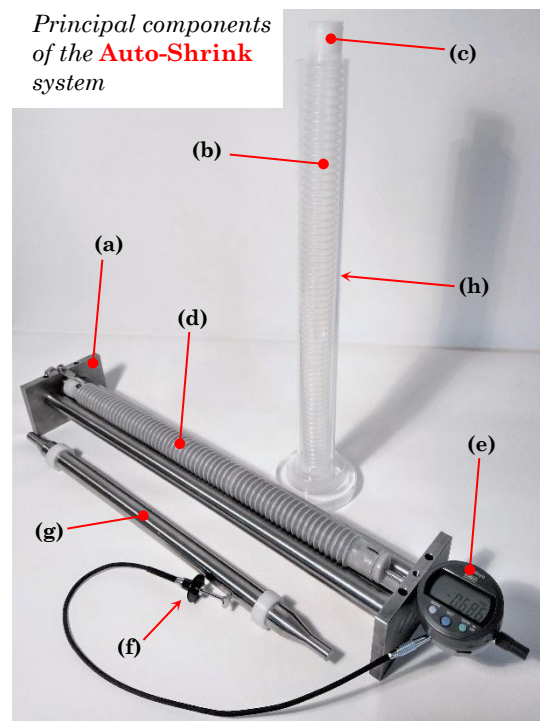
## Auto-Shrink System

The **Auto-Shrink** digital dilatometer is composed of the following basic elements:

- A rigid frame or bench (a) to support the specimen, whose rods are made of Invar, a special steel alloy with a very low coefficient of thermal expansion at room temperatures.
- A corrugated plastic tube mold (b) with 2 sealing plugs (c) to prepare a slender test specimen (d).
- A high precision digital dial gauge (e) with remote control (f) to measure change in specimen length.
- A reference bar (g) made of Invar steel as well.
- A support tube (h) to cast the concrete into the corrugated tube.
- The digital displacement gauge is fixed firmly to the frame with a blunted hex screw. The remote control is mounted on the side of the gauge. A lock function for the remote control is provided.

Specimens are cast vertically by using a support tube, which can be mounted to a vibrating table. To ensure that the cast specimens have approximately the same length, the corrugated mold should not be stretched or

Principal components of the **Auto-Shrink** system



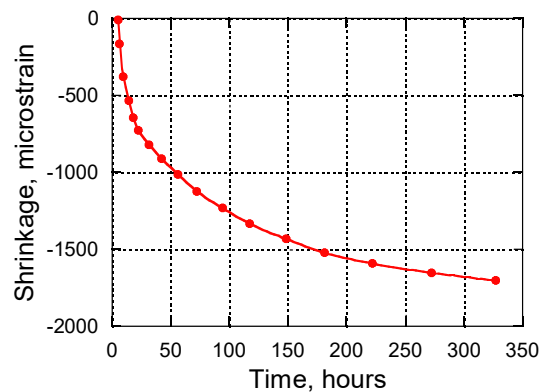
compressed during filling. The mold is filled to approximately 15 mm below the end of the tube to allow room for the top sealing plug. Before the top sealing plug is mounted, the corrugated tube is compressed slightly to bring the cement paste in contact with the sealing plug.

Measurements in the **Auto-Shrink** dilatometer are conveniently done relative to a reference bar. To ensure optimal measuring accuracy, the reference bar as well as the specimens should be placed in the frame in the same orientation during each measurement. A line mark with permanent ink at one end of the corrugated tube may be used to indicate the proper orientation of the specimen during length measurement in the dilatometer.

As an option, a special USB input cable and software can be purchased to connect the displacement gauge to a computer for automatic recording of length change to a spreadsheet file. The software allows gauges from multiple measurement frames to be read automatically. The cables are connected to the computer with a commercial USB hub.

## Testing Example

The following graph is an example of very high autogenous strain measured over 2 weeks on a cement paste ( $w/c$  ratio of 0.25) with 10 % silica fume cured at 30 °C. Time is measured from the addition of water. The strain has been defined as 0 at the time of final setting of the paste (from Mejlhede Jensen and Freiesleben Hansen, 1995).



## Auto-Shrink Specifications

- Support frame and reference bar made of **Invar** steel alloy
- Absolute type linear encoder Digital Gauge with large, easy-to-read LCD rotating display
- Measuring range: 12.7 mm
- Resolution: 0.001 mm
- Accuracy at 20°C: 0.003 mm
- Repeatability at 20°C: 0.002 mm
- 8 mm stem with a 1.5 mm spherical tip (carbide tipped)
- Battery life:  $\approx$  7,000 hours of continuous use
- Service temperature range: 0 to 40°C
- Storage temperature range: 0 to 60°C



## Auto-Shrink AS-1000 Kit Ordering Numbers

Item	Order #
Dilatometer support frame with stop pin	AS-1100
Digital displacement gauge including lifting cable as remote control	AS-1110
Reference bar	AS-1120
Spanner 17 mm	AS-1130
Hex key 2½ mm	AS-1140
Support tube for casting	AS-1170
Grooved support rack for 10 specimens, set of 5 pcs.	AS-1180

## Optional items for automatic data-logging

Item	Order #
USB Input tool direct cable	AS-1200
ITPak software with USB dongle	AS-1210

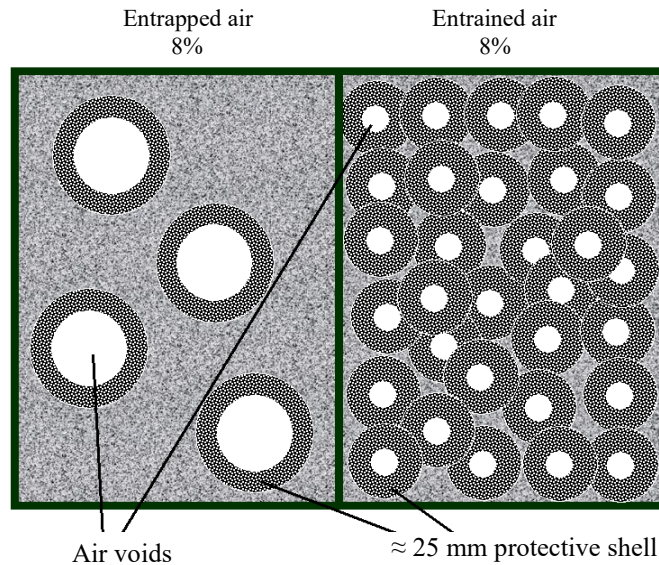
## Consumables

Item	Order #
Corrugated tubes, set of 50 pcs.	AS-1150
Sealing plugs, set of 100 pcs.	AS-1160



## Freeze-Thaw damage, background

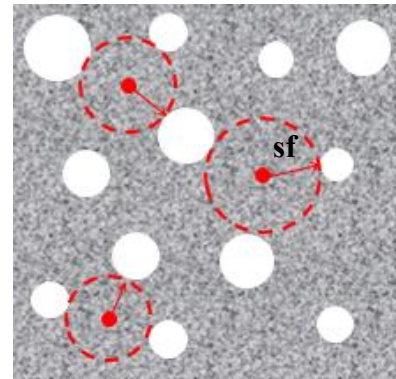
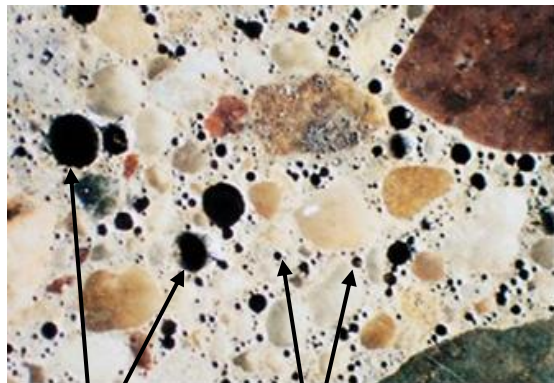
The durability of concrete subjected to wetting and cycles of freezing and thawing can be enhanced by deliberately introducing many, small and closely spaced air bubbles (air voids) in the cement paste. During freezing, the ice formed (about 9% larger volume) in the capillary pores of the paste will expand into adjacent air voids without cracking the paste, provided the air-void spacing and the size distribution of the air voids are within certain limits.



On the left two cases are shown with the same amount of total air, one with few large air-bubbles and one with many small ones in the paste.

In the “shell” around the bubbles, approximately 0.25 mm thick, the ice formed during freezing in the capillary pores in proximity to an air entrained void will expand into the air bubble and not cause cracking of the paste. Upon thawing, the ice will melt in the bubble and be transferred back into the capillary pores.

Consequently, a good frost resistant paste will have to contain many small bubbles closely spaced.



The spacing factor “sf” is the maximum distance from any point in the cement paste to the periphery of an air void. Generally, the spacing factor has to be  $<0.20$  mm for adequate resistance to freezing and thawing. If evaluated by the specific surface (bubble surface / bubble volume), the value has to be  $>25 \text{ mm}^{-1}$ .

*Example of outdoor exposure to Freezing and Thawing after 40 years.*

*Left: Concrete with improper air-void system.*

*Right: concrete with correct air entrainment.*

*Source: PCA*







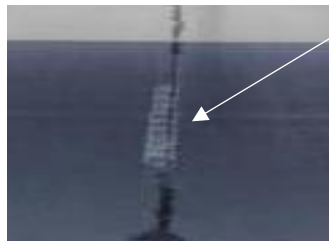
*Example of Freeze and Thaw cracking of the longitudinal joints of a concrete highway due to an improper air-void system in the presence of wet (saturated) concrete and freeze-thaw cycles.*

*Source: KDOT*

*Centerline joint spalling of a highway after 10 years in service in a freeze-thaw environment due to improper air-void structure in the paste and presence of moist/water in the joints*

*Note the centerline joint under the bridge is not spalled. Under winter freezing and thawing conditions, the sun does not reach this area to thaw the concrete, hence reduced numbers of freeze-thaw cycles occurred.*

*Source: KDOT*



## Test Methods

**ASTM C457-16.** Standard Test Method for Microscopical Determination of Parameters of the Air-Void System in Hardened Concrete

The spacing factor and the specific surface of the air-void system are determined typically according to this ASTM standard or according to EN 480-11 "Admixtures for concrete, mortar and grout - Test methods - Part 11: Determination of air void characteristics in hardened concrete."

These methods require obtaining a core from the hardened concrete on-site and preparing a properly polished specimen in the laboratory as illustrated in the photo previous page. This preparation requires specialized equipment, a well-trained technician and it takes time.

The spacing factor and the specific surface are then determined manually by the linear traverse method using a microscope, or by an automated image analyses system like the **RapidAir**. Determination of the air-void structure in this manner cannot produce timely information during construction, which would be needed to make adjustments e.g. to the concrete mixture if the spacing factor and the specific surface are not within specified limits.

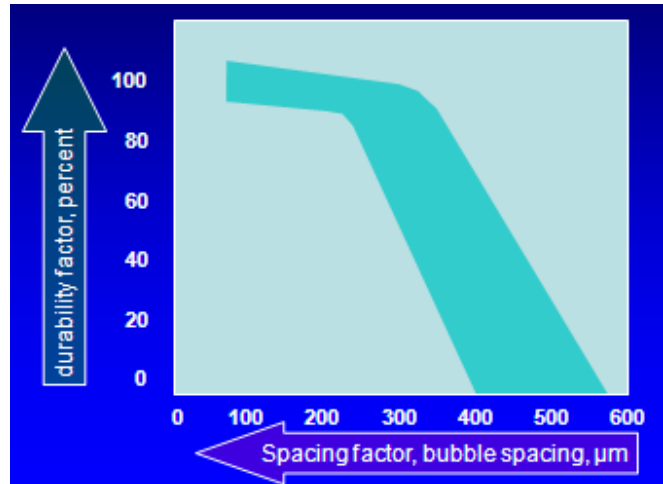
In other words, microscope examination of hardened concrete gives good information, however it is slow, expensive and it gives no timely information.

**ASTM C666-15.** Standard Test Method for Resistance of Concrete to Rapid Freezing and Thawing.

This standard covers the determination of the resistance of concrete specimens to rapidly repeated cycles of freezing and thawing in the laboratory. Each specimen is subjected to maximum 300

freeze/thaw cycles and tested for the relative dynamic modulus of elasticity regularly during cycling. A Durability Factor is then calculated depending on how important the change in the elastic properties is.

The typical relationship between the spacing factor and the durability factor is shown in the figure on the right. It can be seen that durability increases as bubble spacing decreasing, illustrating that a good durability is present if the spacing factor is less than about 0.20 mm.



## The AVA-3000

The AVA (Air Void Analyzer) is used to measure the size distribution of voids and the air-void parameters (spacing factor and specific surface) of the fresh, still-plastic, air-entrained concrete.

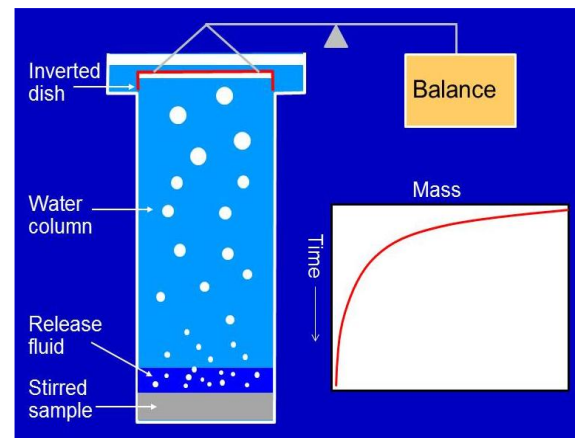


**AVA-3000** System consisting of laptop with installed software, base unit, riser column, water tank and sampling equipment.

## Principle

A mortar sample of the air entrained concrete is obtained from the fresh concrete with a sampling tool and injected into the blue AVA release liquid at the bottom of a riser column with water above. The mortar sample is stirred gently into the release liquid by which the air bubbles are released and start rising through the water following the Stoke's Law: larger bubbles will rise faster than smaller bubbles.

Due to the blue release liquid that has the proper viscosity and hydrophilic character, the air bubbles will retain their original sizes and neither coalesce nor disintegrate into smaller bubbles during



sampling, injection and mixing. The temperature of the liquid and of the water has to be within 21°C and 25°C.

The air bubbles rising through the water column are collected under an inverted and submerged petri dish (buoyancy pan) attached to a sensitive balance. As air bubbles accumulate under the dish, the weight of the dish decreases. The weight of the dish is recorded as a function of time.

Based on the recorded change in apparent mass of the pan, an algorithm calculates the size distribution of the collected air bubbles. From the size distribution, the spacing factor and the specific surface are calculated. The algorithm ensures the parameters are similar to obtained from ASTM C457 linear traverse measurements.

### Test description



- A sample of the mortar of the air-entrained concrete is taken by vibrating a wire cage into the fresh concrete which excludes particles larger than 6 mm. A syringe is used to collect a 20 cm<sup>3</sup> mortar specimen from within the cage.
- The mix proportions for the concrete is entered into the software.
- The riser column has the blue AVA release liquid at the bottom and water above it. The specimen is injected into the riser column and the program started. Mortar and liquid are stirred gently by a magnetic stirrer for 30 seconds by which the air voids are released.
- The bubbles rise through the liquids at rates that depend on their size, which results in a separation in time when different size bubbles arrive at the top of the column and are collected under a submerged and inverted glass dish attached to a high precision balance. The software records the change in mass of the inverted dish as a function of time.
- For each succeeding period, the size of the bubbles collected under the dish decreases. The measurement continues for 25 minutes unless no mass change is recorded for 2 consecutive minutes, in which case the measurement is stopped.
- The AVA software processes the time history of the balance readings and calculates the size distribution of the air bubbles, reported in a graph and a histogram, and the air-void parameters, spacing factor and specific surface.

### System Features

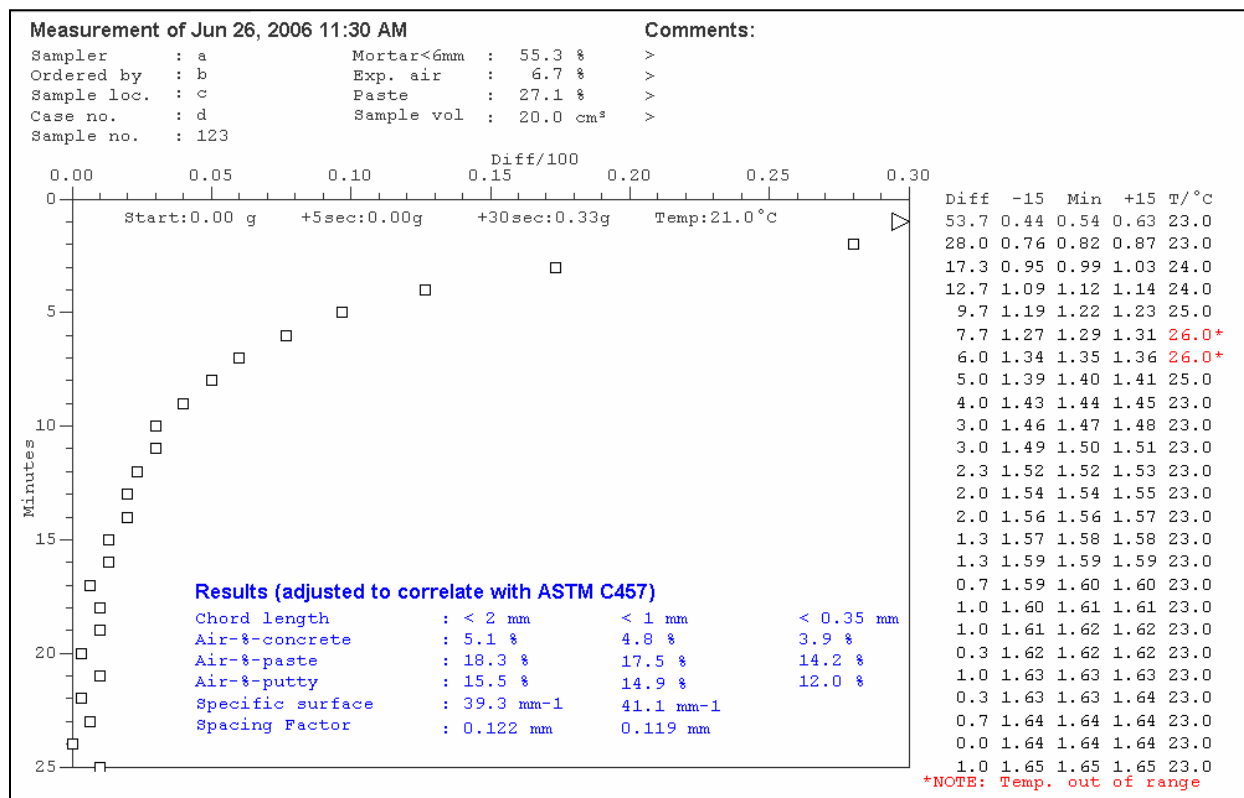
- Accurate measurement of the essential air void parameters, the spacing factor and the specific surface of the air bubbles of air-entrained, still plastic concrete.
- Documenting not only the air void parameters, but also the size distribution in bubble classes and accumulated bubble distribution for bubbles < 2 mm cord size (3 mm diameter).
- Visualization of the air bubbles rising through the riser columns water.
- Scientifically based, documented and investigated in many test programs worldwide.
- Useful to establish a relationship to durability determined by freeze-thaw tests, ASTM C666-15.

- Close relationships to spacing factor and specific surface as determined by ASTM C457-16.
- Easy sampling within 5 minutes and a maximum testing time of 25 minutes.
- Applicable anywhere in the production process, e.g. in the laboratory, at the ready mix plant, on site after transportation, after pumping, manipulation or consolidation of the concrete.
- Real time data acquisition (buoyancy versus time) shown on the laptop.
- Windshield to cover the balance for use on-site.
- 35 liter tank for de-aerating the water used in the riser column and for temperature regulation of the water and the release liquid for releasing the air bubbles in the 20 cm<sup>3</sup> sample.
- AVA-3000 is the latest development in the AVA series
- 15 years of experience among major cement and concrete producers, admixture companies and state / government institutions worldwide.

## Documentation

After the test has been completed, the following documentation is available on the laptop screen, ready for printout:

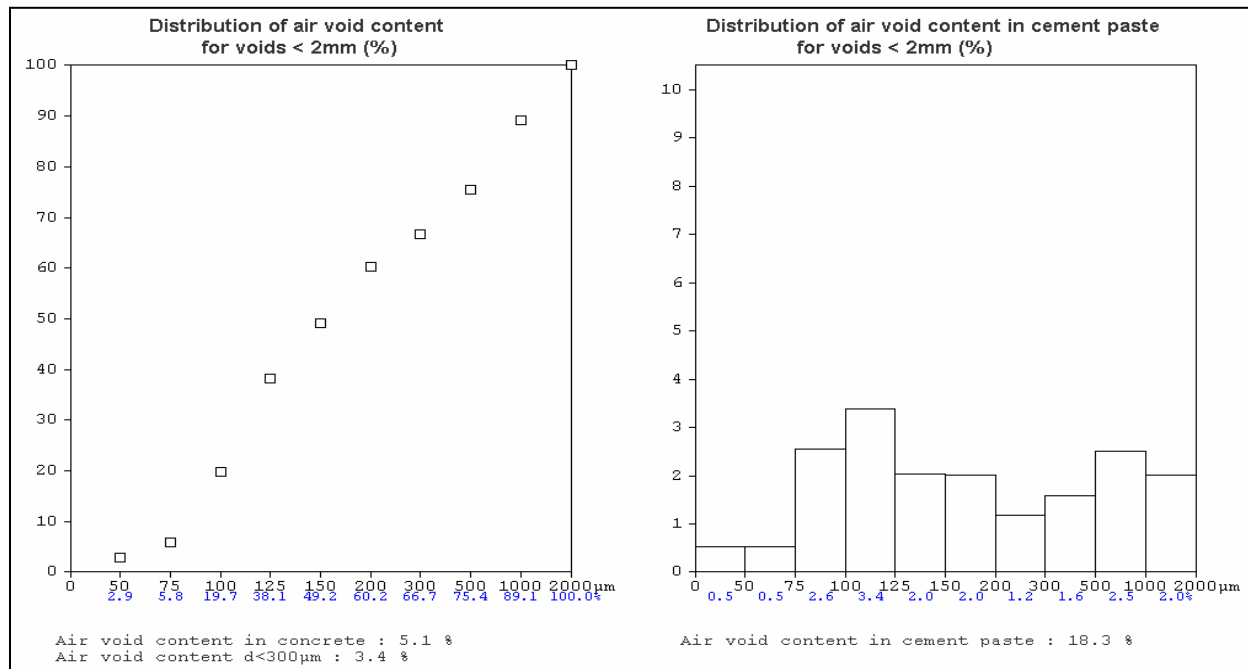
- The change in mass of the buoyancy dish (x-axis) as a function of time (y-axis);
- The results of the analyses, including: air content of the sample, **spacing factor** and **specific surface** for cord length of air bubbles <2 mm and <1 mm.
- The input mix parameters (mortar %, exp. air %, paste % and sample volume)
- Comments



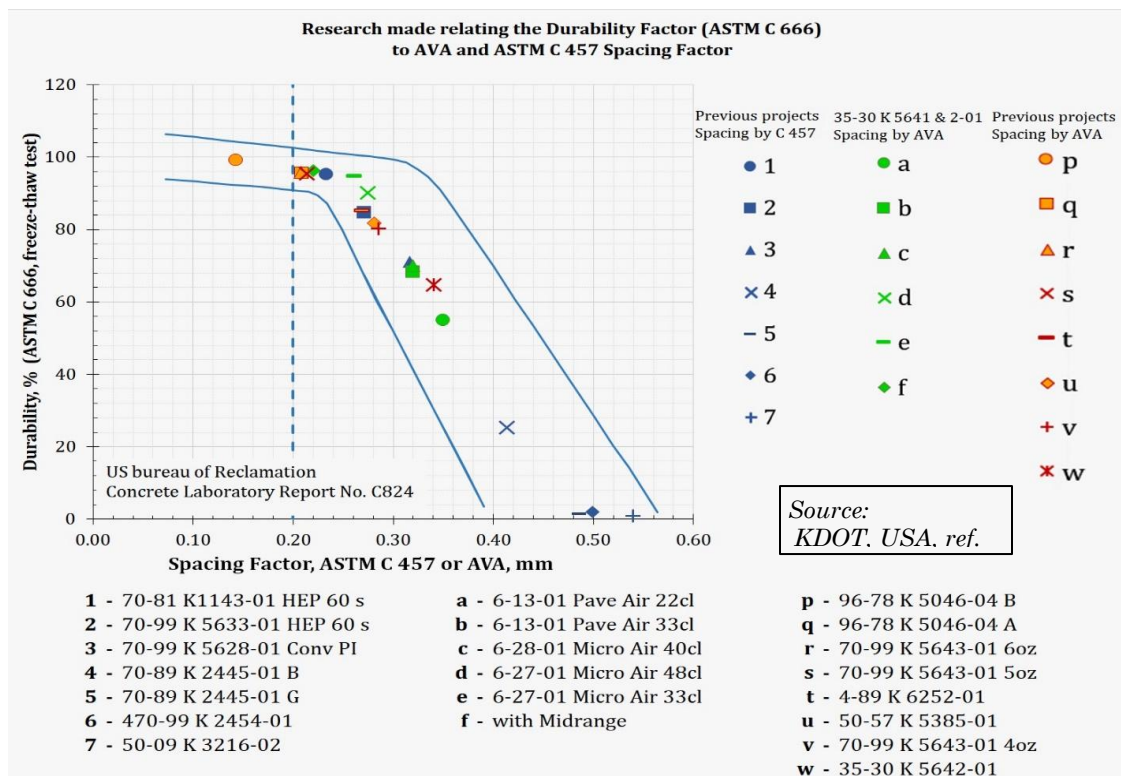
In addition, the following information about the air voids is available:



- The size distribution of air voids less than 2 mm cord size – 3 mm diameter voids (left), and
- A histogram of air-void sizes less than 2 mm cord sizes (right).



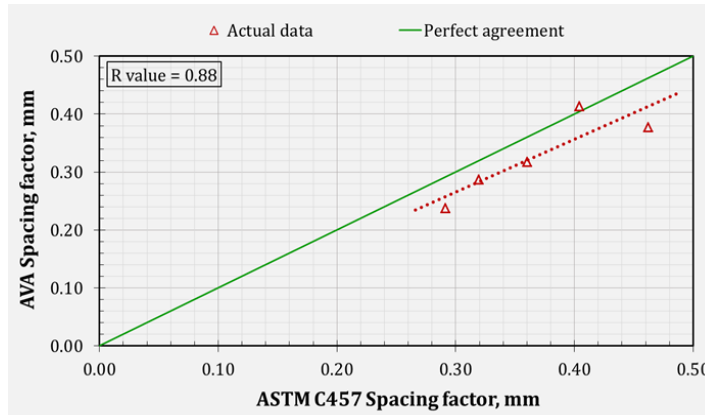
## Comparisons to Durability Factor



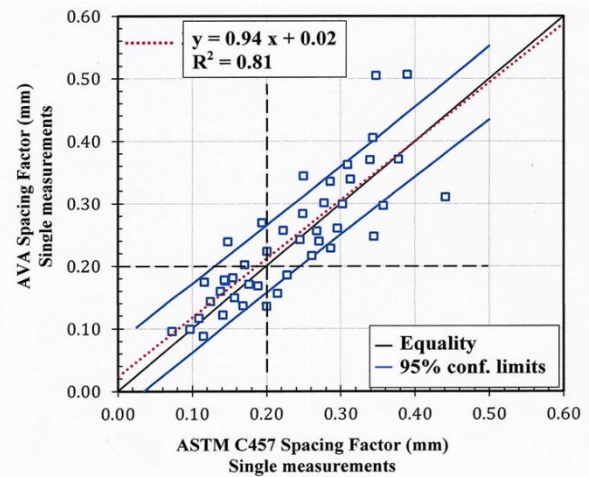
It can be seen that the spacing factor obtained by the two methods, ASTM C 457 and the AVA, are evaluating the durability of the concrete specimens by ASTM C666 almost identically.

## Comparisons between spacing factor evaluated by AVA and ASTM C457:

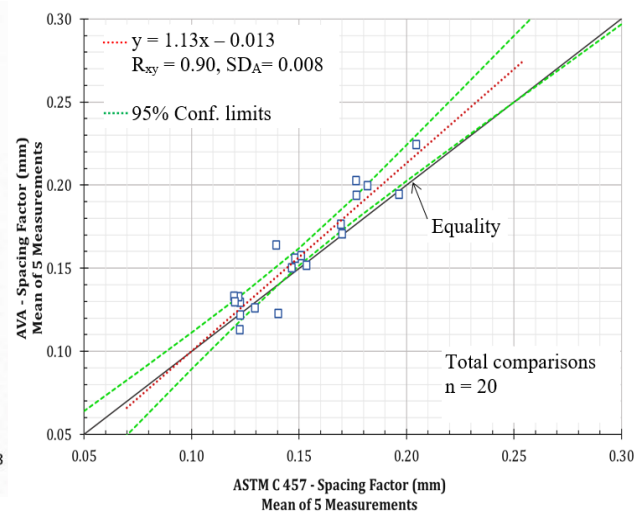
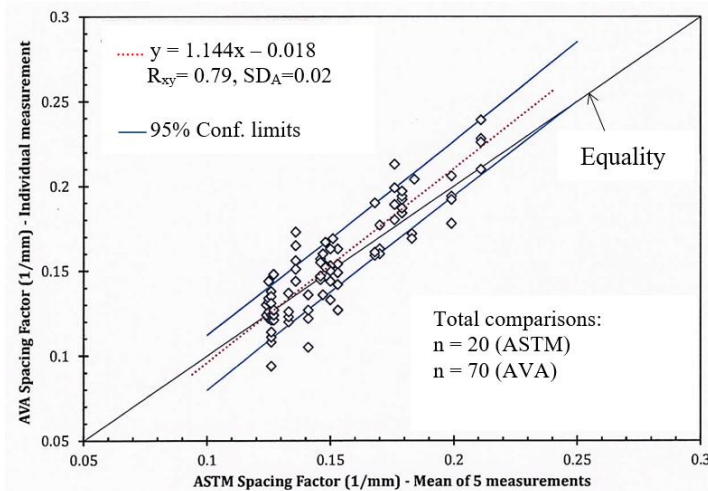
The figures below compare air-void parameters obtained on fresh concrete samples using the **AVA** with the corresponding parameters obtained by microscopical analysis of the hardened concrete and show the good correlation that AVA gives.



Single measurements of AVA spacing factor related to single ASTM C457 measurements, KDOT, USA ref. 11 & 14



Single measurements of AVA spacing factor related to single ASTM C457 measurements, FHWA, USA, ref. 4



AVA spacing factor related to ASTM C457 spacing factor, single AVA measurements to mean of five ASTM measurements (left) and mean of five AVA measurements to mean of five ASTM measurements, DBT, Denmark, ref. 1

## AVA-3000 Specifications

- USB interface
- Measuring time = 25 min./test
- Sample size for a test = 20 mL
- Real time data acquisition (weight vs time) showed on screen.
- Reports voids' curve of size distribution and histogram for void size < 2 mm.
- Algorithm calculates spacing factor and surface area in relation to ASTM C457.

- Operational voltage 240 V AC.
- Weight: 13.8 kg (bath tank) and 7.8 kg (base unit)
- Dimensions: 40 x 40 x 30 cm (bath tank) and 47 x 48 x 21 cm (base unit)
- Mini balance: 300 g capacity, 0.01 g resolution (0.001 g internal accuracy)
- Magnetic stirrer: 150 mNm, 4000 rpm
- 35 L bath tank with de-aerating pump and heater

## AVA-3000 Components

The AVA-3000 is delivered in two cases:



*Aluminum case with base unit and accessories*

*Aluminum case with water tank for de-aerating and tempering, laptop and drill machine*



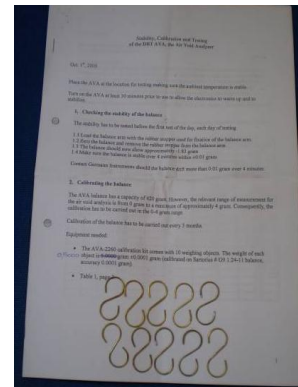
Description	Order #
Alumina case with pouch and foam insert	AVA-3005
Base Unit	AVA-3010
Riser Column	AVA-3020
Windshield	AVA-3022
6 mm Screws, 2 pcs	AVA-3025
Stirrer Pin, with one spare	AVA-3028
Piston	AVA-3030
Buoyancy Pan	AVA-3040
Wire Cage	AVA-3050
Vibrator	AVA-3060
Funnel	AVA-3080
Graduated Sampling Syringes, 3 pcs	AVA-3090
Brush	AVA-3130
Template with center hole	AVA-3140
USB Cord	AVA-3160
Power Cable, 110VAC or 220VAC	AVA-3170
Rubber Suction Ball	AVA-3180
Vaseline, can	AVA-3190
Vaseline, Tube	AVA-3200
CD with AVA Literature	AVA-3210
AVA-3000 software CD	AVA-3220
AVA-3000 Manual	AVA-3230
Flashlight	AVA-3250

Description	Order #
Alumina case with foam insert	AVA-3300
Water tank with temperature regulator and stirring	AVA-3310
Power cable, 110 V or 210 V	AVA-3315
Top Lids, 2 pcs	AVA-3320
2L Containers for release liquid, 2 pcs	AVA-3330
Laptop with installed software	AVA-3340
Electric Drill, 110 V or 210 V	AVA-3350



To be ordered separately:

Description	Order #
AVA Release liquid	AVA-3240
Verification kit	AVA-3260



## References:

1. BRITE/EURAM Project No.: BE-3376-89: "Quality Assurance of Concrete Based on Testing of the Fresh, Still Plastic Concrete", Summary of task 2: "Quantitative and Qualitative Determination of the Air Void Structure of Fresh Concrete", March 1991-February 1994, Brussels, Belgium
2. Price, B.: "High Performance Concrete in Practice", 22nd Annual Convention of the Institute of Concrete Technology, 28-30. March 1994, Swindon, UK
3. Henrichsen A & Vyncke, J.: "Quality assurance of air void structures in concrete", International Symposium Non-Destructive Testing in Civil Engineering (NDT-CE), September 1995, Berlin, Germany
4. Magura, D. D., "Air Void Analyzer Evaluation", FHWA-SA-96-062, May 1996, US Department of Transportation, Federal Highway Administration
5. Price, B.: "Measuring the air voids of fresh concrete", CONCRETE July/August 1996
6. Portland Cement Association 'Control of Air Content in Concrete', Concrete Technology Today, Vol.19, Number 1, April 1998
7. Dansk Beton Teknik (DBT): "Determination of Air Void Structure of the compacted but still plastic concrete using the fresh concrete Air Void Analyzer, E6 Motorway, Sweden", DBT, Copenhagen, Denmark, 1999
8. Henrichsen, A. "Air-entraining and frost resistance properties of concrete", ACI Fall Convention, Phoenix 2002, USA
9. AASHTO Technology Implementation Group: "Air Void Analyzer (AVA), An apparatus that measures the air-void characteristic of fresh concrete", A 2002 Focus Technology, USA
10. US Department of Transportation "Air Void Analyzer", Federal Highway Administration, Washington DC, USA, 2002
11. Wojakowski, J.: "Air in Portland Cement Concrete Pavements", Kansas Department of Transportation, USA, 2002
12. American Concrete Pavement Association "Air Content in Concrete Pavements", Number 4.05, May 2003
13. Crawford, Wathne and Mullarky "A FRESH perspective on measuring air in concrete", 2003 Bridge Conference, USA
14. Wojakowski, J. "Real Air Testing in Real Time", June 2005, PPP, Kansas DOT, Topeka, Kansas, USA
15. Petersen, C.G.: "Air Void Analysis for Fresh Concrete, Latest Advances", 9th ACI Conference, Seville, Spain, October 13-17, 2009
16. Kristensen, L.F. Sammenligning af Unicons og PTE's Air Void Analyzer, Aalborg Portland, Feb.9th 2009, Denmark
17. Germann Instruments: "AVA models between 1986 to 2010", 2011, Copenhagen, Denmark
18. Germann Instruments "AVA for measuring air voids in fresh, air entrained concrete", Copenhagen, Denmark, 2012
19. Qi Yang: "Stability of Air Bubbles in Fresh Concrete", Department of Civil and Environmental Engineering, Division of Building Technology, Building Materials, Chalmers University of Technology, Göteborg, Sweden, 2012
20. Sovannasathya, R. et al: "Critical Size of Entrained Air to Stability of Air Volume in Mortar of Self-Compacting Concrete at Fresh State", Journal of Advanced Concrete technology Vol 15. 29-37, January 2017, Japan Concrete Institute
21. Puthipad, N.: "Effects of Entrained-air Size Distribution and Fly Ash on Self-compactability and Air Volumetric-stability of Fresh Concrete", Kochi University of Technology, Kochi, Japan, March 2018

## Standards related to AVA:

22. AASHTO Designation: TP 75-08: "Provisional Standard Test Method for Air-Void Characteristics of freshly Mixed Concrete by Buoyancy Change", Washington DC, USA
23. ASTM C 457-98: "Standard practice for microscopical determination of air-void content and parameters of the air-void system in hardened concrete", USA
24. EN 480-11: "Determination of air void characteristics in hardened concrete", European Committee for Standardization, Brussels, Belgium
25. US Department of Transportation: "Report Chapter 6. Voids", Federal Highway Administration (FHWA), Washington DC, USA, July 2006

## Purpose

The **BOND-TEST** is used to conduct a pull-off test in accordance with ASTM C1583, "Test Method for Tensile Strength of Concrete Surfaces and the Bond Strength or Tensile Strength of Concrete Repair and Overlay Materials by Direct Tension (Pull-off Method)." The obtained **pull-off strength** can be used for the following purposes:

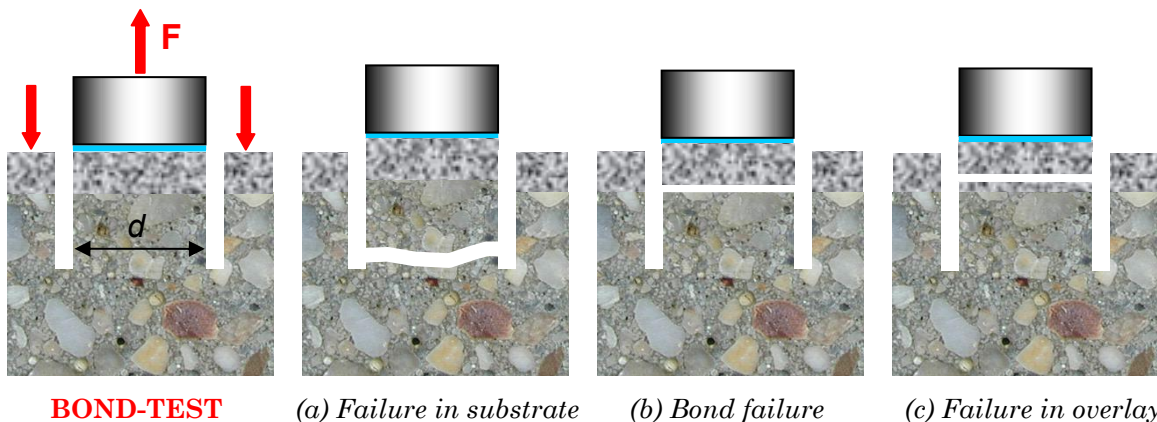
- To evaluate the in-place bond strength between a repair overlay or patch and the substrate
- To evaluate the in-place tensile strength of concrete or other materials
- To evaluate the effect of surface preparation procedures on the tensile strength of the substrate before applying a repair material or overlay
- To evaluate the adhesion of diverse materials like metal plates, tiles, thick coatings, FRP's, etc., on concrete or masonry surfaces.

## Principle

In the **BOND-TEST**, a disc is bonded to a prepared testing surface and the disc is pulled off after a partial core has been cut around the disc (extreme left in following figure). The pull-off force,  $F$ , is divided by the cross-sectional area of the partial core to obtain the pull-off strength  $f_p$ :

$$f_p = \frac{4F}{\pi d^2} \dots (1)$$

where  $d$  is the diameter of the partial core.



The typical failures that can occur in a pull-off test are illustrated above: (a) failure in the substrate indicates that the bond strength is greater than the tensile strength of the substrate; (b) failure at the interface provides a measure of the tensile bond strength between the overlay and the substrate; and (c) failure in the overlay indicates that the bond strength is greater than the tensile strength of the overlay. During a test, it is very important that **negligible bending** is introduced to the disc by the loading system. This is ensured by the **BOND-TEST** pulling machine and its accessories. Otherwise, low and erratic test results will be obtained.

Failure type (a) is preferred because it shows that the bond strength of the overlay is greater than the tensile strength of the substrate. Note that failure occurs at the weakest link of the composite system, and one cannot predict which type of failure will occur. Only tests results with the same type of failure should be averaged in calculating the average pull-off strength.

The nature of the **BOND-TEST** has been investigated by finite element analyses (see Petersen, C.G., Dahlblom, O. and Worters, P., "Bond-Test of Concrete and Overlays," *Proceedings*, International Conference on NDT in Civil Engineering, University of Liverpool, U.K., 1997; Bungey, J.H. and Madandoust, R., Factors influencing pull-off tests on concrete," *Mag. of Concr. Res.*, 1992, 44, No. 158). Failure in the **BOND-TEST** using a 75-mm disc was predicted to occur at a displacement of 0.02 mm

to 0.03 mm and the nominal stress in the partial core before rupture is about 3 % lower than the uniaxial tensile strength of the substrate concrete.

## Procedure

### 1. Surface planing

The surface is ground with a diamond studded planing tool to expose the aggregates and to obtain a plane surface. The center knob that remains is removed with a separate wheel grinder. The dry surface is brushed and any dust or powder is blown away. The suction plate is used to stabilize the planing tool. Note that this operation is done without using cooling water.



### 2. Bonding the disc

A clean disc is bonded to the prepared surface using a rapid-curing adhesive (GRA). The GRA adhesive has a tensile strength of at least 10 MPa when fully cured, which takes 2 to 5 minutes at 15 to 25°C. Lower temperatures will increase its curing time and vice versa. The progress of hardening is observed in the small cup in which the two-component GRA was mixed. In cold weather conditions, the concrete surface and the disc can be heated with a heat gun to accelerate curing of the adhesive.



### 3. Partial coring

A partial core is cut perpendicular to the surface using cooling water; the bonded disc serves as a drill guide (the inner diameter of the coring bit is slightly larger than the disc diameter). The partial core can be cut with the **CORECASE** (see technical data sheet) or any other appropriate coring machine. For tests to measure bond strength, the core is cut to a depth of 25 mm into the substrate or one-half of the core diameter, whichever is greater. For tensile strength of the substrate, cut to a depth of 25 mm.



### 4. Pull-off

The disc is loaded in direct tension at a controlled rate using the calibrated hydraulic pull machine. The machine, which is the same as used for pullout tests (see technical data sheets of **LOK** and **CAPO** tests), bears against a circular counter pressure ring positioned centrally on the planed surface. The peak force in kN is recorded and used to obtain the pull-off strength with equation (1). The type of failure, (a), (b) or (c), as shown before, is recorded.



The procedure and special equipment used for the **BOND-TEST** ensure that the disc is loaded in direct tension without bending. Bending may lower results by 20 to 50 %. The discs have sufficient stiffness to avoid distortion during testing. By bonding a clean disc on a planed, dry surface with the GRA adhesive, failure should not occur at the disc/overlay interface. Failure at the disc/overlay interface is an inconclusive test and must be repeated if the bond strength is to be evaluated.



## Testing Examples



**BOND-TEST** being performed for quality control of the bond between a wear resistant overlay and a concrete slab; coring after bonding the 75- mm disc is shown (left), application of pull-off load (middle), and the bond failure, type (b), between the overlay and the substrate (right) at 1.8 MPa



**BOND-TEST** being performed on granite tiles in a subway station



The bond of a repair on a balcony being evaluated with **BOND-TEST**

## BOND-TEST Specifications

- Battery powered handheld hydraulic pulling machine with robust steel-aluminum body
- Digital display resolution = 0.1 kN
- Maximum force: 100 kN (about 22 MPa for 75 mm discs)
- Maximum stroke: 6 mm
- Accuracy of measurements: < 2%
- Operating conditions: -10 to 50°C, max. RH = 95%
- Memory capacity: 512 measurements (peak-value, time and date of testing)
- AMIGAS Software for PC communication and printout
- Coefficient of variation of replicate test results for the pull-off test method = 8 - 10% for 75 mm discs and 14 - 16% for 50 mm discs

## B-13000 BOND-TEST Pull Machine Kit Ordering Numbers



The pull machine can be used for pullout test (**LOK** and **CAPO** tests)

Item	Order #
Hydraulic pull machine with electronic gauge	L-11-1
AMIGAS printout software	L-13
Cable for printout	L-14
Strength conversion table and manual	B-13001
Counter pressure ring	B-13002
Centering piece	B-13003
Coupling	L-16
Pull bolt	L-17
Bolt handle	L-19
Oil refilling cup	L-24
Oil refilling bottle	L-25
Large screwdriver	C-149
Small screwdriver	C-157
Attaché case	B-13004

## BOND-TEST Accessories and Ordering Numbers



**B-10000 DSV-Kit:** For surface planing, bonding the disc, and attaching the coring rig to produce the partial core without anchoring.

Item	Order #
Diamond planing wheel unit	B-10010
Suction plate with valve and gauge	B-10020
Two adjustable clamping pliers	B-10030
Centering plate for 75 mm disc	B-10040
Optionally, centering plate for 50 mm disc	B-10050
Vacuum pump with hose	B-10060
Wrench, 17 mm	B-10070
Small screwdriver	B-10080
Attaché case	B-10090



**B-11000 BOND-TEST Preparation Kit:** For removing the center knob after surface planing, cleaning the surface, bonding the discs, and heating the discs in cold weather conditions

Item	Order #
Grinder with cup stone	B-11010
Heat gun	B-11020
Steel brush	B-11030
75 mm discs, 6 pcs	B-11040
Optionally, 50 mm discs, 6 pcs	B-11050
GRA glue box (Part A: 100 gr + Part B: 2 x 40 ml)	B-11060
Putty knife	B-11070
Araldite epoxy (for acrylic-based materials)	B-11080
Attaché case	B-11090
Optionally:	
GRA glue Part A, powder, can with 400 gr	B-11100
GRA glue Part B, liquid, 2 x 200 ml bottles	B11110



**CORECASE CS-75:** Coring device for producing the partial core.

Item	Order #
Coring rig with coupling	CC-10
Handles for coring rig, 3 pcs	CC-20
Coring bit, 75 mm x 110 mm	CCB-75/110
Water pump with 2 hoses	CC-30
Clamping pliers, adjustable, 2 pcs	CC-40
Set of anchoring tools, 8 mm	CC-50
8 mm expansion anchors, 20	CC-60
Chisel	CC-70
Hammer	CC-80
Corelifter, 75 mm diameter	CC-90
Wrench, 14 mm	CC-100
Measuring tape	CC-110
Set of spare bearings for coring rig	CC-120
Reinforcement locator	CC-130
Manual	CC-140
Attaché case	CC-150

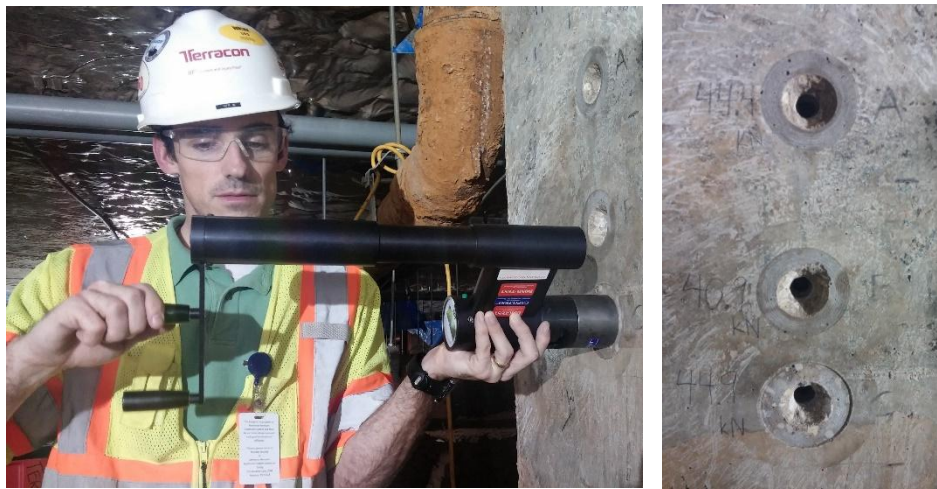
*\*Drill machine not included*



## Purpose

The **CAPO-TEST** system is used to obtain a reliable estimate of the on-site compressive strength of concrete on existing structures in accordance with the pullout test method described in ASTM C900, BS 1881:207, or EN 12504-3. Unlike **LOK-TEST** that requires cast-in inserts, the **CAPO-TEST** can be performed in existing concrete without the need of such pre-installed inserts. The main applications of **CAPO-TEST** are:

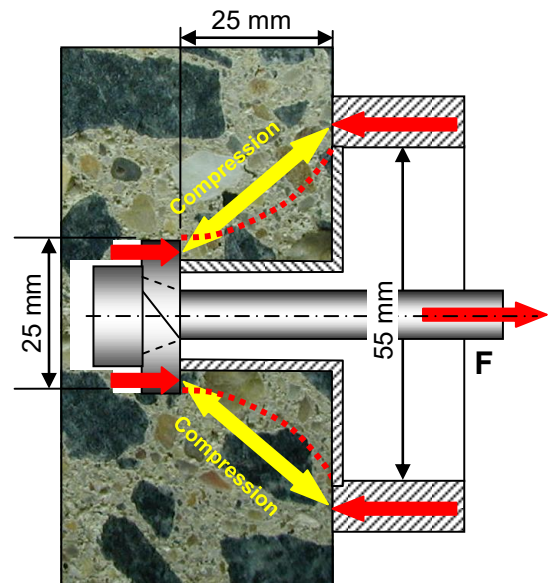
- QA / QC testing of the finished structure.
- Evaluation of curing conditions, testing of the “peel” protecting the reinforcement.
- Verification of in-place strength if strength of standard-cured specimens fails to meet acceptance criteria.
- Estimating strength of concrete in evaluation of existing structures.
- Timing of safe and early loading.
- Evaluation of fire-damaged structures.



## Principle

The surface at the test location is slightly ground (or planned) using a grinding planning tool, and an 18.4 mm hole is cored perpendicular to the surface using a diamond coring bit. A recess is routed in the hole to a diameter of 25 mm and at a depth of 25 mm from the planned surface. A split ring is expanded in the recess and pulled out using a pull machine reacting against a 55 mm diameter counter pressure ring. As in the **LOK-TEST**, the concrete in the strut between the expanded ring and the counter pressure ring is in compression. Hence, the ultimate pullout force  $F$  required to pullout the ring is directly a measure of the compressive strength.

The test is performed until the conic frustum between the expanded ring and the inner diameter of the counter pressure is dislodged. There will be a minor surface damage (the small cone hole), which can be easily patched with a repair mortar for aesthetic purposes or to avoid potential durability problems.



## Correlation and Accuracy

**CAPO-TEST** provides in less than 15 minutes an accurate estimate of in-place strength based on a well-defined general correlation to compressive strength measured using either standard cylinders or cubes.

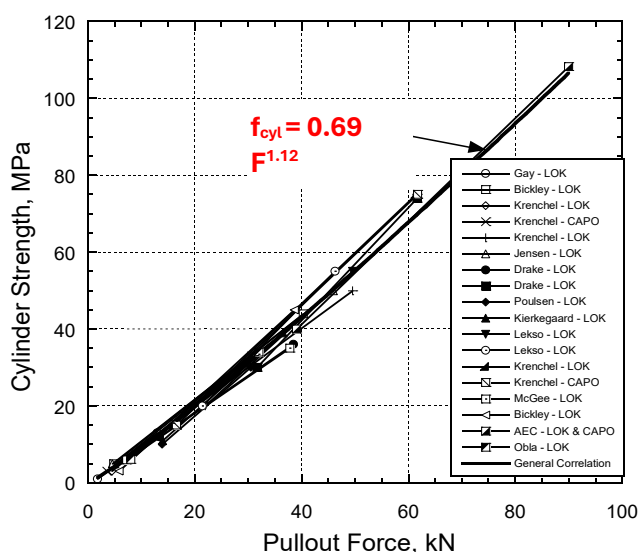
The results are not influenced by surface conditions such as texture, moisture content, hardness or depth of carbonation, as are other methods like the rebound hammer, ultrasound pulse velocity (UPV) or Windsor probe. Thus, the CAPO-Test can be used with confidence without having to take and test a large number of cores to develop a site-specific correlation.

More than 40 years of correlation experience with **LOK-TEST** and **CAPO-TEST** from all over the world indicates that one general correlation can be applicable for all normal density concrete mixtures, with little scattering and very sensitive relationship, <sup>2) 6) 7) 8) 11) and 12)</sup>

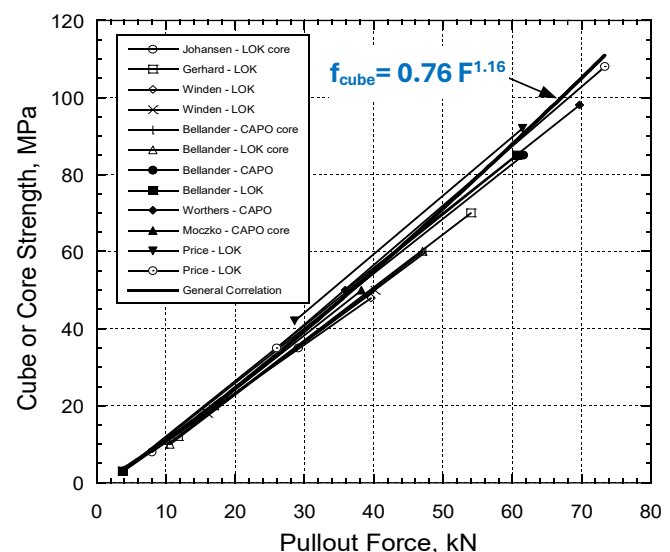
The general correlations between pull-out force and standard compressive strength shown in the following figures are from 30 major independent correlation studies performed by various laboratories in Denmark, Sweden, Norway, Holland, Canada, the United States, Poland, and England. It has been shown that these general correlations are not affected by types of cementitious materials, water-cementitious materials ratio (w/cm), use of self-consolidating concrete, air entrainment admixtures, curing conditions, stresses in the structure, stiffness of the member, carbonation, as well as shape, type, and size of aggregate up to 38 mm.

Several investigations have shown that the pullout strength measured by the **CAPO-TEST** is essentially the same as the pullout strength measured by **LOK-TEST**. This is illustrated next page in the graph on the right, which includes data from six independent studies. Thus, the general correlations are valid for both test systems.

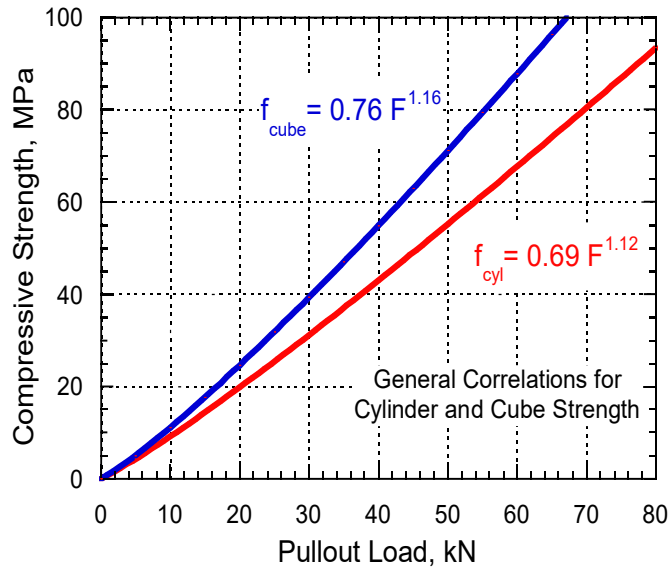
Variation of the **CAPO-TEST** on lab specimens range from 4.5% to 7.5% depending on type of specimen, and on-site from 7.8% to 12.5% for uniform batches delivered. Twenty-five dubious structures, reported in 1984 <sup>6)</sup> exhibited variations from 9.0% to 25.5%, averaging 14.7%. A later report from 1994 <sup>7)</sup> showed similar variations on-site.



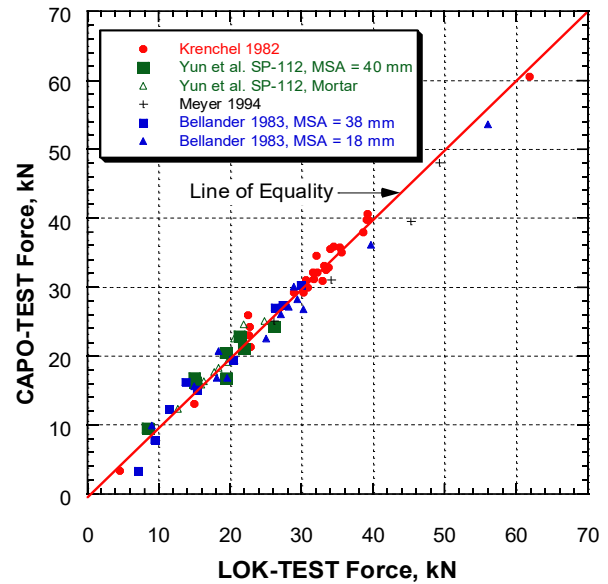
18 correlations between pullout force and standard cylinder strength <sup>4)</sup>



12 correlations between pullout force and standard cube strength or cores (100 mm x 100 mm) <sup>4)</sup>



*The robust general correlations to standard cylinders and cubes (or cores) using either LOK-TEST or CAPO-TEST*



*Comparison of results between the pull-out force given by LOK-TEST and CAPO-TEST*

Performed in accordance with ASTM C900 or EN 12504-3, these robust correlations are documented and discussed in refs 2, 3, 6, 7, 8, 9, 22 and 12. Project specifications, however, may require the development of specific correlations. What is important in such correlations is that they are performed on the same concrete quality. ACI 228.1R gives guidance on how to develop such relationships 18.

## CAPO-TEST Application Examples



*Column being tested for strength acceptance, Mexico*



*Testing the curing conditions of the "peel" protecting the reinforcement, Great Belt Link project, Denmark*

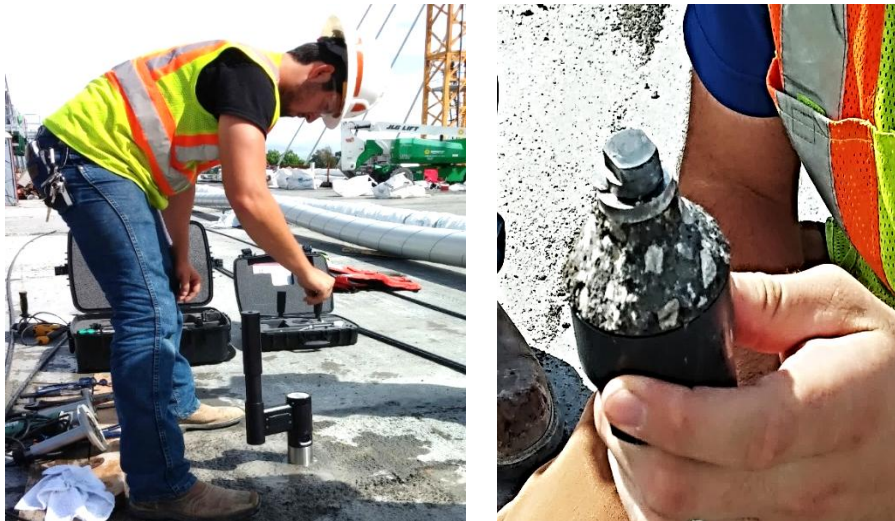


*Dubious beam being tested for strength, Denmark*





*Strength evaluation of 15 bridges (25 to 52 years old) on carbonated concrete, Poland*



*Testing of bridge joint before final loading, USA. Adjacent, the CAPO pullout cone*



*Strength testing of shotcrete, mine shaft, Canada*

*Structural evaluation of a railway bridge, Mexico*

*Quality assurance of tunnel lining segments, Channel Tunnel, UK*

## CAPO-TEST Specifications

- Battery powered handheld hydraulic pulling machine with an electronic precision gauge and robust steel-aluminum body
- Digital display resolution = 0.1 kN
- Maximum force: 100 kN
- Maximum stroke: 6 mm
- Accuracy:  $\pm 1\%$

- Operating conditions: -10 to 50°C, max. RH = 95%
- Memory capacity: 512 measurements (peak-value, time and date of testing)
- USB interface
- AMIGAS Software for PC communication and printout
- 710 W, 24 000 rpm, variable speed, compact electric router
- 650 W, 2 800 rpm, 9 Nm torque, variable speed electric drill

## CAPO-TEST Ordering Numbers

Two versions are available, the C-1000 Capo-Test complete system and the C-2000 Capo-Test Lite.

### C-1000 CAPO-TEST Complete System

Includes vacuum support (base plate and vacuum pump) to facilitate and perform the test in a more controlled manner as well as two independent units for drilling and surface planning. It consists of the C-101 Preparation Kit, the C-102 DSV-Kit, and the C-104 pull machine kit:

#### C-101 CAPO Preparation Kit

For location of reinforcement, planning surface, drilling the center hole and routing the recess to accommodate the expandable insert. It also contains the unit for expanding the insert, counter pressure and other tools for conducting the test.



Item	Order #
Counter pressure	C-142
Expansion unit	C-101-1
Coupling	C-141
Water pump	C-150
Recess router unit	C-101-2
Distance piece, 25 mm	C-136
Bottle w. CAPO-Oil	C-143
Diamond drill unit	C-101-3
Red diamond drill bit	C-101-3-1
Wrench, 13 mm	C-170
Wrench, 14 mm, 2 pcs	C-151
Wrench, 17 mm, 2 pcs	C-171
Wrench, 19 mm, 2 pcs	C-155
Surface planer unit	C-102-1
Diamond planning wheel	C-102-11
Centering brass rod	C-102-5
Reinforcement locator	C-180
Screwdriver	C-149
Tweezers	C-148
Plastic hose, 2 pcs	C-157
Marking chalk	C-160
Allen key, 4 mm	C-156
Wrench, 46 mm	C-147-1
Adjustable wrench	C-147-2
Vernier caliper	C-135
Attaché case with tray	C-160
Electric drill machine	C-101-4



## C-102 SV-Kit

Includes a support suction plate and a vacuum pump as auxiliary tools for testing. The suction plate controls the planning, the coring of the center hole and the routing of the recess. The **green diamond coring bit** is longer than the red one supplied in the preparation kit (C-101-3-1) to accommodate the extra height of the suction plate. There must be sufficient space (350 mm in diameter) and a rather smooth and airtight concrete surface for activation of the suction plate.

Item	Order #
Vacuum pump	C-102-4
Suction plate	C-102-2
Green diamond drill bit	C-101-3-2
Clamping pliers, 2 pcs	C-102-3
Small screwdriver	C-158
Plastic hose with nipple	C-147
Attaché case	C-161



## C-104 CAPO Pull Machine Kit

Includes the hydraulic pull machine, max. 100 kN capacity, and accessories.

The same pull machine can be used for the **LOK-TEST** and the **BOND TEST** with a few additional accessories (see the corresponding technical datasheets).



Item	Order #
Hydraulic pull machine with electronic gauge	L-11-1
AMIGAS printing software	L-13
USB Cable	L-14
Oil refilling cup	L-24
Oil refilling bottle	L-25
Large screwdriver	C-149
Small screwdriver	C-157
Calibration table	L-32
Manual	L-33
Attaché Case	C-104-1



## C-2000 CAPO-TEST Lite

This compact kit includes all the essential parts to perform a CAPO-TEST properly but without the auxiliary vacuum tools. It contains only one unit to perform both the drilling and surface planning. Ideal for places with difficult access or where the concrete surface is irregular, so it is not feasible to use the auxiliary vacuum accessories.



Item	Order #
CAPO-TEST Lite Contains all the parts of the:	C-2000
<ul style="list-style-type: none"> <li>• C-101 CAPO Preparation Kit (except C-101-3)</li> <li>• C-104 CAPO Pull Machine Kit</li> </ul>	



### Additional items for both versions:

**C-112 Expandable inserts** (one per test is used)



### L-30 Load Verification Unit

The calibration of a pull machine is recommended to be verified at least once a year, after servicing or after repair.

The **L-30 Load Verification Unit** has a working range of 0 to 100 kN and ensures that the load displayed by the pull machine is within  $\pm 1\%$  of the actual load, as required by ASTM C900. The load is displayed to the nearest 0.1 kN.



## References

**CAPO-TEST Instruction video on our YouTube channel: "CAPO-TEST ASTM C-900"**

1. Petersen, C.G.: "Capo-Test" Nordisk Betong, 1980, no. 5-6.
2. Moczko, A., Carino, N.J. & Petersen, C.G.: "CAPO-TEST to Estimate Concrete Strength in Bridges", ACI Materials Journal, Nov. – Dec. 2016, No 113-M76.
3. Carino, N.J.: "In-Place Strength without Testing Cores, the Pullout Test", 6th International Seminar on Advances in Cement and Concrete Technology for Sustainable Development, China, March 2018.
4. Carino, N. J., "Pullout Test," Handbook on Nondestructive Testing of Concrete, second edition, V. M. Malhotra and N.J. Carino, eds., CRC Press, Chapter 3, 2004, 36 pp.
5. Petersen, C.G. & Poulsen, E.: "Pullout testing by Lok-Test and Capo-Test with particular reference to the in-place concrete of the Great Belt Link", Danish Concrete Institute, Bredevej 2, 2830 Virum, Denmark, 1992.
6. Krenchel, H. & Petersen, C.G.: "In-Situ Pullout Testing with LOK-TEST, Ten Years Experience", Presentation at Research Session of the CANMET/ACI International Conference on In-Situ/Nondestructive Testing of Concrete, Ottawa, ON, Canada, Oct. 1984, 24 pp.
7. Petersen, C.G.: "Lok-Test and the Capo-Test pullout testing, Twenty Years' Experience", Proceedings, Non-Destructive Testing in Civil Engineering Conference, University of Liverpool, April 8-11th, 1997.
8. Bungey, J.H. & Soutsos, M.N.: "Reliable & Partially Destructive Tests to Assess the strength of Concrete on site", Fifth CANMET/ACI International Conference on Durability of Concrete, Proceedings of Near-to-surface Testing for Strength and Durability of Concrete, Barcelona, Spain, 4-9th June, 2000.
9. Soutsos, M.N., Bungey, J.H. & Long, A.E.: "In-Situ Strength Assessment of Concrete - The European Concrete Frame Building Project", University of Liverpool, UK, 1999.
10. BCA, BRE, Construct, Reinforced Concrete Council & DETR: Early age Strength assessment of Concrete On Site", Best Practice Guide for In-Situ Concrete Frame Buildings, CONCRETE, 2000.
11. Moczko, A.: "Comparison between compressive strength tests from cores, Capo-Test and Schmidt Hammer", Deptm. Of Civil Engr., Wroclaw University, Poland, May 1st, 2002.
12. Yun, C.H., Choi, R.K., Kim, S.Y. & Song, Y.C: "Comparative evaluation of nondestructive test methods for in-place strength determination" SP 112-8, ACI Special Publication, 1988, ACI, Detroit, USA.
13. ASTM C 900-15: "Standard Test Method for Pullout Strength of Hardened Concrete". ASTM International, West Conshohocken, PA, 2015, 10 pp.
14. British Standard BS 1881 pt 207: 1999, "Testing Concrete - Recommendations for the assessment of concrete strength by near-to-surface tests", BSI, London, 16p.
15. European Standard EN-12504-3: "Testing Concrete in Structures – Part 3: Determination of pull-out force". European Committee for Standardization (CEN), Brussels, Belgium, 2005, 10 pp.
16. European Standard EN 13791: "Assessment of In-Situ Compressive Strength in Structures and Precast Concrete Components", European Committee for Standardization (CEN), Brussels, Belgium, 2005, 29 pp.
17. CSA A23.1-14/A23.2-14: "Concrete Materials and Methods of Concrete Construction – Test Methods and Standard Practices for Concrete", Canadian Standards Association, Mississauga, ON, Canada, Aug. 2014, 690 pp.
18. ACI Committee 228, "In-Place Methods to Estimate Concrete Strength", American Concrete Institute.
19. PPT in three sections on Germann Instruments homepage [www.germanninstruments.com](http://www.germanninstruments.com) describing the fundamentals of CAPO-TEST and LOK-TEST
  - Section 1: Theoretical analysis, fracture mechanism and correlations
  - Section 2: Rationale, testing cases and standards
  - Section 3: Hardware, testing procedure and instruments

## Purpose

The **COMA-Meter** (COncrete MAturity-Meter) is used to measure the maturity of newly cast concrete at a depth of 80 mm from the surface for the following purposes:

- Estimating the compressive strength at an early age using a pre-established strength-maturity relationship
- Timing of pullout testing with **LOK-TEST** (consult Technical Data Sheet) for early-age strength measurement
- Evaluating the effective in-place curing temperature

## Maturity Method

The maturity method is a technique to estimate in-place strength after casting by accounting for the effects of temperature and time on the strength gain of concrete. This method is described in ASTM C1074 "Practice for Estimating Concrete Strength by the Maturity Method." The temperature history of the concrete and a maturity function are used to calculate a maturity index that quantifies the combined effects of time and temperature. The strength of a particular concrete mixture is expressed as a function of its maturity index by means of a **strength-maturity relationship**. If portions of the same concrete are subjected to different conditions, the strength-maturity relationship for that concrete and the temperature histories measured at the different locations in the structures can be used to estimate in-place strengths at those locations.

Various maturity functions have been proposed to convert the measured temperature history to a maturity value. The one that has proven to be most accurate over wide temperature ranges is based on the Arrhenius equation:

$$t_e = \sum_0^t e^{\frac{-E}{R} \left( \frac{1}{T} - \frac{1}{T_r} \right)} \Delta t$$

where

- $\Delta t$  = time interval at actual concrete temperature
- $t_e$  = the equivalent age at the reference temperature,
- $E$  = apparent activation energy, J/mol,
- $R$  = universal gas constant, 8.314 J/mol-K,
- $T$  = average absolute temperature of the concrete during interval  $\Delta t$ , Kelvin, and
- $T_r$  = absolute reference temperature, Kelvin.

The exponential function is an **age conversion factor** that converts a time interval at the actual concrete temperature to an equivalent time interval, in terms of strength gain, at the reference temperature. The reference temperature is usually taken as the standard-curing temperature for concrete specimens, typically 20 °C (293 K) or 23 °C (296 K).

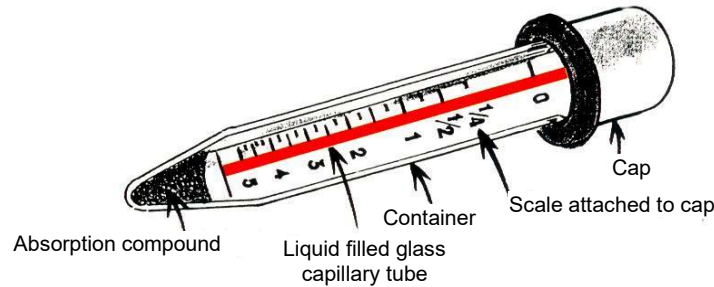
The activation energy represents the temperature sensitivity of the rate of strength gain during the acceleratory period following final setting and it depends on the cementitious materials in the concrete. For ordinary Portland cement it has a value of about 40 kJ/mol, and it is greater for mixtures with slag cement and smaller for mixtures with fly ash (1, 2). ASTM C1074 provides strength-testing procedures for estimating the activation energy for a specific cementitious system. Others have used isothermal calorimetry (2) and setting time tests to evaluate activation energy (3).

To use the maturity method for estimating in-place strength, it is necessary to develop the **strength-maturity relationship** for the particular concrete mixture. As described in ASTM C1074, this can be done by measuring the strength of specimens of the concrete mixture at different values of maturity. The strength-maturity data can then be used for estimating the in-situ strength as a function of age at the locations of the **COMA-Meter** probes.

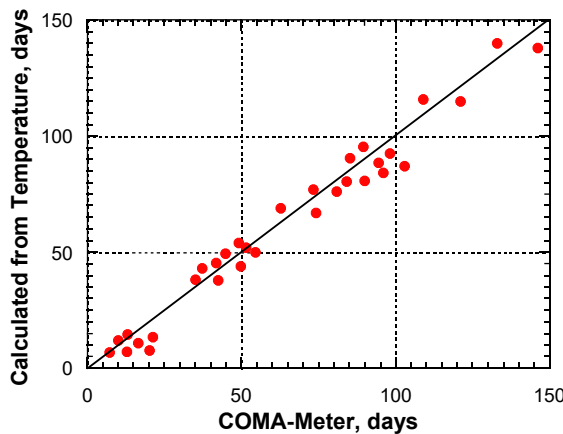


## Principle

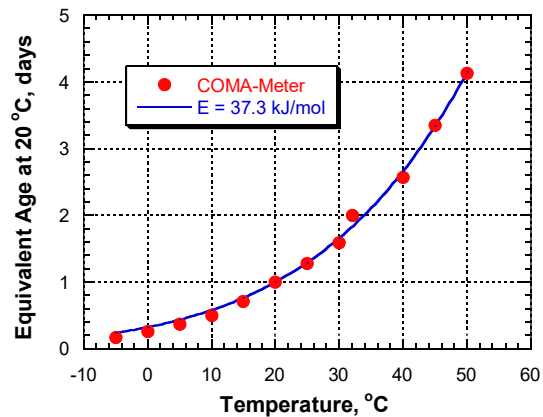
A glass capillary tube contains a special liquid for which the rate of evaporation varies with temperature according to the Arrhenius equation that is used to determine maturity of concrete from its temperature history. The closed capillary tube is placed on a card with a calibrated scale indicating maturity in equivalent age at 20 °C. The card is attached to a cap that fits into a transparent glass container. After the concrete is cast, the capillary tube is snapped at the zero mark on the scale, the cap is pushed into the container, and the container is inserted into the fresh concrete.



The liquid in the capillary tube will evaporate at a rate determined by the concrete temperature and time. The level of the liquid, readable on the scale, measures the maturity of the concrete stated in  $M_{20}$  days, which is the number of equivalent days of curing at 20 °C.



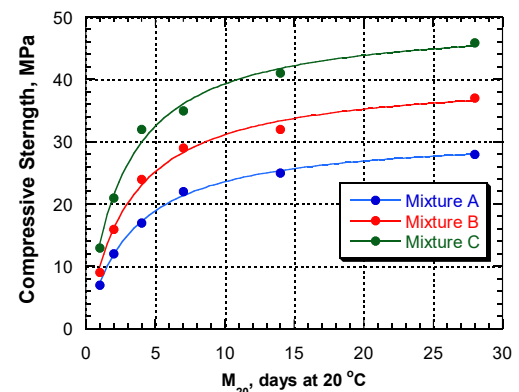
Comparison between **COMA-Meter** maturity and maturity calculated from temperature readings.  
Source: Möller, G. "Evaluation of COMA-test," Report 8335-1983, CBI, Stockholm, Sweden



Maturity calculated by Arrhenius equation with activation energy of 37.3 kJ/mol compared with **COMA-Meter** readings after one actual day at temperatures between -5 °C and 50 °C

## Strength-Maturity Relationship

To estimate the in-place strength, the **strength-maturity relationship** for the concrete mixture needs to be developed beforehand. The detailed procedure is given in ASTM C1074, but basically a set of standard specimens are made in the laboratory. At ages of 1, 3, 7, 14, and 28 days, at least two replicate specimens are tested for strength and the average maturity is calculated from the temperatures registered in two companion specimens with thermocouples. The strength-maturity data are plotted and a best-fit curve is determined and used for estimating the in-place strength. The plot on the right shows examples of strength-maturity curves for three concrete mixtures. A simpler alternative to develop the relationship is using, instead of thermocouples,

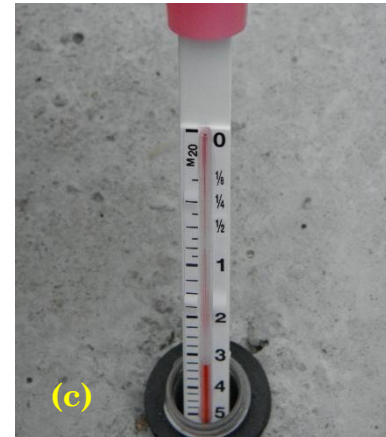
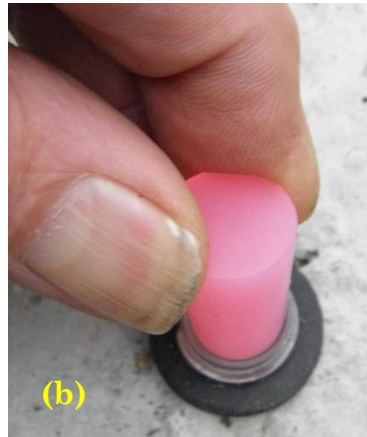


a **COMA-meter** in each of the two companion specimens and test the strengths at the desired maturity ages ( $M_{20}$  days) directly measured by the COMA-meters.

## Application

The basics steps in using the **COMA-Meter** are:

- Break the glass capillary at the 0 mark and introduce the scale card into the container
- Insert the probe into the fresh concrete
- At the desired time, pull out the card and read the maturity days ( $M_{20}$  at  $20^{\circ}\text{C}$ ). Introduce the card again if the expected maturity has not been reached.



## COMA-Meter Specifications

- Measuring ranges:
  - COMA-5** = 0 to 5  $M_{20}$  days
  - COMA-14** = 0 to 14  $M_{20}$  days
- Precision:  $\pm 0.1 M_{20}$  days
- Accuracy:  $\pm 5\%$  compared with maturity values calculated from direct temperature readings
- Activation energy,  $E \approx 40 \text{ kJ/mol}$ .

## Ordering Numbers:

Item	Order #
COMA-Meter 0 to 5 $M_{20}$ days. Pack of five probes.	COMA-5
COMA-Meter 0 to 14 $M_{20}$ days. Pack of five probes.	COMA-14



COMA-5



COMA-14

## References

- Carino, N.J. and Lew, H.S., "The Maturity Method: From Theory to Application" <http://fire.nist.gov/bfrlpubs/build01/PDF/b01006.pdf>
- Schindler, A.K., "Effect of Temperature on Hydration of Cementitious Materials," *ACI Materials Journal*, Vol. 101, No1, Jan-Feb 2004, pp. 72-81.
- Pinto, R.C.A. and Schindler, A.K., "Unified modeling of setting and strength development," *Cement and Concrete Research*, Vol. 40, 2010, pp. 58-65.

## Purpose

**CORECASE** is a portable, lightweight coring rig for quickly obtaining drilled cores of concrete (ASTM C42 or EN 12504-1) that are accurate in diameter, have straight sides, and are perpendicular to the surface. Drilled cores can be used for the following purposes:

- Visual inspection of the concrete interior
- Determination of in-place compressive strength or other mechanical properties
- Verification of flaws identified by NDT methods such as the s'MASH impulse-response system; the DOCTer impact-echo system; and the MIRA and EyeCon pulse-echo systems
- Preparing a partially drilled core for conducting a pull-off test with BOND-TEST following BS 1881:207 or ASTM C1583
- Other laboratory tests such as rapid chloride penetration using the PROOVE'it system, bulk conductivity/resistivity using Merlin, air-void parameters using the RapidAir system, or for petrographic analysis

## Principle

A thin-walled coring barrel with a high-performance diamond bit is attached to a water-cooled drill rig. The drill rig pushes the drill barrel forward concentrically, thereby avoiding bending forces during drilling. A special coupling is used between the electric drill and the coring barrel to minimize vibration of the bit, ensuring a long life for the diamond bit and a smooth core surface. The drill rig is kept securely perpendicular to the surface by adjustable clamps anchored to the surface (or by a suction plate available for the CS-75 version). A hose brings water to the rig from a submersible water pump in a bucket and a second hose allows water recirculation to keep the coring bit cool and well lubricated while is drilling, without spilling water.

The end result is a quickly drilled core that has a smooth surface, accurate diameter, and drilled perpendicular to the surface.

Two versions are available:

**CORECASE CS-75** for a 75-mm core diameter and **CORECASE CEL-100** for a 100-mm core diameter.

## Specifications

Version:	CORECASE CS-75	CORECASE CEL-100
Material	Aluminium rig and barrel with steel diamond bits	
Max. core diameter	75 mm	100 mm
Max. core height	110 mm	220 mm
Rig diameter	125 mm	100 mm
Weight*	4.8 kg	2.6 kg
Length*	600 mm	340 mm
Length, extended*	800 mm	460 mm
Optional vacuum pump and suction plate	Yes	No



\*without drill or coring bit



## Example Applications



Coring with the **CS-75** rig clamped to the surface



The **CS-75** coring rig attached to the suction plate before conducting **BOND-TEST**



Coring with the **CS-75** rig for inspection of cracks following chloride extraction



Coring with the **CEL-100** rig to for testing chloride permeability over the specimen

## Ordering Numbers

### CORECASE CS-75 (75-mm core)

Item	Order #
Coring rig with coupling	CC-10
Handles for coring rig, 3 pcs	CC-20
Coring bit, 75 mm x 110 mm	CCB-75/110
Water pump with 2 hoses	CC-30
Clamping pliers, adjustable, 2	CC-40
Set of anchoring tools, 8 mm	CC-50
8 mm expansion anchors, 20	CC-60
Chisel	CC-70
Hammer	CC-80
Core lifter, 75-mm diameter	CC-90
Wrench, 14 mm	CC-100
Measuring tape	CC-110
Set of spare bearings for coring rig	CC-120
Reinforcement locator	CC-130
Manual	CC-140
Attaché case	CC-150

### Optional items

Suction plate	CC-160
Vacuum pump	CC-170
1150 W electric drill	CC-180



Optional suction plate with vacuum pump

## CORECASE CEL-100 (100 mm core)

Item	Order #
Coring rig with coupling	CC-15
Handles for coring rig, 3 pcs	CC-20
Coring bit, 100 mm x 210 mm	CCB-100/210
Water pump with 2 hoses	CC-30
Clamping pliers, adjustable, 2	CC-40
Set of anchoring tools, 12 mm	CC-55
12 mm expansion anchors, 20	CC-65
Chisel	CC-75
Hammer	CC-80
Core lifter, 100-mm diameter	CC-95
Wrench, 14 mm	CC-100
Measuring tape	CC-110
Set of spare bearings for coring rig	CC-120
Reinforcement locator	CC-130
Manual	CC-145
Attaché case	CC-155

### Optional

1150 W electric drill	CC-180
-----------------------	--------

Extension rods, 100 mm long, for drilling deeper than 110 mm (**CS-75**) or deeper than 210 mm (**CEL-100**) are available on request, Order # CC-190.



### Additional coring bits

#### For CORECASE CS-75

Core diameter × length	Coring bit #
25 mm × 110 mm	CCB-25/110
35 mm × 110 mm	CCB-35/110
50 mm × 110 mm	CCB-50/110
75 mm × 110 mm	CCB-75/110

#### For CORECASE CEL-100

Core diameter × length	Coring bit #
25 mm × 210 mm	CCB-25/210
35 mm × 210 mm	CCB-35/210
50 mm × 210 mm	CCB-50/210
75 mm × 210 mm	CCB-75/210
100 mm × 210 mm	CCB-100/210

## Purpose

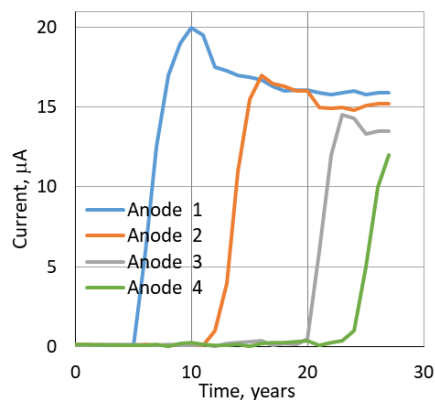
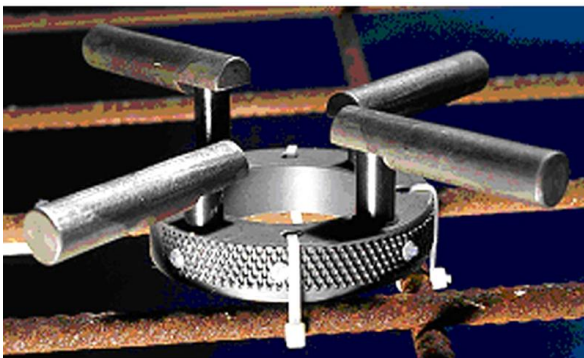
**CorroWatch** is a 4-probe monitoring system for early warning of the onset reinforcement corrosion. It can be used to estimate the time before corrosion of reinforcement begins so that corrective measures may be taken early enough to minimize repair costs. Applications:

- Monitoring of reinforcement in critical areas for corrosion such as construction joints, splash zones in marine structures, bridge decks, bottoms of bridge columns exposed to ingress of chlorides, etc.
- Monitoring of the ingress of the depassivation front, due to chloride penetration or carbonation.

## Principle

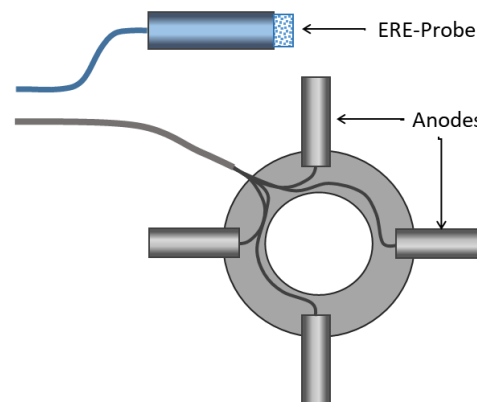
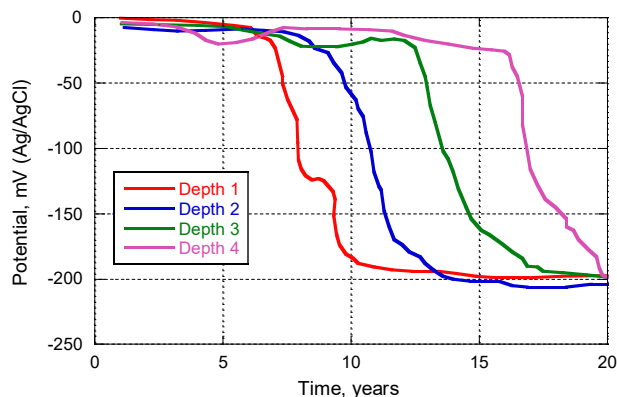
The **CorroWatch** is a multi-probe device consisting of four black steel bars acting as anodes and a noble metal as the cathode. It is attached to the rebars with plastic strips and the anodic bars are positioned at different elevations and when concrete is cast, **CorroWatch** allows determination of corrosion activity as a function of cover distance. The height of the anodes may be adjusted according to the thickness of the concrete cover.

In order to predict when corrosion activity has reached the anodes, the current between the individual anodes and the cathode is measured, either with a handheld Zero Ohm Ammeter or a datalogger. When corrosion starts, the measured current increases significantly.



**CorroWatch** measurements after long exposure in sea water

In addition, the **ERE-Probe** (see technical data sheet) may be cast into the concrete along with the **CorroWatch** for monitoring the electrical potentials of its four black steel anodes. By monitoring the potential drop of the four anodes as a function of time, the gradual penetration of the depassivation front can be tracked and the service life can be estimated reliably, based on the actual depth of the reinforcement.

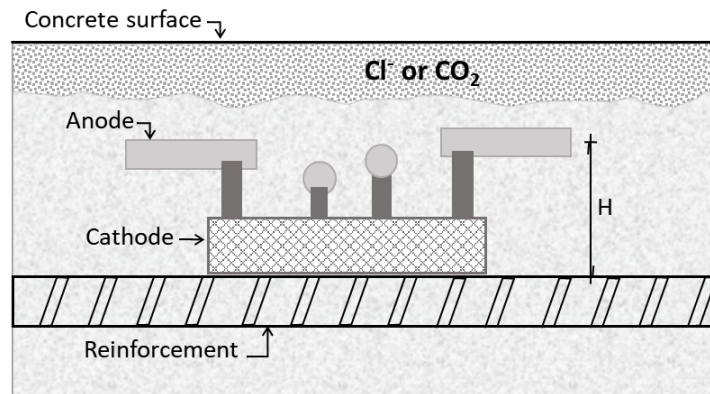


**CorroWatch and ERE-Probe** potential measurements from a marine structure showing the advancement of the depassivation front



## CorroWatch Specifications

- Anodes: 4 black steel bars
  - Length = 60 mm
  - Diameter = 12 mm
- Anode default heights, H: 33, 38, 43 and 48 mm
- Cathode's chamber:
  - External diameter = 85 mm
  - Thickness = 20 mm
- Overall weight = 500 g



## Ordering Numbers:

Item	Order #
<b>CorroWatch</b> with 3 meter cables	CW-3
<b>CorroWatch</b> with 5 meter cables	CW-5
<b>CorroWatch</b> with 10 meter cables	CW-10

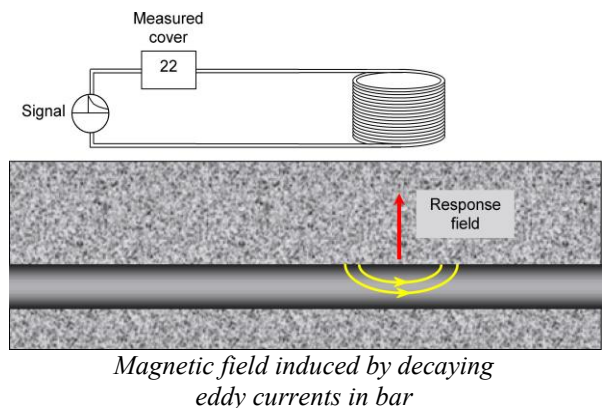
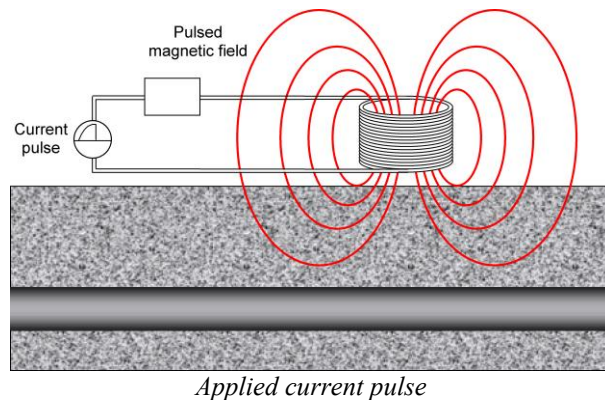
## Purpose

**CoverMaster (Elcometer 331)** is a portable, convenient, accurate rebar locator and concrete covermeter that can be used in reinforced concrete structures for the following applications:

- Locate position and orientation of reinforcing bars and metal cable ducts in concrete structures
- Measure the cover depth of reinforcement
- Estimate the diameter of reinforcing bars
- Locate other metal objects embedded in concrete

## Principle

The instrument is based on the pulse-induction technique. A repetitive current pulse is applied to the coils in the search head (below left). During each pulse, current increases gradually in the coils but is turned off rapidly. The sudden end of the pulse causes a sudden collapse in the magnetic field produced by the coils, which induces eddy currents in a bar located within the coils' influence zone. As the eddy currents decay, a decaying magnetic field induces a secondary current in the coils (below right). The instrument measures the amplitude of the induced current, which depends on the orientation, depth, and size of the bar. The search head is directional, so the maximum signal is obtained when the bar is aligned with the long axis of the search head. The pulse-induction technique is uniquely stable, is not affected by moisture in concrete or magnetic aggregates and is immune to temperature variations and electrical interference.



To identify the location and orientation of the rebar under the surface of the concrete, a search head is connected to the covermeter and is used to scan across the designated search area. When the search head approaches a reinforcement bar, the covermeter will start to emit a sound which increases in pitch and the signal strength indicator bar on the display increases in length. When the bar is positioned below the center of the search head, the pitch of the sound will be at its highest and the signal strength indicator bar will be at its maximum. At this moment, the depth of cover will be shown on the display.



pitch and the signal strength indicator bar on the display increases in length. When the bar is positioned below the center of the search head, the pitch of the sound will be at its highest and the signal strength indicator bar will be at its maximum. At this moment, the depth of cover will be shown on the display.

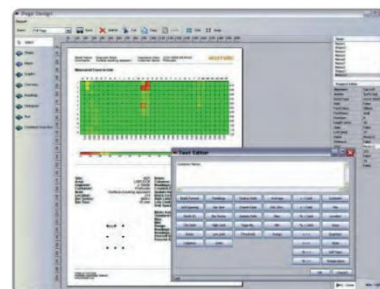
The case is designed to meet IP65 protection so the instrument can be used in harsh environments.

A range of fully interchangeable search heads are available to suit different requirements. Changing

from one search head to another is quick and simple. All functions can be accessed through 4 buttons on the search head.

The **Elcometer 331** can also be used with half-cell electrode probes to measure half-cell potentials in accordance with ASTM C876, in a similar manner to the **Mini Grate Dane** (see its technical data sheet).

The Covermaster™ software, available for some models, is a data management tool to store cover and half-cell readings and produce professional reports.



## Elcometer 331 Specifications and Features

- Power supply: 7.4V battery pack
- Battery life: 32 hours of continuous use (20 hours with backlight)
- Recharging time: 4 hours
- Dimensions: 230 x 130 x 125 mm
- Weight: 1.6 kg (without accessories)
- Half-Cell measurements: -999 mV to +999 mV,  $\pm 5$  mV
- Operation temperature: 0 to 50°C
- Rugged case IP65

Description of feature	Model				
	B	BH	SH	TH	THD
Rebar location, orientation and depth of cover	•	•	•	•	•
Cover thickness reading in mm and inches	•	•	•	•	•
Graphics display with backlight	•	•	•	•	•
Multiple language menu	•	•	•	•	•
Signal strength bar displayed	•	•	•	•	•
Interchangeable heads with LED and keypad	•	•	•	•	•
Adjustable beep volume and earphone socket	•	•	•	•	•
Measurement sound modes:	•	•	•	•	•
Locate ( <i>tone increases as head approaches rebar</i> )	•	•	•	•	•
Under Cover ( <i>tone only sounds for low cover</i> )			•	•	•
Maxpip™ ( <i>tone only as head passes rebar center</i> )			•	•	•
Half-cell potential measurements capability		•	•	•	•
Auto size mode for bar diameter estimation			•	•	•
Orthogonal mode for bar diameter estimation			•	•	•
RS232 output to printer or PC			•	•	•
CoverMaster™ Software			•	•	•
Statistics			•	•	•
Minimum and maximum cover limits			•	•	•
Date and time			•	•	•
Memory			•	•	•
Linear batch memory (No. batches / Readings per batch)			10 / 1000	200 / 1000	200 / 1000
Grid batch memory (No. batches / Readings per batch)				1000 / 240000	1000 / 240000
User customized batch size				•	•
Graphics plot				•	•
Threshold plot				•	•
Stainless steel probe					•



## Search Heads

<p><b>Standard</b></p> 	<p>General purpose</p> <p>Cover layer range: 15 to 95 mm for 40 mm bar 8 to 70 mm for 8 mm bar</p> <p>Sensing area: 120 x 60 mm</p>	<p><b>Narrow Pitch</b></p> 	<p>For resolving closely-spaced bars</p> <p>Cover layer range: 8 to 80 mm for 40 mm bar 5 to 60 mm for 8 mm bar</p> <p>Sensing area: 120 x 60 mm</p>
<p><b>Deep Cover</b></p> 	<p>For deep-located bars</p> <p>Cover layer range: 35 to 180 mm for 40 mm bar 25 to 160 mm for 8 mm bar</p> <p>Sensing area: 160 x 80 mm</p>	<p><b>Dual Search</b></p> 	<p>For high strength and stainless steel (only for model THD)</p> <p>Cover layer range: 35 to 180 mm for 40 mm bar 25 to 160 mm for 8 mm bar</p> <p>Sensing area: 160 x 80 mm</p>

### Bar Diameter Ranges

Metric	5 to 50 mm in 21 values
U.S. Bar Numbers	#2 to #18 in 16 values
ASTM/Canadian	10 to 55M in 8 values
Japanese	6 to 57 mm in 17 values

## Half-Cells Kit



Suitable for models BH, SH, TH and THD. Consists of either a copper / copper sulphate electrode or a silver / silver chloride electrode. Each half cell is a sealed unit, no need to mix chemicals.

It is supplied with a 25 m cable.

## Borehole probe

Borehole probes are also available for locating a second layer of reinforcement or deeply embedded tendon ducts. The borehole probe can be switched from the “forward looking” to the “side looking” mode.

Measurement depth:

Short probe = up to 400 mm / Long probe = up to 1000 mm



## Elcometer 331 Ordering Numbers

Elcometer 331 Covermeters are delivered with your selected search head and/or half-cell electrode, including connecting cables, rechargeable battery pack and charger, earphone, shoulder strap, plastic carry case, operating instructions, CoverMaster™ software (for SH, TH & THD models) & PC cable (for SH, TH & THD models).

## Purpose

The **CrackScope CRS-100** can be used for accurate measurement of the width of surface opening cracks as well as measurement of the depth of surface holes or irregularities.

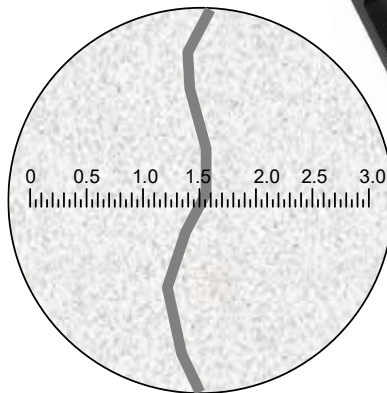
## Principle

The **CrackScope** is a small size, lightweight and conveniently portable microscope with a 25× magnification. It has a built-in scale for crack-width measurement and another scale on the focusing adjustment ring for depth indication.

Depth measurements are made by means of the scale engraved on the focusing ring and the needle of the lens barrel. For a depth measurement, a reading in the scale is taken after focusing at the bottom of a depression and then a second reading is taken after focusing at the surface (top) perimeter of the depression. The difference of both readings gives the depth of the depression measured with an accuracy of  $\pm 0.1$  mm.

## CrackScope Specifications

- Magnification = 25x
- Built-in 3-mm scale with 0.05 mm divisions
- Accuracy:  $\pm 0.025$  mm on crack width
- Attachable/detachable rubber eyepiece
- Scale engraved on the focusing ring with 0.1 mm divisions for depth indication
- Size: 125 x 42 mm
- Net weight: 85 g



## Ordering Number:

Item	Order #
CrackScope	CRS-100

## Purpose

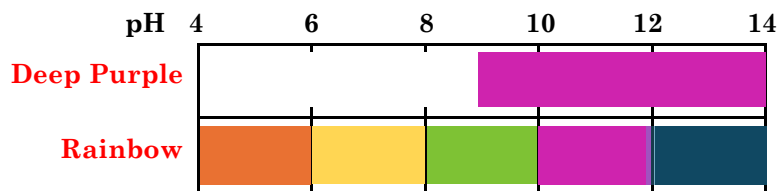
**Deep Purple** and **Rainbow Indicators** are used to determine the depth of carbonation in samples of field concrete by means of its pH. Carbonation depth can be used for the following purposes:

- To evaluate the cause of corrosion when conducting corrosion surveys
- To estimate service life where penetration of the carbonation front is critical
- To monitor the effectiveness of protective coatings, sealers or procedures for re-alkalization of the cover layer
- To make a rough estimate of concrete strength from the age of concrete and the relative humidity

## Principle

The natural alkalinity of cement paste in concrete results in a protective oxide coating on steel reinforcement that prevents the steel from rusting. When carbon dioxide ( $\text{CO}_2$ ) in the air penetrates into concrete, it reacts with the calcium hydroxide ( $\text{CaOH}_2$ ) in the cement paste producing calcium carbonate ( $\text{CaCO}_3$ ). This reaction is called **carbonation**, and it causes the alkalinity of the paste to decrease, that is, the pH decreases below its normal value of about 13. When the pH drops below 9, the protective oxide coating is destroyed and, in the presence of moisture and oxygen, the steel will corrode. Thus measurement of the depth of carbonation is an essential step for corrosion evaluation of a reinforced concrete structure.

To measure the pH of the cement paste, a freshly broken piece of concrete or a newly cut core is sprayed with the indicator, and allowed to dry. The approximate pH of the paste is indicated by a color index as illustrated below.



## Accuracy

The carbonation front or depth of carbonation measured with the **Deep Purple Indicator** represents the traced line where the cement paste has a pH within the range of 8.5 to 9.5 as shown above.

The carbonation front measured with the **Rainbow Indicator** was correlated with the depth of carbonation determined by petrographic thin section analysis for a wide range of concretes with varying slump, with or without calcium chloride or fly-ash, different water-cement ratios, varying degrees of consolidation and different finishing methods:

Campbell, D.H., Sturm, R.D. and Kosmatka, S.H., "Detecting Carbonation," *Concrete Technology Today*, Vol. 12, No. 1, March 1991, Portland Cement Association, USA

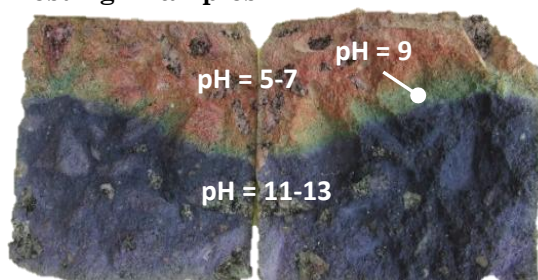
The results show that the depth of carbonation determined from thin section analysis correlated well with the depth where the **Rainbow Indicator** indicated a green color or pH of 9 as shown above.

On normal concrete, the depth of the carbonation front indicated by the Deep Purple Indicator can be determined with an accuracy of  $\pm 10\%$  to  $\pm 15\%$ .

One study with several mortar mixes exposed to accelerated carbonation showed that the standard deviation for measurements of depth of carbonation with the Rainbow Indicator is about 0.8 mm:

A. Belda, K. De Weerd, M.R. Geiker, "Carbonation front characterization with pH colour indicators," 35th Cement and Concrete Science Conference, University of Aberdeen, Scotland (2015)

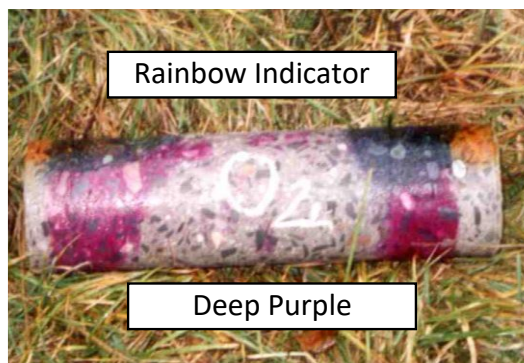
## Testing Examples



The depth of carbonation evaluated by spraying the surfaces of a freshly broken core with the **Rainbow Indicator**. Depth of carbonation varied from 27 mm to 41 mm.



## Purple and Rainbow Indicators

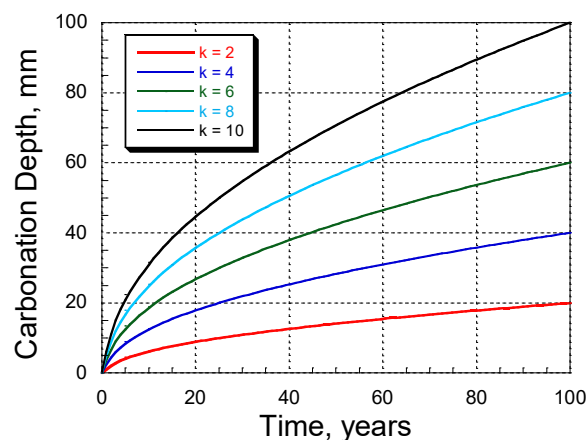


Shown in the photo to the left, the pH profile of a newly cut core was evaluated by the **Rainbow Indicator** (top of core) and by the **Deep Purple Indicator** (bottom of core). The core was drilled through the exterior beam of a bridge. Both indicators show that the depth of carbonation was greater on the right side of the core. The left side of the core was the exterior face of the beam, which was exposed to the weather. The right side of the core is the interior surface of the beam, where the environmental conditions were more favorable for diffusion of carbon dioxide and resulted in greater penetration of the carbonation front.

### Carbonation Depth versus Time

The penetration of the carbonation front depends on many factors, such as the penetrability characteristics of the concrete, the in-place moisture content, and the CO<sub>2</sub> concentration in the environment. Penetration is slow in dry and wet concrete, and is greatest when the concrete has an internal relative humidity between 50 and 75 %. For a given concrete and constant exposure conditions, the depth of penetration of the carbonation front  $d_c$ , varies approximately with the square root of time.

$$d_c = k\sqrt{t}$$



The constant  $k$  depends on the factors mentioned above. The graph shows the depth of carbonation versus time for different values of  $k$ . If the depth of carbonation  $d_{c1}$  is measured at a time  $t_1$  and it is assumed that conditions in the future will be similar to those in the past, the depth of the carbonation front at a later time  $t_2$  can be approximated as follows:

$$d_{c2} = d_{c1} \sqrt{\frac{t_2}{t_1}}$$

### Ordering Numbers



**RI-7000 Deep Purple Indicator**  
Set of 4 spray bottles, 80 mL each



**RI-8000 Rainbow Indicator**  
Set of 4 spray bottles, 80 mL each

## Purpose

The use of traditional ultrasonic pulse velocity testers to identify the presence of anomalies in structures requires access to both faces of a member and it is not possible to determine the depth to anomalies. These drawbacks are eliminated by using the impact-echo method, which requires access to only one face. The impact-echo method is based on monitoring the periodic arrival of reflected stress waves and is able to obtain information of the depth of the internal flaws or the thickness of a solid member.

The **DOCTer** is a versatile, portable system, accompanied with the **Viking** software, based on the impact-echo method, that can be used for the following applications:

- Measure the thickness of pavements, asphalt overlays, plate-like concrete elements like slabs or walls, etc.
- Detect the presence and depth of voids and honeycombing
- Detect voids below slabs-on-ground
- Evaluate the quality of grout injection in post-tensioning cable ducts or joints for precast elements
- Integrity of a membrane below an asphalt overlay protecting structural concrete
- Delamination surveys of bridge decks, piers, cooling towers, chimneystacks, etc.
- Detect debonding of overlays and patches
- Detect ASR damage and freezing-and-thawing damage
- Measure the depth of surface-opening cracks
- Estimate early-age strength development (with proper correlation)

## Principle

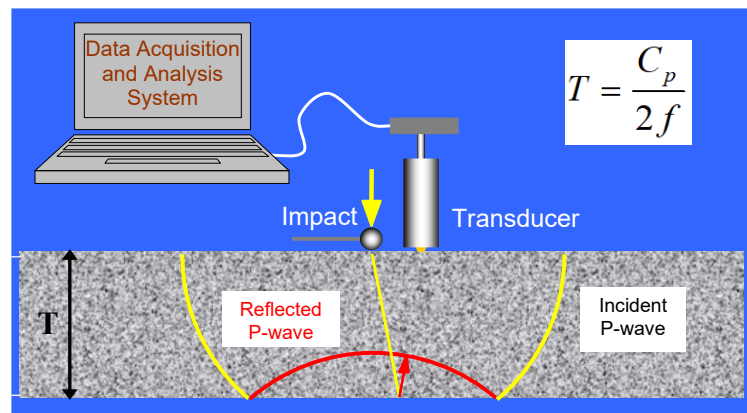
A short-duration stress pulse is introduced into the member by a small mechanical impact. This impact generates stress waves that propagate away from the impact point. A surface wave (R-wave) travels along the top surface, and a P-wave and an S-wave travel into the member. In impact-echo testing, the P-wave is used to obtain information about the member.

When the P-wave reaches the back side of the member, it is reflected and travels back to the surface where the impact

was generated. A sensitive displacement transducer next to the impact point picks up the disturbance due to the arrival of the P-wave. The P-wave is then reflected back into the member and the cycle begins again. Thus, the P-wave undergoes multiple reflections between the two surfaces and the recorded waveform of surface displacement has a periodic pattern that is related to the thickness of the member and the wave speed.

The displacement waveform is transformed into the frequency domain to produce an **amplitude spectrum**, which shows the predominant frequencies in the waveform. The frequency of P-wave arrival is determined as the frequency with a high peak in the amplitude spectrum. The thickness ( $T$ ) of the member is related to this thickness frequency ( $f$ ) and wave speed ( $C_p$ ) by the simple approximate equation shown on the image.

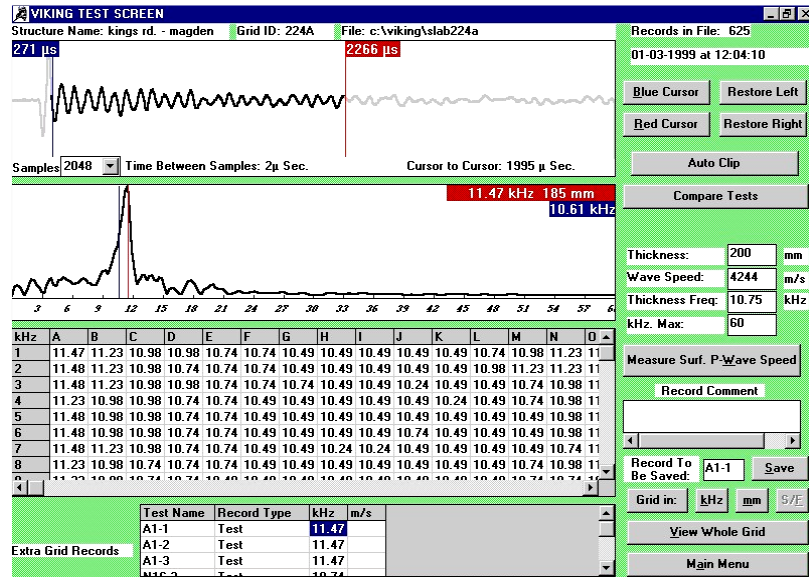
The same principle applies to reflection from an internal defect (delamination or void). Thus, the impact-echo method is able to determine the location of internal defects as well as measure the thickness of a solid member.



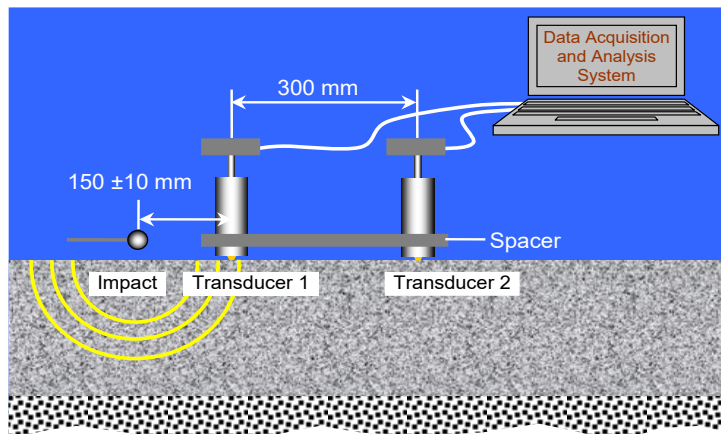
### Example

The upper plot in this example shows the surface displacement waveform (displacement vs time) obtained from a test of a solid concrete slab. The figure below is the amplitude spectrum (amplitude vs frequency) obtained by transforming the waveform into the frequency domain by applying the Fast Fourier Transform algorithm. The peak at 11.47 kHz (red cursor) is the thickness frequency. For a measured wave speed of 4240 m/s, this frequency corresponds to a thickness of:

$$4240 / (2 \times 11,470) = 0.185 \text{ m,} \\ \text{or } 185 \text{ mm.}$$

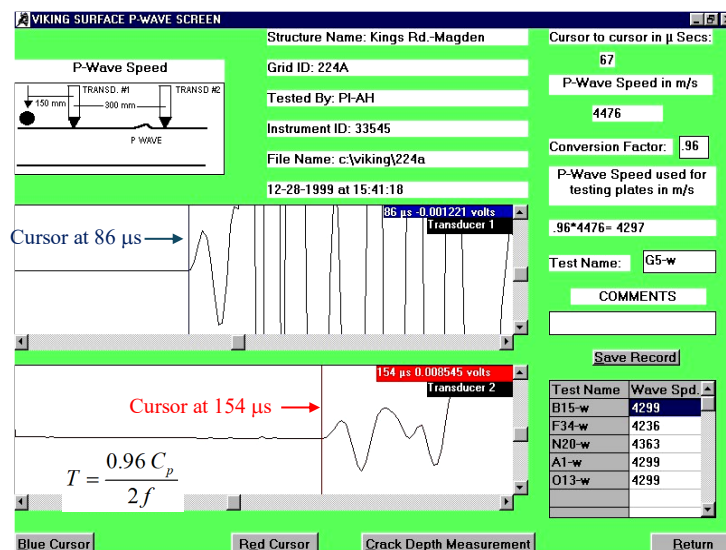


### Thickness Measurement by ASTM C1383



Accurate measurement of thickness requires knowledge of the in-place P-wave speed. ASTM C1383, "Test Method for Measuring the P-Wave Speed and the Thickness of Concrete Plates Using the Impact-Echo Method," permits two methods for obtaining the P-wave speed. One method is by determining the thickness frequency and then measuring the actual plate thickness at that point. The equation in this case is solved for  $C_p$ , i.e.,  $C_p = 2 f T$ .

Alternatively,  $C_p$  can be determined by measuring the time for the P-wave to travel between two transducers with a known separation. With the **LONGSHIP** assembly, the transducers are placed 300 mm apart and the impactor is about 150 mm from one of the transducers one the line passing through the transducers. The distance  $L$  (300 mm) between the transducers, is divided by time difference  $\Delta t$  between arrival of the P-wave at the second and first transducers. In the figure on the left,  $\Delta t$  was  $154 - 86 = 67 \mu\text{s}$ , and the P-wave speed is  $0.3 / 0.000067 = 4480 \text{ m/s}$ . If the wave speed is determined by the surface measurement method, the resulting value is multiplied by 0.96 when it used to calculate thickness <sup>[1]</sup>.





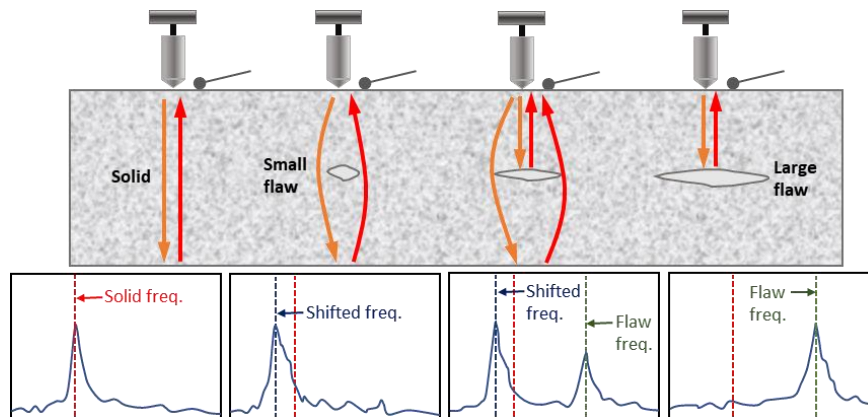
### Detection of Internal Defects

The P-wave generated by impact will reflect at interfaces within the concrete where there is a change in **acoustic impedance**, which is defined as the product of the density and wave speed of a material. The following table lists the reflection coefficients of a P-wave travelling through concrete and incident normal to an interface with air, water, soil, or steel. A negative reflection coefficient means that the stress changes sign when the stress wave is reflected; for example, a compressive stress would be reflected as a tensile stress. Steel is "acoustically harder" than concrete and the stress does not change sign when reflected at a concrete-steel interface.

Interface	Reflection Coefficient
Concrete-air	-1.0
Concrete-water	-0.65 to -0.75
Concrete-soil	-0.3 to -0.9
Concrete-steel	0.65 to 0.75

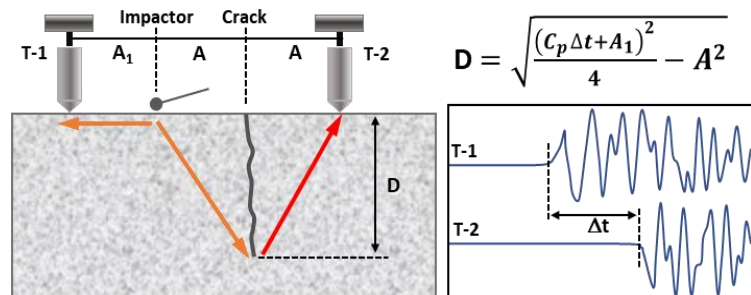
It is seen that at a concrete-air interface, there is complete reflection of the P-wave (1.0 = 100%). This makes the impact-echo method inherently powerful for detecting air interfaces, such as those due to cracks, delaminations, cavities, and honeycombed concrete. If the area of the reflecting interface is large, the impact-echo response will be similar to that of a solid plate except that the thickness frequency will be shifted to the higher value corresponding to the depth of the interface. If the defect is just large enough to be detectable, the amplitude spectrum will show two peaks: a high frequency

peak corresponds to reflection from the interface and the low frequency peak corresponds to the portion of the P-wave that travels around the defect and reflects from the opposite surface of the plate. The frequency associated with the portion of the P-wave that travels around the defect will be shifted to a lower frequency value than the solid plate thickness frequency. This is because the wave has to travel a longer distance as it diffracts around the flaw. The frequency shift is a good indicator of the presence of a flaw if it is known that the plate thickness is constant.



### Depth of Surface-Opening Cracks

The **DOCTer** can also be used to measure the depth of surface-opening cracks, using a time domain analysis. The **LONGSHIP** is used with the transducers on opposite sides of the crack and the impact is generated on the line passing through the transducers. When the P-wave reaches the tip of the crack, the crack tip acts as a P-wave source by **diffraction**. The diffracted P-wave is detected by the second transducer on the opposite side of the crack. By measuring the time interval between the arrival of the direct P-wave at the first transducer and the arrival of the diffracted wave at the second transducer, the depth of the



crack can be calculated. The example shown is from testing a fire-damaged structure, and a crack depth of 87 mm was estimated for a time difference ( $\Delta t$ ) of 35  $\mu$ s and a P-wave speed of 3155 m/s.



## Testing Examples



*Detection of delaminations and honeycomb in sewer pipe*



*Measurement of P-wave speed by surface method*



*Testing for quality of grout injection in cable ducts*

## DOCTer Specifications

- Data Acquisition System:
  - 2 channels, 4 MB/channel
  - 8 bits resolution, 50 MHz bandwidth
  - -5V to 5V Input Voltage Range
  - USB interface
- Dry contact, high sensitivity, piezoelectric handheld transducers
- Accuracy (assuming a constant P-wave speed):
  - Thickness measurement, direct calibration:  $\pm 2\%$
  - Thickness measurement by surface P-wave speed measurement:  $\pm 3\%$
  - Depth of surface-opening cracks:  $\pm 4\%$
- Operating conditions: Temperature: -10 to 50 °C, RH  $\leq 95\%$

## DOCTer Ordering Numbers

### DOC-700

Item	Order #
Laptop computer	DOC-10
Data acquisition module with USB cable	DOC-20
<b>Viking</b> software	DOC-30
Mark IV transducer	DOC-40
Star support with 5, 8 and 12 mm impactors	DOC-60
Impactors on spring rods, 5, 8, and 12 mm	DOC-70
Protection caps for transducer tips, 4 pcs	DOC-80
BNC cable	DOC-90
User Manual for Viking software	DOC-150
Operation manual	DOC-160
Binder with testing case studies	DOC-170
Attaché case	DOC-120

With **Viking** Software and one Mark IV transducer for flaw detection and thickness measurements. Can be later upgraded to DOCTer-4000.



### DOC-4000

Item	Order #
Laptop computer	DOC-10
Data acquisition module with USB cable	DOC-20
<b>Echolyst</b> software	DOC-30
Viking <b>LONGSHIP</b> with long handle and two Mark IV handheld transducers	DOC-50
Star support with 5, 8 and 12 mm impactors	DOC-60
Impactors on spring rods, 5, 8, and 12 mm	DOC-70
Short handle for crack depth measurement	DOC-80
Protection caps for transducer tips, 8 pcs	DOC-90
BNC cable, 2 pcs.	DOC-100
Manual for <b>Echolyst</b> software	DOC-150
Operation manual	DOC-160
Binder with testing case studies	DOC-170
Attaché case	DOC-130

With **Viking** Software and **LONGSHIP** assembly with two Mark IV transducers for flaw detection, thickness measurement, crack depth measurement, and P-wave speed measurement according to ASTM C1383.

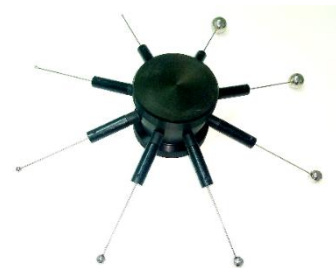


## Optional Items

### **Spider**, Order # DOC-210

It contains 8 spherical impactors, with diameters ranging from 2 mm to 15 mm and covering a frequency content from approximately 1.2 kHz to 100 kHz on a hard concrete surface.

**References:** [1] The explanation for the 0.96 factor can be found in: Gibson, A. and Popovics, J.A., 2005, "Lamb Wave Basis for Impact-Echo Method Analysis," *J. of Engineering Mechanics* (ASCE), Vol. 131, No. 4, pp. 438-443.





## Purpose

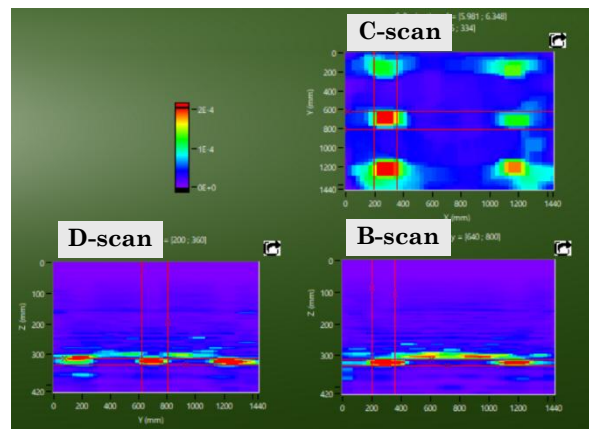
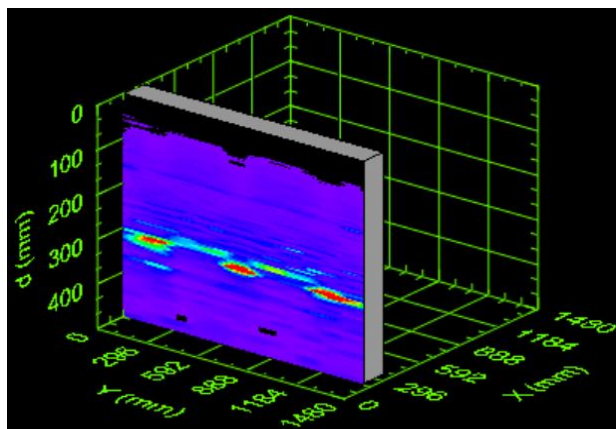
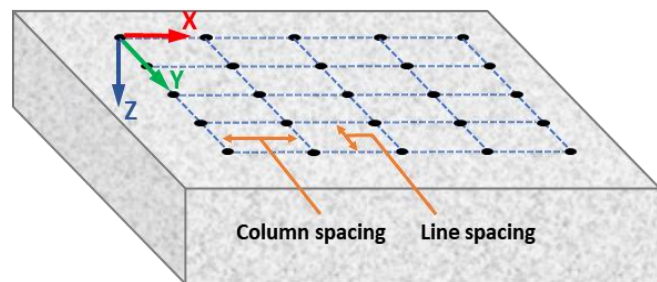
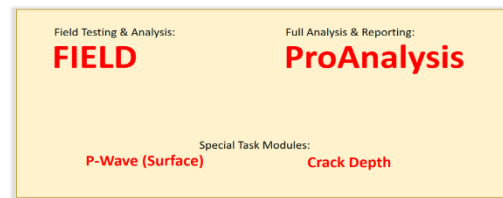
**Echolyst** is an advanced data acquisition and data analysis software for the impact-echo method. It is used along with the **Mirador** system (see datasheet) or other commercially available hardware for Impact-Echo. Besides the traditional use for interpretation of results of the impact-echo method, the **Echolyst** software incorporates innovative techniques to create 2-dimensional (2-D) and 3-dimensional (3-D) visual representations of measurements obtained from a grid test points. The key features of the software include:

- Simple interfaces for setting up data acquisition parameters and defining the testing grid
- Audio assisted prompts during testing to speed up data acquisition
- Visualization of impact-echo tests results by creating a 3-D volume model of the test region
- Ability to look at reflecting interface on different cutting planes
- Ability to superimpose test results on real world image of a test location
- Report generation

## Principle

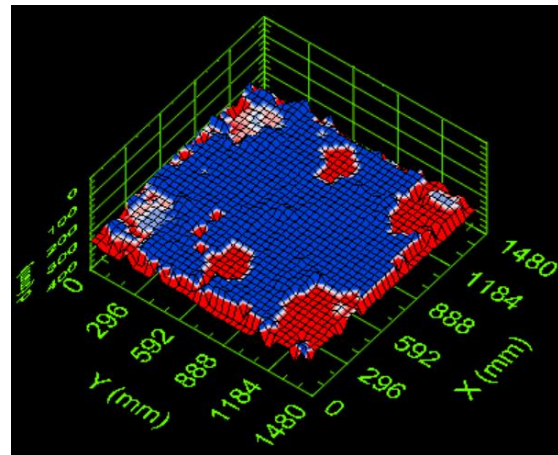
The principle of the impact-echo method is described in the **Mirador** system's datasheet. To take full advantage of **Echolyst**, the user can generate a grid of test points at the inspection site. A series of equally-spaced scan lines of equal length are marked on the test surface, and equally spaced test points are marked along each line. The distance between test points on a scan line defines the column spacing. The combination of "lines" and "columns" defines the 2-D grid that is the basis for subsequent displays. An X-Y-Z coordinate system is defined as shown, where the X-axis is parallel to the scan lines, and the Y-axis is parallel to the columns. The Z-axis is the depth axis into the test object.

The essence of **Echolyst** is the technique for using the amplitudes of the different frequency components obtained at the grid points to construct a volumetric model of the test region from which locations of reflecting interfaces can be presented as images. Each spectrum along a scan line is represented as a vertical strip, with a width equal to the test point spacing. The vertical axis of the strip corresponds to frequency and color coding is used to represent the relative amplitude of each



frequency. The strips are placed side-by-side, and the end result is a cross-section picture of the frequency peaks along a scan line. This image is called a **B-scan** (XZ-plane view) and all the B-scans obtained from all the scan lines are used to create a 3-D model of the test region, from which **D-scans** (YZ-plane view) and **C-scans** (XY-plane view) can also be generated. In addition to views on individual planes, there is the option to create **B-, C-, and D-projections** which are based on averaging the amplitude spectra from two or more adjacent planes.

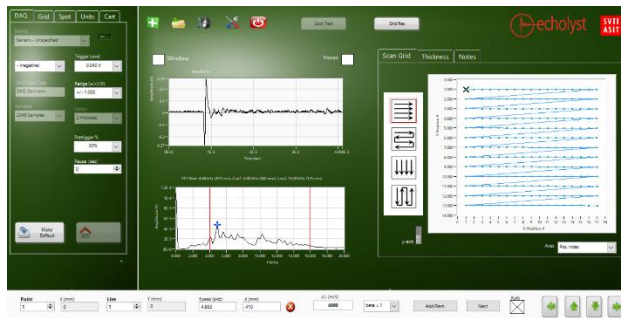
Since the measured frequency is related to an equivalent depth according to the basic equation of impact-echo, the measured depths can also be plotted along the scan grid to generate 2-D and 3-D representations (e.g. depth plot on the right) with depth values instead of frequency values representing the Z-axis.



## The Four Modules

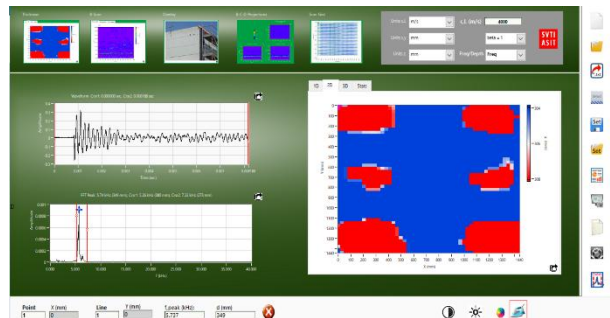
### FIELD Module

Acquisition and analysis of individual waveforms collected. It contains the tools for setting the acquisition parameters, calibration of wave speed and collecting data points.



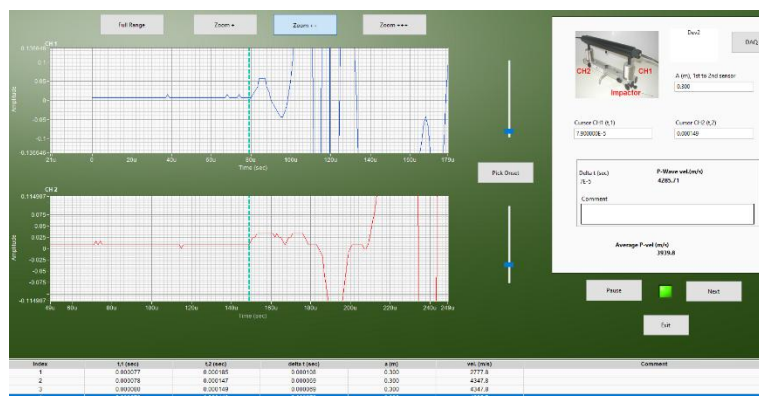
### ProAnalysis Module

Full analysis of grid data and reporting. It contains the tools for statistical analysis, creating 2D and 3D thickness plots, 2D and 3D tomographic images and projections on imported photos or drawings.



### P-Wave Module

For measuring wave velocity at the surface according to ASTM C1383.



### Crack Depth Module

For the standard method to measure the depth of surface opening cracks.

## Data Acquisition Parameters

A full menu of parameters to set up the data acquisition system is available: Number of samples, delta t between samples, trigger level, pre-trigger length, input signal voltage range, etc.

## Sound Settings

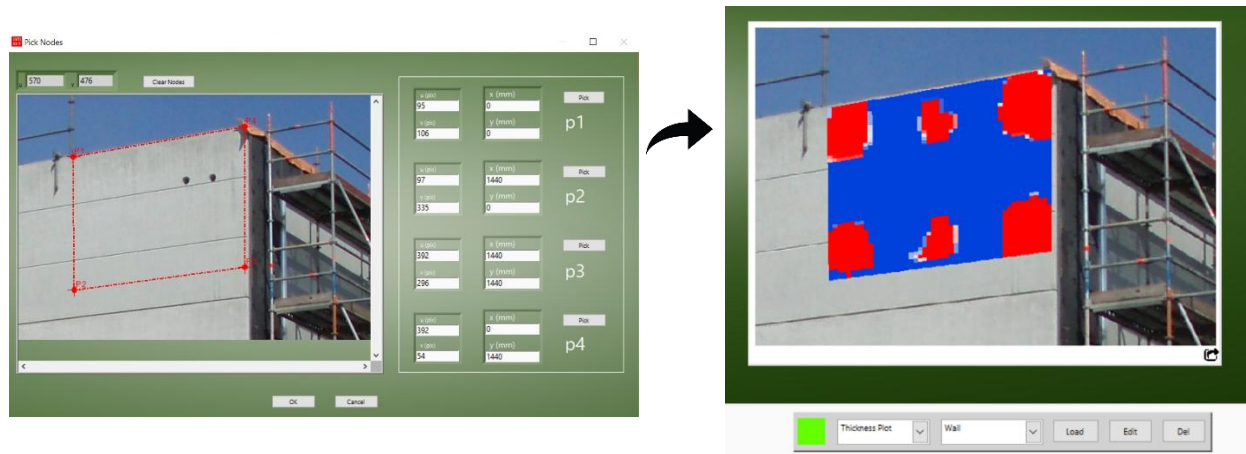
To speed up data acquisition, a voice output provides full control for the user, who can focus on the measurement without having to watch the screen. The voice output can be configured according to the specific needs and preferences of the user.

## Scans and Projections

**Echolyst** generates layer thickness profiles and displays them in various modes, in 1D, 2D and 3D. It also provides volumetric slicing capabilities for tomographic B-Scan, C-Scan and D-Scan imaging. The slicing is controlled intuitively, including options for color bar selection and customization, smoothing, contrast and threshold adjustment.

## Overlay of Results

One of the unique features of **Echolyst** software for interpretation and reporting is the ability to superimpose an image created during data analysis onto a photograph of the test site. This provides an effective way to present test results to the client. Any volumetric slice or projection generated with an unlimited number of imported pictures (photos, drawings, CAD models, etc.) of the inspection object can be used.



## Report

During analysis, images and results can be exported, commented and compiled so the user can create a comprehensive analysis report. **Echolyst** is the only impact-echo software making the reporting flexible, easy and efficient.



*Echolyst with Mirador-3000 being used*



*Echolyst with Mirador-5000 being used*



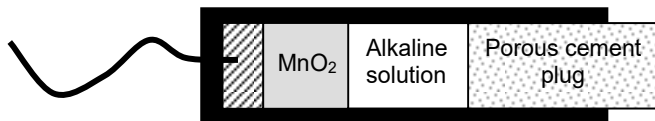
## Purpose

The **ERE-Probe** is a half-cell reference electrode to be embedded in concrete that can be used to:

- Monitor the reinforcement potentials in critical areas for corrosion such as construction joints, splash zones in marine structures, bridge decks, bottoms of bridge columns exposed to ingress of chlorides, etc.
- Monitor the efficiency of cathodic protection
- Monitor the ingress of the depassivation front, due to chloride penetration or carbonation, in combination with installing the **CorroWatch** (see technical data sheet)

## Principle

The **ERE-Probe** (Embeddable Reference Electrode) is a stable, long life reference electrode for monitoring the half-cell potential of reinforcement in concrete structures. It is based on a manganese dioxide electrode in a steel housing with a chloride-free, alkaline gel and having a porous fiber reinforced cement plug at one end. The housing is made from a corrosion resistant material. Diffusion of ions through the porous cement plug is low because the pH of the alkaline gel corresponds to that of pore water in normal concrete.



In new structures, the **ERE-Probe** is attached to the reinforcement by plastic straps before placement of the concrete. In existing structures, a hole is drilled to the required depth and the **ERE-Probe** is embedded using an appropriate cementitious mortar. The probe can be used for concrete exposed to chlorides or carbonation and will not induce corrosion or change the natural potential of the steel. A high impedance voltmeter is connected to the cable and used to measure the half-cell potential between the probe and the reinforcement.

## ERE-Probe Specifications

- Diameter  $\approx 18$  mm
- Length  $\approx 85$  mm (without protective cap)
- Typical potential =  $+205 \pm 20$  mV measured in a saturated  $\text{Ca(OH)}_2$  solution at  $23^\circ\text{C}$  vs Ag/AgCl electrode\*
- Internal resistance  $< 5,000$  Ohm measured in a saturated  $\text{Ca(OH)}_2$  solution at  $23^\circ\text{C}$
- Variation:  $\pm 5$  mV compared with the initial value at the same temperature and electrolyte environment
- Operating temperature:  $0$  to  $+40^\circ\text{C}$   
(false readings are expected during frost but they are recovered after thawing)
- Service life  $> 30$  years



\***ERE-Probes** come with a calibration certificate stating their actual potential value

## Ordering Numbers:

Item	Order #
<b>ERE-Probe</b> with 3 meter cable	ERE-Probe-3
<b>ERE-Probe</b> with 5 meter cable	ERE-Probe-5
<b>ERE-Probe</b> with 10 meter cable	ERE-Probe-10

## EyeCon

### Purpose

The **EyeCon (A1220 Monolith 3D)** is a portable hand-held instrument, one channel, pulse-echo tester, for flaw detection and thickness measurements. The device is based on the ultrasonic pitch-catch method and uses an antenna composed of an array of dry point contact (DPC) transducers, which emit shear waves into the concrete. The 4 by 6 transducer array is under computer control and the recorded data are analyzed to create 2-D images of the reflecting interfaces within the cross sections below the antenna. Test results can be displayed as individual A-Scans (reflection amplitude versus time or depth) or as B-scans or D-scans showing cross sections of the test object along scan lines.

The series of 2-D images obtained from the test object can also be transferred to a computer with **IntroView** imaging software. The software assembles the 2-D slices into a 3-D image of the test object. The 3-D reconstruction can then be manipulated for interpretation of test results.

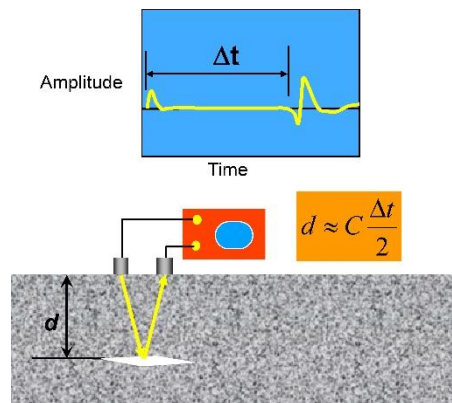
With additional transducers, the **EyeCon** can also be used for traditional ultrasonic pulse velocity measurements.

**EyeCon** can be used for the following applications:

- Thickness measurement
- Detection of voids and honeycombing in concrete members
- Detection of voids in grouted tendon ducts
- Detection of poor quality bond in overlays and repairs
- Detection of delaminations

### Principle

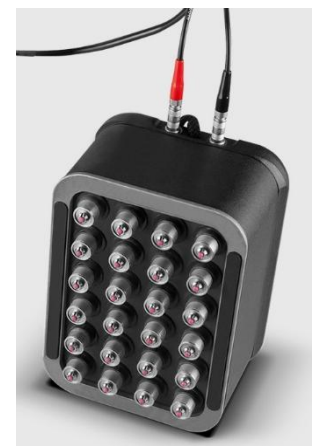
**EyeCon** is based on the ultrasonic pulse-echo method using transmitting and receiving transducers in a "pitch-catch" configuration as shown on the right. In the pitch-catch method, one transducer sends out a stress-wave pulse and a second transducer receives the reflected pulse. The time from the start of the pulse until the arrival of the echo is measured. If the wave speed  $C$  is known, the depth of the reflecting interface can be calculated as shown. The equation assumes that the two transducers are close to each other.



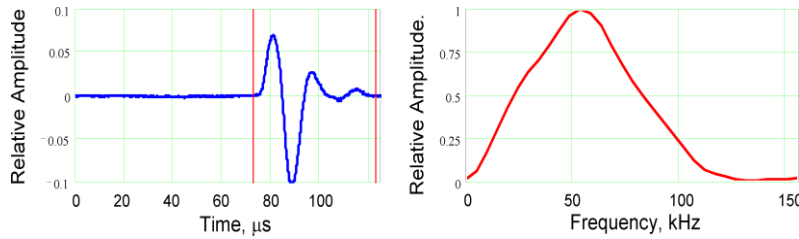
Key features:

- Use of dry point transducers (DPC) to introduce into the concrete pulses of **shear waves** with an adjustable frequency of 25 to 250 kHz. Each transducer is spring loaded to conform to irregular surfaces and they do not require a coupling medium, that is, testing is done in the dry.
- The handheld, light-weight electronic unit with display facilitates the job in areas with difficult access.
- Transit times are analyzed using the synthetic aperture focusing technique (SAFT) to reconstruct, in real time, 2-D color images of the cross section below the antenna which can be displayed as B-Scans or D-Scans along each scan line.
- The data captured can be transferred to a computer and the 3-D visualization software allows views of different slices of the reconstructed internal structure.

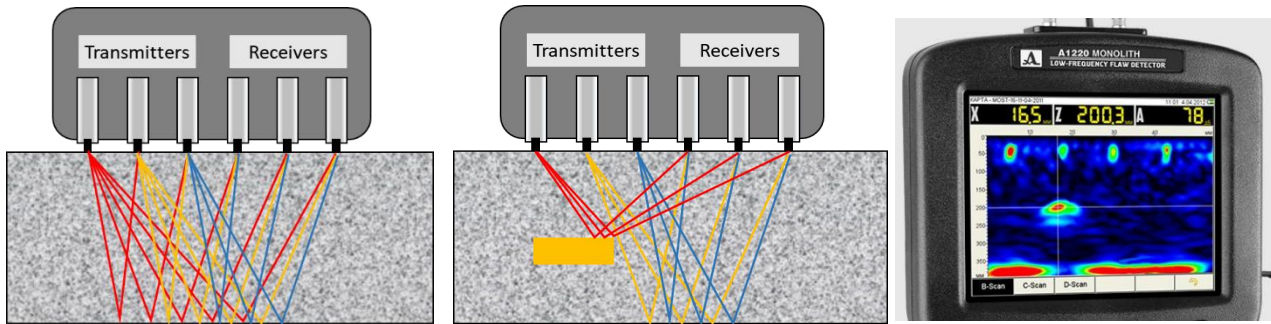
The antenna is composed of 24 transducers arranged in a 4 by 6 array of point transducers. The transducers are heavily damped so that a short



duration pulse is created. The plot in blue shows the typical shape of the received pulse after it has reflected from an air interface. The plot in red to the right shows the amplitude spectrum of the pulse (the nominal center frequency is about 50 kHz but can be varied from 25 to 250 kHz, allowing the user to control both penetration depth and image resolution).



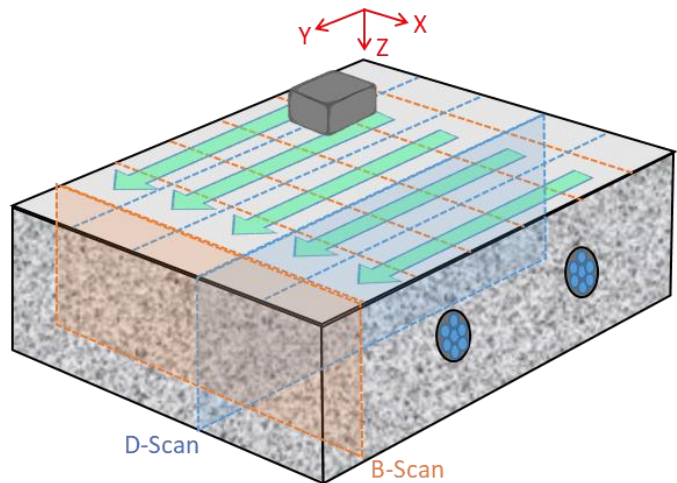
Basically, the first three rows of transducers act as a single transmitter and the other three rows act as a single receiver. In this way, the signal noise ratio is improved because random reflections from aggregate particles will tend to cancel out, while reflections from large concrete-air interfaces will be superimposed. The averaged signal recorded is stored in the hand-held unit as a time-domain waveform (A-Scan). Multiple stored A-Scans taken on a testing line can be used to create cross-sectional views: B-scans or D-scans. These reconstructed images show the locations of the reflecting interfaces, which could be the opposite side of the member (back wall reflection), reinforcing bars, and most importantly, internal concrete-air interfaces (such as voids, cracks, delaminations, etc.).



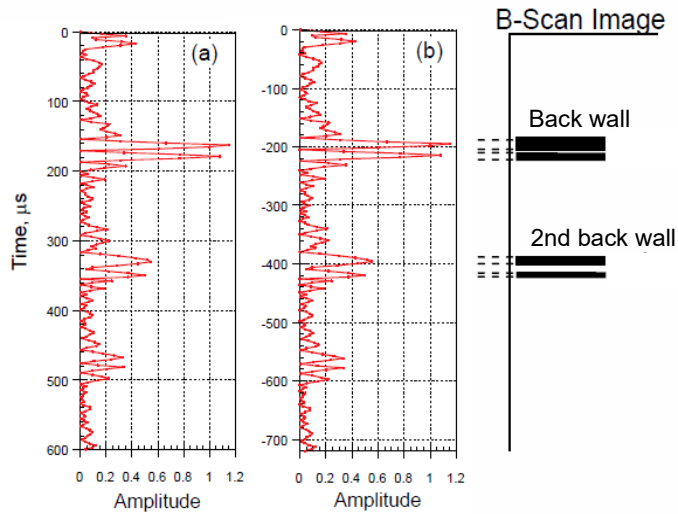
As illustrated in the right figure above, because of the shorter ray paths, reflections from a defect will arrive at the receivers sooner than reflections from the back wall. The instrument uses the arrival times of the reflected pulses to determine the location of the defect within the member. Note in the figure that some transducers do not receive the reflection from the back wall because the flaw intercepts the rays. This behavior accounts for the so-called "shadow" zones in 2-D images.

## Method of operation

Setup parameters for recording and displaying signals are entered using a menu system. To carry out a complete inspection of a specific area of a concrete member, the user first lays out a 2-dimensional grid on the testing surface. The step spacing depends on the size of defects to be detected, with a smaller spacing for smaller defects. The long axis of the antenna is preferably oriented perpendicular to the longitudinal direction of long objects like tendon ducts. The data are recorded at each step along each scan line. The grid layout (step distance, number of steps per line, and the number of lines) is entered into the hand-held unit and that information is used in referencing the displayed test results to the testing position on the test object.



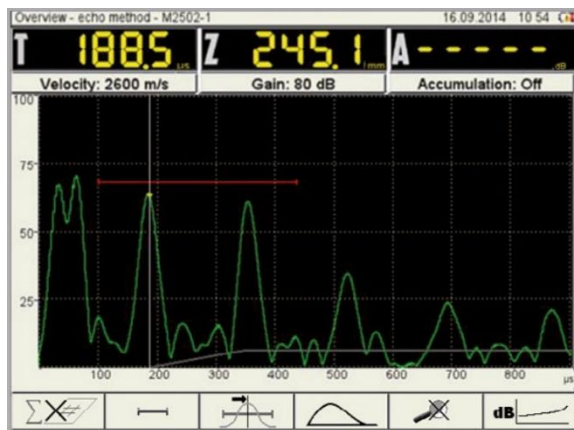




After the scanning is completed, the signal at each test point is plotted as an **A-scan** with time in the vertical direction as exemplified in the left hand figure (a). If the shear-wave speed in the concrete is known, the time axis can be converted to distance from the surface by multiplying by one-half of the wave speed (because the travel time is for a round trip equal to twice the depth). If the shear wave speed is assumed to be 2400 m/s, the distance axis is as shown in figure (b). To construct a cross-sectional view, a threshold level of signal amplitude is chosen and a colored dash (in this representation black) is drawn at the depth where the signal exceeds the threshold amplitude. In this example, a low threshold is used and the second echo from the back wall

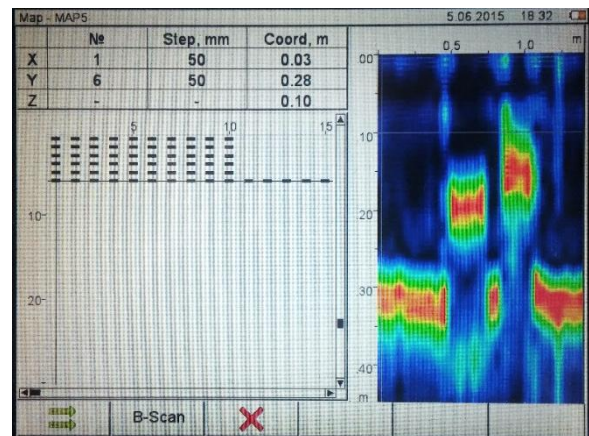
is plotted. If a higher threshold were used, only the first back wall echo would be shown. This process is repeated for each test point along the scan line, and the end result is a 2-dimensional representation of the locations of reflecting interfaces along that scan line. Each scan line in the X-axis has therefore an associated **B-Scan** plane and each scan line in the Y-axis has an associated **D-Scan** plane that can be displayed.

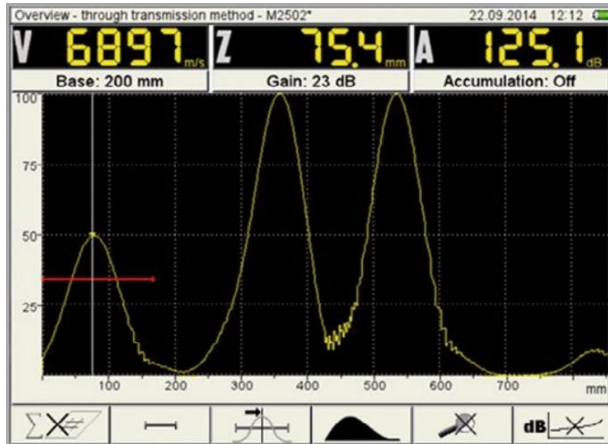
The three operation modes available in **EyeCon** are:



**A-SCAN Echo Method:** The recorded signal at a single antenna position is processed. The signal can be from one set of pulses or an average of several sets of pulses. Different display formats are available. In this case, the signal has been rectified and is not filled in. The horizontal axis is in units of time (microseconds), but it could also be displayed in units of distance if the wave speed is entered. Various measurements can be made such time to first peak or peak-to-peak interval. A portion of the signal can be zoomed in for a more detailed view.

**MAP:** This mode is used to review results acquired if a 2-dimensional testing grid is used. The upper left box shows the grid layout. The horizontal cursor is used to select the scan line for which the B-Scan cross section is to be shown on the right side. The vertical cursor is used to select the scan line for which the D-Scan cross section is to be shown. The lower box is used to select the scan (B or D) that is going to be displayed. In this case the locations of reflecting interfaces are assigned a color to indicate intensity of reflection from those elements (constructive superposition). The end result is 2-D color images of the B or D cross sections.





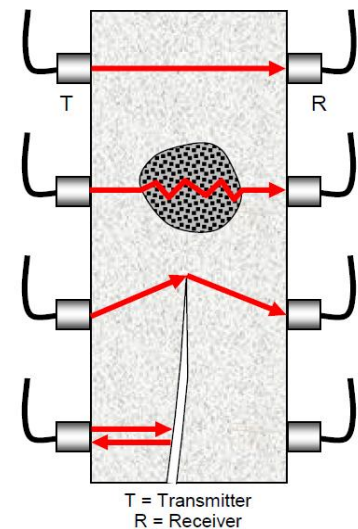
**A-SCAN Propagation method:** The **EyeCon** can be also used to measure the speed of ultrasonic stress waves between two points by the well-known ultrasonic pulse through transmission method. Dedicated pairs of transducers are available as optional accessories for performing this test method which is governed by various standards like ASTM C597, BS 1881:203 and EN 12504-4.

The interface of this mode is very similar to the echo method and most of the display options and functions are also available.

Provided there is access to both sides of the element, this method can be used for applications like:

- Evaluating the uniformity of concrete within a structural member
- Inferring the presence internal voids and cracks
- Estimating the depth of surface-opening cracks
- Estimating severity of deterioration
- Estimating depth of fire damaged concrete
- Evaluating effectiveness of crack repairs
- Identifying anomalous regions for invasive sampling with drilled cores
- Estimating early-age strength (with project specific correlation)

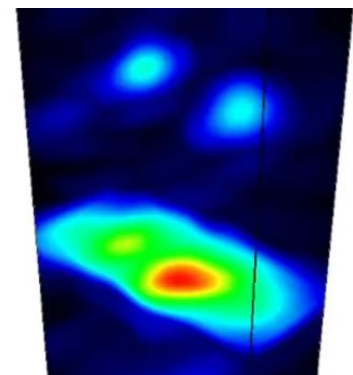
The figure illustrates different conditions that may be encountered when testing an element using the UPV method. At the top, the path between the transducers is through solid concrete, and the travel time would be the shortest. Below that is the case where there is an internal pocket of porous concrete, such as honeycombed concrete. The pulse is scattered as it travels through the contiguous portions of the honeycombed concrete. As a result, the actual travel path and time are longer and this results in a reduced pulse velocity. In the next case, the transducers are located so that the direct travel path is near the edge of a crack. The pulse cannot travel across a concrete-air interface but it is able to travel from the transmitter to the receiver by diffraction at the crack edge. Because the travel path is longer than the distance between the transducers, the apparent pulse velocity is lower than through sound concrete. In the lowermost case, the pulse is reflected completely by the crack, and travel time is not measurable.



### 3-D Image Reconstruction

At the completion of testing, the data can be transferred to a laptop computer that contains the **IntroView** 3-D visualization software. The software "stitches" together all the 2-D images to create a 3-D model of the test object. The resolution of the reconstruction depends on how close the test points of the grid are. As an example, the figure on the right is the 3-D model from a scan of a portion of a concrete block with two defects. The bottom of the block is indicated.

The user can manipulate the 3-D model by rotating it or looking at different orthogonal planes cutting through the model. A C-scan shows the reflecting interfaces on a plane parallel to the test surface and at different depths (Z-axis); that is, it provides a "plan view" of the reflectors. A B-scan provides an "end view" of the reflectors. The D-scan provides a side view of the reflectors. The user can look at

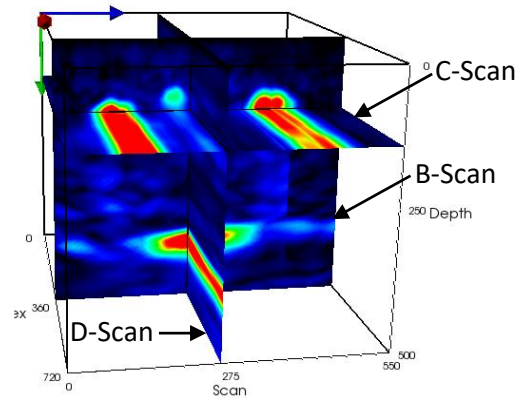


## EyeCon

specific "slices" through 3-D model by defining the Z-coordinate for a C-scan image, the Y-coordinate for a B-scan image, and the X-coordinate for a D-scan image. For example the right figure below shows three slicing planes through a 3-D model.

### EyeCon (A1220 Monolith 3D) Specifications

- Dry point contact shear-wave transducers with wear-resistant ceramic tip
- Spring loaded 4 x 6 transducers antenna array
- 25 to 250 kHz working frequency range
- Nominal frequency converter = 50 kHz
- Ultrasound speed range: 1,000 to 10,000 m/s
- Dimensions of the electronic unit: 260 × 153 × 43 mm
- Weight of the electronic unit: 0.8 kg
- Dimensions of the antenna array: 139 × 105 × 89 mm
- Weight of the antenna array: 1.1 kg
- Testing depth: 10 to 600 mm (depending on the concrete quality, member dimensions and amount of reinforcement)
- TFT (640 x 480) color screen
- 11.2 V rechargeable battery, 8 h operating life
- USB 2.0 interface
- Maximum number of A-scans in memory = 200
- Protection class IP54
- 3-D tomographic display with **IntroView** software
- Operating conditions: -20 °C to 45 °C, < 95% RH
- Error of the depth of a defect, mm, where H is the measured depth:  $\pm (0.1 \cdot H + 5)$
- Minimum flaw diameter to be detected: 30 mm
- Maximum area in MAP mode = 2 m<sup>2</sup>



### EyeCon-1000 Kit Ordering Numbers

Item	Order #
EyeCon (A1220 Monolith 3D) electronic unit	EYE-1001
Antenna array for flaw detection with 24 low-frequency DPC transducers, shear wave.	EYE-1010
IntroView software license	MIR-1003
AC Charger	EYE-1004
USB Cable	EYE-1005
Double LEMO 00 – LEMO 00 cable 1,2 m	EYE-1006
Soft cover	EYE-1007
Carrying case	EYE-1008
Laptop with NVIDIA GeForce graphics card (optional)	MIR-1002





**Optional antenna arrays and transducers**

Item	Order #
<b>For the echo method</b>	
Antenna array for flaw detection with 24 low-frequency DPC transducers, longitudinal wave.	EYE-1020
<b>For the through transmission UPV method<sup>(1)</sup></b>	
Antenna array with 12 DPC transducers, deep penetration, shear wave, 50 kHz.	EYE-1030
Antenna array with 12 DPC transducers, deep penetration, longitudinal wave, 100 kHz.	EYE-1031
DPC <sup>(2)</sup> transducer, shear wave, 50 kHz	EYE-1040
DPC <sup>(2)</sup> transducer, longitudinal wave, 100 kHz	EYE-1041
DPC <sup>(2)</sup> transducer, shear wave, 250 kHz	EYE-1042
<sup>(3)</sup> Liquid contact transducer, longitudinal wave, 25 kHz	EYE-1050
<sup>(3)</sup> Liquid contact transducer, longitudinal wave, 50 kHz	EYE-1051
<sup>(3)</sup> Liquid contact transducer, longitudinal wave, 100 kHz	EYE-1052

<sup>(1)</sup>For the through transmission method 2 antennas or transducers are needed.

<sup>(2)</sup>DPC = Dry Point Contact transducers.

<sup>(3)</sup>Liquid contact transducers require a coupling medium.



*EYE-1030  
or  
EYE-1031*



*EYE-1040, EYE-1041  
or EYE 1042*



*EYE-1050, EYE-1051  
or EYE 1052*

# GalvaPulse

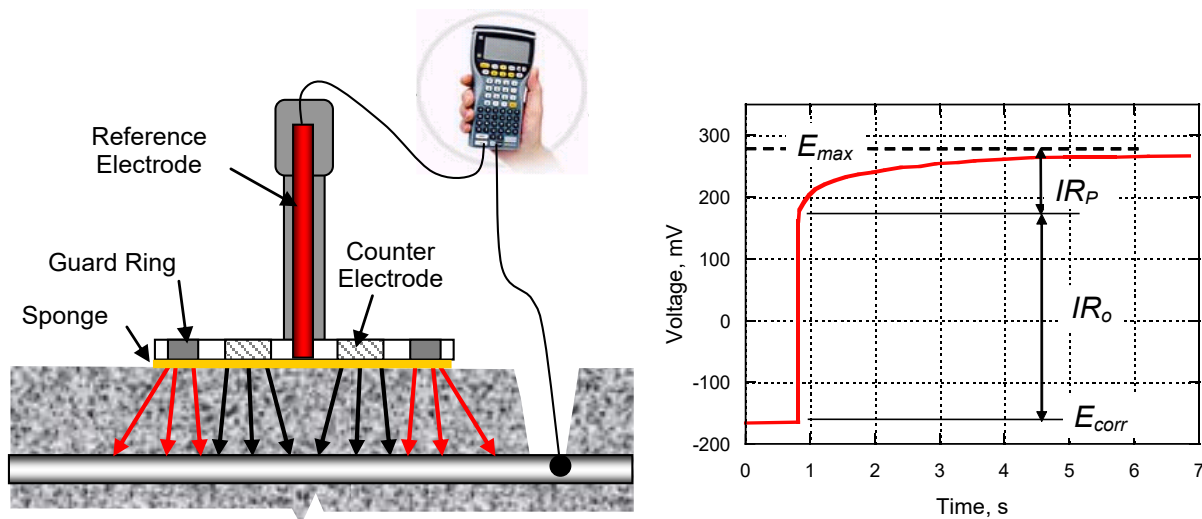
## Purpose

The **GalvaPulse** is used to measure half-cell potentials, electrical resistance and particularly the corrosion rate of reinforcement in concrete for the following typical applications:

- Monitoring corrosion activity in reinforced concrete structures
- Service life estimation
- Evaluating the efficiency of corrosion arresting measures such as application of inhibitors, membranes, electrochemical removal of chlorides, concrete realkalinization, etc.
- Condition surveys of suspect reinforced structures, especially structures in wet environments where the classic half-cell potential mapping may provide misleading or insufficient information
- Measuring corrosion activity in repaired areas

## Principle

The **GalvaPulse** evaluates the corrosion rate of reinforcement by measuring polarization resistance using the **galvanostatic pulse** technique, as described below.



A current pulse  $I$  is imposed on the reinforcement from a counter electrode placed on the concrete surface. A guard ring confines the current to an area  $A$  of the reinforcement below the central counter electrode.

The applied current is usually in the range of 5 to 400  $\mu A$  and the typical pulse duration is 5 to 10 seconds. The reinforcement is polarized in the anodic direction compared to its free corrosion potential,  $E_{corr}$ . The resulting change of the electrochemical potential of the reinforcement is recorded as a function of time using a silver chloride reference electrode (Ag/AgCl). A typical potential response for reinforcement actively corroding is shown in the right figure above.

When the current is applied, there is an ohmic potential drop  $IR_o$  as well as change in potential due to polarization of the reinforcement,  $IR_p$ . Assuming the Randles circuit model, the polarization resistance of the reinforcement  $R_p$  is calculated by curve fitting to the transient portion of the potential data. By means of the Stern-Geary equation for active corrosion ( $I_{corr} = (26 A)/R_p$ ) and Faraday's law of electrochemical equivalence, the corrosion rate is estimated as:

$$\text{Corrosion Rate } (\mu\text{m/year}) = 11.6 \ I_{corr} / A$$

where  $A$  is the confined area (in  $\text{cm}^2$ ) of the reinforcement below the central counter electrode. The factor 11.6 is for black steel.

The value of  $R_o$ , the electrical resistance of the concrete between the counter electrode and the reinforcement, is also determined.

### Variation and Accuracy

The accuracy of the corrosion rate estimation can only be evaluated by comparison with actual mass loss measurement of the reinforcement subjected to long term corrosion conditions. One such laboratory investigation produced the following comparison between corrosion rates calculated from measured mass loss measurements of actual steel bars and from the **GalvaPulse**.

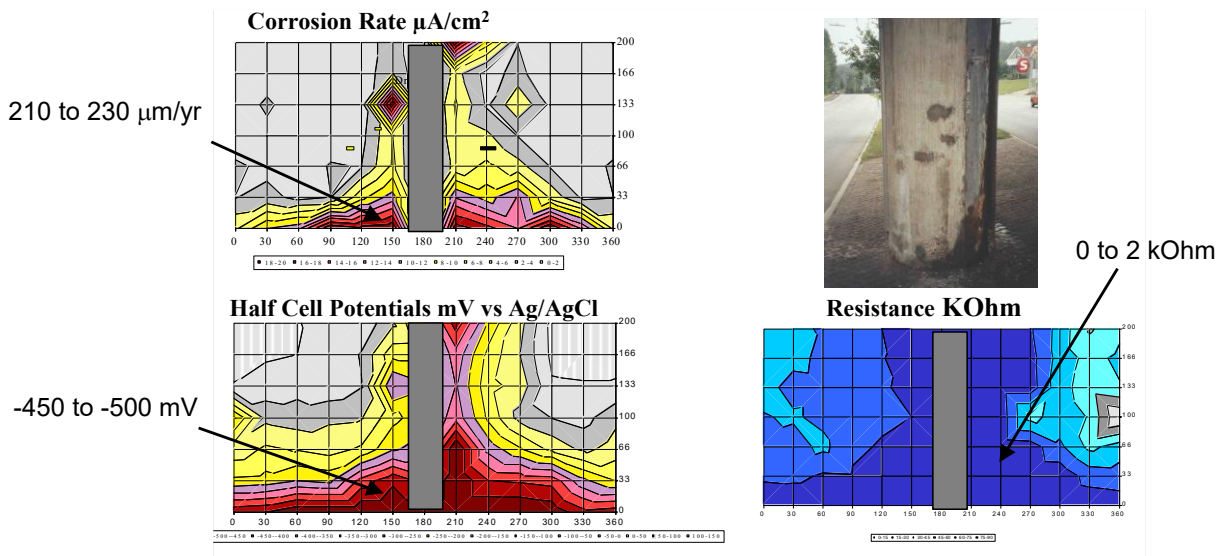
Reinforcement	Corrosion Rate ( $\mu\text{m}/\text{year}$ )	
	Mass Loss	GalvaPulse
A	53	36
B	56	29
A+B connected	55	61

Reference: Baessler, R. and Burkert, A., "Laboratory Testing of Portable Equipment," Brite/Euram Project Integrated Monitoring System for Durability Assessment of Concrete Structures, BAM (Federal Institute for Materials and Testing), Berlin, Germany, 2001

The findings support the general conclusion that the **GalvaPulse** is accurate well within a factor of two for estimating the corrosion rate in anodic areas. In addition, other uncertainties should be taken into account when evaluating on-site test results, e.g., the actual area of the reinforcement being polarized and the variation over time in corrosion rates due variation in temperature and moisture conditions.

In passive regions (corrosion rates  $< 1 \mu\text{m}/\text{year}$ ), the **GalvaPulse** may overestimate the corrosion rate by a factor of 3 to 4. Such areas are, however, not interesting in terms of corrosion risk.

In a long term field study, 30-year old bridge columns subjected to deicing salts were examined regularly over a 20-year period since corrosion began. The chloride levels and moisture content in the concrete of the bridge were high. When the last measurements were performed, the temperature was  $15^\circ\text{C}$  and the following test results were obtained.



The fairly constant corrosion rate measured over the 20-yr period corresponds to a cross section loss of the reinforcement of 20 years times  $0.22 \text{ mm}/\text{y} = 4.4 \text{ mm}$ . Removal of concrete at several locations at the bottom of the columns revealed also approximately 4 mm cross section loss of the reinforcement.



# GalvaPulse

## Testing Examples



Evaluation of corrosion rate in balcony slab of seaside condominium with the **GalvaPulse**



Highway bridge column being tested for corrosion rate with the **GalvaPulse**



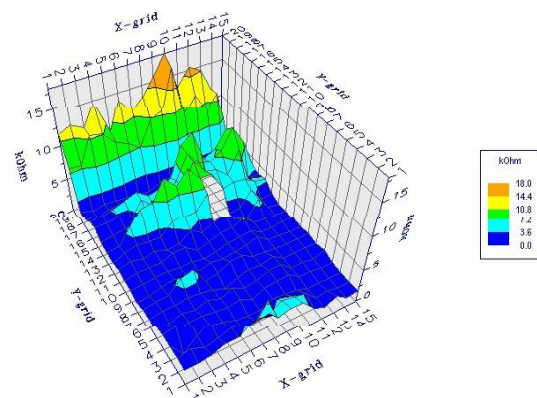
Corrosion activity being evaluated on a bridge wall with the **GalvaPulse**



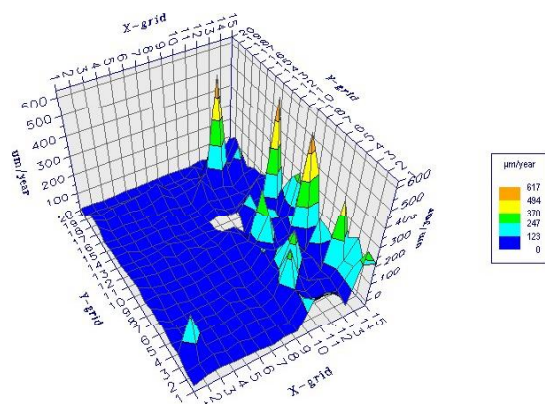
**GalvaPulse** (older model) testing in progress for corrosion activity of a heavily corroded column

## Examples of the Graphic Displays to View **GalvaPulse** Data

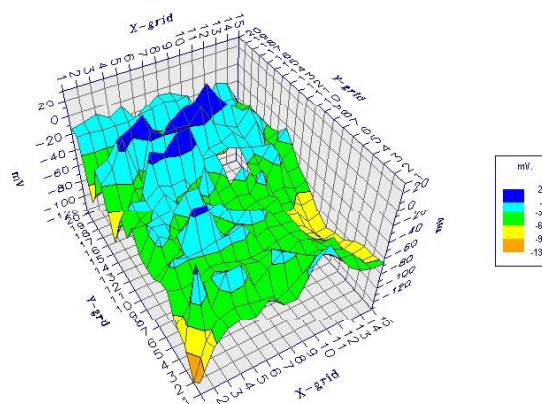
Following testing, the handheld computer is connected to a PC with the installed viewing and reporting software. The records are transferred to the PC and data can be viewed using 2D or 3D graphic displays. Here we see 3-D displays of the corrosion rates, the half-cell potential, and the electrical resistance. Such plots permit the display of a large amount of data in a concise manner for preparing test reports.



**3-D Plot of resistance**



**3-D Plot of corrosion rate**



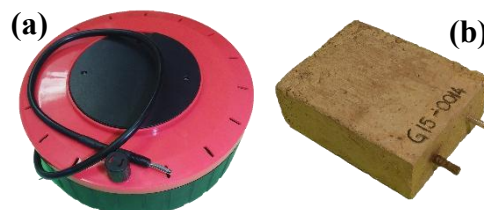
**3-D Plot of half-cell potential**

## GalvaPulse Features and Specifications

- Reliable evaluation of reinforcement corrosion in anaerobic concrete environment
- Lightweight, handheld equipment, easy to operate
- Kit includes a calibration box and a check concrete block with embedded bars
- Easy-to-use software for reporting test results in 2D or 3D graphics
- Two operation modes:
  - (1) only for half-cell potentials and electrical resistance (1 to 2 s/test)
  - (2) for corrosion rate, half-cell potentials and electrical resistance (5 to 10 s/test).
- The first mode is normally used to identify the anodic and cathodic areas, while the second mode is used in anodic areas, where corrosion rate is a decisive parameter to be measured
- Suitable for testing on rough or curved surfaces
- Uses Ag/AgCl (silver / silver chloride) reference electrode
- Storage capacity: 20,000 records
- Current pulse generated: 5 to 400  $\mu$ A from 1 to 20 seconds
- Pulse guard ring diameter: 70 mm

## GalvaPulse-5000 Kit Ordering Numbers

Item	Order #
Handheld computer with pulse generator	GP-5010
Calibration unit for pulse generator	GP-5020
Measuring cell with 3 meter cable	GP-5031
Sponge for measuring cell	GP-5040
Reinforcement locator	GP-5050
Reinforcement conductivity meter	GP-5060
Cable for data transfer to PC	GP-5070
Measuring cable	GP-5080
Two adjustable reinforcement clamps	GP-5090
Two reinforcement adaptors	GP-5100
12 mm and 18 mm drill bits	GP-5110
10 mm Allen key	GP-5120
Sponge for grinding of electrode rings	GP-5130
Hammer and chisel	GP-5140
Measuring tape and chalk	GP-5150
<b>GalvaPulse</b> software for data viewing/reporting	GP-5160
User Manual	GP-5170
Attaché case	GP-5180
Cable drum with 15 meters of cable <b>(a)</b>	GP-5190
Check block with embedded a corroding black steel bar and a stainless steel bar <b>(b)</b>	GP-5200





## Purpose

The **GWT** (Germann Water permeation Test) is used for on-site evaluation of

- Water permeation of the skin-concrete in finished structure
- Water permeation of masonry panels
- Water tightness of construction joints and sealed control joints
- Effectiveness of waterproofing admixtures, additives, membranes, coatings or other surface applied compounds
- Approximate estimation of the coefficient of water permeability of concrete or other material alike by the penetration method

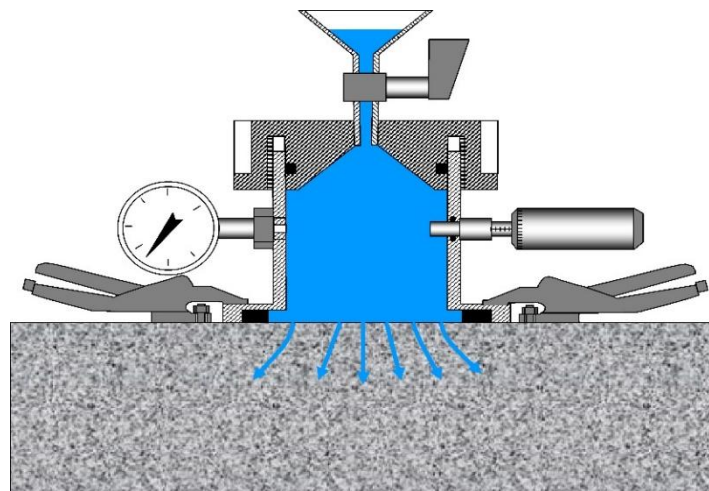
## Principle

The **GWT** measures the permeation of water into the test surface under an applied pressure.

A pressure chamber containing a watertight gasket is secured tightly to the surface by two anchored clamping pliers or by means of a suction plate. Alternatively, the gasket may be bonded to the surface with a proper sealant.

The chamber is filled with water and the water is allowed to be absorbed by the test surface for a certain time (from 10 minutes to several hours depending on the purpose of the test). The filling valve is closed, and the top cap of the chamber is turned until a desired water pressure is displayed on the gauge. As water permeates into the concrete, the selected pressure is maintained by means of a micrometer gauge pushing a piston into the chamber. The piston movement compensates for the volume of water penetrating into the material.

The travel of the piston as a function time is recorded and the speed the piston travel in  $\mu\text{m/s}$  is used to characterize the permeation of the test surface.



## Application Examples

### 1. Permeation of Concrete Surface



On the left, the cap of the **GWT** is being tightened to bring the water pressure to 1 bar (100 kPa). On the right the **GWT** is being used on a vertical concrete surface. An elbow is used to permit initial filling of the chamber. The micrometer is turned to advance the piston and maintain the water pressure



constant at 1 bar (100 kPa). The micrometer position is recorded as a function of time as a qualitative parameter to characterize the velocity of water penetration.

$$\Delta_g = g_n - g_{n+1} \quad (1)$$

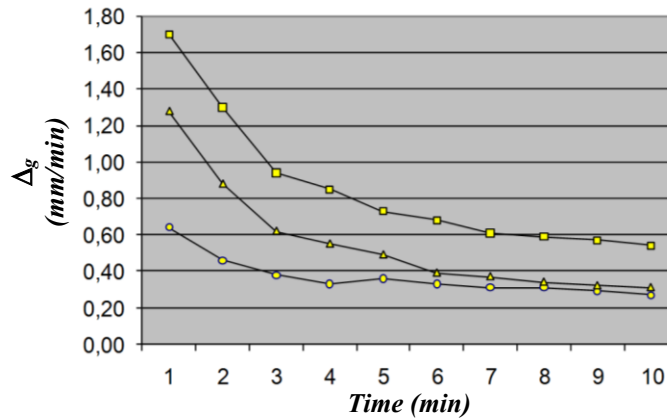
where

$\Delta_g$  = speed of the micrometer piston travel (mm/min)

$g_n$  = the micrometer gauge reading after n minutes of testing (mm)

$g_{n+1}$  = the micrometer gauge reading after n+1 minutes of testing (mm)

When  $\Delta_g$  is plotted over the testing time, the curves are a good guide to compare the performance of different surfaces. The figure below shows curves for 3 different concretes during 10 minutes of test, which is usually a good duration for a quick test.



## 2. Laboratory Evaluations

With the use of the optional laboratory kit a set of extension rods, clamps and bench, the **GWT** can be used to determine the water penetration characteristics of specimens of alternative concrete mixtures. While a standard method for evaluating test data exists, one approach is to calculate the "depth" of water penetration as a function of time using the following relationship:

$$h(t) = \left(\frac{d}{D}\right)^2 (g_1 - g_2(t)) \quad (2)$$

where

$h(t)$  = depth of water penetration at time  $t$ , mm

$d$  = diameter of micrometer piston, 10 mm,

$D$  = inside diameter of gasket, 62 mm,

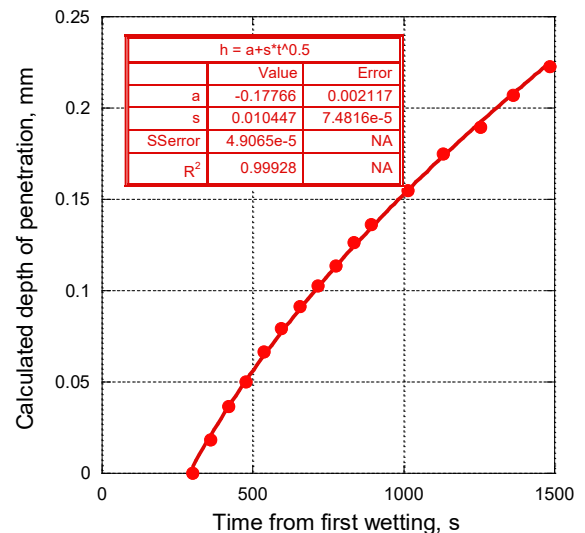
$g_1$  = initial micrometer gauge reading at start of measurement, mm, and

$g_2(t)$  = final micrometer gauge reading at time  $t$ , mm.

It has been found that the depth of water penetration is a linear function of the square root of time [1], where time is measured from when water is first added to the GWT chamber. Therefore, the following function can be fitted to the data:

$$h(t) = a + s \sqrt{t} \quad (3)$$

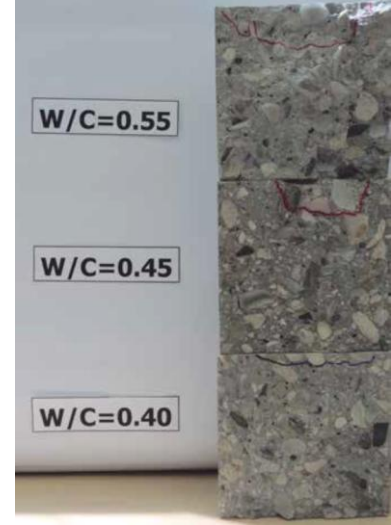
where  $a$  is the intercept and  $s$  is called the **sorptivity index** in units of  $\text{mm}/t^{0.5}$ . The plot to the right is an example of typical data of depth of water penetration



versus time. In this case, measurement of water penetration began after a 5-minute delay from the time water was introduced into the chamber. The chamber pressure was 1 bar (100 kPa). The best-fit of Eq. (3) is shown, and the sorptivity index from the regression analysis is  $0.01 \text{ mms}^{0.5}$ .

### 3. In-place Quality Assurance Testing

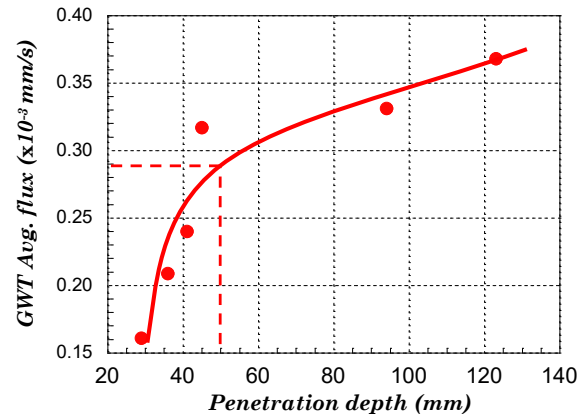
In the standard EN 12390-8 "Testing Hardened Concrete-Part 8: Depth of Penetration of Water Under Pressure", the depth of water penetration is measured on companion specimens. This method requires the specimens to be taken to the compression machine to split it transversally into two halves (Brazilian test) and the depth of penetration, indicated by the moisture stain, is visually measured. The figure on the right shows an example of three split specimens after being tested. The moisture stain was marked to compare the difference in water penetration depth after 72 hours of exposure to 5 bar. Project specifications often require that the concrete meets a maximum water penetration using this test.



For quicker permeability assessments, correlations can be established between the average flux of water measured by the GWT in a given short time and the depth of water penetration measured on companion specimens using the described EN 12390-8. The next graph is an example of such a correlation by testing 6 different mixes [3]. For example, a maximum depth of 50 mm is specified typically for concrete in non-corrosive conditions. Using the established correlation, the GWT can be used for in-place testing to demonstrate that the concrete in the structure conforms to the water penetration requirements.

Specimen	$f_c$ (MPa)	Avg. penetration depth (mm)	GWT Avg. flux* ( $\times 10^{-3} \text{ mm/s}$ )
1	57.0	29	0.161
2	38.5	94	0.331
3	43.3	41	0.240
4	56.4	36	0.209
5	45.9	45	0.317
6	37.9	123	0.368

\*10 minutes at 1 bar. Correlations curves for different testing times and applied pressures may be obtained.



### 4. Masonry Permeability

The GWT is shown being used for testing the water tightness of a brick masonry wall. It was found that when it rained and for a normal wind pressure, water penetrated the wall. The first thought was that there was a problem with the mortar joints. By using the GWT, however, the problem was shown to be related to the brick units, not to the mortar joints. The brick units had been burned at a higher temperature than normal to produce the required color, but the higher burning temperature increased the permeability of the brick.



## GWT Features and Specifications

- Lightweight, handheld equipment, easy to operate in the lab and in-situ
- Strong aluminum/stainless steel chamber
- Kit includes 2 pressure gauges
- 4 bar (400 kPa) maximum pressure
- High precision micrometer for registering water volume
- 2 types of watertight gaskets for different surface conditions

## GWT-4000 Kit Ordering Numbers

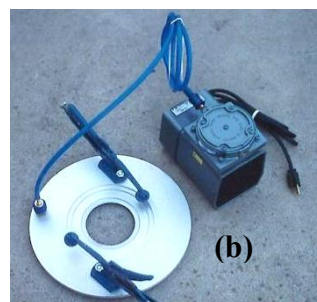
Item	Order #
Pressure chamber unit with 0-1.5 bar* gauge and micrometer	GWT-4010
Wrench for pressure lid	GWT-4020
Extra 0 - 6 bar gauge	GWT-4030
Water filling cup with L-joint	GWT-4050
Adjustable clamping pliers	GWT-4060
Set of anchoring tools	GWT-4080
Wrenches: 14 and 17 mm	GWT-4090
Sealant tape	GWT-4100
Bottles with boiled water, 3	GWT-4110
Foam gaskets, 15 mm thick, 4	GWT-4130
Rubber gaskets, 15 mm thick, 3	GWT-4131
Manual	GWT-4140
Attaché case	GWT-4150

\*1 bar = 100 kPa



## Optional Items:

Item	Order #
Laboratory Kit (a). Set of extension rods, clamps and bench for testing on 150 x 300 mm or 100 x 200 mm cylinders, and on 150 mm cubes	GWT-4260
Suction plate & vacuum pump (b) for testing without anchoring	GWT-4230
Hammer drill machine	GWT-4240



## References

- [1] Mohammadi, B and Nokken, M.R., "Influence of Moisture Content on Water Absorption in Concrete," 3<sup>rd</sup> Specialty Conference on Material Engineering & Applied Mechanics, Montreal, May 29-June 1, 2013.
- [2] Valenta O. (1970) "The permeability and durability of concrete in aggressive conditions". Proceedings of 10th International Congress on Large Dams, Montreal.
- [3] Moczko Andrzej, Moczko Marta. GWT – "Testing System for "in-situ" Measurements of Concrete Water Permeability", Wrocław University of Technology, Poland, 2015.



## Purpose

The **ICAR Plus Rheometer** is a rugged, portable instrument for measuring fundamental flow (rheological) properties of fresh concrete. The instrument was developed at the International Center for Aggregate Research (ICAR) located at The University of Texas at Austin to fill the need for a method to characterize the true flow behavior of concrete mixtures. The traditional methods of measuring slump or slump flow are not capable of characterizing the fundamental rheological properties of concrete that exist during the processes of mixing, transporting, and placement. As a result, the true performance of innovative concrete mixtures cannot be measured with these traditional methods. The **ICAR Plus** appears as a low-cost and simple to operate instrument that can be used for:

- Research and development to characterize the influence of new materials on concrete rheology
- Optimizing mixture proportions so that the resulting concrete flows readily but is resistant to segregation (especially important for self-consolidating concrete or pumped concrete)
- On-site quality control of mixtures

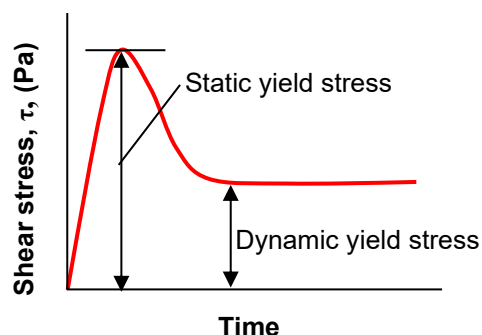
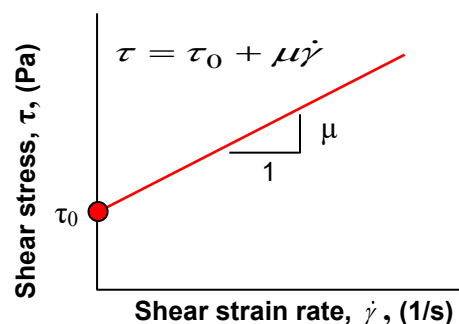


## Principle

Fresh concrete can be considered as a fluid, which means that it will flow under the action of shear stresses. The flow behavior of concrete can be represented by the following two-parameter relationship:

$$\tau = \tau_0 + \mu \dot{\gamma}$$

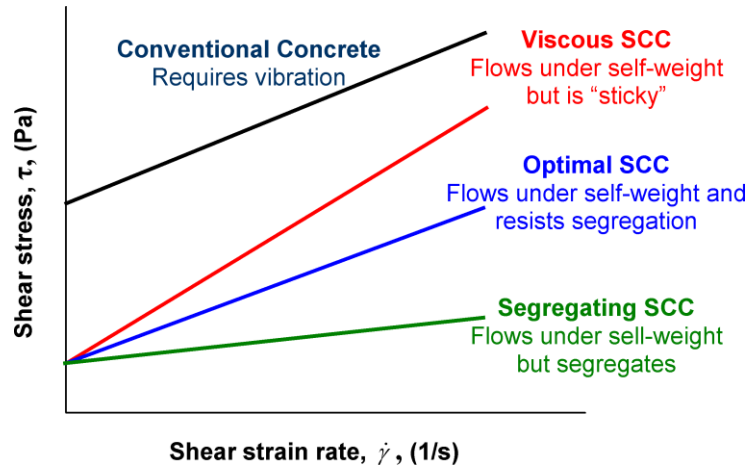
which is known as the **Bingham model**: The parameter  $\tau_0$  is the **yield stress** and represents the shear stress required to initiate flow. The slope of the line is the **plastic viscosity**,  $\mu$ , and it affects the resistance to flow after the yield stress has been surpassed. These two parameters, which define the **flow curve**, provide a complete description of the flow behavior of a fluid.



Concrete, however, is not a simple fluid because it displays **thixotropic** behavior, which means that the shear stress required to initiate flow is high if the concrete has been in an “at rest” condition, but a lower shear stress is needed to maintain flow once it has begun. This type of behavior is summarized in the schematic plot shown to the left, which shows the variation in shear stress with time for the case of a **low** applied shear strain rate. At the start, the shear stress increases gradually with time but there is no flow. When the stress reaches the **static yield stress**, the concrete begins to flow and the stress required to maintain flow is reduced to the **dynamic yield stress**. If the applied shear strain rate is reduced to zero and the concrete is

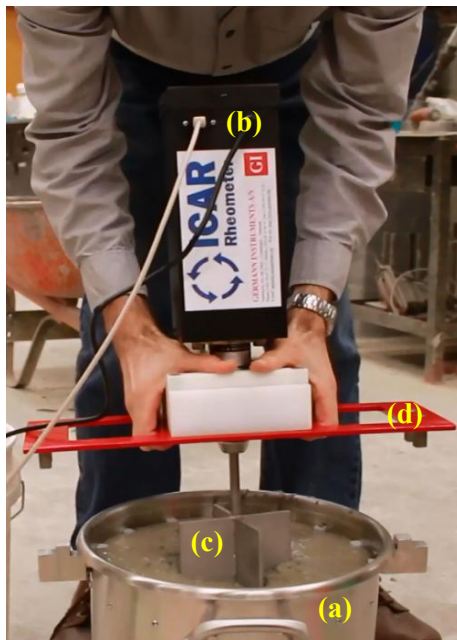
allowed to rest, inter-particle forces create a weak framework that restores the static yield stress. With time, the static and dynamic yield stresses increase as the effectiveness of water-reducing admixtures diminish and hydration proceeds, which is commonly referred to as “slump loss.”

The **ICAR Plus** is designed to characterize the **static yield stress**, the **dynamic yield stress** and **plastic viscosity** of the concrete. A high static yield stress is desirable because it reduces formwork pressure and increases the resistance to segregation. But for ease of pumping, placement, and self-consolidation, a low dynamic yield stress is necessary. The dynamic viscosity provides cohesiveness and contributes to reducing segregation when concrete is flowing. The schematic plot to the right shows dynamic flow curves for conventional concrete and different types of self-consolidating concrete (SCC) mixtures. The conventional concrete has a high dynamic yield stress and additional energy (vibration) is needed to consolidate the concrete after it is placed in forms. The self-consolidating mixtures all have low dynamic yield stress and will consolidate due to self-weight, but they have different rheological properties. The SCC with a high plastic viscosity (red line) will be sticky and difficult to place and strike off. On the other hand, the mixture with low plastic viscosity (green line) will be prone to segregation. Thus, by determining the dynamic flow curves of concretes with different mixture proportions and type of admixtures, and optimum balance between ease of flow and resistance to segregation can be realized. These types of determinations cannot be done using conventional slump-based tests.



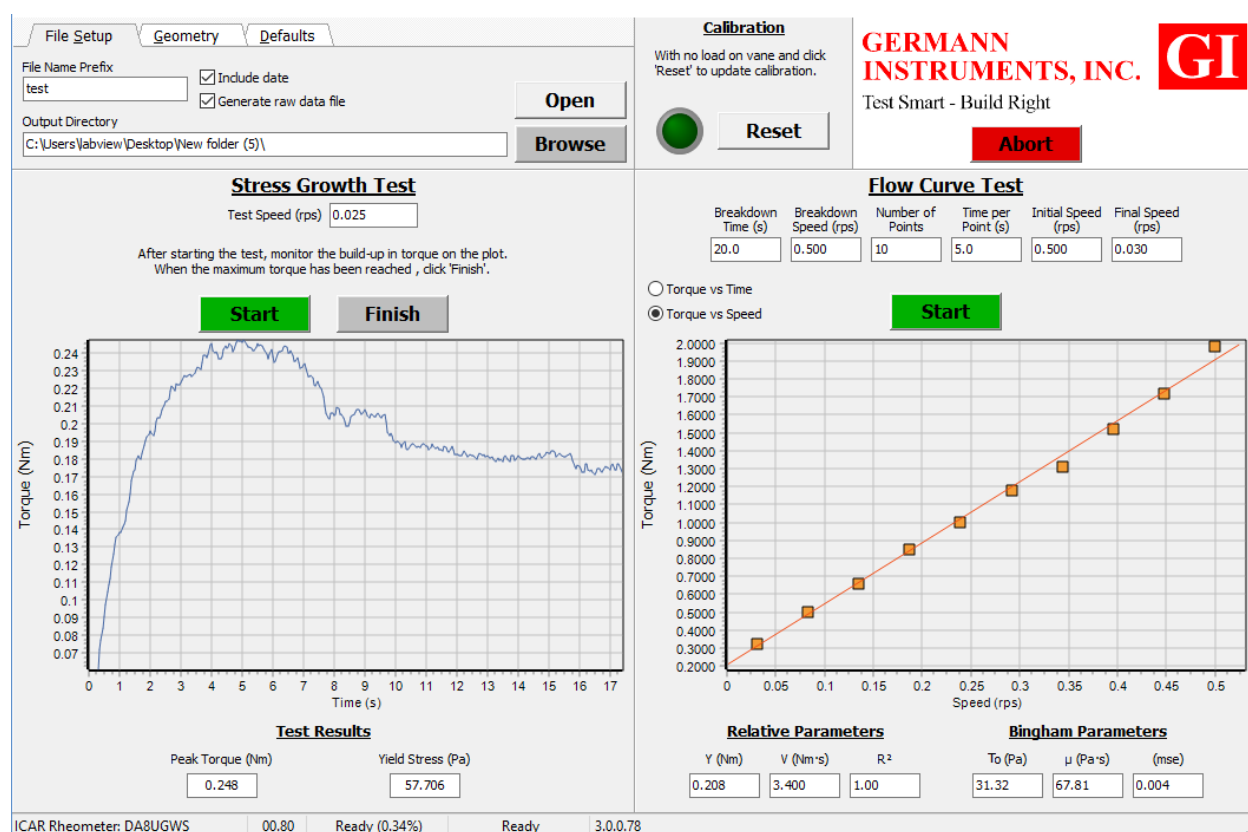
### Method of Operation

The **ICAR Plus Rheometer** is composed of a container (a) to hold the fresh concrete, a driver head (b) that includes an electric motor and torque meter; a four-blade vane (c) that is held by the chuck on the driver; a frame (d) to attach the driver/vane assembly to the top of the container; and a laptop computer to operate the driver, record the torque during the test, and calculate the flow curve parameters. The container contains a series of vertical rods around the perimeter to prevent slipping of the concrete along the container wall during the test. The size of the container and length of the vane shaft are selected based on the nominal maximum size of the aggregate. The vane diameter and height are both 127 mm. A multiple blade “**Carrousel**” vane (e) is also available to be used with a container for maximum aggregate size of 13 mm (f). This vane generates a more uniform flow velocity profile and provides more accurate and stable measurements for flow curve tests on materials like high flow self-consolidating concrete (e.g. slump flow > 600 mm), flowable mortars or grouts (e.g. self-leveling), mortars for 3D printing, etc.



Two types of tests are performed. The first type is a **stress growth test** in which the vane rotates at a constant slow speed of 0.025 rev/s. The initial increase of torque is measured as a function of time. The maximum torque measured during this test is used to calculate the **static yield stress**. The second type is a **flow curve test** to determine the **dynamic yield stress** and the **plastic viscosity**. The flow curve test begins with a “breakdown” period in which the vane is rotated at maximum speed to breakdown any thixotropic structure that may exist and to provide a consistent shearing history before measuring the Bingham parameters. The vane speed is then decreased in a specified number of steps, which is selected by the user but at least six steps are recommended. During each step, the vane speed is held constant and the average speed and torque are recorded. The plot of torque versus speed of vane rotation defines the **flow curve** from which the Bingham parameters are calculated. The equipment also allows us to set the steps of speeds in ascending order if required, such as for thixotropy measurements.

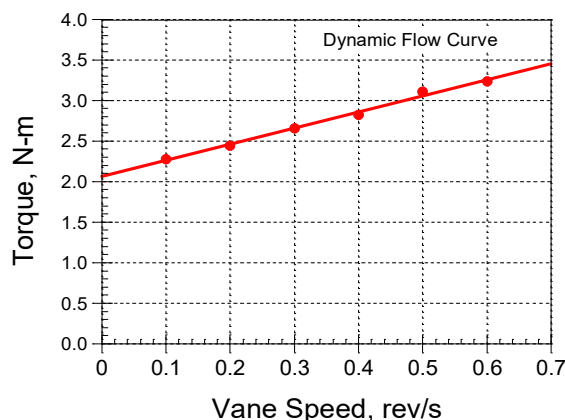
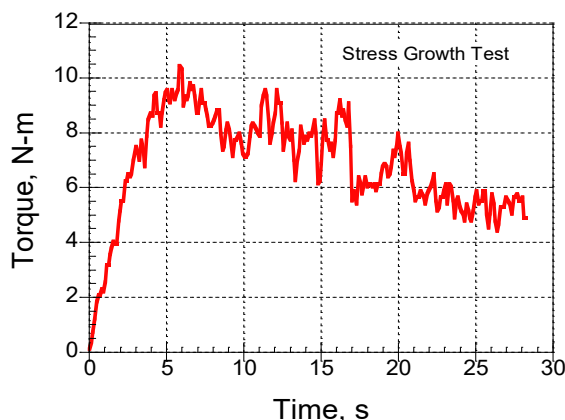
The **ICAR software** operates and calibrates the driver, records the torque, computes test results, and stores data. The entire testing is controlled from a single screen as shown below. A simple press of the “Start” button initiates the stress growth test or the flow curve test. Both tests are completed within 1 minute. The automatic digital calibration allows users to always have a ready to use system. After calibration, the uncertainty torque measurement value is displayed, which is typically less than 0.5%.



## Example Results

The next figure on the left shows the results of a stress growth test. The program uses the peak torque and test geometry to calculate the static yield stress, which is displayed at the bottom of the computer display. The figure on the right shows the average torque versus average vane rotation measured during six steps of the flow curve test. The software computes a best-fit line to the data and reports the intercept and slope as relative parameters. Based on the test geometry, the software computes the Bingham parameters: dynamic yield stress and plastic viscosity.





### ICAR Plus Features and Specifications

- Minimum slump: The concrete has to have a slump greater than 75 mm, otherwise, the concrete is too stiff for being tested
- Nominal maximum size of aggregate (NMSA): up to 32 mm for the largest available container
- Vane rotation speed: 0.001 to 0.667 rev/s
- Motor type: Integrated Servo Motor
- Accuracy:  $\pm 0.1\%$
- Resolution: 0.001 Nm
- Minimum Torque: 0.01 Nm
- Peak Torque: 90 Nm for not more than 2 seconds
- Continuous Maximum Torque: 32 Nm
- Power Supply: Input of 100-240 VAC 50-60 Hz – 3.5A.
- Digital Calibration can be performed by user at any time
- Performs static stress growth and dynamic flow curve tests
- Software computes static yield stress, dynamic yield stress, and plastic viscosity in fundamental units
- Motor drive dimensions: 11 x 11 x 43 cm
- Motor console weight: 7.5 kg
- Carrying Case dimensions: 67 x 52 x 28 cm
- Carrying Case weight: 20 kg, including motor drive, base frame, vane, power supply and cables



### RHM-4000 ICAR Plus Kit. Ordering Numbers

Item	Order #
Motor drive/torque meter unit	RHM-4001
Power cord for motor drive unit	RHM-4002
Base frame	RHM-3003
Container for max. 19 mm NMSA *	RHM-3005
Four-blade vane for 19 mm NMSA *	RHM-3009
USB cable	RHM-3012

Item	Order #
Laptop computer with software	RHM-4013
Software on CD-ROM	RHM-4014
User manual	RHM-4015
Carrying case for laptop computer	RHM-4016
Carrying case for Rheometer	RHM-4017

\*Default size supplied along with the RM-4000 ICAR Plus Kit if another size is not specified.

**Available containers and vanes for different NMSA**

	Nominal Maximum Size of Aggregate (NMSA)			
	13 mm	19 mm	25 mm	32 mm
<b>Container</b>	RHM-3004	RHM-3005*	RHM-3006	RHM-3007
<b>Four-blade vane</b>	RHM-3008	RHM-3009*	RHM-3010	RHM-3011
<b>Carrousel vane</b>	RHM-3020			

**Optional Items**

Item	Order #
30,000 centistokes silicone oil for verification of instrument (25 L or 19 L pail)	RHM-3018



## Purpose

The **LOK-TEST** system is used to obtain a reliable measurement of the in-place compressive strength of concrete in newly cast structures in accordance with the pullout test method described in ASTM C900, BS 1881:207, or EN 12504-3. **LOK-TEST** can be used for:

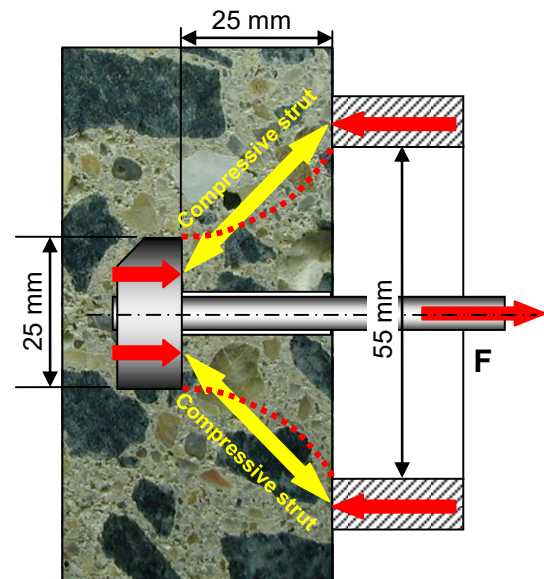
- Determining whether in-place concrete strength is sufficient for timing of early and safe loading operations, such as due to formwork removal or application of prestressing.
- Determining whether the in-place strength is sufficient for terminating curing and thermal protection.
- Quickly evaluating the quality of the critical cover layer protecting the reinforcement in the finished structure.
- Substituting laboratory testing cylinders or cubes for testing final strength of structures on-site.

## Principle

An insert with a steel disc, 25 mm in diameter at a depth of 25 mm, is cast into concrete either by attaching it to formwork before placing concrete or by inserting it manually into the fresh concrete. Various **LOK-TEST** inserts are available. Deeper testing is shown in the Canadian Standard CSA A23.2-15C<sup>14</sup>.

Once the concrete has hardened, the disc is pulled centrally against a 55 mm diameter counter pressure ring bearing on the testing surface. The force **F** required to pullout the insert generates compression stresses in the strut between the disc and the counter pressure ring. Therefore, the pullout force **F** is a direct measure of the compressive strength.

Loading is performed either to a required force, in which case the test is nondestructive, or to the peak-load, which results in a slightly raised, 55-mm diameter circular crack on the surface. If pulled out, the conical hole can be easily patched with a repair non-shrink mortar.



## Correlation and Accuracy of Estimated Strength

**LOK-TEST** provides a quick and accurate estimate of in-place strength as the peak pullout force has a robust correlation to compressive strength measured either by standard cylinders or cubes. Test methods to estimate compressive strength like rebound hammer (Schmidt hammer), ultrasonic pulse velocity or Windsor probe, require individual correlations for every concrete mixture that are usually insensitive and present large scatter. By contrast, the more than 30 years of correlation experience with **LOK-TEST** and **CAPO-TEST**, from all over the world, indicates that **one general correlation** can be applicable for all normal density concrete mixtures. A significantly different correlation, however, has been found for concrete made with lightweight (low density) aggregate.

The general correlations between pull-out force and standard compressive strength shown in the following figures are summarized from 32 major independent studies performed by various laboratories in Denmark, Sweden, Norway, Holland, Canada, the United States, Poland, and England.<sup>1,2,5</sup> It has been shown that these general correlations are not affected by types of cementitious materials, water-cementitious materials ratio (w/cm), maturity, use of self-consolidating concrete, air entrainment, use of admixtures, fibers, curing conditions, stresses in the structure, rigidity of the member, carbonation, as well as shape, type, and size of aggregate up to 38 mm.

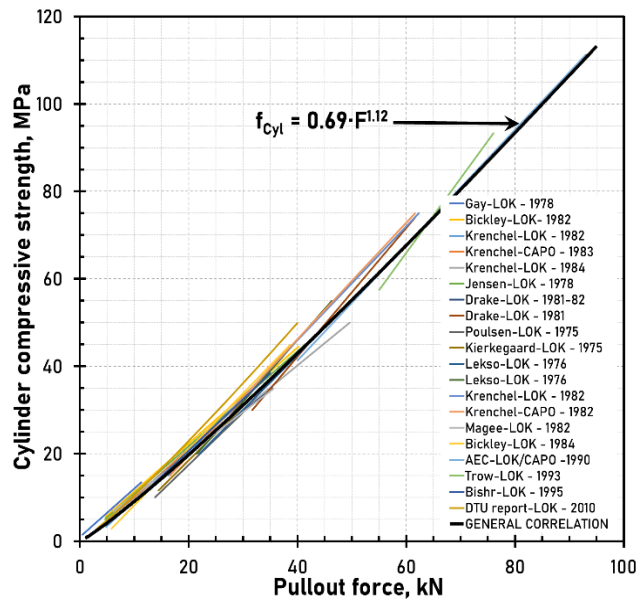
Correlations have separately been performed in a large project at the University of Liverpool<sup>3</sup> aimed at methods for assessing early-age strength and whose efforts led to a Best Practice Guide by the British Cement Association<sup>4</sup> in which the pullout test is recommended for assessing early-age strength



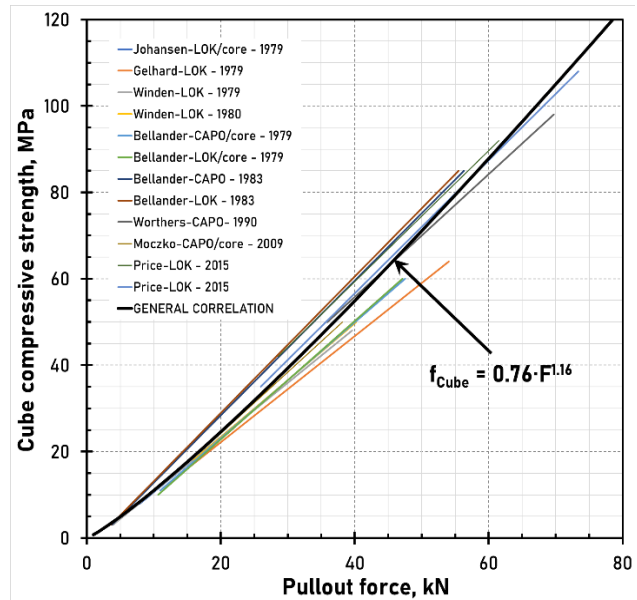
in new structures. In this British research, the general correlation between LOK-TEST and 150 mm cube strength was confirmed again for the normal-density concrete mixtures investigated.

Similarly, many reports have confirmed these findings<sup>5,6,7,8</sup>. In-place testing with pullout have even been used instead of using standard cylinders<sup>7</sup>.

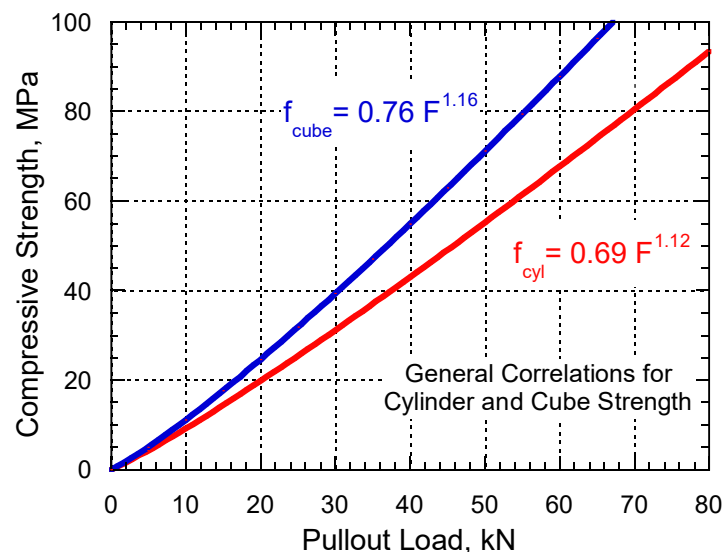
At the 95 % confidence level and for an average of 4 pullout tests, the estimated compressive strength based on the **LOK-TEST** and the general correlations indicated is within  $\pm 4$  % of the strength measured from tests of standard specimen (cylinders or cubes) for a maximum aggregate size of 38 mm. The coefficient of variation of individual **LOK-TEST** results is about 6 to 8 % for normal density concrete.



The best-fit curve to 18 correlations between pullout force and the compressive strength of 150 x 300 mm (6 x 12 in.).



The best-fit curve to 12 correlations between pullout force and compressive strength of 150 mm (6 in.) cubes



**LOK-TEST** inserts are supplied in four different configurations and in two strength classes: (normal strength) 0 to 50 kN and (high strength) 0 to 100 kN pullout force.

- **L-40** and **L-41**: Control inserts for nailing to wooden formwork. The formwork is removed before testing.
- **L-42** and **L-43**: Early stripping inserts, with a steel plate for attachment to a removable plug through a porthole in the formwork, for use if testing is performed before the formwork is removed.
- **L-45** and **L-46**: Disc and stem, only, for replacement of used inserts.
- **L-49** and **L-50**: Floating inserts for insertion into the top surface of newly cast concrete.

Normal strength, 0 to 50 kN



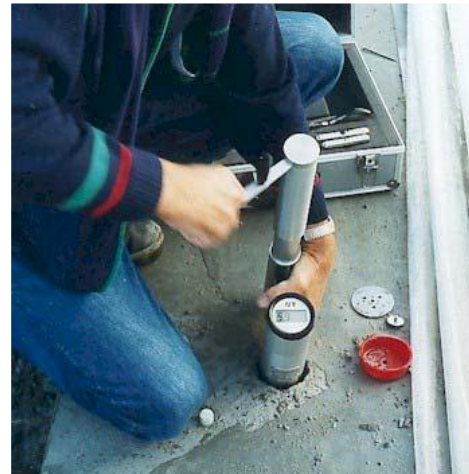
High strength, 0 to 100 kN



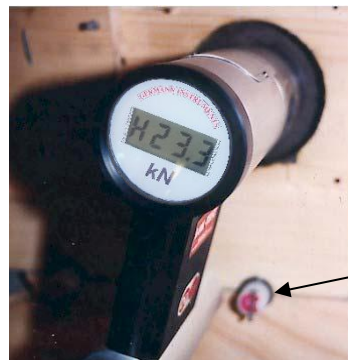
## Example Applications



**LOK-TEST** being performed on a wall for quality control of the finished structure. “H” on the display shows the highest pullout force. The L-40 Insert is used.



Testing for in-place quality control on a slab. The L-49 floating insert is used. Maturity was measured with the **COMA-Meter**, shown in front of technician’s knee.



**COMA-Meter** reading 2  $M_{20}$  days.

**LOK-TEST** performed from the bottom of a slab, through the formwork, for safe and early form removal. The L-42 early stripping insert was used with the L-44 steel plate attached to a removable plug through a porthole in the formwork. **COMA-Meters** are used for timing of the **LOK-TEST**.

## LOK-TEST Specifications

- Handheld hydraulic pulling machine with electronic gauge.
- Digital display resolution = 0.1 kN
- Maximum force: 100 kN
- Maximum stroke: 6 mm
- Accuracy of measurements:  $\pm 0.1$  kN
- Operating conditions: -10 to 50°C, max. RH = 95%
- Memory capacity: 512 measurements (peak-value, time and date of testing)
- AMIGAS Software for PC communication and printout

## LOK-TEST Ordering Numbers



The **L-11-1** pull machine can be also used for **CAPO-TEST** and **BOND-TEST**.  
See their Technical Data Sheets.

### LOK-TEST L-11 Kit

Item	Order #
Hydraulic pull machine with electronic gauge	L-11-1
AMIGAS Printout software	L-13
Cable for printout	L-14
Centering plate	L-15
Coupling	L-16
Pull bolt	L-17
Stem removal tool	L-18
Bolt handle	L-19
Adjustable pliers	L-20
Oil refilling cup	L-24
Oil refilling bottle	L-25
Large screwdriver	C-149
Small screwdriver	C-157
Calibration table	L-32
Manual	L-33
Attaché case	L-34

## Inserts

### Normal strength, 0 to 50 kN



Item	Order #
Control insert	L-40
Early stripping insert with L-44 steel plate	L-42
Disc and stem, thread locked and coated	L-45
Floating insert	L-49

### High strength\*, 0 to 100 kN



Item	Order #
Control insert	L-41
Early stripping insert with L-44 steel plate	L-43
Disc and stem, thread locked and coated	L-46
Floating insert	L-50

\*For testing high strength inserts, a special high-strength pull bolt with flange is needed, **L-17-1**, along with the high-strength coupling device **C-141**.



Undamaged inserts may be re-used provided the discs are thread locked to the stems and coated with a coating agent, **L-29**.

## Load Verification Unit

The calibration of a pull machine is recommended to be verified at least once a year, after servicing or after repair.

The **L-30** Load Verification Unit has a working range of 0 to 100 kN.

The load is displayed to the nearest 0.1 kN.



## References

1. Petersen, C. G., "LOK-TEST and CAPO-TEST Pullout Testing, Twenty Years' Experience," NDT in Civil Engineering Conference, Liverpool, UK, Apr. 1997, 19 pp.
2. Krenchel, H., and Petersen, C. G., "In-Situ Pullout Testing with LOK-TEST, Ten Years' Experience," Presentation at Research Session of the CANMET/ACI International Conference on In Situ/Nondestructive Testing of Concrete, Ottawa, ON, Canada, Oct. 1984, 24 pp.
3. Soutsos, M. N.; Bungey, J. H.; and Long, A. E., "In-Situ Strength Assessment of Concrete, the European Concrete Frame Building Project," Department of Civil Engineering, the University of Liverpool, Liverpool, UK, 1999, 10 pp.
4. British Cement Association, "Best Practice Guides for In-Situ Concrete Frame Building: Early Age Strength Assessment of Concrete On Site," Crowthorne, Berkshire, UK, 2000, 4 pp.
5. Moczko, Carino, and Petersen, "CAPO-TEST to Estimate Concrete Strength in Bridges", ACI Materials Journal, Technical Paper No. 113-M76, V. 113, No. 6, November-December 2016, pp. 827 – 836.
6. Bickley, J.A.: "The variability of pullout tests and in-place concrete strength", Concrete International, Apr. 1982.
7. Bickley, J.A.: "Trinity Square: Commentary on Concrete Test Data", Cement and Concrete Aggregates, ASTM, 1984.
8. Bickley, J.A. & Hindo, K.: "How to Build Faster for Less- The Role of In-Place Testing in Fast construction", ACI 1994 Spring Convention.
9. Bickley, J.A.: "A Brief History of Pullout Testing: With Particular Reference to Canada, A Personal Journey", Tenth ACI Conference, Sevilla, Spain, Oct 2009.
10. Carino, N. J., "Pullout Test," Handbook on Nondestructive Testing of Concrete, second edition, V. M. Malhotra and N.J. Carino, eds., CRC Press, Chapter 3, 2004, 36 pp.
11. ACI Committee 228, "In-Place Methods to Estimate Concrete Strength", American Concrete Institute.
12. ASTM C 900-19: "Standard Test Method for Pullout Strength of Hardened Concrete".
13. EN 12504-3: "Testing concrete in structures – Part 3: Determination of pull-out force"
14. Canadian Standard, CSA Group: "Evaluation of concrete strength in place using the pullout test", A23.2-15C, 2014.

## Purpose

**Merlin** is used to measure the **bulk electrical resistivity**, or its inverse, the **bulk electrical conductivity**, of saturated specimens or cores. This test is governed by **ASTM C1876** “Standard Test Method for Bulk Electrical Resistivity or Bulk Conductivity of Concrete”. The operation is simple and a measurement is obtained within two seconds. The conductivity of a saturated concrete specimen provides information on the resistance of the concrete to penetration of ionic species, chloride ions for instance, by diffusion. The term **bulk** is used to indicate that the measurement is made through the specimen as opposed to a surface-based measurement.

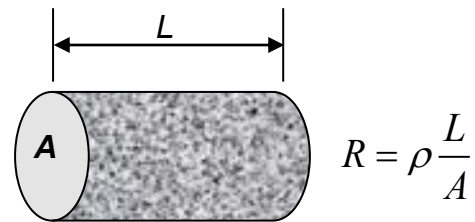
**Merlin** can be used for the following purposes:

- Research and development to characterize the influence of new materials on the electrical resistivity of concrete.
- Optimizing mixture proportions and blends of supplementary cementitious materials to increase concrete service life.
- On-site durability quality control and quality assurance.
- Evaluation of in-place concrete (using cores).



## Principle

The electrical resistance  $R$  of a conductor of length  $L$  and uniform cross-sectional area  $A$  is given by the equation shown in the figure to the right. The quantity  $\rho$  is the **electrical resistivity** and is a material property, with units of resistance multiplied by length, such as ohm·m. If the electrical resistance  $R$  of a specimen of length  $L$  and area  $A$  is measured, the resistivity can then be calculated as  $\rho = R A/L$ . The inverse of electrical resistivity is the electrical conductivity,  $\sigma = 1/\rho$ . The inverse of ohms is a unit called siemens (S). Therefore, electrical conductivity has units of S/m. For concrete, it is convenient to express electrical conductivity in millisiemens per meter or mS/m.



In assessing the ability of a concrete mixture to resist penetration of a particular type of ion, one of the key properties is the **diffusivity**, which defines how readily that ion will migrate through saturated concrete in the presence of a concentration gradient. For a saturated porous material, such as concrete, the diffusion coefficient of a given type of ion can be related to electrical conductivity through the **Nernst-Einstein equation** as follows (Snyder et al. 2000; Nokken and Hooton 2006):

$$\frac{\sigma}{\sigma_p} = \frac{D}{D_w} \quad (1)$$

where  $\sigma$  = bulk electrical conductivity of the saturated porous material

$\sigma_p$  = conductivity of the pore fluid

$D$  = bulk diffusion coefficient of the specific type of ion through the porous material, and

$D_w$  = diffusion coefficient of the specific ion through water (Mills and Lobo 1989).

If the conductivity of the pore fluid is assumed to be similar among different concretes, the measured bulk electrical conductivity is related directly to the bulk diffusion coefficient (Berke and Hicks 1992). Measurement of the bulk diffusion coefficient of a particular type of ion through concrete is a time-consuming process, while electrical conductivity can be measured with **Merlin** in a matter of seconds.

The electrical conductivity of saturated cement paste is related to the volume of pores and how they are connected within the paste. The paste porosity is related to the water-cement ratio ( $w/cm$ ), the types of supplementary cementitious materials (SCMs), and the degree of hydration. For the same

$w/cm$  and degree of hydration, the use SCMs reduces pore size and increases the tortuosity of the pores and, thereby, reduces electrical conductivity and the ease of fluid penetration.

### Method of operation

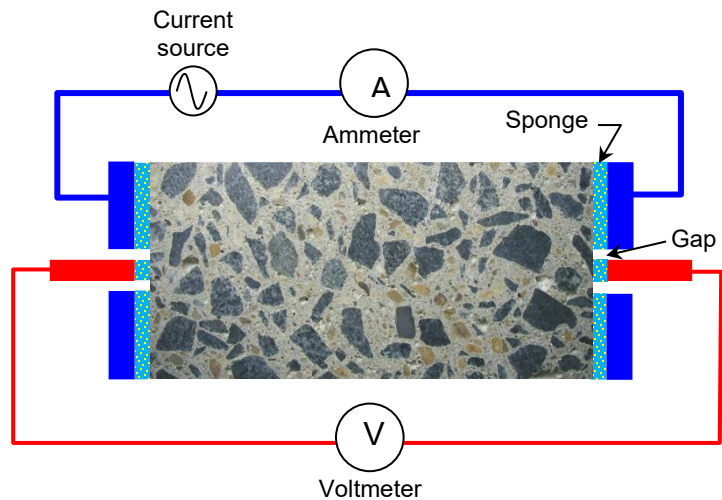
The **four-point** measurement method that is used provides an accurate measure of specimen resistance by minimizing the effects of the conductive sponges and the pressure applied to the electrodes.

An alternating current (325 Hz) is applied through the saturated specimen or core. A voltmeter measures the voltage drop across the specimen, and an ammeter measures the current through the specimen. From the measured current  $I$  and voltage  $V$ , the bulk conductivity is calculated as follows:

$$\sigma = \frac{I}{V} \frac{L}{A} \quad (2)$$

The bulk **resistivity** is the inverse of the bulk conductivity,  $\rho = 1/\sigma$ .

A 100 by 200 mm verification cylinder is supplied to check that the **Merlin** system is operating correctly. The cylinder includes a switch to select one of several precision resistors from 10  $\Omega$  to 1 M $\Omega$  and the **Merlin** should display the right conductivity and resistivity values for each of these resistors.



### Application

Measuring the bulk electrical conductivity also provides an indication of the diffusivity properties of the concrete. If the test is conducted at a consistent degree of hydration for a given combination of cementitious materials, the variation in measured bulk electrical conductivity can be used as an indicator of variation of  $w/cm$  using a pre-established correlation. If the conductivity of the approved concrete mixture for a project is known, that value can be used for quality control and quality assurance. Thus **Merlin** can be considered as a **surrogate test** to verify the  $w/cm$  of a specimen.

The bulk conductivity measured with **Merlin** is related directly to the charge passed through a specimen as measured by ASTM C1202 using the **PROOVE'it** system (see data sheet), provided that the current remains constant during the 6 h test duration. This is typically not the case for highly conductive concretes due to electrical heating of the specimen, which increases the pore fluid conductivity and the current. If we assume, however, that current is constant during the test, we can convert the ASTM C1202 coulomb limits for the different categories of "chloride ion penetrability" into bulk conductivity limits using the following relationship:

$$\sigma = \frac{QL}{VtA} \quad (3)$$

where  $Q$  = charge passed in the **PROOVE'it** test  
 $V$  = applied voltage in the **PROOVE'it** test (60V)  
 $L$  = length of the **PROOVE'it** specimen  
 $A$  = area of the **PROOVE'it** specimen  
 $t$  = measurement time (6 h = 21,600 s) of the **PROOVE'it** test

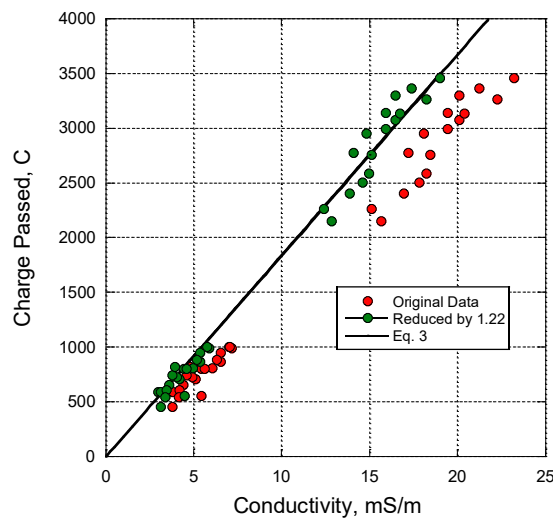


For a specimen length of 50 mm and a diameter of 95 mm (the reference dimensions specified in ASTM C1202), the conversion from charge passed using ASTM C1202 to bulk conductivity values (Eq. 3) and bulk resistivity values is as follows:

Permeability Class (ASTM C1202)	Charge passed using <b>PROOVE'it</b> , Coulombs <sup>†</sup>	<b>Merlin</b> Bulk Conductivity, mS/m	<b>Merlin</b> Bulk Resistivity, $\Omega \cdot m$
High	> 4,000	> 21.8	< 45.9
Moderate	4,000 – 2,000	21.8 – 10.9	45.9 – 91.9
Low	2,000 – 1,000	10.9 – 5.4	91.9 – 183.7
Very Low	1,000 – 100	5.4 – 0.54	183.7 – 1,837
Negligible	< 100	< 0.54	> 1,837

<sup>†</sup>It is assumed that current is constant during the 6 h test duration, which is typically not true for high conductivity concrete

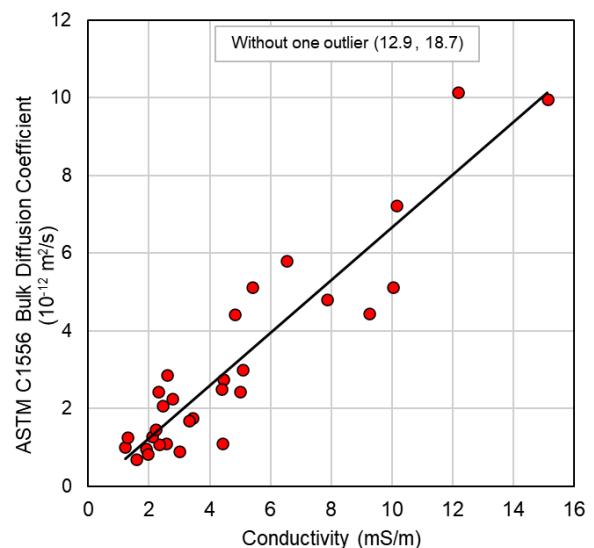
### Test Data



Data have been published on the relationships between bulk conductivity and other durability related properties, such as permeability, chloride diffusion, and charge passed. E. Karkar (2011) performed a study from which bulk conductivity can be compared with results of other test methods. The study involved nine concrete mixtures, made with different cementitious materials, and with  $w/cm$  values between 0.40 and 0.50. The specimens were tested at ages of 35 and 56 days. Bulk electrical conductivity was measured after applying current for 1 minute and 5 minutes using the ASTM C1202 apparatus and compared with bulk conductivity using the **Merlin**. Charge passed in accordance with ASTM C1202 was also measured. The graph on the left shows the Coulomb values measured by ASTM C1202 versus conductivity measured with **Merlin** on the same

specimens. The straight line is the relationship given by Eq. (3) for a specimen diameter of 95 mm and length of 50 mm. It is seen that the bulk conductivity measured with **Merlin** is systematically greater than expected based on Eq. (3). Hence the measured values have been reduced by a factor of 1.22. The reduced values, which are plotted as green points, are now in agreement with Eq. (3). The reason for this discrepancy was not addressed by Karkar (2011), but the important conclusion is that a rapid measurement of bulk conductivity will provide the same information as the 6-h ASTM C1202 test.

According to the **Nernst-Einstein equation**, Eq. (1), the bulk chloride ion diffusion coefficient is expected to vary linearly with bulk electrical conductivity of concrete, assuming that the pore fluid conductivity is the same. The plot on the right shows data (Kessler et al. 2008) of mixes made with different cementitious materials and  $w/cm$  values between 0.29 and 0.45. The **chloride bulk diffusion coefficient** determined by ASTM C1556 after 1 year of chloride exposure is plotted as a function of bulk conductivity. While there is data scatter, it is clear that there is a consistent relationship between them.



The chloride ion migration coefficient determined by Nordtest Build 492 is not identical to the chloride diffusion coefficient, but it has been shown that the two are correlated to each other (Frederiksen et al. 1997). Thus we would expect the migration coefficient to also be a linear function of bulk conductivity assuming the same pore fluid conductivity. The data by Karkar (2011) also allow presenting the migration coefficient plotted as a function of bulk conductivity measured by **Merlin**.

### Specimen Conditioning and Test Interpretation

For an electrical conductivity test according to ASTM C1876, it is essential that the specimens obtained from cores or cast in molds, the ends are submerged in a simulated pore solution prepared with NaOH, KOH, and  $\text{Ca(OH)}_2$  for at least 6 days, or from time of demolding in the case of molded cylinders.

The purpose of this conditioning is to bring the specimen to a level of near-complete saturation of the capillary and gel pores and to prevent leaching of ions from the pore solution of concrete as this is known to affect measured conductivity values.

The conductivity of the pore solution affects the measured bulk conductivity of concrete. Thus comparisons should not be made between concretes with widely different pore solution conductivities. For example, the use of calcium nitrite as a corrosion inhibitor will increase the conductivity of the pore fluid, and the measured bulk conductivity of the concrete will be higher than for another concrete without calcium nitrite but with a similar chloride ion diffusion coefficient. On the other hand, concrete with supplementary cementitious materials may have a reduced pore fluid conductivity, which will reduce the measured bulk conductivity while the actual diffusion coefficient may not be reduced (Liu and Beaudoin 2000).

### Variability

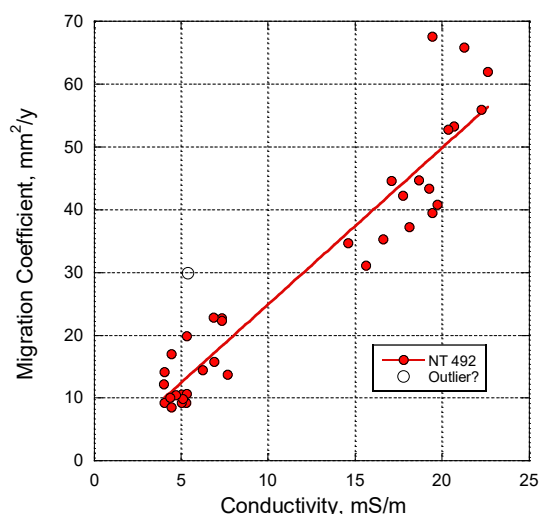
The single-operator variation is reported to be 4.3 % in ASTM C1876 and the multi-laboratory variation was found to be 13.2 %.

### Merlin Specifications

- 220 VAC / 60 Hz or 110 VAC / 50 Hz power supply
- Measurement time:  $\approx 2$  seconds
- Frequency: 325 Hz AC
- Sampling rate: 5 Hz
- Precision:  $\pm 0.1$  % for 20 to 4,000  $\Omega \cdot \text{m}$  at 23°C
- Test results displayed in terms of bulk resistivity or conductivity
- Test results can be stored for preparing test reports
- USB connection
- Compatible with Windows 7 / 8 / 10 operating systems

Two versions of the **Merlin** system are available:

	Merlin	Merlin Grande
Size of specimens	For 200 mm long and 100 mm diameter cylindrical specimens.	For up to 300 mm long and 150 mm wide specimens, <b>cylinders or cubes</b> .
	Minimum length = 25 mm Minimum diameter/width = 75 mm	



## Merlin Ordering Numbers

### Merlin, MRLN-1000 Kit

Item	Order #
<b>Merlin</b> unit	MRLN-1001
Netbook computer	MRLN -1002
<b>Merlin</b> software	MRLN-1003
<b>Merlin</b> verification cylinder	MRLN-1004
Insulating specimen support	MRLN-1005
Spray bottle	MRLN-1007
Carrying case	MRLN-1008



### Merlin Grande, MRLN-2000 Kit

Item	Order #
<b>Merlin Grande</b> unit	MRLN-2001
Netbook computer	MRLN -1002
<b>Merlin</b> software	MRLN-1003
<b>Merlin</b> verification cylinder	MRLN-1004
Spray bottle	MRLN-1007
Carrying case	MRLN-1008



## Optional Items

Item	Order #
Precision steel mold, reusable	MRLN-1009
<b>CORECASE</b> for 100 mm cores	CEL-100
Drilling machine, 1150W	CC-29
Diamond saw for trimming cores	PR-1060

## References

- Berke, N.S. and Hicks, M.C., 1992, "Estimating the Life Cycle of Reinforced Concrete Decks and Marine Piles Using Laboratory Diffusion and Corrosion Data," **Corrosion Forms and Control for Infrastructure**, ASTM STP1137, pp. 207-231.
- Berke, N.S. and Roberts, L.R., 1989, "Use of Concrete Admixtures to Provide Long-Term Durability from Steel Corrosion," Third CANMET/ ACI International Conference on Superplasticizers and Other Chemical Admixtures in Concrete, Ed. V.M. Malhotra, Ottawa, Canada, October 4-6, 1989, ACI SP 119, American Concrete Institute, p. 383-403.
- Frederiksen, J.M., Sørensen, H.H., Andersen, A., and Klinghoffer, 1997, "The Effect of the w/c Ratio on Chloride Transport into Concrete- Immersion, Migration, and Resistivity Tests," Report 54, HETEK, Road Directorate of Denmark.
- Karkar, E., 2011, "Developing and Evaluating Rapid Test Methods for Measuring the Sulphate Penetration Resistance of Concrete in Relation to Chloride Penetration Resistance," MSc Thesis, Department of Civil Engineering, University of Toronto.
- Liu, Z. and Beaudoin, J. J., 2000, "The Permeability of Cement Systems to Chloride Ingress and Related Test Methods," *Cement, Concrete, and Aggregates*, CCAGDP, Vol. 22, No. 1, June, pp. 16-23.
- R. Mills and V. M. M. Lobo, 1989, Self-Diffusion in Electrolyte Solutions, Elsevier, New York.
- Nokken, M.R. and Hooton, R.D., 2006, "Electrical Conductivity Testing," *Concrete International*, October, pp. 58-63.
- Snyder, K.A., Ferraris, C. Martys, N.S. and Garboczi, E.J., 2000, "Using Impedance Spectroscopy to Assess the Viability of the Rapid Chloride Test for Determining Concrete Conductivity," *J. Res. Natl. Inst. Stand. Technol.* 105, pp. 497-509.
- Kessler, Powers, Vivas, Paredes, Virmani, 2008, "Surface Resistivity as an Indicator of Concrete Chloride Penetration Resistance," 2008 Concrete Bridge Conference, St. Louis MO, United States. Transportation Research Board (TRB), TRID database, Accession Number: 01104992.



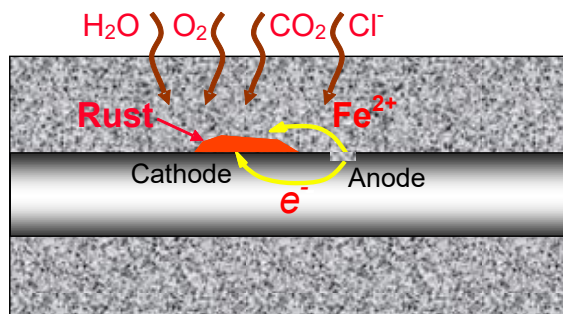
## Purpose

The **Mini Great Dane** is used to measure the half-cell potential of uncoated reinforcing steel in concrete (in accordance with ASTM C876) and the electrical resistance of the concrete's cover layer. Typical applications include:

- Condition surveys of suspect reinforced concrete (RC) structures to identify areas with corrosion activity for further analysis (testing for chlorides or sulphates, depth of carbonation, presence of flaws, etc.) to establish the cause of such corrosion and estimate remaining service life
- Monitoring RC structures for changes in corrosion activity
- Checking the effect of re-alkalization, electrochemical removal of chlorides or cathodic protection
- Measuring the corrosion activity in repaired or protected areas



## Principle

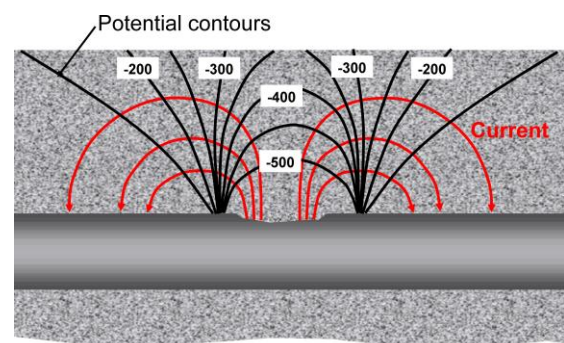


The highly alkaline pore fluid of concrete, with a pH of about 13, creates a protective film on the reinforcement. This passive layer may, however, be destroyed by the ingress of chloride ions or by a reduction in pH due to carbonation and a corrosion process may be triggered in the presence of moisture and oxygen.

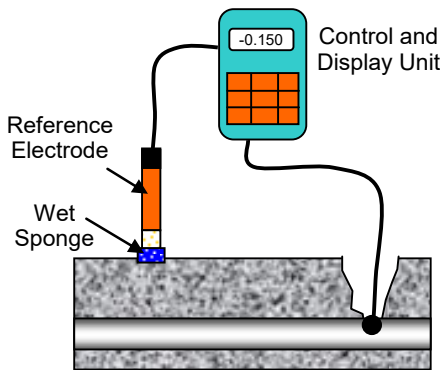
During the corrosion activity, anodic and cathodic areas are formed on the reinforcement. At the anodes, iron atoms dissolve losing electrons and diffuse into

the concrete as ferrous ions. At the cathodic sites, these ions combine with water and oxygen to form an expansive corrosion product, i.e., rust. The rate of corrosion is controlled by how easily the iron ions can move through the concrete from the anodes to the cathodes and it depends on the availability of oxygen and moisture at the cathodes.

This flow of iron ions is associated with a potential field as shown on the right. The **Mini Great Dane** measures the surface potentials (relative to an Ag/AgCl reference electrode) and the electrical resistance of the cover concrete between the electrode and the reinforcement. The potential,  $E_{corr}$ , is indicated in mV. The risk of corrosion is evaluated by means of the steepness of the potential gradients measured at the concrete surface and the level of the electrical resistance of the cover concrete. A large potential gradient and a low concrete resistance will normally indicate a high corrosion rate, except in saturated concrete because of the low oxygen content available.



After areas with the lowest potential, highest gradients, and lowest electrical resistance are identified, additional tests may be performed to establish the cause of corrosion, or the concrete may be removed at several "hot spots" to verify the actual degree of corrosion on the rebars. If, for example, the chloride ion content profile and depth of carbonation are determined, the remaining service life may be estimated (e.g., by using diffusion theory) or an appropriate protection and/or repair strategy may be developed.



Potential levels indicative of active corrosion depending on the cover condition (Ag/AgCl electrode)

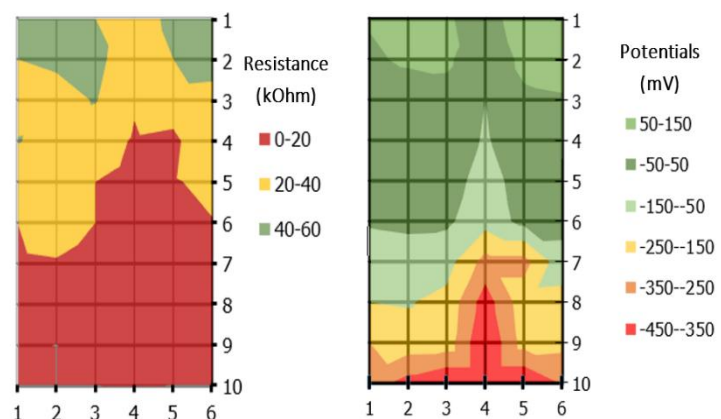
	Cover Condition		
	Dry w/o Cl <sup>-</sup> ions	Wet w/o Cl <sup>-</sup> ions	Wet with Cl <sup>-</sup> ions
E <sub>corr</sub> , mV	60 to -90	-140 to -240	-290 to -490
Gradient			
R, kOhm	20 to 50	5 to 10	0 to 1

## Testing Examples

1) The access slabs of a housing complex had been subjected to de-icing salts for 18 years. No major rust stains or spalling were observed. Shown to the right are the electrical resistance and the potentials measured with the **Mini Great Dane** on one of the slabs. The relatively low electrical resistance towards the railings indicates a water saturated concrete and/or the presence of chlorides in the concrete. A large potential gradient is noted from the wall towards the railing. The potentials are in terms of a Cu/CuSO<sub>4</sub> electrode (CSE), which are -110 mV lower in value than for the Ag/AgCl electrode. When the concrete was removed at several locations towards the railing, the bars were found to have heavy corrosion with a 1 to 20 % reduction of the cross section. Based on further testing with the **RCT** and the **Rainbow Indicator**, service life was estimated and a repair strategy was developed.

kOhm			mV (CSE)		
72	55	5	-50	-110	-390
70	64	5	-40	-120	-125
68	60	5	-30	-100	-135
71	65	8	-45	-120	-120
64	62	14	-50	-90	-110
59	55	10	-45	-95	-380
81	49	19	-50	-110	-390
73	59	20	-45	-110	-380
78	54	15	-60	-125	-365
82	68	27	-55	-135	-405
89	74	19	-45	-100	-355
98	72	21	-50	-90	-325
92	87	35	-60	-85	-310
99	90	44	-50	-75	-115
102	103	65	-55	-70	-65
Line A	Line B	Line C	Line A	Line B	Line C

2) The columns of a Danish bridge were tested. A testing grid of 6 columns and 10 rows was set up to cover the entire surface of the bottom part of each column. The resulting data was processed in an Excel spreadsheet to generate contour plots for a better visualization. The typical results from one column are presented on the right. The electrical resistance is lowest at the footing of the column where it is exposed to splashing of deicing salts in the wintertime from passing cars. The potentials show a similar trend in the vertical direction where the lowest values and largest gradients are found on the footing. A further extraction of a core for laboratory and visual inspection in the bottom of the column confirmed a high chloride content at the depth of the reinforcement and the presence of pitting corrosion with more than 10% of lost of cross section on the rebars.



## Mini Great Dane Specifications

- Input Impedance: 1,012 Ohm
- Battery Type / Life: 1 x 9V / approx. 150 hours
- Auto-off after 20 minutes of non-use
- Range:  $\pm 1,999$  mV
- Resolution: 0.1 mV for  $\pm 700$  mV and 1 mV for  $\pm 2,000$  mV
- Operating conditions: Temperature:  $-10$  to  $50$  °C, RH  $\leq 95$  %
- Reference electrode type: Ag/AgCl with BNC connection.  
The variation of the potential readings with the Ag/AgCl electrode is normally within  $\pm 5$  mV.  
The electrical resistance variation is less than  $\pm 5$  %

## The Mini Great Dane-2000 Ordering Numbers

Item	Order #
Digital meter with signal box	GD-2001
Ag/AgCl measuring cell	GD-2002
Connecting cable	GD-2003
Cable drum, 15 meters	GD-2004
Reinforcement locator	GD-2005
Drill bits, 10 mm and 18 mm	GD-2006
Two reinforcement adaptors	GD-2007
Allen key	GD-2008
Two reinforcement clamping pliers	GD-2009
Hammer and chisel	GD-2010
Telescoping extension rod	GD-2011
Multimeter	GD-2012
KCl solution	GD-2013
Manual	GD-2020

### Optional Items

Verification cell	GD-2014
Temperature probe	GD-2015
Electric hammer drill	GD-2016





## MIRA Classic

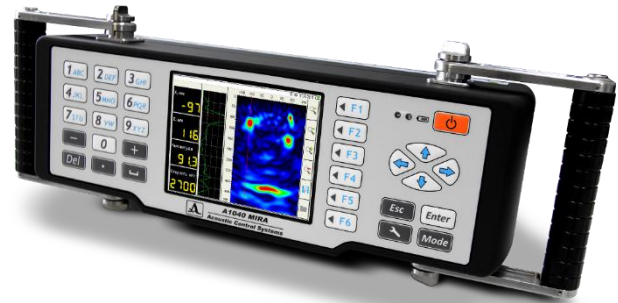
### Purpose

The **MIRA** Ultrasound Tomo-grapher is a state-of-the-art instrument for creating three-dimensional (3-D) representation (tomogram) of internal defects that may be present in a concrete element. **MIRA** is based on the ultrasonic pitch-catch method and uses an antenna composed of an array of dry point contact (DPC) transducers, which emit shear waves into the concrete. The 4 by 12 transducer array is under computer control and the recorded data are analyzed to create a 2-D image of the reflecting interfaces within the cross section below the antenna. The series of 2-D images obtained from the test object are transferred to a computer with the **IntroView** imaging software. The software assembles the 2-D slices into a complete 3-D image of the test object. The 3-D image can then be manipulated for interpretation of test results.

**MIRA** can be used for the following applications:

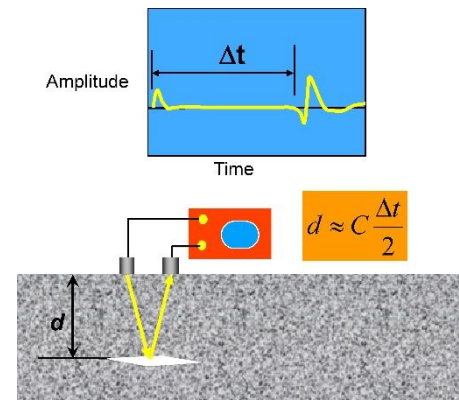
- Thickness measurement
- Detection of voids in grouted tendon ducts
- Detection of poor quality bond in overlays and repairs
- Detection of delaminations
- Detection of voids and honeycombing in concrete members
- Detection of voids behind tunnel linings and below slabs on ground.

While not intended for that purpose, **MIRA** is also capable of detecting steel reinforcement.



### Principle

**MIRA** is based on the ultrasonic pulse-echo method using transmitting and receiving, low-frequency, broad banded transducers in a "pitch-catch" configuration as shown on the right. In the pitch-catch method, one transducer sends out a stress-wave pulse and a second transducer receives the reflected pulse. The time from the start of the pulse until the arrival of the echo is measured. If the wave speed  $C$  is known, the depth of the reflecting interface can be calculated as shown (the equation assumes that the two transducers are close to each other).



The key features that distinguish **MIRA** from other flaw detection devices include:

- The use of dry point transducers to introduce into the concrete pulses of **shear waves** with an adjustable frequency of 10 to 100 kHz, that display the cross section (B-Scan) of the object in real time with a frame rate of 10 Hz
- Each transducer is spring loaded to conform to an irregular surface and they do not require a coupling medium, that is, testing is done in the dry
- The handheld, light-weight electronic unit with a TFT, 5.7" color display and adjustable handles, provides a comfortable use on horizontal, vertical and overhead surfaces
- Positioning laser beams and a rule installed in the unit facilitate the user to perform the testing and localize with precision the defects relative to the position of the antenna
- Transit times are analyzed using the synthetic aperture focusing technique (SAFT) to reconstruct a 2-D image of the cross section below the antenna

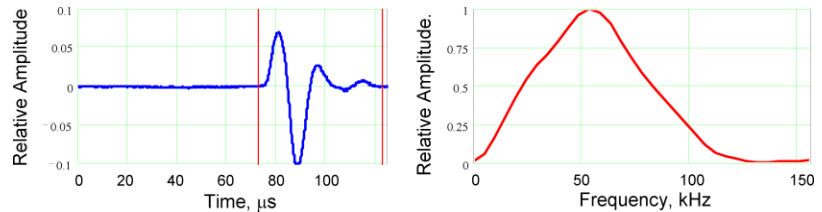


## MIRA Classic

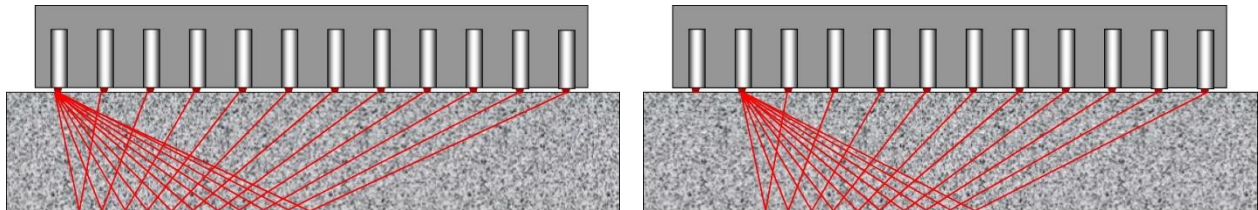
- The data captured by **MIRA** are transferred to a computer and the 3-D visualization software allows views of different slices of the reconstructed internal structure

The following provides additional descriptions of the principles involved in the **MIRA** system. The antenna is composed of a 4 by 12 array of point transducers and a control unit that operates the transducers. The transducers are heavily damped so that a short duration pulse is created. The plot in blue below shows the typical shape of the received pulse after it has reflected from an air interface.

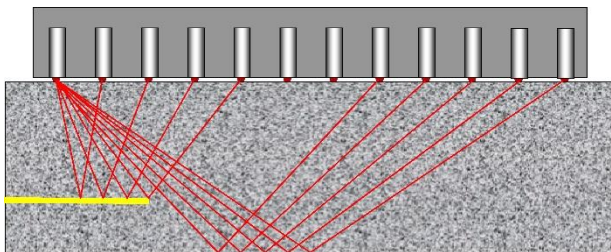
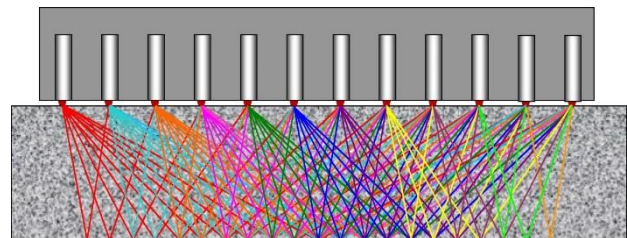
The plot in red to the right shows the amplitude spectrum of the pulse (the nominal center frequency is about 50 kHz but can be varied from 10 to 100 kHz, allowing the user to control both penetration depth and image resolution).



Basically, the control unit within the antenna excites one row of transducers and the other rows of transducers act as receivers. The left side figure below shows the ray paths of the measured transit times of the first row of transducers acting as transmitters and the remaining rows of transducers acting as receivers. Then, as shown in the figure on the right, the next row of transducers is excited and the other rows to the right act as receivers. This process is repeated sequentially until each of the rows of transducers has acted as transmitters.



The figure to the right shows the 66 ray paths for the 4 x 12 array generated during a measurement at one test location. The reconstructed image shows the locations of the reflecting interfaces, which could be the opposite side of the member (back wall reflection), reinforcing bars, and most importantly internal concrete-air interfaces (such as voids, cracks, delaminations, etc.).



If there is a sufficiently large concrete-air interface, like a defect within the member, a portion of the emitted stress pulse will be reflected by the defect. As illustrated in the figure to the left, because of the shorter ray paths, reflections from the defect will arrive at the receivers sooner than reflections from the back wall. The instrument uses the arrival times of the reflected pulses at each row of transducers to

determine the location of the defect within the member. Note in the figure that some transducers do not receive a reflection from the flaw or the back wall. This is because the flaw intercepts the rays that would normally be reflected from the back wall. This behavior accounts for a so-called "shadow" zones in some 2-D images.

### Method of operation

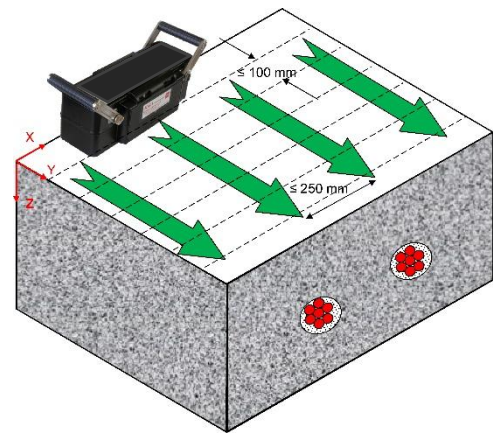
There are three modes of operation of the **MIRA** system as follows:

## MIRA Classic

- **SETUP**— This mode is used for setting up the device parameters, managing stored data, and defining the scanning grid that will be used in the SCAN mode. The system can be set up to use a designated shear wave speed for depth calculations or to measure the shear wave speed at each test location before gathering time-of-flight information.
- **REVIEW-SCAN**— This mode is intended for preliminary testing at arbitrary locations on the surface of the test object. Ideally, preliminary tests should be done at locations where the internal conditions are known. Based on the appearance of the B-scan image, it can be determined whether the correct device settings are being used before starting actual surface area scans.
- **MAP**— This mode is used for gathering a complete data set by testing at pre-defined grid locations on the surface of the test object. This mode automatically saves the B-scan data at each test location after the B-scan image is displayed. The system also stores the current system settings and an image of **MIRA** screen display at each grid point. These images can be inserted in the project report to document key features in the testing results

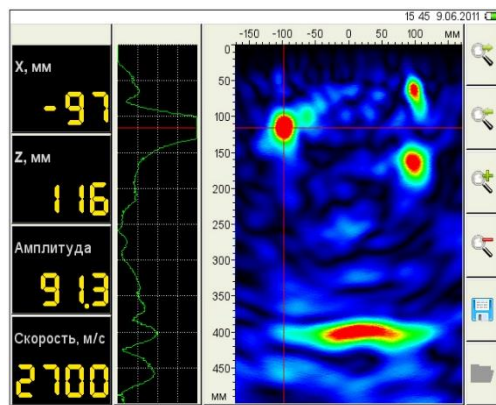
### Performing a Scan

To carry out a detailed inspection of a portion of the member, the user lays out a series of parallel scan lines on the testing surface, which are shown as green arrows. The distance between the scan lines is the same as the "horizontal step" distance entered in the SETUP mode. If the entire interior of the object is to be examined, the distance between the scan lines should not exceed 200 mm. Another series of lines perpendicular to the scan lines is laid out, which are shown as dashed lines. The distance between these lines is the same as the "vertical step" entered in the SETUP mode. If the complete interior of the test object is to be inspected, the distance between the "vertical steps" should not exceed 100 mm. The antenna is oriented perpendicular to the direction of the scan lines and data are recorded at each "vertical step" along each scan line. After taking data along the first scan line, the operator moves to the beginning of the next scan line. The testing layout entered into the system in the SETUP mode is used during image reconstruction to establish the locations of the reflecting interfaces within the test object.

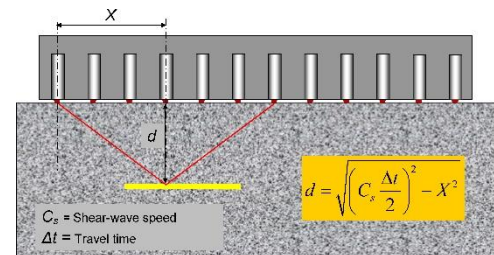


### Data Analysis

After transit time data are acquired at a test location, a signal processing technique called **synthetic aperture focusing (SAFT)** is used to reconstruct a 2-D image of the interior of the concrete member at the test location. In simple



terms, the region below the antenna



is subdivided into small elements (analogous to finite elements used for stress analysis). From the pulse arrival times and the known positions of the transmitter-receiver pairs, the depth of the reflecting interface can be established. Because of the inclined ray paths, the depth of the reflector is calculated using the formula for the relationship between the lengths of the sides of a right triangle. In the formula shown in the above figure,  $C_s$  is the shear wave speed determined by **MIRA** at the start of each measurement or the value entered by the user in the SETUP mode. Volume elements

that correspond to locations of reflecting interfaces are assigned a color to indicate intensity of reflection from those elements (constructive superposition). The end result is a 2-D image representing the locations of reflecting interfaces in the region below the antenna.

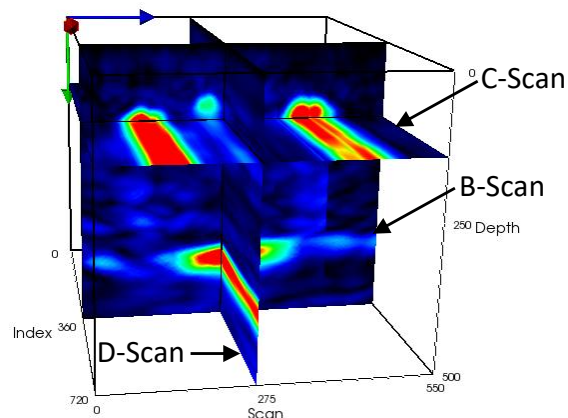
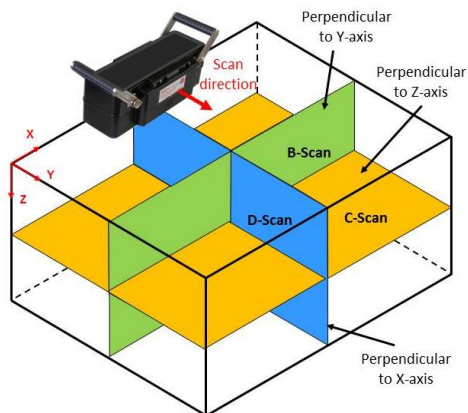
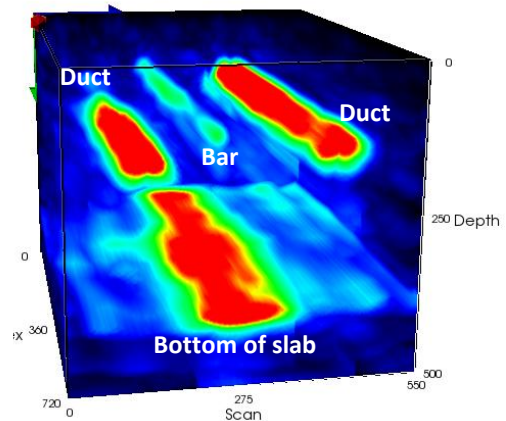


## MIRA Classic

### 3-D Image Reconstruction

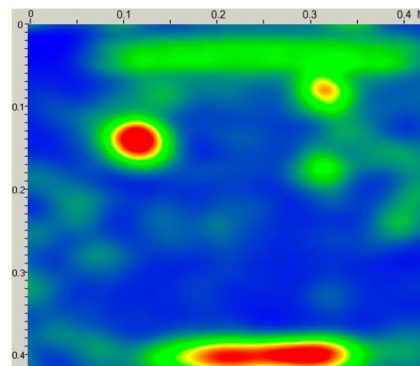
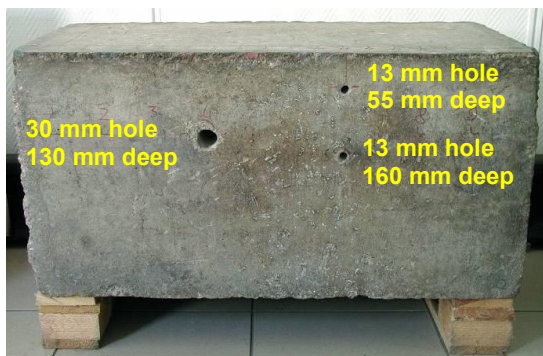
At the completion of testing, the data are transferred to a laptop computer that contains the **IntroView** 3-D visualization software. The software "stitches" together all the 2-D images to create a 3-D model of the test object. As an example, the figure at the right is the reconstructed 3-D model from a scan of a portion of a slab containing two tendon ducts and a reinforcing bar. The bottom of the slab is indicated.

The user can manipulate the 3-D model by rotating it or looking at different orthogonal planes cutting through the model. The views on the three orthogonal planes have formal names as shown in the left figure below. A **C-scan** shows the reflecting interfaces on a plane parallel to the test surface and at different depths (Z-axis); that is, it provides a "plan view" of the reflectors. A **B-scan** provides an "end view" of the reflectors. The B-scan views are the same images created at each test location by the **MIRA**. The **D-scan** provides a side view of the reflectors. The user can look at specific "slices" through 3-D model by defining the Z-coordinate for a C-scan image, the Y-coordinate for a B-scan image, and the X-coordinate for a D-scan image. For example the right figure below shows three slicing planes through the 3-D model of the slab with the ducts.



### Examples

**Plain concrete block with holes:** The test object is a 0.8 m long by 0.43 m wide by 0.43 m deep plain concrete block into which three holes were cast as shown.



The antenna was scanning along the top of the block parallel to the direction of the holes. The resulting B-scan image is shown to the right. The three holes are seen clearly and the red band at the bottom

## MIRA Classic

represents reflections from the bottom of the block. Because of the inclined ray paths, it is possible to see the deeper 13-mm hole directly below the upper 13-mm hole.

**Testing for voids in grouted cable ducts:** MIRA was used to evaluate the conditions of grouted post-tensioning ducts near the anchorage zone in the webs of a box-girder bridge. Before testing, the locations of the ducts were marked on the face of the web using information on the construction drawings (center photo below). One of the test records is shown below. The B-scan is at the cross section shown as a dashed line in the C-scan. The large amplitude signal in the B-scan at the location of the duct indicated a high probability that the duct was not fully grouted. This was confirmed by drilling a core to reveal bare strands as shown in the photo on the right. (Courtesy of Ramboll Finland Ltd.)



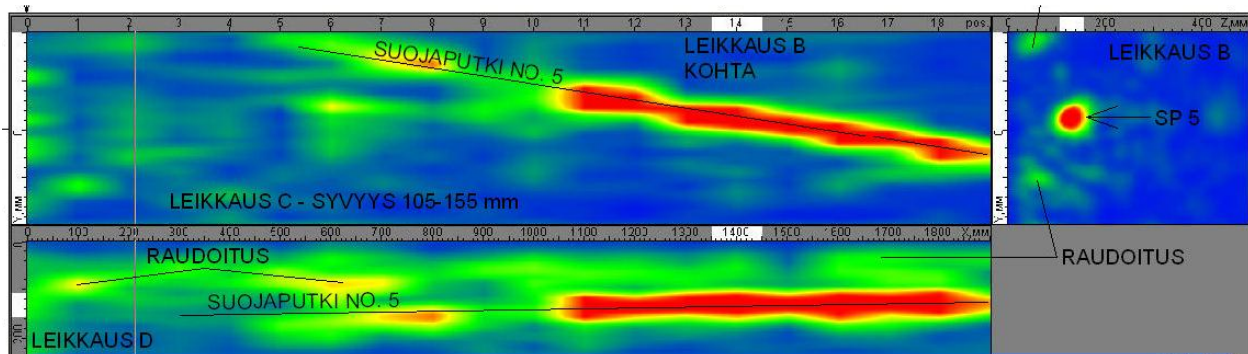
Scanning along web



View of web and drilled core

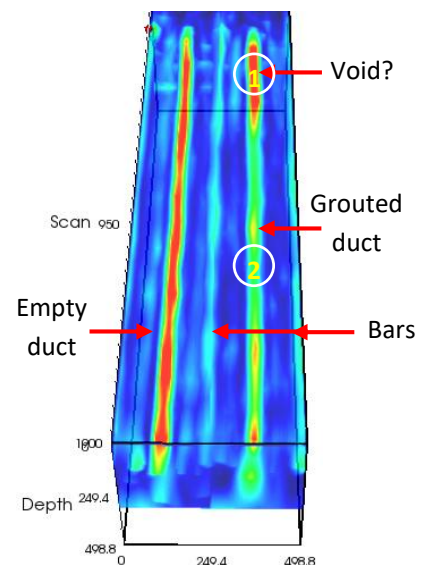


Condition of duct



**Tendon Ducts in Slab Specimen at Copenhagen Training Facility:** A 400-mm thick slab-on-ground has been constructed at the **Germann Instruments** training facility in Copenhagen. The slab contains two 100-mm diameter metal tendon ducts with a nominal cover of 100 mm. One duct is empty and the other contains 10 grouted, 16-mm diameter strands. A non-shrink grout was used to prepare the grouted duct specimen, which was then cast into the slab. In addition, ordinary reinforcing bars were located in the top of the slab parallel to the ducts.

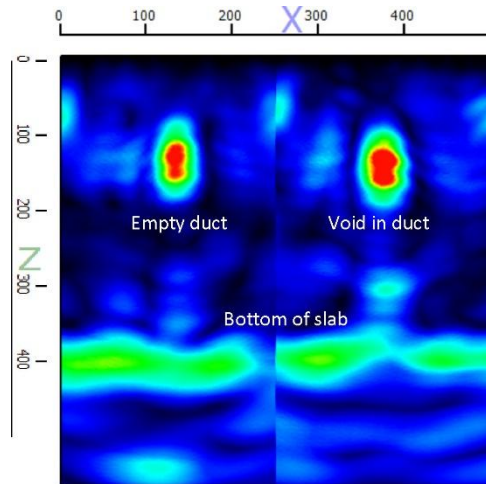
The figure to the right is the 3-D model constructed from the B-scan images obtained from scanning the surface of the portion of the slab containing the ducts. The depth of the 3-D model has been cutoff to eliminate the image of the bottom of the slab so that the ducts can be seen easily. The empty duct is displayed with red color, which indicates strong reflections from the air interface. The grouted duct is shown in a greenish-yellow color, indicating lower amplitude reflections from the steel strands. The reinforcing bars





between the ducts and to the right of the grouted duct are indicated in light blue. It is seen that at the far end of the grouted duct the image of the duct is in red, indicating a strong reflection that is characteristic of an air void. To verify that the duct is not grouted fully, the grouted duct was excavated at two locations: (1) 150 mm from the edge at the end where the air void is indicated and (2) at the approximate mid-length of the duct where no air void is indicated.

The following show the B-scan image and the corresponding photographs of the excavated duct at location 1. The B-scan image shows a similar pattern for the empty duct and the grouted duct, which is a strong indication that the grouted duct is not fully grouted. The corresponding photo of the excavated duct shows that some of the strands are not embedded in grout. Thus the presence of the air void is confirmed.

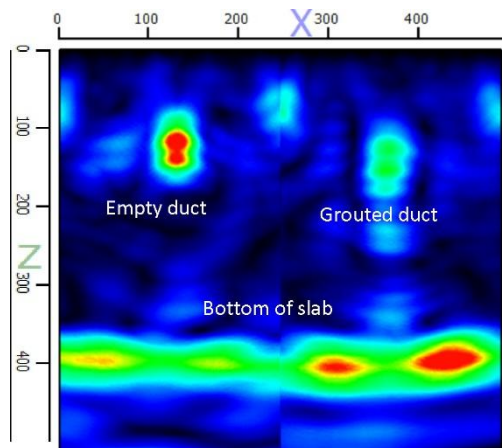


*B-scan showing cross section image of slab at location(1) with suspected void in grouted duct*



*The excavated duct at location (1) reveals that some of the strands are not embedded in grout*

The following shows the results at location 2. The B-scan image shows lower amplitude reflections (from the 10 strands) at the location of the grouted duct compared with the empty duct. The reflection coefficient at the grout-steel interface is lower than at an interface with air, and that is why the grouted duct does not appear in red. The excavated portion of the grouted duct shows that the strands were encased with the grout although this was fractured during the removal of the metal duct.



*B-scan at location (2) with no voids indicated in grouted duct. The excavation reveals the strands encased with grout; some of it was fractured in the process and this exposed some wires.*



## MIRA Classic

### MIRA Specifications

- Integrated 5.7" TFT color screen.
- Low frequency, broadband, dry point contact shear-wave transducers with wear-resistant ceramic tips
- Spring loaded 4 x 12 transducers in the antenna array
- 10 to 100 kHz working frequency range
- Nominal frequency converter = 50 kHz
- Ultrasound speed range: 1,000 to 10,000 m/s
- Dimensions: 370 × 150 × 145 mm (without handles)
- Weight: 4.5 kg
- Testing depth: 40 to 2,000 mm (depending on the concrete quality, member's lateral dimensions and amount of reinforcement)
- 7 Gb flash memory
- USB 2.0 interface
- 11.2 V rechargeable battery, 5 h operating life
- Protection class IP54
- **IntroView** software for 3-D tomographic display
- Operating conditions: -10 °C to 50 °C, < 95% RH
- Error of the depth of a defect, mm, where H is the measured depth =  $\pm (0.05 \cdot H + 10)$



### MIRA (MIR-1000) Tomographer Ordering Numbers

Item	Order #
MIRA system	MIR-1001
IntroView software license	MIR-1003
AC Charger	MIR-1004
USB Cable	MIR-1005
Verification sample plate	MIR-1006
Wheeled carrying case	MIR-1007
Laptop with NVIDIA GeForce graphics card <b>(optional)</b>	MIR-1002



## MIRA 3D

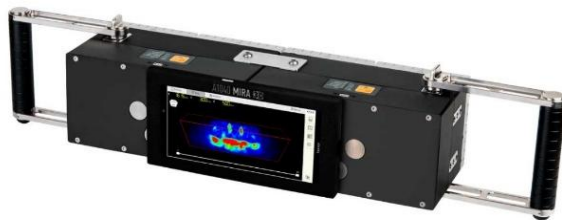
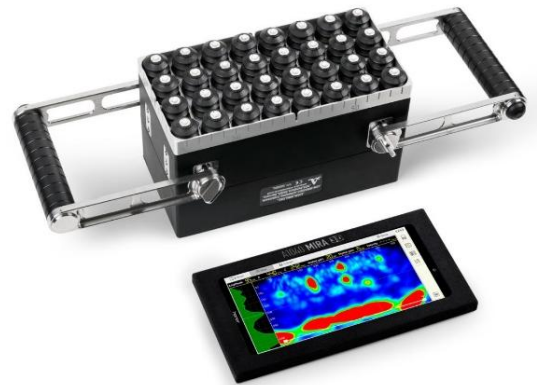
### Purpose

The **MIRA 3D** is the advanced version of the well-known, state-of-the-art, MIRA Ultrasound Tomographer. It creates a three-dimensional representation (tomogram) of internal defects that may be present in a concrete element. **MIRA 3D** is based on the ultrasonic pitch-catch method and uses an antenna composed of an array of active dry point contact (A-DPC) transducers with enhanced penetration depth, which emit shear waves into the concrete and receive them. The 4 by 8 transducer array is under wireless control by a powerful smartphone and the recorded data are analyzed to create a 2-D image of the reflecting interfaces within the cross section below the antenna. A series of 2-D images obtained from the test object can be processed into a complete 3-D reconstruction and displayed on the smartphone's screen. The information can also be transferred to a computer with the **IntroView** imaging software. The software gives additional tools to manipulate the 3-D images for interpretation and reporting of test results.

Furthermore, the best novelty of the **MIRA 3D** is that it also has available an operation mode which uses a technique of data collection known as Full-Matrix-Capture (FMC) where the signal is produced and received by each individual transducer in the antenna array so the pitch-catch, time-of-flight measurements are captured for every possible transmitter-receiver combination in the antenna. Thus, real-time, 3D and cross-sectional visualizations are possible for individual measurements, i.e., at each instrument position (true 3D tomography).

**MIRA 3D** can be used for the following applications:

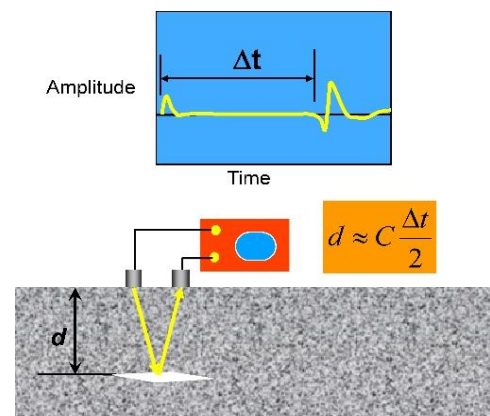
- Thickness measurement
- Detection of voids in grouted tendon ducts
- Detection of poor-quality bond in overlays and repairs
- Detection of delaminations
- Detection of voids and honeycombing in concrete members
- Detection of voids behind tunnel linings and below slabs on ground.
- While not intended for that purpose, **MIRA 3D** is also capable of detecting steel reinforcement.



For better and faster scan coverage, the active aperture of the instrument can be extended by attaching and synchronizing a second antenna array. This enlarged version is the **MIRA 3D PRO**.

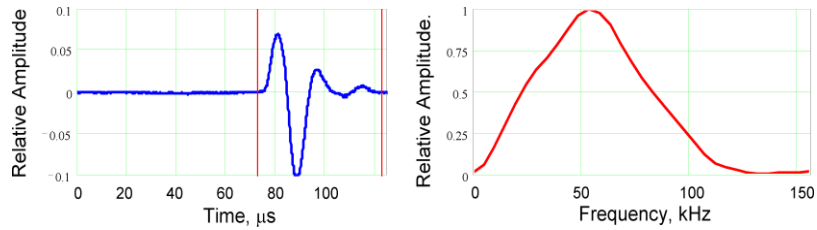
### Principle

**MIRA 3D** is based on the ultrasonic pulse-echo method using transmitting and receiving transducers in a "pitch-catch" configuration as shown on the right. In the pitch-catch method, one transducer sends out a stress-wave pulse and a second transducer receives the reflected pulse. The time from the start of the pulse until the arrival of the echo is measured. If the wave speed  $C$  is known, the depth of the reflecting interface can be calculated as shown (the equation assumes that the two transducers are close to each other).

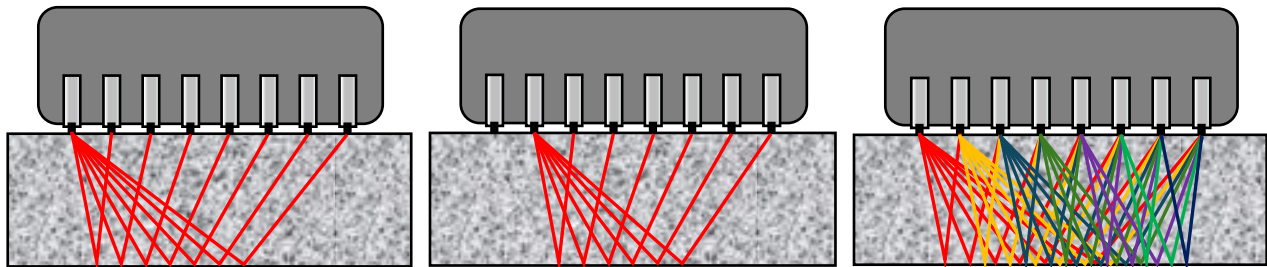


## MIRA 3D

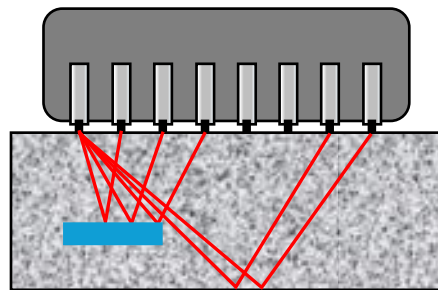
In the **MIRA 3D** system, the antenna is composed of a 4 by 8 array of point transducers and a control unit that operates them. The transducers are heavily damped so that a short duration pulse is created. The plot in blue below shows the typical shape of the received pulse after it has reflected from an air interface. The plot in red to the right shows the amplitude spectrum of the pulse (the nominal center frequency is about 50 kHz but can be varied from 10 to 100 kHz, allowing the user to control both penetration depth and image resolution).



Basically, in the traditional mode of operation, the control unit excites one row of transducers and the other rows of transducers act as receivers. The left side figure below shows the ray paths of the measured transit time of the first row of transducers acting as transmitters and the remaining rows of transducers acting as receivers. Then, as shown in the figure in the center, the next row of transducers is excited and the other rows to the right act as receivers. This process is repeated until each of the rows of transducers has acted as transmitter.



The figure to the right shows the 28 ray paths for the 4 x 8 array that are involved during a measurement at one test location. Data processing and visualization of the B-Scan (2-D image of the cross section below the antenna) are made in real time at each location. The reconstructed image shows the locations of the reflecting interfaces, which could be the opposite side of the member (back wall reflection), reinforcing bars, and most importantly, internal concrete-air interfaces such as voids, cracks, delaminations, etc.



If there is a sufficiently large concrete-air interface, like a defect within the member, a portion of the emitted stress pulse will be intercepted and reflected by the defect instead of traveling all the way to the back wall. As illustrated in the figure to the left, because of the shorter ray paths, reflections from the defect will arrive at the receivers sooner than reflections from the back wall. The instrument uses the arrival times of the reflected pulses to determine the location of the defect within the member.

In the **new MATRIX operation mode** that **MIRA 3D** is also equipped with, the Full-Matrix-Capture (FMC) data collection technique is used together with the processing algorithm known as Total Focusing Method (TFM) to compute the arrival-time data acquired from all directions of the many transducer pairs in the antenna array and directly reconstruct 3D images of the reflecting interfaces within the volume of the object below the antenna at each test position. This “true 3D tomography” system provides greater imaging resolution and precision compared to standard phased array ultrasonic measurements.

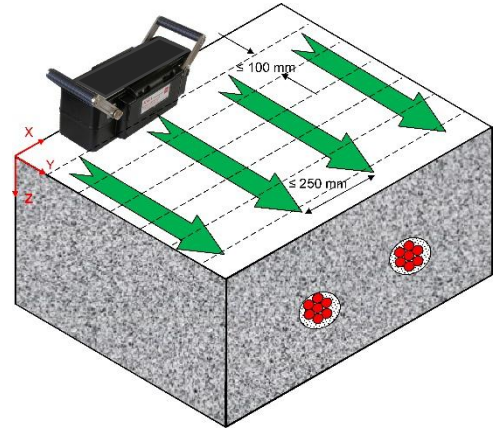




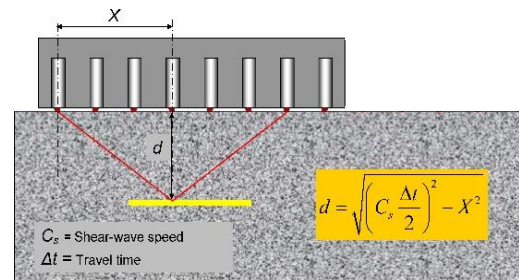
## MIRA 3D

### Full-area Scanning and 3D Reconstruction

To carry out a detailed inspection of a portion of the member, the user lays out a series of parallel scan lines on the testing surface, which are shown as green arrows in the figure on the right. Another series of lines perpendicular to the scan lines is laid out, which are shown as dashed lines. The antenna is oriented perpendicular to the direction of the scan lines and data are recorded at each "vertical step" along each scan line. After taking data along the first scan line, the operator moves to the beginning of the next scan line. This testing grid is then used during image reconstruction to establish the locations of the reflecting interfaces within the test object under the whole scanned area.

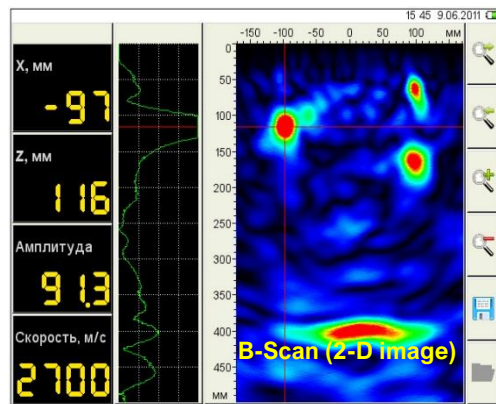


After transit time data are acquired at a test location, the signal processing technique reconstructs the interior of the concrete member at the test location by subdividing the region below the antenna into small discrete elements (analogous to finite elements used for stress analysis). From the pulse arrival times and the known positions of the transmitter-receiver pairs, the depth of the reflecting interface can be established. Because of the inclined ray paths, the depth of the reflector is calculated using the

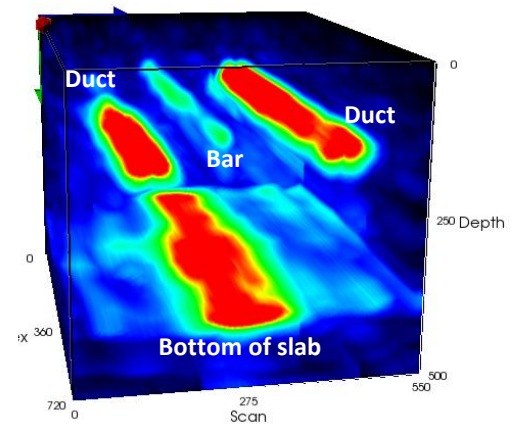


formula for the

relationship between the lengths of the sides of a right triangle. In the formula shown in the above figure,  $C_s$  is the shear wave speed determined by **MIRA 3D** itself at the start of each measurement or the specific value entered by the user in the setup. Volume elements that correspond to locations of reflecting interfaces are assigned a color to indicate intensity of reflection from those elements (constructive superposition). The end result is, depending on the operating mode chosen, either a 2-D or a 3-D image (for classic linear mode or matrix mode, respectively) representing the locations of reflecting interfaces in the region below the antenna at each position on the grid.

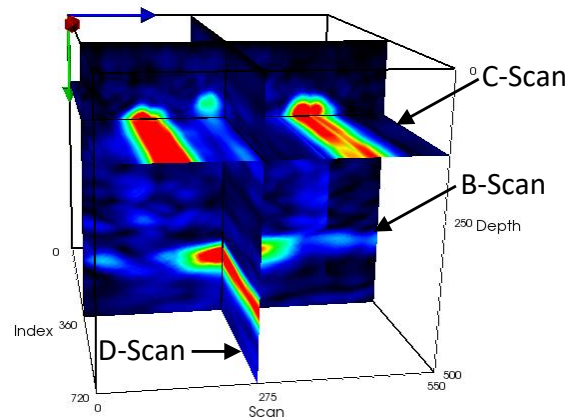
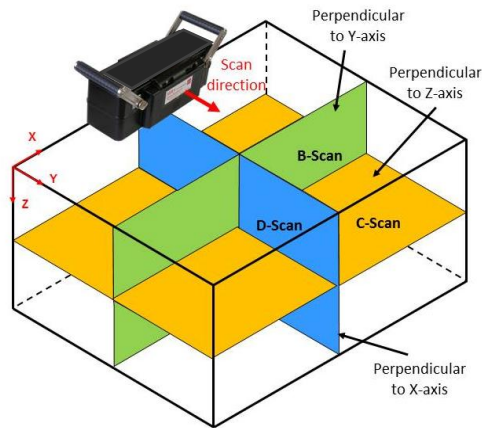


After completion of the measurements over all the points on the testing grid, the individual scans are "stitched" together to create a full 3-D model of the test object that can be visualized directly in the screen of the **MIRA 3D** control unit. Alternatively, the data can also be transferred to a laptop computer that contains the **IntroView** 3-D visualization software. As an example, the figure on the right is the reconstructed 3-D model from a scan of a portion of a slab containing two tendon ducts and a reinforcing bar. The bottom of the slab is indicated.



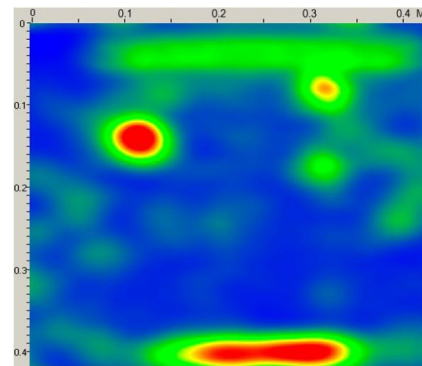
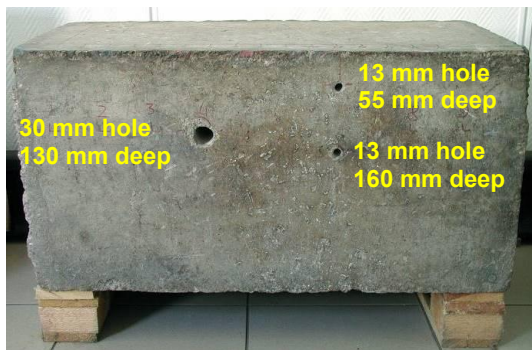
The user can manipulate the 3-D model by rotating it or looking at different orthogonal planes cutting through the model. In left figure below a **C-scan** shows the reflecting interfaces on a plane parallel to the test surface and at different depths (Z-axis); that is, it provides a "plan view" of the reflectors. A **B-scan** provides an "end view" of the reflectors and the **D-scan** provides a side view of the reflectors. The user can look at specific "slices" through the 3-D model by defining

the coordinates of any of the three X, Y or Z axes. For example, the right figure below shows three slicing planes through the 3-D model of the slab with the ducts.



## Examples

**Plain concrete block with holes:** The test object is a 0.8 m x 0.43 m x 0.43 m plain concrete block into which three holes were cast as shown. The scanning was along the top of the block parallel to the direction of the holes. The resulting B-scan image is shown to the right. The three holes are seen clearly and the red band at the bottom represents reflections from the bottom of the block. Because of the inclined ray paths, it is possible to see the deeper 13-mm hole directly below the upper 13-mm hole.



**Testing for voids in grouted cable ducts of bridge girders:** The instrument was used to evaluate the conditions of grouted post-tensioning ducts near the anchorage zone in the webs of a box-girder bridge. Before testing, the locations of the ducts were marked on the face of the web (center photo below). One of the test records is shown below. The B-scan is at the cross section shown as a dashed



*Scanning along web*



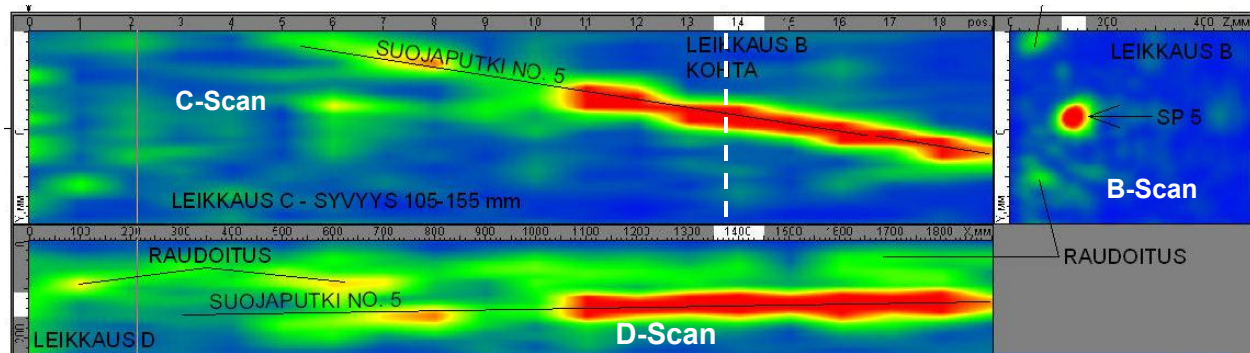
*View of web and drilled core*



*Condition of duct*

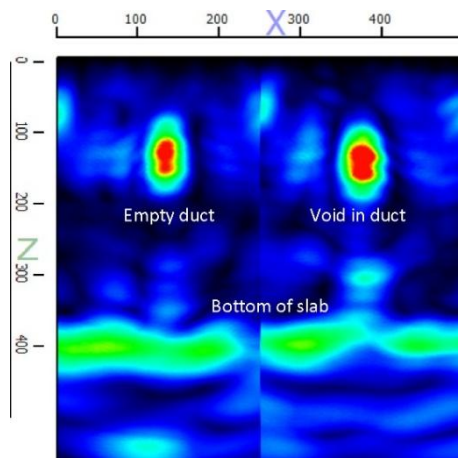
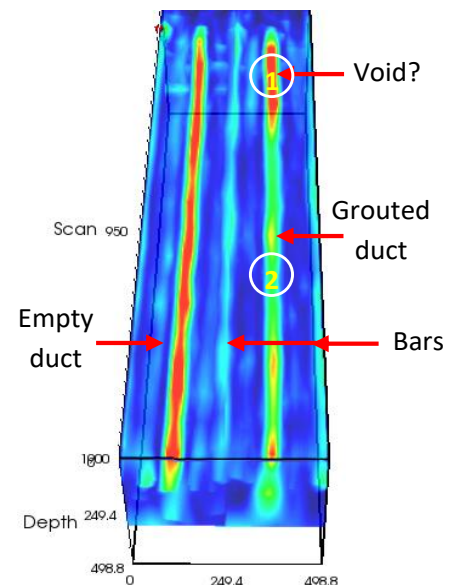


white line in the C-scan. The large amplitude signal in the B-scan at the location of the duct indicated a high probability that the duct was not fully grouted. This was confirmed by drilling a core and carefully removing the duct to reveal bare strands as shown in the photo on the right. (Courtesy of Ramboll Finland Ltd.)



**Tendon Ducts in Slab Specimen:** A 400-mm thick slab-on-ground was cast at the Germann Instruments' facilities in Copenhagen. The slab contains two 100-mm diameter metal tendon ducts with a cover of 100 mm. One duct is empty and the other contains 10 grouted, 16-mm diameter strands. A non-shrink grout was used to prepare the grouted duct specimen, which was then cast into the slab. In addition, ordinary reinforcing bars were located in the top of the slab, parallel to the ducts.

The figure to the right is the 3-D model obtained from scanning the surface of the portion of the slab containing the ducts. The empty duct is displayed with red color, indicating strong reflections from the air interface. The grouted duct is shown in a greenish-yellow color, indicating lower amplitude reflections from the steel strands. The reinforcing bars between the ducts and to the right of the grouted duct are indicated in light blue. It is seen that at the far end of the grouted duct the image of the duct is in red, indicating a strong reflection that is characteristic of an air void.



*B-scan showing a cross section image of slab at location (1) with suspected void in grouted duct*



*The excavated duct at location (1) reveals that some of the strands are not embedded in grout*

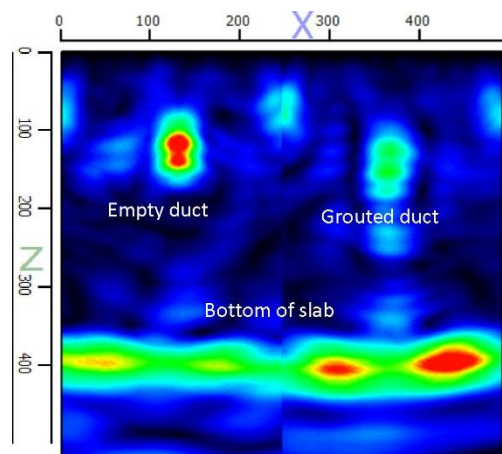


## MIRA 3D

To verify that the duct is not grouted fully, the grouted duct was excavated at two locations: (1) at the end where the air void is indicated and (2) at the approximate mid-length of the duct where no air void is indicated.

The left image is the B-scan at location (1) showing a similar pattern for the empty duct and the grouted duct, which is a strong indication that the pretended grouted duct is not actually fully grouted. The corresponding photo of the excavated duct shows that indeed some of the strands are not embedded in grout. Thus, the presence of the air void is confirmed.

The following shows the results at location 2. The B-scan image shows lower amplitude reflections (from the 10 strands) at the location of the grouted duct compared with the empty duct. The reflection coefficient at the grout-steel interface is lower than at an interface with air, and that is why the grouted duct does not appear in red. The excavated portion of the grouted duct shows that the strands were encased with the grout although this was fractured during the removal of the metal duct.



*B-scan at location (2) with no voids indicated in grouted duct. The excavation reveals the strands encased with grout; some of it was fractured in the process and this exposed some wires.*

### MIRA 3D Specifications

- Active dry point contact (A-DPC), shear-wave transducers with wear-resistant ceramic tips and integrated pulser-receiver electronics
- Spring loaded, 32 transducers, wireless, light and compact antenna array. Extendable to 64 transducers (MIRA 3D PRO)
- The spring-loaded transducers conform to irregular surfaces, and they do not require a coupling medium, that is, testing is done in the dry
- Positioning laser beams in the antenna to facilitate its centering during scanning
- 10 to 100 kHz working frequency range
- Nominal frequency = 50 kHz
- Ultrasound speed range: 1,000 to 4,000 m/s (shear wave)
- Dimensions without handles and weight: 200 × 125 × 100 mm, 3.5 kg (400 × 125 × 100 mm, 5.6 kg for MIRA 3D PRO)
- Testing depth: 20 to 3,000 mm, depending on the concrete quality, member's lateral dimensions and amount of steel reinforcement (20 to 4,000 mm for MIRA 3D PRO)
- Rechargeable battery, 10 h operating life
- USB interface
- 3-D tomographic display in a PC with IntroView software
- Operating conditions: -10 °C to 50 °C, < 95% RH
- Error of the depth of a defect, mm, where H is the measured depth =  $\pm (0.05 \cdot H + 10)$

## MIRA 3D Ordering Numbers

Item	Order #
MIRA 3D control unit and protective case	M3D-1001
MIRA 3D antenna array	M3D-1002
Adjustable handle x 2	M3D-1003
Type C, AC Charger x 2	M3D-1004
USB Type C data cable x 2	M3D-1005
USB-A to USB-C cable	M3D-1006
Verification sample plate	M3D-1007
Exchangeable battery pack (inside the antenna)	M3D-1008
Carrying case	M3D-1009
IntroView software license	MIR-1003
Laptop with NVIDIA GeForce graphics card ( <b>optional</b> )	MIR-1002



## MIRA 3D PRO Ordering Numbers

Item	Order #
MIRA 3D control unit and protective case	M3D-1001
MIRA 3D antenna array x 2	M3D-1002
Adjustable handle x 2	M3D-1003
Type C, AC Charger x 2	M3D-1004
USB Type C data cable x 2	M3D-1005
USB-A to USB-C cable	M3D-1006
Verification sample plate	M3D-1007
Exchangeable battery pack x 2 (inside the antenna)	M3D-1008
Carrying case	M3D-1009
H-Fastener	M3D-1010
M6x10 stainless screw x 4	M3D-1011
IntroView software license	MIR-1003
Laptop with NVIDIA GeForce graphics card ( <b>optional</b> )	MIR-1002



## Purpose

The use of traditional ultrasonic pulse velocity testers to identify the presence of anomalies in structures requires access to both faces of a member and it is not possible to determine the depth to anomalies. These drawbacks are eliminated by using the impact-echo method, which requires access to only one face. The impact-echo method is based on monitoring the periodic arrival of reflected stress waves and is able to obtain information on the depth of the internal flaws or the thickness of a solid member.

The **Mirador** is a versatile, portable system, empowered by **Echolyt** software (see datasheet), based on the impact-echo method, that can be used for the following applications:

- Measure the thickness of pavements, asphalt overlays, plate-like concrete elements like slabs or walls, etc.
- Detect the presence and depth of voids and honeycombing
- Detect voids below slabs-on-ground
- Evaluate the quality of grout injection in post-tensioning cable ducts or joints for precast elements
- Integrity of a membrane below an asphalt overlay protecting structural concrete
- Delamination surveys of bridge decks, piers, cooling towers, chimneystacks, etc.
- Detect debonding of overlays and patches
- Detect ASR damage and freezing-and-thawing damage
- Measure the depth of surface-opening cracks
- Estimate early-age strength development (with proper correlation)

## Principle

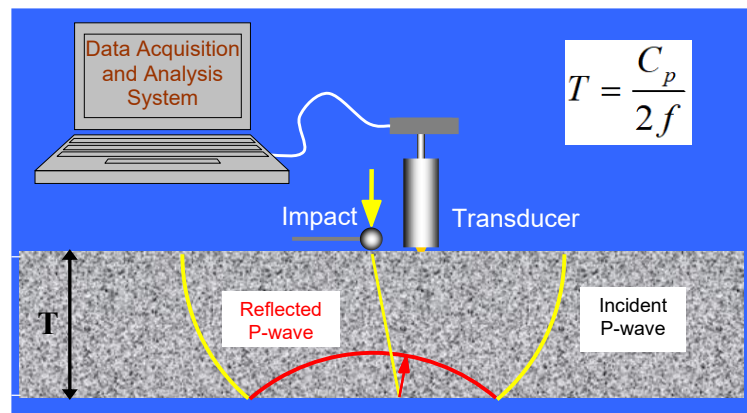
A short-duration stress pulse is introduced into the member by a small mechanical impact. This impact generates stress waves that propagate away from the impact point. A surface wave (R-wave) travels along the top surface, and a P-wave and an S-wave travel into the member. In impact-echo testing, the P-wave is used to obtain information about the member.

When the P-wave reaches the back side of the member, it is reflected and travels back to the surface where the impact was generated. A sensitive displacement transducer next to the impact point picks up the disturbance due to the arrival of the P-wave. The P-wave is then reflected back into the member and the cycle begins again. Thus, the P-wave undergoes multiple reflections between the two surfaces and the recorded waveform of surface displacement has a periodic pattern that is related to the thickness of the member and the wave speed.

A sensitive displacement transducer next to the impact point picks up the disturbance due to the arrival of the P-wave. The P-wave is then reflected back into the member and the cycle begins again. Thus, the P-wave undergoes multiple reflections between the two surfaces and the recorded waveform of surface displacement has a periodic pattern that is related to the thickness of the member and the wave speed.

The displacement waveform is transformed into the frequency domain to produce an **amplitude spectrum**, which shows the predominant frequencies in the waveform. The frequency of P-wave arrival is determined as the frequency with a high peak in the amplitude spectrum. The thickness ( $T$ ) of the member is related to this thickness frequency ( $f$ ) and wave speed ( $C_p$ ) by the simple approximate equation shown on the image.

The same principle applies to reflection from an internal defect (delamination or void). Thus, the impact-echo method is able to determine the location of internal defects as well as measure the thickness of a solid member.

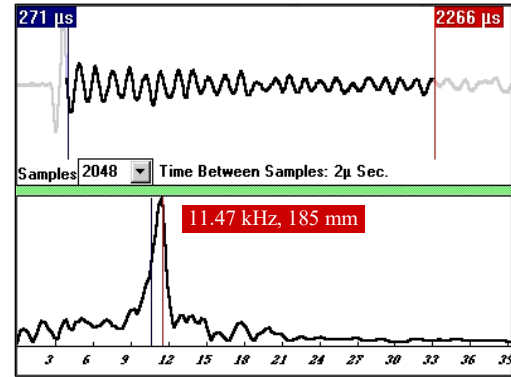




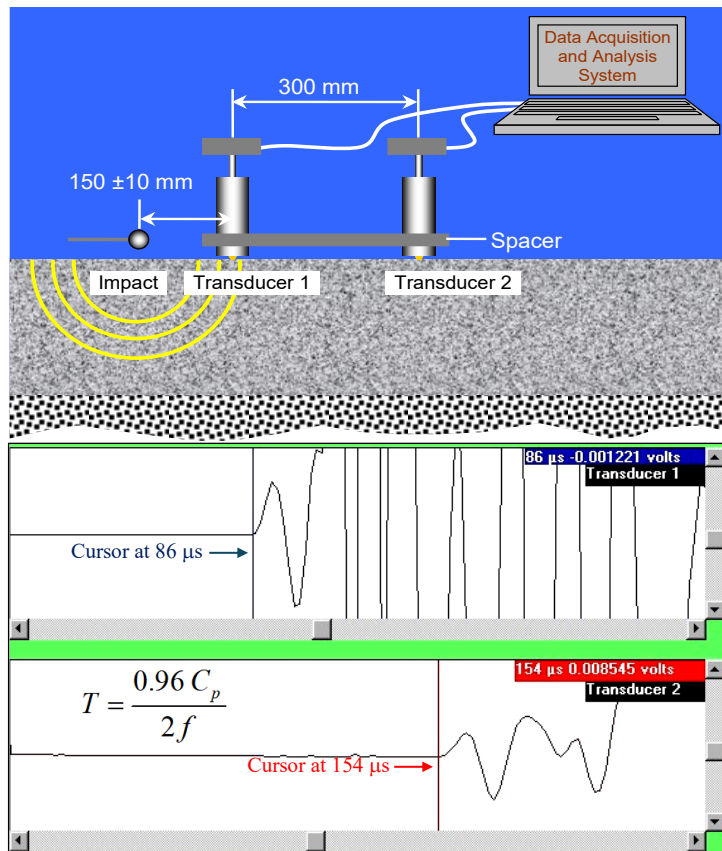
## Example

The upper plot in this example shows the surface displacement waveform (displacement vs time) obtained from a test of a solid concrete slab. The figure below is the amplitude spectrum (amplitude vs frequency) obtained by transforming the waveform into the frequency domain by applying the Fast Fourier Transform algorithm. The peak at 11.47 kHz (red cursor) is the thickness frequency. For a measured wave speed of 4240 m/s, this frequency corresponds to a thickness of:

$$4240 / (2 \times 11,470) = 0.185 \text{ m, or } 185 \text{ mm.}$$



## Thickness Measurement by ASTM C1383



Accurate measurement of thickness requires knowledge of the in-place P-wave speed. ASTM C1383, "Test Method for Measuring the P-Wave Speed and the Thickness of Concrete Plates Using the Impact-Echo Method," permits two methods for obtaining the P-wave speed. One method is by determining the thickness frequency and then measuring the actual plate thickness at that point. The equation in this case is solved for  $C_p$ , i.e.,  $C_p = 2 f T$ .

Alternatively,  $C_p$  can be determined by measuring the time for the P-wave to travel between two transducers with a known separation. With the **LONGSHIP** assembly, the transducers are placed 300 mm apart and the impactor is about 150 mm from one of the transducers one the line passing through the transducers. The distance L (300 mm) between the transducers, is divided by time difference  $\Delta t$  between arrival of the P-wave at the second and first transducers. In the figure on the left,  $\Delta t$  was measured to be  $154 - 86 = 67 \mu s$ , and the P-wave speed is  $0.3 / 0.000067$

= 4480 m/s. If the wave speed is determined by the surface measurement method, the resulting value is multiplied by 0.96 when it used to calculate thickness <sup>[1]</sup>.

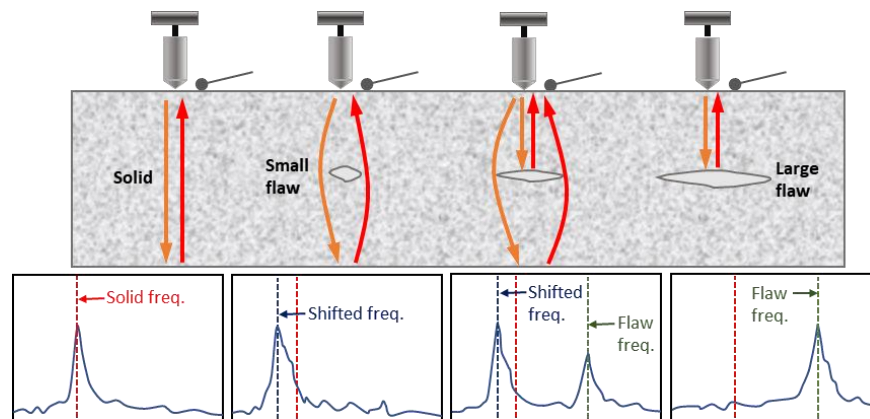
## Detection of Internal Defects

The P-wave generated by impact will reflect at interfaces within the concrete where there is a change in **acoustic impedance**, which is defined as the product of the density and wave speed of a material. The following table lists the reflection coefficients of a P-wave travelling through concrete and incident normal to an interface with air, water, soil, or steel. A negative reflection coefficient means that the stress changes sign when the stress wave is reflected; for example, a compressive stress would be reflected as a tensile stress. Steel is "acoustically harder" than concrete and the stress does not change sign when reflected at a concrete-steel interface.

Interface	Reflection Coefficient
Concrete-air	-1.0
Concrete-water	-0.65 to -0.75
Concrete-soil	-0.3 to -0.9
Concrete-steel	0.65 to 0.75

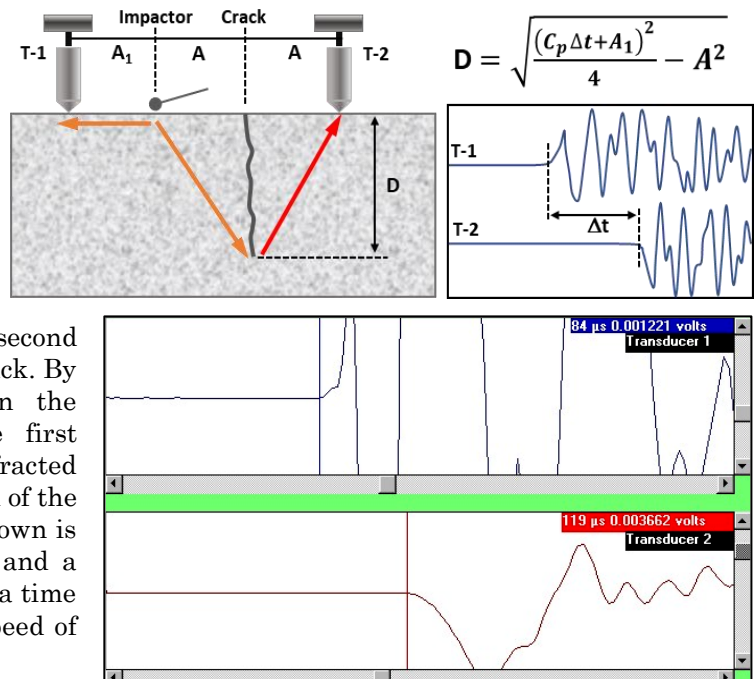
It is seen that at a concrete-air interface, there is complete reflection of the P-wave (1.0 = 100%). This makes the impact-echo method inherently powerful for detecting air interfaces, such as those due to cracks, delaminations, cavities, and honeycombed concrete. If the area of the reflecting interface is large, the impact-echo response will be similar to that of a solid plate except that the thickness frequency will be shifted to the higher value corresponding to the depth of the interface. If the defect is just large enough to be detectable, the amplitude spectrum will show two peaks: a high frequency

peak corresponds to reflection from the interface and the low frequency peak corresponds to the portion of the P-wave that travels around the defect and reflects from the opposite surface of the plate. The frequency associated with the portion of the P-wave that travels around the defect will be shifted to a lower frequency value than the solid plate thickness frequency. This is because the wave has to travel a longer distance as it diffracts around the flaw. The frequency shift is a good indicator of the presence of a flaw if it is known that the plate thickness is constant.



### Depth of Surface-Opening Cracks

The **Mirador** can also be used to measure the depth of surface-opening cracks, using a time domain analysis. The **LONGSHIP** is used with the transducers on opposite sides of the crack and the impact is generated on the line passing through the transducers. When the P-wave reaches the tip of the crack, the crack tip acts as a P-wave source by **diffraction**. The diffracted P-wave is detected by the second transducer on the opposite side of the crack. By measuring the time interval between the arrival of the direct P-wave at the first transducer and the arrival of the diffracted wave at the second transducer, the depth of the crack can be calculated. The example shown is from testing a fire-damaged structure, and a crack depth of 87 mm was estimated for a time difference ( $\Delta t$ ) of 35  $\mu s$  and a P-wave speed of 3155 m/s.



## Testing Examples



*Detection of delaminations and honeycomb in sewer pipe*



*Measurement of P-wave speed by surface method*

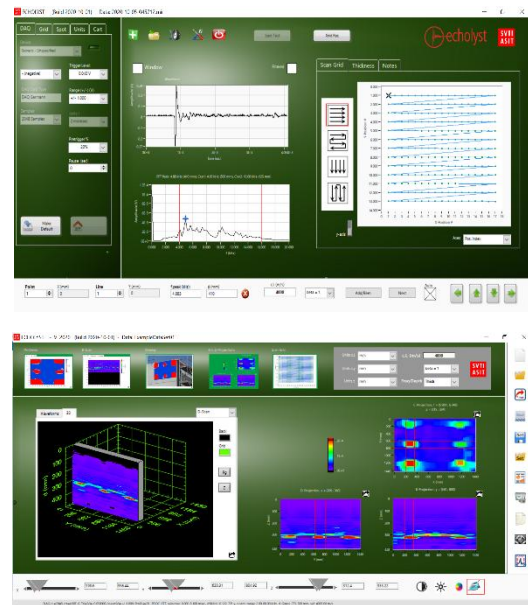


*Testing for quality of grout injection in cable ducts*

## Mirador Specifications

- Data Acquisition System:
  - 2 channels, 4 MB/channel
  - 8 bits resolution, 50 MHz bandwidth
  - -5V to 5V Input Voltage Range
  - USB interface
- Dry contact, high sensitivity, piezoelectric handheld transducers
- Equipped with **Echolyst** software that allows:
  - real-time waveform display while testing
  - create 2-D and 3-D visual representations
  - look at reflecting interface on different cutting planes
  - audio assisted prompts to speed up data acquisition
  - superimpose test results on real image of test location
  - report generation
- Accuracy (assuming a constant P-wave speed):
  - Thickness measurement, direct calibration:  $\pm 2\%$
  - Thickness measurement by surface P-wave speed measurement:  $\pm 3\%$
  - Depth of surface-opening cracks:  $\pm 4\%$
- Operating conditions: Temperature:  $-10$  to  $50$  °C, RH  $\leq 95\%$

## Echolyst screenshots



## Marador Ordering Numbers

Mirador-3000	Mirador-5000
With <b>Echolyst</b> Software and one Mark IV transducer for flaw detection and thickness measurements.  Can be later upgraded to Mirador-5000	With <b>Echolyst</b> Software and <b>LONGSHIP</b> assembly with two Mark IV transducers for flaw detection, thickness measurement, crack depth measurement, and P-wave speed measurement according to ASTM C1383.



## Mirador -3000

Item	Order #
Laptop computer	MRD-10
Data acquisition module with USB cable	MRD-20
<b>Echolyst</b> software	MRD-30
Mark IV transducer	MRD-40
Star support with 5, 8 and 12 mm impactors	MRD-60
Impactors on spring rods, 5, 8, and 12 mm	MRD-70
Protection caps for transducer tips, 4 pcs	MRD-80
BNC cable	MRD-90
User Manual for <b>Echolyst</b> software	MRD-150
Operation manual	MRD-160
Attaché case	MRD-120



## Mirador-5000

Item	Order #
Laptop computer	MRD-10
Data acquisition module with USB cable	MRD-20
<b>Echolyst</b> software	MRD-30
Viking <b>LONGSHIP</b> with long handle and two Mark IV handheld transducers	MRD-50
Star support with 5, 8 and 12 mm impactors	MRD-60
Impactors on spring rods, 5, 8, and 12 mm	MRD-70
Short handle for crack depth measurement	MRD-80
Protection caps for transducer tips, 8 pcs	MRD-90
BNC cable, 2 pcs.	MRD-100
Manual for <b>Echolyst</b> software	MRD-150
Operation manual	MRD-160
Attaché case	MRD-130



### Optional Items

#### **Spider**, Order # MRD-210

The **Spider** contains 8 spherical impactors, with diameters ranging from 2 mm to 15 mm and covering a frequency content from approximately 1.2 kHz to 100 kHz on a hard concrete surface.



### References

[1] The explanation for the 0.96 factor can be found in: Gibson, A. and Popovics, J.A., 2005, "Lamb Wave Basis for Impact-Echo Method Analysis," *J. of Engineering Mechanics* (ASCE), Vol. 131, No. 4, pp. 438-443.

## Purpose

The **Profile Grinder** is used to obtain concrete powder samples by precision grinding at small depth increments for accurate determination of the chloride ion profile for the following applications:

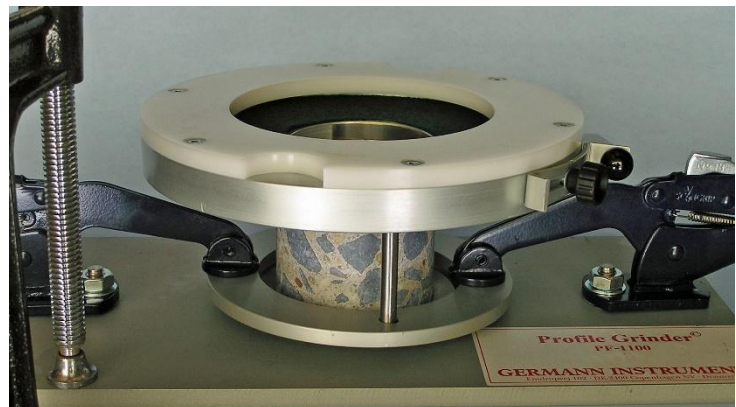
- Following immersion of specimens in a chloride solution in the laboratory, e.g., according to NT Build 443 "Concrete, Hardened: Accelerated Chloride Penetration" or ASTM C1556 "Test Method for Determining the Apparent Chloride Diffusion Coefficient of Cementitious Mixtures by Bulk Diffusion"
- Directly on-site on existing structures that have been exposed to chloride ion ingress or on cores extracted from them.

From the chloride ion content profile, the chloride ion diffusion coefficient can be estimated in accordance with ASTM C1556 or NT Build 443 and used for estimating the remaining service life.

## Principle

A high performance grinding bit, 18 mm in diameter, grinds the concrete to a fine powder at exact depth increments, which can be selected between 0.5 mm to 2.0 mm. The bit is attached to a grinding machine that is held against the surface by a support plate. Grinding is accomplished by rotating the grinder within the support plate so that the bit removes a circular portion of the surface. The grinding area is 73 mm in diameter and the maximum depth is 40 mm. For **in-situ testing**, the **Profile Grinder** can be attached to horizontal or vertical surfaces using the anchor bolts and clamping pliers shown in the image on the right. On horizontal surfaces, the powder produced at each depth increment is collected with a battery-operated vacuum cleaner (Dust Buster) containing a re-usable filter. On a vertical face, the powder at each depth increment is collected in a plastic bag attached to the grinding plate, as shown to the right. For every depth increment of 1 mm, approximately 9 grams of powder is obtained for analysis. It takes 4 to 6 minutes to obtain each sample and about 5 minutes to determine the chloride content using the **RCT Kit** (see **RCT** data sheet for details).

For **laboratory testing**, a grinding bench plate is available to permit profile grinding of small specimens, e.g. 100 mm in diameter. These can be specimens molded in the laboratory and used in diffusion testing such as ASTM C1556 of NT Build 443, or cores drilled directly from the structure.



## Data Analysis

For laboratory tests in accordance with ASTM C1556 or NT Build 443, the chloride content profile obtained after a given period of immersion in the specified chloride solution is subjected to regression

analysis to obtain the apparent chloride diffusion coefficient. The testing condition is assumed to result in one-dimensional diffusion and the chloride ion content as a function of depth is assumed to obey the following solution to Fick's second law of diffusion (1):

$$C(x,t) = C_s - (C_s - C_i) \operatorname{erf}\left(\frac{x}{2\sqrt{D_a t}}\right) \quad (1)$$

where,

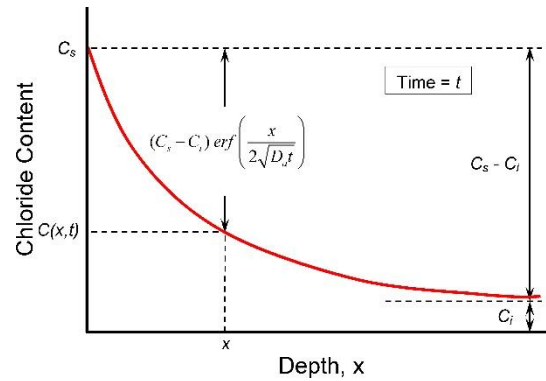
$C(x,t)$  = the chloride ion concentration at a depth  $x$  in mm from the exposed surface for an elapsed time  $t$  in years since the start of chloride exposure;

$C_s$  = the chloride concentration at the surface, expressed as a % of concrete mass;

$C_i$  = the initial (or background) chloride concentration of the concrete, expressed as a % of concrete mass;

$\operatorname{erf}$  = the error function (a special function related to the integral of the normal probability function); and

$D_a$  = the apparent chloride diffusion coefficient in  $\text{mm}^2/\text{year}$



Equation (1) describes the variation of chloride ion content as a function of the distance  $x$  from the surface after an elapsed time  $t$  since initial exposure to a constant surface chloride concentration of  $C_s$ . This function is shown as the red curve in the above figure. The values of the equation parameters ( $C_s$ ,  $C_i$ , and  $D_a$ ) are determined using least-squares curve fitting, which can be implemented using for example the "Solver" function in Microsoft Excel or using statistical software that permits general non-linear regression analysis. The value of  $C_i$  would be zero (0) if there is no background chloride present initially in the concrete.

The diffusion coefficient in research reports is reported often in units of  $10^{-12} \text{ m}^2/\text{s}$ . To convert to units of  $\text{mm}^2/\text{y}$ , multiply by  $3.15576 \times 10^{13}$ . For good quality concrete, typical values of the chloride diffusion coefficient are 10 to 100  $\text{mm}^2/\text{y}$ .

## Service Life Estimation

A common application of the **Profile Grinder** is to obtain powder samples from existing structures to establish the exiting chloride profile. If the structure has been exposed to moist conditions so that diffusion has been the primary transport mechanism for chloride ions, Eq. (1) can be fitted to the data to obtain an apparent chloride diffusion coefficient. If it is assumed that the surface chloride concentration and diffusion coefficient do not change in the future, Eq. (1) can also be used to estimate the chloride ion content at the depth of the reinforcement at a particular time in the future. Thus it is possible to determine at what time  $t$ , the chloride content at the depth of the reinforcement would reach the **chloride ion threshold** for initiation of corrosion.

## Chloride Ion Threshold

There is no single unique value for the amount of chlorides in concrete that will breakdown the protective oxide film and initiate corrosion of steel reinforcement. The value depends on many variables, among others, the exposure conditions, the water-cementitious materials ratio, the types of cementitious materials in the concrete, etc. (1, 2, 3). The figure to the right shows a proposed equation for estimating the chloride ion threshold based on the exposure condition and the amounts of cement ( $C$ ), water ( $W$ ), fly ash ( $FA$ ), and silica fume ( $SF$ ) in the concrete (1). For example, for a concrete with  $w/cm = 0.4$ , with 15 % of the binder being fly ash and 5 % being silica

$$C_{cr} = k e^{-1.5 (w/c)_e}$$

$$(w/c)_e = \frac{W}{C - 1.4 \times FA - 4.7 \times SF}$$

$C_{cr}$  = Chloride threshold percent mass of binder  
 $(w/c)_e$  = Equivalent  $w/cm$   
 $k$  = 1.25 for marine exposure and splash zone  
 $k$  = 3.35 for submerged in seawater



fume, and exposed to a splash zone, the chloride ion threshold is estimated to be about 0.23 % of the mass of the binder.

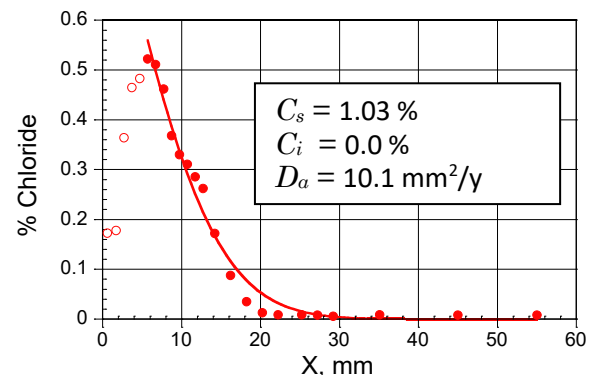
In the literature, the threshold chloride ion content may be expressed in different units. In the U.S., it is commonly expressed in terms of mass of chloride per unit volume of concrete. In Europe, it is commonly expressed as a mass percentage of chloride per mass of binder (the cementitious materials). The chloride ion content measured with the **RCT Kit** (see data sheet) is in terms of mass percentage of chloride per mass of concrete. To convert from a threshold value expressed as a mass percentage of binder to a value expressed as a mass percentage of concrete, it is necessary to multiply the former by the ratio of binder content (in  $\text{kg/m}^3$ ) to the density of the concrete. For example, if the binder content is  $450 \text{ kg/m}^3$  and the concrete density is  $2250 \text{ kg/m}^3$ , a threshold chloride ion content expressed as 0.23 % of binder would be  $0.23 (450/2250) = 0.046 \%$  of the mass of concrete, or approximately 0.05 %.

## Testing Example

The following example illustrates the analysis of the chloride profile obtained from a structure exposed to marine environment for 5 years. The **Profile Grinder** was used to obtain powder samples at approximately 1-mm depth increments. As the powder samples were obtained, chloride content was determined on site using the **RCT Kit**.



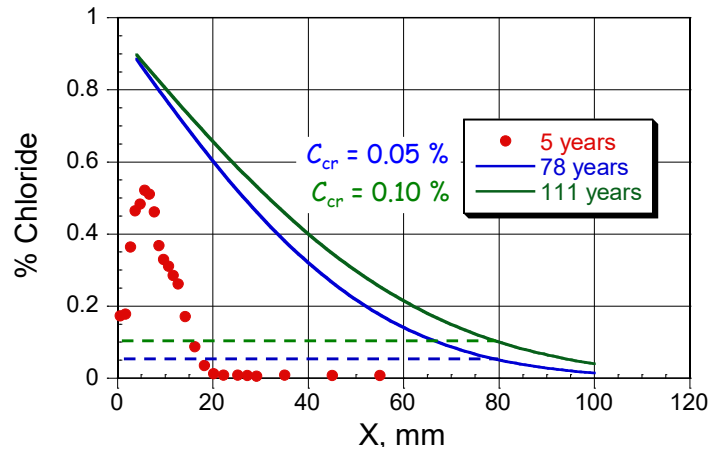
The data points in plot on the right show the measured chloride content profile expressed as % mass of concrete. It is seen that the first points within the outer 5 mm show less chloride than expected based on the diffusion model given by Eq. (1). Several explanations have been proposed for this behavior, such as washout by exposure to rain and an interaction effect due to carbonation. In any case, the data points shown as open circles were neglected in doing the least-squares regression analysis to obtain the best-fit values of the three parameters in Eq. (1), which are shown within the box. It is seen that background chloride content is 0 % and the apparent chloride diffusion coefficient is  $10.1 \text{ mm}^2/\text{y}$ .



The nominal depth of cover for the structure is 80 mm. Based on the assumption that the surface chloride ion concentration and chloride diffusion coefficient do not change with time, calculations can be done to estimate the remaining service life, which is defined as when the chloride content reaches the threshold value at the reinforcement depth. Two values of threshold chloride concentration were used 0.05 % and 0.10 %. By trial and error, the exposure time,  $t$ , was determined when the chloride content at  $x = 80 \text{ mm}$  would reach the threshold values. The results are shown in the graph on the next page. Thus it is concluded that the remaining service life is in the range of 80 to 110 years. Keep in mind that these estimates of remaining service life are approximate values and based on several simplifying assumptions:

- Chloride migration is governed by diffusion
- The apparent diffusion coefficient does not change with time
- The concentration of chloride at the surface remains constant
- Effects of temperature and chloride binding are not considered

In practice, the chloride profile in the structure should be reevaluated at regular intervals in the future. This will allow updating the effective chloride ion diffusion coefficient and calculating a new expected service life.



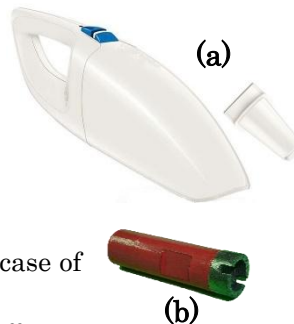
The curves in green and blue are the chloride ion profiles calculated using Eq. (1) for the times that would result in the threshold chloride content at a depth of 80 mm

## References

- (1) Poulsen, E. and Mejlbro, L., **Diffusion of Chlorides in Concrete, Theory and Application**, Modern Concrete Technology Series, Taylor and Francis, 2006, ISBN13: 9-78-0-419-25300-6
- (2) Nilsson, L.O., Sandberg, P., Poulsen, E., Tang, L.M. Andersen, A. and Frederiksen, J.M., "A System for Estimation of Chloride Ingress into Concrete: Theoretical Background," HETEK Report 83, 1997, <http://www.hetek.teknologisk.dk/english/16507>
- (3) Frederiksen, J.M. and Poulsen, E. "Chloride penetration into concrete—Manual," HETEK Report 123, 1997, <http://www.hetek.teknologisk.dk/english/16507>

## Profile Grinder Specifications

- No-load speed: 2,500 – 8,700 rpm
- Rated input power: 950 W
- Output power: 510 W
- Thumbwheel for speed selection
- Electronic overload protection
- Electronic safety motor shutdown in case of unexpected stop
- Grinding diamond bit diameter: 18 mm
- Depth increments: 0.5 to 2.0 mm ( $\pm 2\%$ )
- Maximum grinding depth: 40 mm
- Grinding area: 4,185 mm<sup>2</sup> (73 mm diameter)
- Powder sample:  $\approx 9$  g per each mm of grinded depth



## Profile Grinder Kit (PF-1100) Ordering Numbers

Item	Order #
Grinder unit consisting of grinding machine, housing, handle cover with flange and counter nut, two handles and grinding diamond bit	PF-1101
Grinding support plate with green felt	PF-1102
Grinding bench plate with screws and nuts	PF-1103
Attachment ring and two bolts	PF-1104
Allen key, 4 mm	CC-25
2 adjustable clamping pliers	C-102-3
Set of anchoring tools	CC-30
2 seating rubber rings	PF-1105
Plastic bags, 50 pcs	PF-1106

Item	Order #
Brush	PF-1107
Measuring tape	RCT-1028
14 and 17 mm wrenches	C-155/151
Sponge	PF-1108
Dust mask	PF-1109
Silicone oil bottle	L-24
Spare green felt	PF-1111
User Manual	PF-1112
<b>Optional Items</b>	
Dust Buster, portable vacuum cleaner (a)	PF-1200
PF-1110 Spare grinding diamond bit (b)	PF-1110

## Purpose

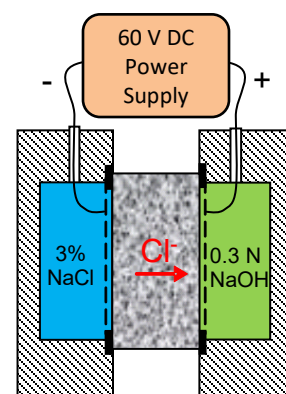
The **PROOVE'it** system is used to evaluate the resistance of concrete to the ingress of chloride ions in 3 ways:

- By determining the total electrical charge that passes through a saturated concrete specimen by applying an electrical potential across the specimen in accordance with AASHTO T 277 or ASTM C1202. This is known as the "Rapid Chloride Permeability Test (RCPT)" or as the "Coulomb test".
- By measuring the penetration depth of chloride ions, after an electric potential is applied to the specimen in accordance with Nordtest Build 492 or EN 12390-18 to determine the "Chloride Migration Coefficient," which can be used to estimate the chloride diffusion coefficient for service life estimations.
- By measuring the current passing through a saturated concrete specimen and determining the bulk conductivity in accordance with ASTM C1760.

## Principles

### ASTM C1202: RCPT Test

ASTM C1202 "Standard Test Method for Electrical Indication of Concrete's Ability to Resist Chloride Ion Penetration" is actually a test of electrical conductance, rather than chloride permeability as it is often stated. In this test, a water-saturated concrete specimen, nominally 100 mm diameter and 50 mm thick, is positioned in a test cell (right) containing fluid reservoirs on both ends of the specimen. One reservoir is filled with a 3 % NaCl solution and the other with a 0.3N NaOH solution. An electrical potential of 60 VDC is applied across the cell. The negative terminal of the potential source is connected to the electrode in the NaCl solution and the positive terminal is connected to the electrode in the NaOH solution. The negatively charged ions will migrate towards the positive terminal resulting in current through the specimen.



The more permeable is the concrete, the more negative ions will migrate through the specimen, and a higher current will be measured. The current is measured for 6 hours and the area under the curve of current versus time is determined, which represents the total charge or Coulombs passed across the specimen. Test results are corrected for a standard specimen diameter of 95 mm. The Coulomb values are used for classifying the concrete as follows (ASTM C1202):

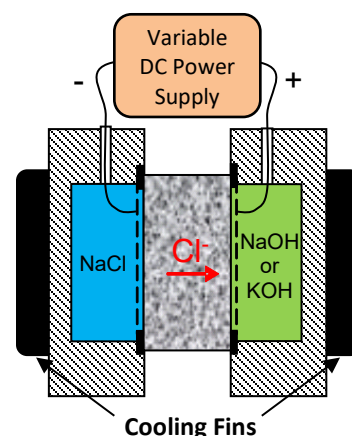
**Table 1**

Coulombs	Permeability Class	Typical of
>4000	High	$w/c^* > 0.5$
4000-2000	Moderate	$w/c = 0.4$ to $0.5$
2000-1000	Low	$w/c < 0.4$
1000-100	Very Low	Latex-modified concrete
<100	Negligible	Polymer concrete

\* $w/c$  = water-cement ratio

### NT Build 492 or EN 12390-18: Chloride Migration Test

The electrical conductivity of concrete is related to its diffusion coefficient. To use **PROOVE'it** for the NT Build 492 or EN 12390-18 "Chloride Migration Coefficient from Non-Steady State Migration Experiments". While there are some differences between the two test methods, the general procedure consists in filling the reservoir surrounding the negative terminal with a solution rich in NaCl and the reservoir surrounding the positive terminal is filled with a NaOH or KOH solution. An initial 30 VDC potential is applied across the specimen, and the corresponding current is measured. Based on this measurement, the test voltage and test duration are selected accordingly, with the intention that the chloride penetration reaches a





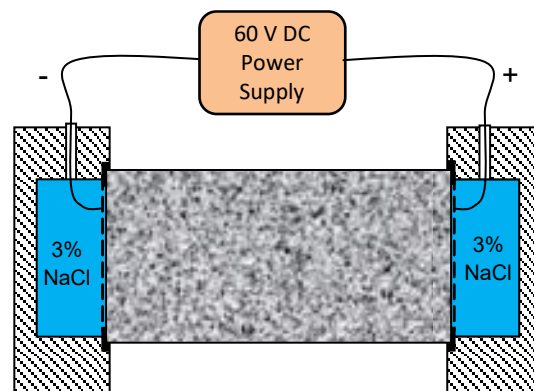
depth of between 10 and 30 mm. After the test is completed, the specimen is split, and the chloride ion penetration is measured by spraying the split surface with a 0.1 M silver nitrate solution, which precipitates as white AgCl where chlorides are present. From the penetration depth and test conditions, the chloride ion migration coefficient is calculated. Because, it is required to maintain a constant temperature in the solutions in the reservoirs, the measuring cells with cooling fins (Part No. PR-1100) are recommended for this test.

There is also an AASHTO test method TP-64, "Standard Method of Test for Predicting Chloride Penetration of Hydraulic Cement Concrete by the Rapid Migration Procedure," that uses the same procedure as NT Build 492. The test result, however, is reported as a rate of penetration, by dividing the depth of penetration, in mm, by the product of applied voltage (V) and the test duration (h).

### ASTM C1760: Bulk Electrical Conductivity

ASTM C1760, "Standard Test Method for Bulk Electrical Conductivity of Hardened Concrete," involves the same basic testing procedure as ASTM C1202, with the following exceptions: 1) both reservoirs contain the 3 % NaCl solution; 2) the specimen length (  $L$  ) can be up to 200 mm; and 3) the current (  $I$  ) is measured for just 1 minute. With the area of the cross section of the specimen (  $A$  ), the bulk electrical conductivity (  $\sigma$  ) in millisiemens per meter is calculated:

$$\sigma = \frac{I}{V} \cdot \frac{L}{A}$$



Bulk conductivity is related directly to the charge passed through a specimen as measured by ASTM C1202, provided that the current remains constant during the 6 h test duration. If we assume that is valid, the ASTM C1202 coulomb limits can be converted into bulk conductivity limits:

**Table 2**

Charge passed using ASTM C1202, Coulombs <sup>†</sup>	Bulk Conductivity mS/m
50	0.27
100*	0.54
1,000*	5.44
2,000*	10.89
4,000*	21.77
10,000	54.43

<sup>†</sup>It is assumed that current is constant during the 6 h test duration, which is typically not true for high conductivity concrete. Specimen length of 50 mm and a diameter of 95 mm.

\*Limiting values in ASTM C1202 used to define different categories of "chloride ion penetrability" (Table 1)

### Variability

The repeatability of the RCPT or Coulomb Test is reported to be about 12 % (ASTM C1202), and the repeatability of the migration test is reported to be about 9 % (NT Build 492).

### Testing Examples

**RCPT:** The next image shows the screen display showing the details when **PROOVE'it** is used for the RCPT test (ASTM C1202). The "Status" line for the eight cells indicates OFF, ON, or FIN, depending on whether power to the cell is turned off, if the cell is operating, or if the test has finished. The "Actual voltage" line indicates the test voltage, which has to be the same for all cells. The "Actual current" line indicates the instantaneous current during testing. Readings are updated every 5 seconds. The "Temperature" line indicates the instantaneous temperature in the reservoir solutions

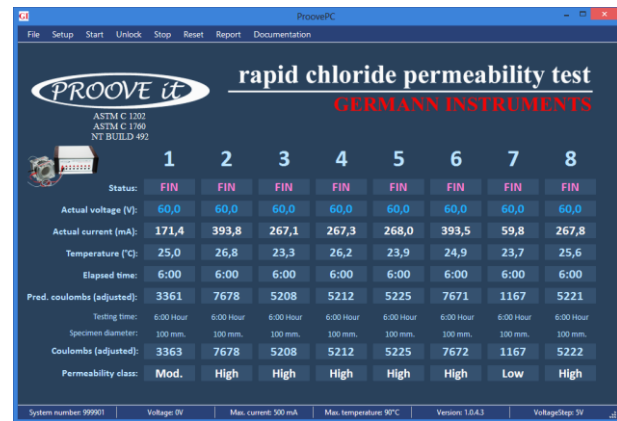
during testing if temperature probes are used. “Elapsed time” indicates the cumulative time since the cell was turned on. The “Pred. coulombs (adjusted)” line indicates the predicted Coulombs at 6 hours, which are estimated continuously every 5 minutes while the test is running. “Testing time” indicates the selected testing time, and the “Specimen diameter” indicates the actual diameter of the specimen. The “Coulombs (adjusted)” line indicates the measured Coulombs at any time during testing, which have been adjusted for a specimen diameter of 95 mm as required by ASTM C1202; so when the test ends, it indicates the test result. The last line shows the “Permeability class” according to ASTM C1202 (Table 1).

**Migration:** For using **PROOVE'it** to determine the chloride migration coefficient, a two-step process is used. First the cells are set up for a voltage of 30 V and the initial current is recorded. Based on the initial current, the operator selects the test voltage and test duration in accordance with NT Build 492 or EN 12390-18. Test voltage may be from 10 to 60 V, and test duration may be from 6 to 168 h, depending on the standard method used. A higher voltage and longer test duration are required for higher quality concrete mixtures. Cell temperature must be measured during the test. At the end of the test, the specimen is split in half, the surface is sprayed with a 0.1 M silver nitrate solution, and the average depth of chloride penetration is determined by making several measurements in the central part of the specimen as shown above. The average chloride penetration, the applied voltage, average temperature of the sodium hydroxide solution, test duration, and specimen thickness are used to calculate the *non-steady-state migration coefficient*.

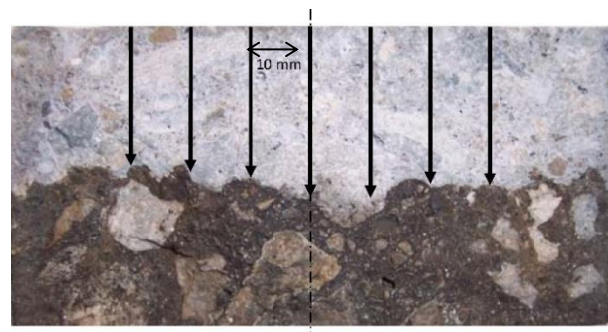
**Conductivity:** The image to the right shows the screen display when **PROOVE'it** is used to measure bulk electrical conductivity in accordance with ASTM C1760. A separate module is used for this test. The user sets up the test by entering the length and diameter of the specimens for each cell. The voltage is set to 60 V and the cells are turned on. The test runs for 1 minute, at which time the currents recorded during the last 3 readings are saved, averaged, and used to calculate the bulk conductivity, which is displayed in units of mS/m. For concrete with adjusted Coulomb values in the range of 500 to 4000 C, the bulk conductivity is expected to be in the range of 3 to 20 mS/m (see Table 2).

## Test Report

The software includes a **Report Manger** for preparing professional quality test reports, which can be customized with the purchaser's company logo. Data recorded during each test are stored in a database allowing a complete review of data if anomalous results are encountered. Customized labels can be



	1	2	3	4	5	6	7	8
Status:	FIN	FIN	FIN	FIN	FIN	FIN	FIN	FIN
Actual voltage (V):	60,0	60,0	60,0	60,0	60,0	60,0	60,0	60,0
Actual current (mA):	171,4	393,8	267,1	267,3	268,0	393,5	59,8	267,8
Temperature (°C):	25,0	26,8	23,3	26,2	23,9	24,9	23,7	25,6
Elapsed time:	6:00	6:00	6:00	6:00	6:00	6:00	6:00	6:00
Pred. coulombs (adjusted):	3361	7678	5208	5212	5225	7671	1167	5221
Testing time:	6:00 Hour	6:00 Hour	6:00 Hour	6:00 Hour	6:00 Hour	6:00 Hour	6:00 Hour	6:00 Hour
Specimen diameter:	100 mm	100 mm	100 mm	100 mm	100 mm	100 mm	100 mm	100 mm
Coulombs (adjusted):	3363	7678	5208	5212	5225	7672	1167	5222
Permeability class:	Mod.	High	High	High	High	High	Low	High



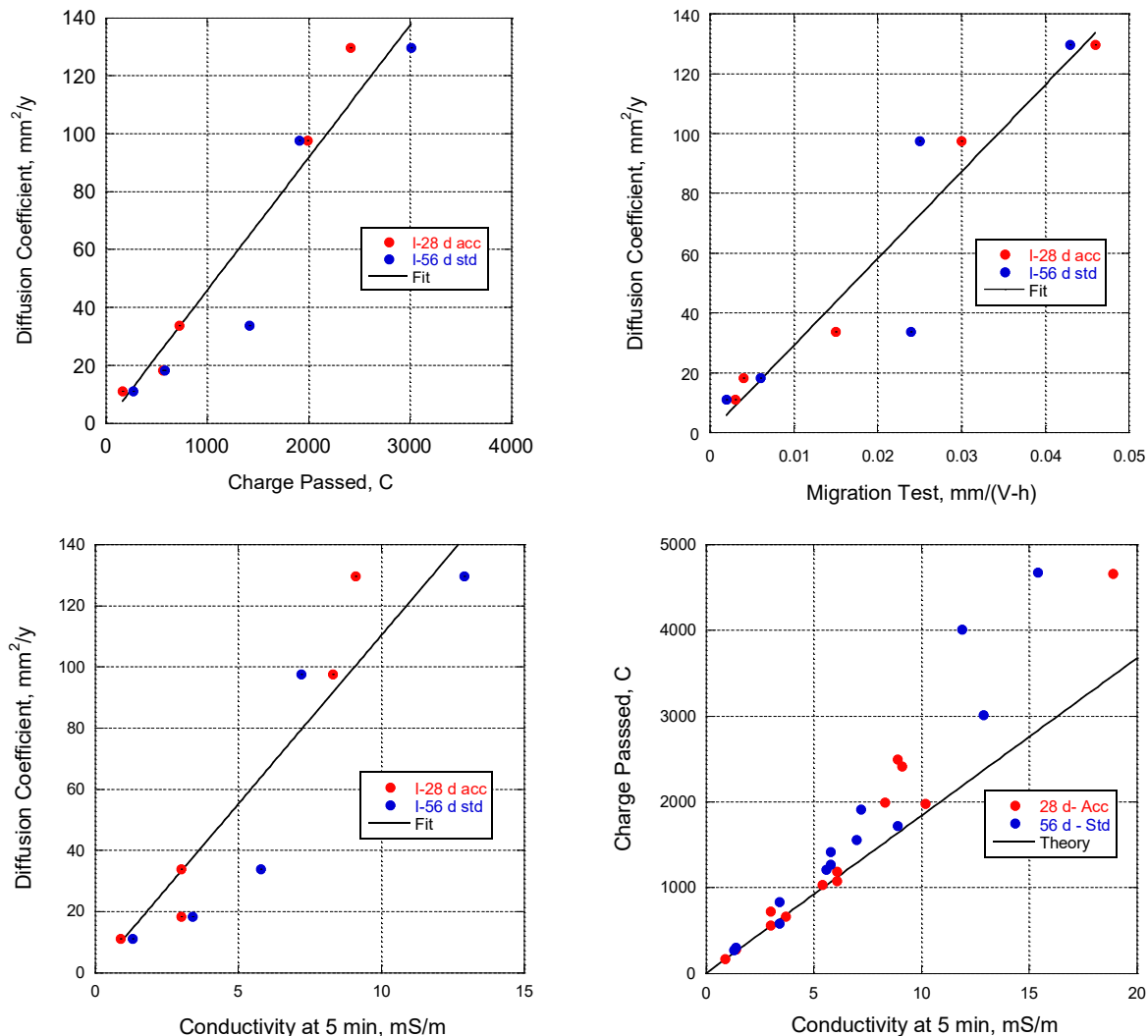

	1	2	3	4	5	6	7	8
Status:	OFF	OFF	OFF	OFF	OFF	OFF	OFF	OFF
Actual voltage (V):	---	---	---	---	---	---	---	---
Actual current (mA):	---	---	---	---	---	---	---	---
Temperature (°C):	---	---	---	---	---	---	---	---
Elapsed time:	0:00	0:00	0:00	0:00	0:00	0:00	0:00	0:00
Current after 60 second:	---	---	---	---	---	---	---	---
Testing time:	1 minute	1 minute	1 minute	1 minute	1 minute	1 minute	1 minute	1 minute
Specimen diameter:	100 mm	100 mm	100 mm	100 mm	100 mm	100 mm	100 mm	100 mm
Specimen length:	200 mm	200 mm	133 mm	200 mm	200 mm	200 mm	200 mm	200 mm
Conductivity mS/m:	---	---	---	---	---	---	---	---

attached to each test for complete project documentation. Test results can be exported to Excel for statistical analysis of the results and preparing user defined control charts.

### Correlations to Chloride Diffusion Coefficient

There is a theoretical relationship between the chloride diffusion coefficient and electrical conductivity whose validity has been experimentally investigated. The chloride diffusion coefficient can be determined directly by profile grinding (see **Profile Grinder** data sheet) and testing for chloride content (see **RCT** data sheet) after ponding with NaCl solution as per NT Build 443 "Concrete, Hardened: Accelerated Chloride Penetration" or ASTM C1556 "Test Method for Determining the Apparent Chloride Diffusion Coefficient of Cementitious Mixtures by Bulk Diffusion." The required ponding period is at least 35 days. A correlation can then be developed between the diffusion coefficient and any of the other properties determined with the **PROOVE<sup>it</sup>**. The following shows a good example:

In a study by Obla, Kim, and Lobo (2014), the apparent chloride diffusion coefficient was determined as per ASTM C1556. Specimens from 5 concrete mixtures were subjected to 59 days of standard curing and then 16 months of immersion in NaCl solution. Companion specimens were tested as per ASTM C1202 and AASHTO TP 64, after standard curing at 23 °C for 56 days or standard curing for 7 days plus 21 days curing at 38 °C. For the ASTM C1202 tests, the current at 5 minutes was used to calculate the electrical conductivity. The following plots show the correlations between various test results and the relationship between the charge passed and the 5-minute electrical conductivity test.





## Reference

Obla, K.H., Kim, H, and Lobo, C.L., 2014, "Selection of Rapid Index Tests and Criteria for Concrete Resistant to Chloride Penetration," presented at Transportation Research Board Meeting, Washington D.C., Jan. 2014.

## PROOVE'it Specifications

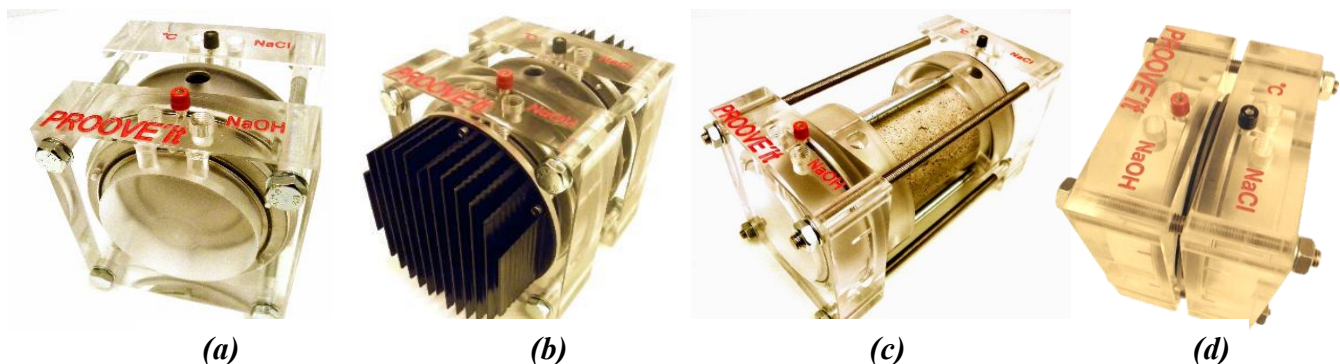
### Power supply unit and software:

- 8-channel unit for testing simultaneously.
- 220 VAC / 60 Hz or 110 VAC / 50 Hz power supply.
- RS-232 serial connection to PC, convertible to USB.
- Short circuit protection Channel locking option.
- Dimensions: ~ 40 x 30 x 15 cm.
- Compatible with Windows 7 / 8 / 10 operating systems.
- Easy and friendly display.
- Auto-correction of measured Coulombs using ASTM C 1202-14 when the diameter of the specimens differs from the standard's 95 mm.
- Customizable voltage: 5 V to 60 V in steps of 5 V (e.g. for NT BUILD 492 or EN 12390-18).
- Max. testing current for protection: 500 mA per Channel.
- Current accuracy  $\pm 0.5\%$  at 1 to 500 mA.
- Voltage accuracy  $\pm 0.1$  V at 5 to 60 V.
- Maximum testing temperature: 90°C (system shuts down to prevent boiling of the solutions).
- Temperature probes with  $\pm 1^\circ\text{C}$  accuracy at 20 – 25°C.
- Report Manager with detailed data.

### Measuring cells:

Robust, easy to assemble, auto-seal cells available in different versions:

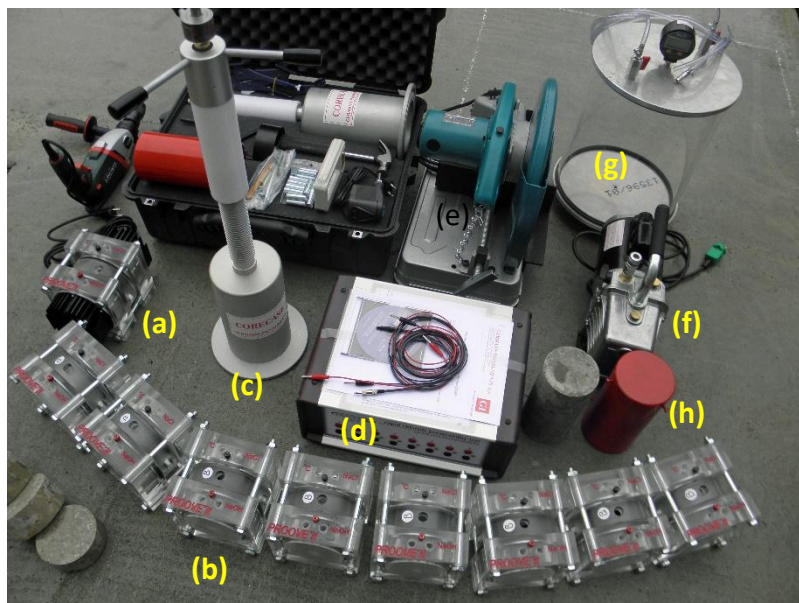
- ✓ (a) PR-1000 cell: Regular cell as specified by ASTM C 1202-14.
- ✓ (b) PR-1100 cell: Enhanced cell with cooling fins to keep the temperature of the liquids at room temperature, preventing heating of the specimen. Used for NT BUILD 492, EN 12390-18 or as a modified cell for ASTM C 1202 with control of temperature.
- ✓ (c) PR-1200 cell: Measuring cell for 200 mm long specimens for ASTM C 1760-12 Bulk Conductivity.
- ✓ (d) PR-1000-113-20: Modified cell for the French standard XP P 18-461 for 113 mm dia. and 20 mm thick specimens (cooling fins can also be mounted here).



The following gaskets are available for different specimen diameters. All cells are supplied with the PR-1010B gaskets, unless otherwise specified. The PR-1010B gaskets match the 100-mm core diameter produced by the CEL-100 coring equipment (see **CORECASE** data sheet):

Specimen Diameter	Gasket Ordering #
104 to 102 mm	PR-1010A
101 to 97 mm	PR-1010B
96 to 93 mm	PR-1010C

## PROOVE<sup>it</sup> System components



- (a) Cell with cooling fins (PR-1100)
- (b) Eight standard cells (PR-1000)
- (c) **CORECASE** for producing cores of 100 mm in diameter (CEL-100)
- (d) **PROOVE<sup>it</sup>** microprocessor power supply (PR-1050) and software (PR-1040)
- (e) Diamond saw for cutting 50 mm slices (PR-1090)
- (f) Vacuum pump, <10 mmHg or 1.3 kPa (PR-1081)
- (g) Vacuum desiccator for max. 16 specimens (PR-1070)
- (h) Precision steel mold, reusable for casting 100 mm x 200 mm specimens (MRLN-1009)

**NOTE:** A computer is also required with a Windows® operating system.

## PROOVE<sup>it</sup> Ordering Numbers\*

Item	Order #
<b>PROOVE<sup>it</sup></b> power supply for 8 cells	PR-1050
<b>PROOVE<sup>it</sup></b> software for Windows®	PR-1040
Power cable for power supply 230 VAC	PR-1064
Power cable for power supply 110 VAC	PR-1065
RS-232C serial cable for power supply	PR-1066
<b>PROOVE<sup>it</sup></b> cell, standard	PR-1000
<b>PROOVE<sup>it</sup></b> cell, with cooling fins	PR-1100
<b>PROOVE<sup>it</sup></b> cell for bulk conductivity	PR-1200
<b>PROOVE<sup>it</sup></b> cell for bulk conductivity	PR-1000-113-20
Red connecting cord, one per cell	PR-1001
Black connecting cord, one per cell	PR-1002
Temperature probe, one per cell	PR-1005

Item	Order #
User manual	PR-1090
Spare steel mesh for cell	PR-1003
Verification unit	PR-1055
Vacuum desiccator for max. 16 specimens	PR-1070
Vacuum pump, < 50 mm Hg (6.7 kPa)	PR-1080
Vacuum pump, < 10 mm Hg (1.3 kPa)	PR-1081
<b>CORECASE</b> for 100 mm cores	CEL-100
Drilling machine, 1150W	CC-29
Diamond saw for trimming cores	PR-1090
300 mL bottle of 3.0 % NaCl solution	PR-1020
300 mL bottle of 0.3N NaOH solution	PR-1030
Precision steel mold, reusable	MRLN-1009

\*These items can be selected as needed to assemble a system to meet the desired requirements

The PR-1055 verification unit is used to verify that the microprocessor power supply is working properly. The unit is connected to line power, 110 VAC or 220 VAC. Each channel of the **PROOVE<sup>it</sup>** power supply is set up for testing at a selected voltage and connected to the verification unit. If the **PROOVE<sup>it</sup>** system is operating properly, the “Actual current” indicated on the computer screen should be within  $30 \text{ mA} \pm 0.1 \text{ mA}$  or  $300 \text{ mA} \pm 0.1 \text{ mA}$  for the two switch settings on the verification unit.



## Purpose

**Pulsar** (A1410) is a compact, hand-held, coupling-free instrument for measuring the speed of a pulse of ultrasonic longitudinal stress waves propagating within concrete; that is, it measures the ultrasonic pulse velocity (UPV).

The instrument incorporates two antenna arrays, each one with a set of 7 dry-point-contact (DPC) transducers that are brought into contact with the surface of the test object. The receiving antenna is fixed to the electronic unit while the transmitting antenna is connected by a 3 meter cable.

**Pulsar** can be used for the following applications:

- Assessment of concrete uniformity
- Locating internal voids and cracks
- Estimation of the extent and severity of deterioration
- Estimating depth of fire damaged concrete
- Evaluation of damage to test specimens during durability testing (freeze and thaw, sulfate attack, alkali-silica reaction)
- Estimation of depth of surface-opening cracks
- Estimation of early-age strength (with project/mixture specific correlation)
- Evaluation of condition or elastic properties of solid materials like rocks, bricks or composites.



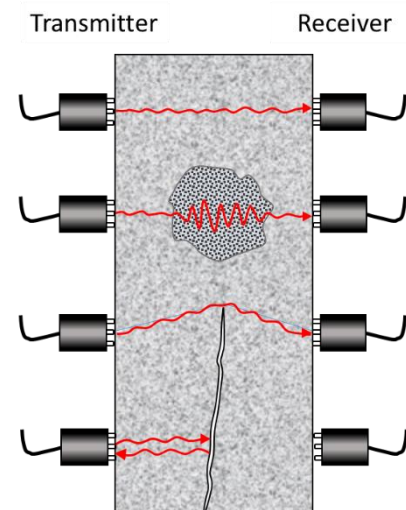
## Principle

A pulse of ultrasonic longitudinal stress waves is introduced into one surface of a concrete member by the transmitting antenna. The pulse travels through the concrete, is received by a similar antenna on a different surface and its transit time is determined by the instrument. If the distance between the transducers is divided by the transit time, the pulse velocity can be obtained. The longitudinal pulse velocity,  $C_p$ , of an elastic solid is a function of the elastic constants (modulus of elasticity,  $E$ , and Poisson's ratio,  $\nu$ ) and the density,  $\rho$ .

$$C_p = \sqrt{\frac{E(1-\nu)}{\rho(1+\nu)(1-2\nu)}}$$

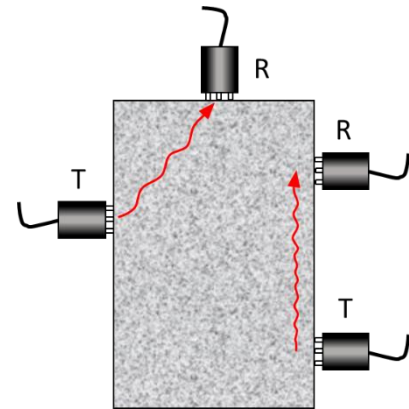
In contrast with traditional pulse velocity instruments, the antennas are built with dry-point-contact (DPC) transducers in order to work without a coupling material (grease or gel). These transducers allow to make measurements much quicker.

The figure to the right illustrates examples of different conditions that may be encountered when testing an element. At the top, the path between the transducers is through solid concrete, and the travel time would be the shortest. Below that is the case where there is an internal pocket of porous concrete, such as honeycombed concrete. The pulse is scattered as it travels through the contiguous portions of the honeycombed concrete. As a result, the travel path is longer and the pulse travel time is longer as well. This results in a reduced pulse velocity. In the next case, the transducers are located so that the direct travel path is near the edge of a crack. The pulse cannot travel across a concrete-air interface, but it is able to travel from the transmitter to the receiver by diffraction at the crack edge. Because the travel path is longer than the distance between the transducers, the apparent pulse velocity is lower than through sound concrete. In the lowermost case, the pulse is reflected completely by the crack, and travel time is not measurable.





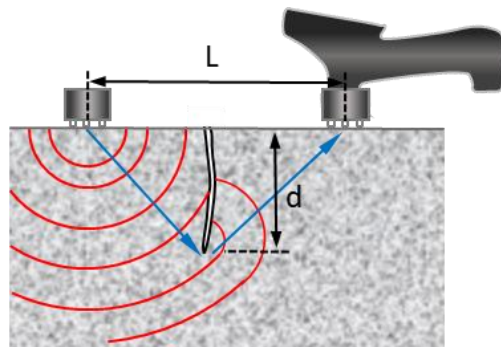
These examples correspond to the direct thru-transmission method where the transducers are positioned in opposite parallel faces of the concrete element. There are however cases where access to the opposite side of the element is restricted. The semi-direct and indirect transmission methods are alternatives in such situations although surface conditions of the concrete or the presence of steel reinforcement might interfere in the measurements. The relevant standards and guidelines for Ultrasonic Pulse Velocity testing give advice on what aspects the user have to take care of if these techniques are to be used.



The UPV test method is governed by various standards including ASTM C597, BS 1881:203, and EN 12504-4. The method is totally nondestructive and it is possible to repeat the test at the same point at different times to determine changes of UPV with time. It is also highly repeatable. For tests of sound concrete, the coefficient of variation for repeated measurements at the same location is 2 %. The accuracy of the pulse velocity is a direct function of the accuracy of the measured distance between the transducer faces.

## Crack depth estimation

**Pulsar** can also be used to estimate the depths of surface-opening cracks. When the stress pulse reaches the tip of a surface-opening crack, the pulse is diffracted by the crack tip. The diffracted pulse travels away from the crack tip and is detected by the receiver. Because the crack increases the length of the travel path from transmitter to receiver, the transmit time will be greater than if no crack were present. Crack depth is determined by making two transit time measurements. The first one is made with the transducers aligned parallel to the crack, and the second one is made with the transducers perpendicular to the crack (figure below). For the second measurement, the crack should be at the midpoint between the transducers. By using these transit times and the distance between the transducers, the crack depth can be calculated:



$$d = \frac{L}{2} \sqrt{\left(\frac{t_c}{t_p}\right)^2 - 1}$$

Where  $L$  is the distance between the transducers,  $t_p$  is the transit time measured with the transducers parallel to the crack, and  $t_c$  is the transit time with transducers perpendicular to the crack.

## Estimating In-place Strength

To use **Surfer** to estimate early-age strength development of concrete, a relationship needs to be established between concrete strength and pulse velocity. Such a relationship can be established by making pulse velocity measurements on standard strength test specimens and then measuring their compressive strength. The resulting data can be used to develop a regression equation to represent the relationship between concrete strength and pulse velocity. Refer to ACI 228.1R (In-Place Methods to Estimate Concrete Strength) for guidance on developing and using the strength relationship. The relationship that is developed is applicable only to that specific concrete mixture.

## Elastic Modulus Degradation

Because the modulus of elasticity is proportional to the square of the pulse velocity, **Pulsar** can be used as an alternative to resonant frequency testing to monitor deterioration of specimens used in standard durability tests, such as freezing and thawing. In such tests, the decrease in the dynamic

modulus of elasticity is used as an indicator of deterioration. The elastic modulus ratio is equal to the square of the pulse velocity ratio:

$$\frac{E_n}{E_i} = \left( \frac{V_n}{V_i} \right)^2$$

Where  $V_i$  and  $E_i$  are the initial values of pulse velocity and modulus of elasticity; and  $V_n$  and  $E_n$  are the values of pulse velocity and modulus of elasticity after exposure to the test conditions.

## Pulsar Specifications

- Antennas with an array of 7 dry point contact, undamped, longitudinal-wave transducers
- The signal waveform can be displayed
- Operating frequency: 50 kHz
- Rechargeable battery with 16 hours life
- 2.8", 320 × 240 LCD screen
- Data transfer to computer via USB
- Transit time measurement range: 0.1 to 10,000  $\mu$ s
- Pulse velocity measurement range: 1,000 to 15,000 m/s
- Transit time (t) measurement accuracy:  $\pm (0.02 \cdot t + 0.1)$   $\mu$ s
- Resolution: 0.1  $\mu$ s (transit time), 10 m/s (pulse velocity)
- Maximum distance to measure: 2,500 mm
- Automatic Gain Control (AGC) function.
- Storage capacity: 50,000 results
- Metric and inch-pound units
- Instrument's weight: 420 g
- Instrument's dimensions: 230 x 125 x 65 mm
- Operating conditions: Temperature: -10 to 50 °C, RH  $\leq$  95 %



## Pulsar (PUL-1000) Ordering Numbers

tem	Order #
Hand-held electronic unit, Pulsar A1410, with carrying case	PUL-1001
Transmitter antenna array with 7 DPC transducers, longitudinal wave	PUL-1002
LEMO-LEMO cable, 3 m	PUL-1003
Charger and USB cable for connection to PC	PUL-1004
Reference specimen with calibration certificate	PUL-1005
User manual	PUL-1006



## Purpose

The **RapidAir** is an image analysis system for **automatic determination** of the air void structure parameters in hardened concrete according to the linear traverse method (procedure A) or the point count method (procedure B) as described in ASTM C457, "Test Method for Microscopical Determination of Parameters of the Air-Void System in Hardened Concrete," or in EN 480-11, "Admixtures for concrete, mortar and grout - Test methods - Part 11: Determination of air void characteristics in hardened concrete."

**RapidAir** is used to:

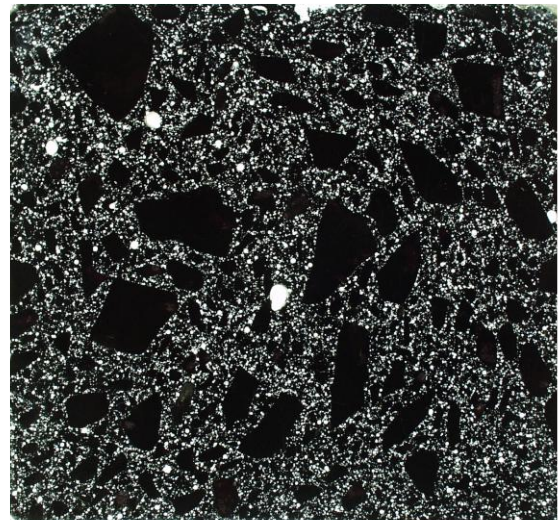
- Determine the total air content, spacing factor, and specific surface in hardened concrete.
- Effectively and rapidly study and quantify the air void system: volume, spacing, and size distribution of the air bubbles.

## Principle

A core is taken from the structure, and then sliced, ground, and lapped in the laboratory. The resulting surface is plane, smooth, and with sharp edges along the perimeter of air voids. Before final specimen preparation, the lapping quality is checked under a stereomicroscope.

The lapped surface is colored black with a black ink marker pen and a white barium sulphate powder is worked into the air voids using a rubber stopper. The quality of the black-white contrast is checked under a stereomicroscope. The voids should be filled totally with white powder and no white regions should be visible on the surface. Finally, voids in aggregates and obvious cracks are also colored black under the stereomicroscope.

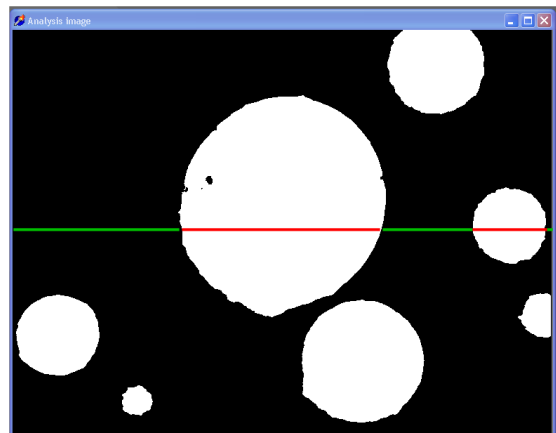
The photo on the right shows a properly prepared specimen. The preparation of a well-lapped specimen surface for analysis takes about 30 minutes. The **RapidAir** measurement is done within 12 min for linear traverse analysis and within 30 min for modified point count. This should be compared with a time of 4 to 6 hours normally required for manual analysis in accordance with ASTM C457 or EN 480-11.



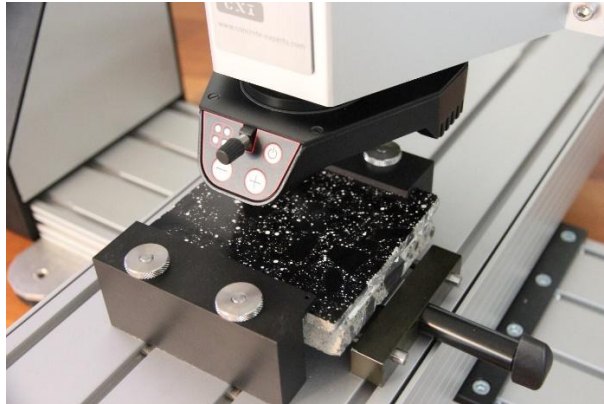
## Operation

Following contrast enhancement, the prepared specimen is mounted on a moving X-Y-Z stage positioned below a video camera. The **RapidAir** control unit automatically moves the stage, and the software determines the portion of the total traverse length that passes through the white air voids, as shown in the magnified view to the right. After the scan is completed, the air-void parameters are calculated as per ASTM C457 or EN 480-11.

The specimen scan is saved automatically in a report file documenting the air content, spacing factor, and specific surface. In addition, graphical presentation of the air-void distribution and the raw data are available.







*Prepared specimen positioned on the moveable stage ready for image analysis.*

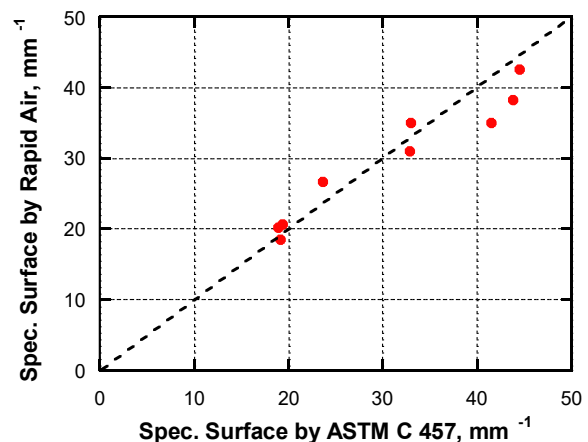
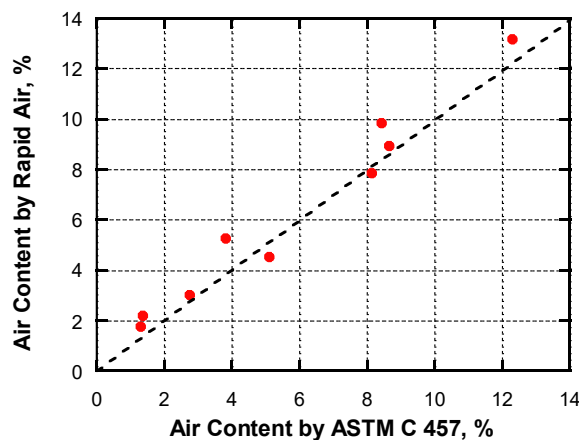


**RapidAir** system in operation.

## Correlation with ASTM C457 and Precision

As reported by Pade, C. et al.<sup>(1)</sup>, very good agreement was found between the air-void system parameters measured by the **RapidAir** system and by the ASTM C457 standard method. The study involved thirteen European laboratories and concluded that the repeatability of the automatic analysis system not only conforms to the precision statement of ASTM C 457 but is better than when the tests are performed manually. The standard deviations of the air-void parameters determined by **RapidAir** were as follows:

- Air content: 0.37 %
- Specific surface: 1.57 mm<sup>-1</sup>
- Spacing factor: 0.011 mm

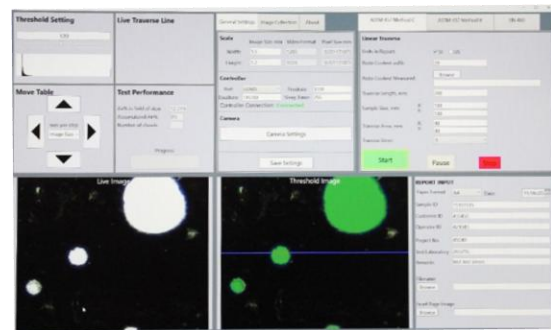


*Comparison between **RapidAir** and ASTM C457 measurements of air content and specific surface*

The very good results for reproducibility and repeatability of the **RapidAir** system were also validated in an international Round Robin study where seven laboratories participated <sup>(2)</sup>. The results are better than those obtained from traditional manual analysis of air-entrained concrete because these ones have been shown to be significantly operator-dependent since the person that observes the specimen defines the air void edges subjectively <sup>(3)</sup>. In contrast, the automatic programmed procedure performed by the **Rapid Air** importantly reduces this sensitivity to bias errors.

## RapidAir Specifications

- X,Y,Z-stage with electronic stepper motor for accurate X-Y displacement, 230/120 VAC, equipped with emergency switch
- LED ring lightening system
- Color digital camera, 2  $\mu$ m resolution
- Microscope objective for op to 100x magnification
- Windows based software with user friendly interface
- Self-calibration with a reference sample
- Exporting of data to MS Excel
- Print out reports for ASTM C 457 and EN 480-11



## RapidAir Ordering Numbers

Item	Order #
RapidAir System Delivered with computer and software, pre-configured, aligned, tested, and ready for Plug-and-Play use.	RAP-3000



## References

15. Pade, C., Jakobsen, U.H. and Elsen, J., "A New Automatic Analysis System for Analyzing the Air Void System in Hardened Concrete," International Cement Microscopy Association Conference, San Diego, CA, USA, April 2002.
16. U.H. Jakobsen, C. Pade, N. Thaulow, D. Brown, S. Sahu, O. Magnusson, S. De Buck, and G. De Schutter, "Automated air void analysis of hardened concrete — a Round Robin Study", Cement and Concrete Research Vol. 36 – 8, Pages 1444-1452, August 2006
17. Schlorholtz, S. Image Analysis for Evaluating Air Void Parameters of Concrete. Iowa DOT Project HR-396; Final Report; Iowa Department of Transportation: Ames, IA, USA, 1998.

## Purpose

The **RAT** (Rapid Alkali Test) measures the amounts of sodium and potassium ions that contribute to alkali-silica reaction (ASR) if reactive aggregates are present. ASR leads to expansive products that can cause extensive cracking in concrete structures. The alkalies (potassium and sodium ions) in the cement paste react with reactive (amorphous) silica particles in fine or coarse aggregate and cause expansion and cracking, provided sufficient moisture is present.

To reduce the risk of ASR in new concrete structures, the quantity of sodium and potassium ions in the cement paste of fresh concrete should be reduced so as not to exceed the critical limit defined in standards, guidelines or particular project specifications.

The **RAT** measures the amount of sodium and potassium ions in fresh concrete or in its constituents and can also be used for testing powder samples of hardened concrete. Concrete powder samples from existing structures can be obtained by drilling or by using the **Profile Grinder** (see Technical Data Sheet) if sampling at controlled depths is desired.

## Principle

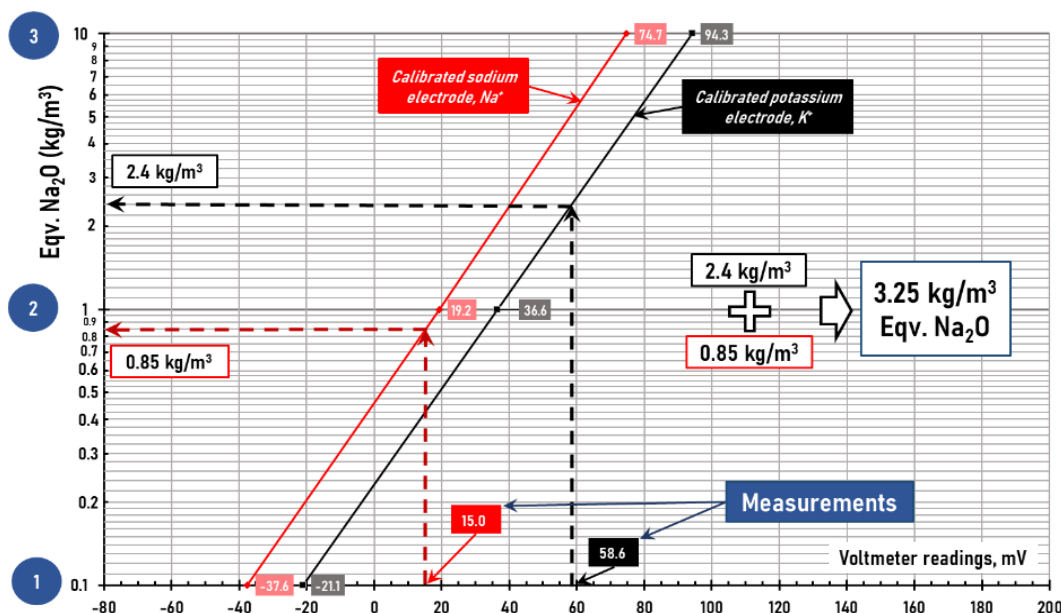
A sample of the fresh concrete, or its constituents, is taken and dissolved in a specific amount of acid extraction liquid. A calibrated set of ion-selective electrodes, one for measuring the sodium ions and one for measuring the potassium ions, is submerged into the solution and the corresponding electrode readings (in mV) are taken with a high impedance voltmeter. Calibration of the electrodes is performed using calibration liquids, three for sodium and three for potassium, so that two calibration curves are plotted.

The mV-readings are transformed directly into amount of  $\text{Na}_2\text{O}$  and  $0.658 \times \text{K}_2\text{O}$  in  $\text{kg/m}^3$  by means of calibration curves. The two values are added together to give the equivalent amount of total  $\text{Na}_2\text{O}$ .

Similarly, for hardened concrete, a powder sample may be analyzed. If aggregates containing reactive material need to be excluded, a core is taken, the core is fractured, and the aggregate particles are removed. The remaining material is then pulverized and analyzed.

## Testing Example

In this example, the mV-reading for the  $\text{Na}^+$  electrode is 15 mV and for the  $\text{K}^+$  electrode it is 58.6 mV. The corresponding amounts of equivalent  $\text{Na}_2\text{O}$  and  $\text{K}_2\text{O}$  are  $0.85 \text{ kg/m}^3$  and  $2.4 \text{ kg/m}^3$ , respectively, which give a total equivalent  $\text{Na}_2\text{O}$  content of  $3.25 \text{ kg/m}^3$ . Once the calibration curves are plotted, a test takes about 10 minutes to perform.





The limit of the total alkalis in the mix to prevent or minimize ASR varies for different aggregate types and binder alkali classification and depends also on the size of the concrete member and the environmental exposure. Typical alkali limit values for controlling expansion from reactive aggregate (in kg per m<sup>3</sup> of concrete) for various countries and from RILEM, are given here as a reference only.

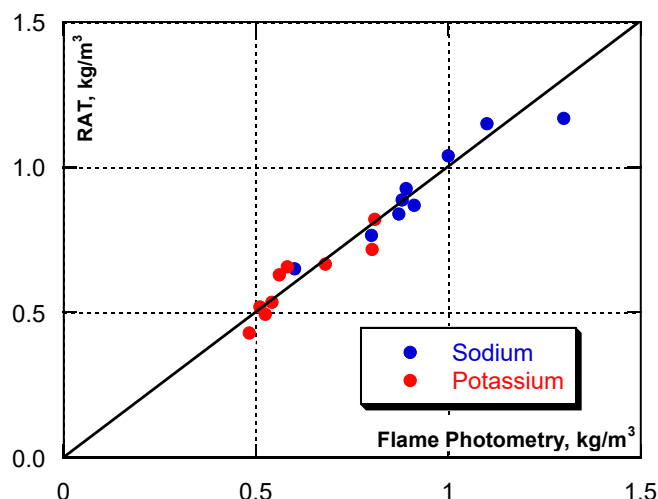
Country	Specified Total Alkali Limit in Concrete (kg/m <sup>3</sup> )	Comments and Performance Guidelines
United States (ASTM C1567, 2013; ASTM C1293, 2018)	1.8 – 3.0	Prescriptive and performance approach used. Performance using ASTM C1293 and C1567
Canada (CSA A23.1&2, 2014)	2.0 – 3.0	Limits based on environment and risk for each structure
United Kingdom (BRE Digest 330.2, 2004)	3.5	Alkali limits based on cement alkali limits and aggregate reactivity
RILEM AAR 7.1—2016	2.5 – 3.5	Limits based on aggregate reactivity, with classification being low, medium, or high
Japan (JIS A5308, 2009)	3	Prescriptive limit based on andesite data Performance limits from 1.2 to 3.0 kg/m <sup>3</sup>
Australia (HB 79, 2015)	2.8	Risk with reactive aggregate almost always controlled using SCMs <sup>a</sup>
New Zealand (CCANZ TR3, 2012)	2.5	Prescriptive limit widely used Performance limits from 1.8 to 3.0 kg/m <sup>3</sup>
South Africa (SANS 6245, 2006)	2.0 – 4.0	Limits based on aggregate reactivity SCMs widely used to control ASR

<sup>a</sup> - SCM: Supplementary cementitious material, such as fly ash or slag; also termed “addition” or “extender”.  
Source: Mark G Alexander, 2019, “Developments in the Formulation and Reinforcement of Concrete (Second Edition). Adapted from Mackechnie, J. R. (2020). Alkali silica reaction in concrete. In Alexander, M. G. (Ed.), Fulton’s concrete technology (10th (rev.) ed.). Midrand, South Africa: The Concrete Institute.

### Correlations and Variability

The graph shows the correlation between alkali contents determined by flame photometry and **RAT**, for tests performed on the same solutions prepared from different concrete mixtures. The test solutions were prepared by acid extraction of the alkalis.

The correlation coefficient for these results is 0.97 and the alkali contents determined by **RAT** are within ±5 % of the values determined by flame photometry.



## RAT Specifications

- Input Impedance: 1,012 Ohm
- Battery Type / Life: 1 x 9V / approx. 150 hours
- Auto-off after 20 minutes of non-use
- Environment: 0 to 50°C; RH max 95%
- Range:  $\pm 1,999$  mV
- Resolution: 0.1 mV for  $\pm 700$  mV and 1 mV for  $\pm 2,000$  mV
- Accuracy: 0.2 mV for  $\pm 700$  mV and 1 mV for  $\pm 2,000$  mV



## RAT-1000 Kit Ordering Numbers

Item	Order #
K <sup>+</sup> electrode	RAT-700
Spare cover for K <sup>+</sup> electrode	RAT-701
Na <sup>+</sup> electrode	RAT-800
Spare cover for Na <sup>+</sup> electrode	RAT-801
Reference electrode	RAT-900
Holster for electrodes	RAT-910
Electrometer w. spare battery	RAT-950
Adaptor switch box	RAT-960
Wetting agent for K <sup>+</sup> electrode	RAT-970
Wetting agent for Na <sup>+</sup> electrode	RAT-980
Wetting agent for ref. electrode	RAT-990
Set of filling syringes, three	RAT-1005
Spray bottle with distilled water	RAT-1010
Calibration liquid # 1	RAT-1020
Calibration liquid # 2	RAT-1030
Calibration liquid # 3	RAT-1040
Cleaning tissues	RAT-1050
Calibration sheets, 30 pcs	RAT-1060
Data sheets, 30 pcs	RAT-1070
Pencils (black and red) and ruler	RAT-1080
Spatula, 5 pcs	RAT-1090
Safety goggles	RAT-1100
Rubber gloves	RAT-1110
Mixing container	RAT-1120
Sampling cup for fresh concrete	RAT-1130
Plastic lid with holes for electrodes	RAT-1140
Temperature probe	RAT-1150
Vials for hardened concrete	RAT-1160
Vials for fresh concrete	RAT-1170
Manual	RAT-1180



**RAT-1000 Kit**

## Purpose

The **RCT** and **RCTW** systems are used to accurately and quickly determine the chloride ion content from powder samples of concrete obtained on-site or in the laboratory using the **Profile Grinder** (see Data Sheet) or other means. The test results can be used for:

- Establishing the chloride ion profile for service life estimation
- Establishing the depth of removal of a chloride ion contaminated surface layer
- Diagnosing a structure for corrosion activity, in combination with other test systems such the **Mini Great Dane**, **GalvaPulse**, and **Rainbow Indicator** (see relevant data sheets)
- Monitoring the chloride ion content during electrochemical removal of chlorides
- Measuring the chloride ion content of fresh concrete or its constituents

## Principle

A powder sample of hardened concrete is obtained by drilling or grinding the cover concrete in the structure, or a sample is obtained from the fresh concrete. The sample is mixed with a specific amount of extraction liquid and shaken for 5 minutes. The extraction liquid is designed to neutralize disturbing ions that may interfere the measurements, such as sulfide ions, and extracts the chloride ions in the sample. A calibrated chloride selective electrode is then submerged into the solution to determine the amount of chloride ion, which is expressed as percentage of concrete mass.

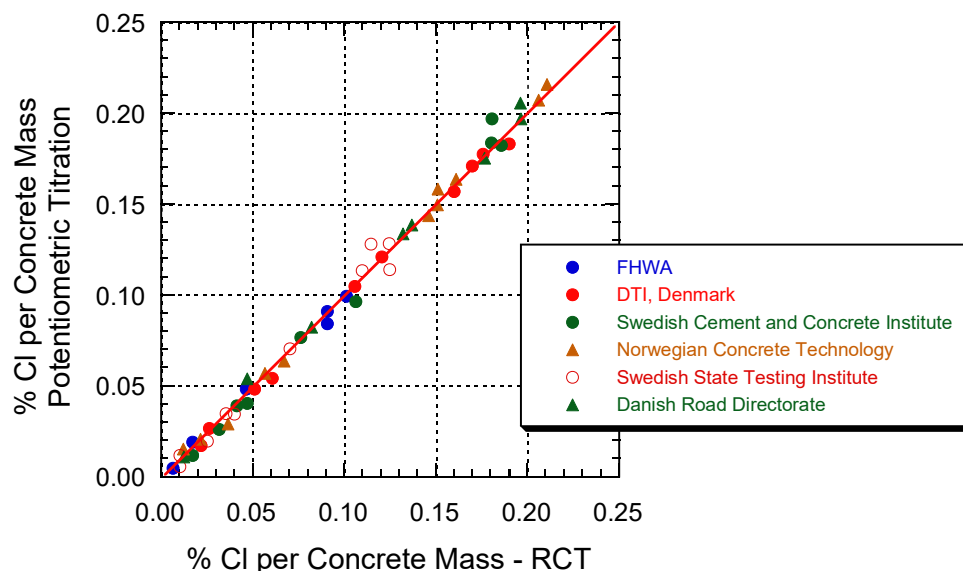
Two extraction methods can be used:

- The **RCT** (**R**apid **C**hloride **T**est) to determine the amount of acid-soluble chlorides
- The **RCTW** (**R**apid **C**hloride **T**est **W**ater) to determine the amount of water-soluble chlorides

The two methods use different kinds of extraction liquids. The type of method to use will depend on the specification criteria for maximum allowable chloride ion content in either hardened or fresh concrete. Note that the acid extraction does not remove chemically bound chlorides.

## Accuracy

Numerous correlations have been made between **RCT** test results and chloride ion content determined by standard laboratory potentiometric titration methods such as AASHTO T 260, ASTM C114, EN 14629. The following graph shows the results of such correlations made by various laboratories in the Scandinavian countries and in the U.S.



In one comparison whose results are illustrated in the next table, the Swedish National Testing Institute produced concrete powders made with different binders and containing known amounts of chloride ion introduced into the concrete by diffusion. Parallel testing was done in accordance with AASHTO T 260 and with the **RCT** system. The **RCT** readings were taken after the powder samples were kept in the extraction liquid overnight to obtain full extraction of acid-soluble chlorides.



Alternatively, if the result is obtained after 5 minutes of shaking of the vial, a correction factor can be applied to the measured chloride ion content.

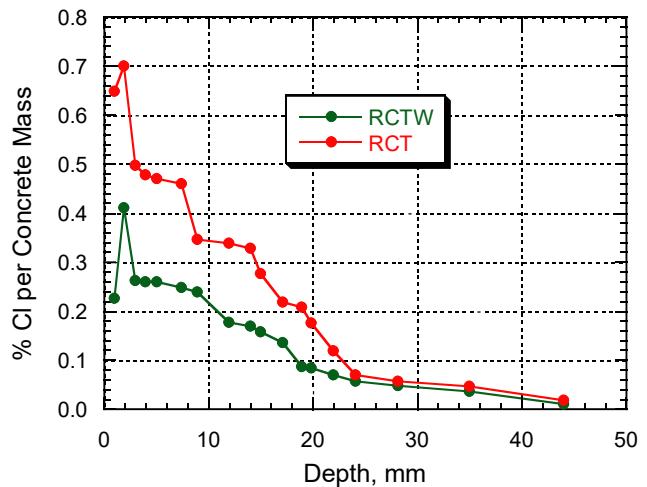
Material	% Cl <sup>-</sup> per Mass of Concrete		
	Known Amount	AASHTO T 260	<b>RCT</b>
Portland Cement (CEM I)	0.023	0.024	0.022
	0.071	0.070	0.072
	0.328	0.314	0.321
–Fly Ash Cement (CEM II/B-V)	0.020	0.019	0.019
	0.057	0.052	0.061
	0.244	0.229	0.238
Slag Cement (CEM III/B)	0.020	0.019	0.019
	0.056	0.052	0.059
	0.244	0.231	0.238

The accuracy of the **RCT** results compared with the known amount of chlorides is as good as with the AASHTO T 260 potentiometric titration method. The average deviation of the **RCT** results from the known amount of chlorides is within  $\pm 4\%$ .

For repeated testing with the **RCT** on the same concrete powder, the coefficient of variation of test results is on average 5 %. The precision and accuracy of the **RCTW** test for water-soluble chlorides is similar to **RCT** results.

## Testing Examples

The graph to the right shows two profiles obtained from on-site profile grinding on a highway bridge column exposed to deicing salts for 4 years. Concrete powder samples were obtained at depth increments of 1 to 2 mm and were analyzed for acid-soluble chlorides with the **RCT** and for water-soluble chlorides with the **RCTW**. A depth of carbonation of 2 mm measured using the **Rainbow Indicator** (see data sheet), corresponding to the initial peaks of the chloride ion profiles obtained.



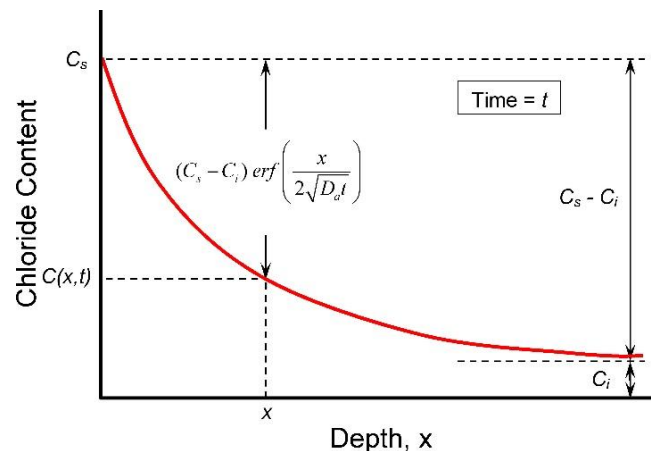
## Data Analysis

For laboratory tests in accordance with ASTM C1556 or NT Build 443, the chloride content profile obtained after a given period of immersion in the specified chloride solution can be subjected to regression analysis to obtain the apparent chloride diffusion coefficient. The testing condition is assumed to result in one-dimensional diffusion and the chloride ion content as a function of depth is assumed to obey the following solution to Fick's second law of diffusion (1):

$$C(x,t) = C_s - (C_s - C_i) \operatorname{erf} \left( \frac{x}{2\sqrt{D_a t}} \right) \quad (1)$$

where;

$C(x,t)$  = the chloride ion concentration at a depth  $x$  in mm from the exposed surface for an elapsed time  $t$  in years since the start of chloride exposure;



$C_s$  = the chloride concentration at the surface, as a % of concrete mass;  
 $C_i$  = the initial (or background) chloride concentration of the concrete, as a % of concrete mass;  
 $erf$  = the error function (function related to the integral of the normal probability function); and  
 $D_a$  = the apparent chloride diffusion coefficient in mm<sup>2</sup>/year

Eq. (1) describes the variation of chloride ion content as a function of the distance  $x$  from the surface after an elapsed time  $t$  since initial exposure to a constant surface chloride concentration of  $C_s$ . This function is shown as the red curve in the above figure. The values of the equation parameters ( $C_s$ ,  $C_i$ , and  $D_a$ ) are determined using least-squares curve fitting, which can be implemented using, for example, the "Solver" function in Microsoft Excel or using statistical software that permits general non-linear regression analysis. The value of  $C_i$  will be zero (0) if there is no background chloride present initially in the concrete.

The diffusion coefficient in research papers is reported often in units of 10<sup>-12</sup> m<sup>2</sup>/s. To convert to units of mm<sup>2</sup>/y, multiply by 3.15576 × 10<sup>13</sup>. For good quality concrete, typical values of the chloride diffusion coefficient are 10 to 100 mm<sup>2</sup>/y.

## Service Life Estimation

If the structure has been exposed to moist conditions so that diffusion has been the primary transport mechanism for chloride ions, a common application of the chloride profile obtained by **RCT** or **RCTW** and the apparent chloride diffusion coefficient given by the best fit regression of Eq. (1) is to determine at what time  $t$ , the chloride content at the depth of the reinforcement would reach the chloride ion threshold for initiation of corrosion. This service life time estimation assumes that the surface chloride concentration and diffusion coefficient do not change in the future and the effect of ambient temperature is not considered. Therefore in practice, the chloride profile should be reevaluated at reasonable regular intervals in order to update the expected service life of the structure.

## Chloride Ion Threshold

There is no a single unique value for the amount of chloride ions in concrete that will breakdown the protective oxide film and initiate corrosion of steel reinforcement. The value depends on many variables, among others, the exposure conditions, the water-cementitious materials ratio, the types of cementitious materials in the concrete, etc. For estimating the chloride ion threshold, a model given by **Eq. (2)** and **Eq. (3)** has been proposed (1,2,3):

$$C_{cr} = ke^{-1.5(W/c)_e} \quad (2)$$

$$(W/c)_e = \frac{W}{C - 1.4 \times FA - 4.7 \times SF} \quad (3)$$

where;

$C_{cr}$  = Chloride threshold percent by mass of binders

$(W/c)_e$  = Equivalent w/cm ratio (W = water, C = cement,  
FA = fly ash, SF = silica fume)

$k$  = 1.25 for marine exposure and splash zone

$k$  = 3.35 for submerged exposure in seawater

## RCT Electrometer and Electrode Specifications

- Input Impedance: 1,012 Ohm
- Battery Type / Life: 1 x 9V / approx. 150 hours
- Auto-off after 20 minutes of non-use
- Environment: 0 to 50°C; RH max 95%
- Temperature and pH measuring capacity (pH electrode and temperature probe are sold separately)
- Range: ±1,999 mV
- Resolution: 0.1 mV for ±700 mV and 1 mV for ±2,000 mV
- Accuracy: ±0.2 mV for ±700 mV and ±1 mV for ±2,000 mV
- Electrode type: Combination chloride ion selective electrode with waterproof BNC connection



**RCT-500 Kit**

## RCT-500 Kit Ordering Numbers

Item	Order #
RCT chloride selective electrode	RCT-770
Electrometer for mV, pH and °C	RCT-990
Electrode wetting agent, 80 mL, with spout	RCT-1000
Distilled water, spray bottle	RCT-1001
Polishing strips for electrode	RCT-1002
Plastic bags for powder sampling	RCT-1003
Powder collecting bowl	RCT-1004
Powder collecting pan, circular	RCT-1005
Powder collecting square w. clip	RCT-1006
Adjustable pliers	RCT-1007
Set of anchoring tools	RCT-1008
Mandrel	RCT-1009
Hammer	RCT-1010
Powder compression pin	RCT-1011
Powder weighing ampoules, 6 pcs	RCT-1012
Digital pocket balance, 115 x 0.01 g	RCT-2700

Item	Order #
Calibration liquid, 0.005 % Cl <sup>-</sup>	RCT-1013
Calibration liquid, 0.020 % Cl <sup>-</sup>	RCT-1014
Calibration liquid, 0.050 % Cl <sup>-</sup>	RCT-1015
Calibration liquid, 0.500 % Cl <sup>-</sup>	RCT-1016
Cleaning tissues	RCT-1017
Calibration sheets for hardened concrete	RCT-1018
Calibration sheets for fresh concrete	RCT-1019
Rubber ball dust remover	RCT-1020
Pencil and ruler	RCT-1021
Measuring tape	RCT-1022
Extraction vials, hardened concrete, 10 pcs	RCT-1023
Manual	RCT-1024
RCT testing cases and applications, binder	RCT-1025
Attaché case	RCT-1026

The **RCT-1025** binder contains 20 years of testing experience, including theory and applications for chloride diffusion modeling.

It is recommended to always have an extra set of clean **RCT-1030** calibration liquids to ensure that the chloride electrode is working properly if deviations occur from the usual obtained calibration curve.

### Extra Parts



**RCT-1030** set of calibration liquids, 0.005, 0.020, 0.05 & 0.5 % Cl<sup>-</sup>



**RCT -1032** mixing container and cup. For samples of fresh concrete



**RCT -1000-1** electrode wetting agent (EWA), 300 mL. For refilling the RCT-1000 bottle with spout

### Consumables

Extraction liquids for **RCT** testing for acid-soluble chlorides in hardened concrete or fresh concrete:



**RCT-1023** vials, set of 25, for testing hardened concrete

**RCT-1031** vials, set of 4, for testing fresh concrete





Extraction liquids for **RCTW** testing for water-soluble chlorides in hardened concrete or fresh concrete:



**RCTW-1023-1** vials, set of 25,  
**RCTW-1023-2** buffer vials, set of 25,  
for testing hardened concrete



**RCTW-1031-1** vials, set of 4,  
**RCTW-1031-2** buffer vials,  
set of 4, for testing fresh concrete

## Optional items



**RCT-1027 Certified Reference Powders**  
9 jars, each containing 70 grams of concrete powder, with  
known amounts of chlorides and titrated according to  
AASHTO T 260

Cement type*	Known amounts of Cl <sup>-</sup>		
Portland cement	0.023 %	0.071 %	0.328 %
Fly ash cement	0.020 %	0.057 %	0.244 %
Slag cement	0.020 %	0.056 %	0.244 %

\*According to ENV- 197-1

### RCT-1028 pH-electrode



- Range: 0.0 to 12.0 pH
- Temperature: -5.0 to 70.0°C
- Meter resolution: 0.01 pH
- Meter accuracy: ±0.01 pH

### RCT-1029 temperature probe



- Range: -20.0 to 120.0°C / -4.0 to 248.0°F
- Meter resolution: 0.1°C / 0.1°F
- Meter accuracy: ±0.4°C / ±0.8°F

## References

- (1) Poulsen, E. and Mejlbro.L., **Diffusion of Chlorides in Concrete, Theory and Application**, Modern Concrete Technology Series, Taylor and Francis, 2006, ISBN13: 9-78-0-419-25300-6
- (2) Nilsson, L.O., Sandberg, P., Poulsen, E., Tang, L.M. Andersen, A. and Frederiksen, J.M., "A System for Estimation of Chloride Ingress into Concrete: Theoretical Background," HETEK Report 83, 1997, <http://www.hetek.teknologisk.dk/english/16507>
- (3) Frederiksen, J.M. and Poulsen, E. "Chloride penetration into concrete—Manual," HETEK Report 123, 1997, <http://www.hetek.teknologisk.dk/english/16507>

## Purpose

For a long time, users of NDT systems have wished for a rapid, easy to use method for rapid screening of the integrity of structures. The **s'MASH** impulse-response test system fulfills this wish. The idea is to quickly screen a structure for flaws and identify suspect areas for subsequent detailed investigation, e.g. by the impact-echo method (using **DOCTer**, or **Mirador**), ultrasonic-echo testing (using **MIRA**), or by invasive inspection with drilled cores (using **CORECASE**).

With the **s'MASH**, rapid evaluation can be conducted for:

- Detecting voids beneath concrete slabs in highways, spillways, and floors
- Detecting curling of slabs on ground
- Evaluating the integrity of anchoring systems of wall panels
- Locating delaminations and honeycombing in bridge decks, slabs, walls and large structures such as dams, chimney stacks, and silos
- Detecting the presence of damage due to freezing and thawing
- Detecting the presence of alkali-silica reaction (ASR)
- Detecting debonding of asphalt or concrete overlays and repair patches from concrete substrates
- Evaluating the effectiveness of the load transfer system in transmitting forces across joints in concrete structures



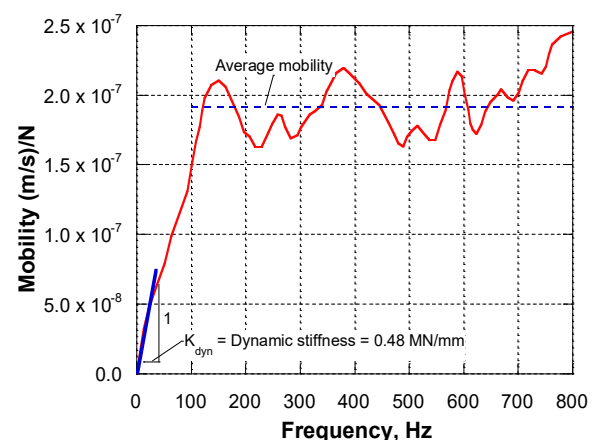
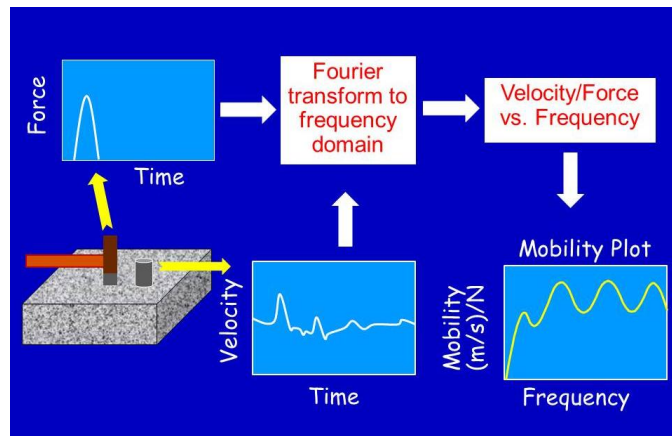
*Dr. Allan Davis testing the stiffness of concrete segments in Wrigley Building, Chicago, USA*

The application of impulse-response to plate-like structures is governed by ASTM C1740, "Standard Practice for Evaluating the Condition of Concrete Plates Using the Impulse-Response Method."

## Principle

The **s'MASH** uses a low-strain impact, produced by an instrumented rubber tipped hammer, to send stress waves through the tested element. The impact causes the element to vibrate in a bending mode and a velocity transducer, placed adjacent to the impact point, measures the amplitude of the response. The hammer load cell and the velocity transducer are connected to a portable computer with **s'MASH** software for data acquisition, signal processing, data display, and data storage.

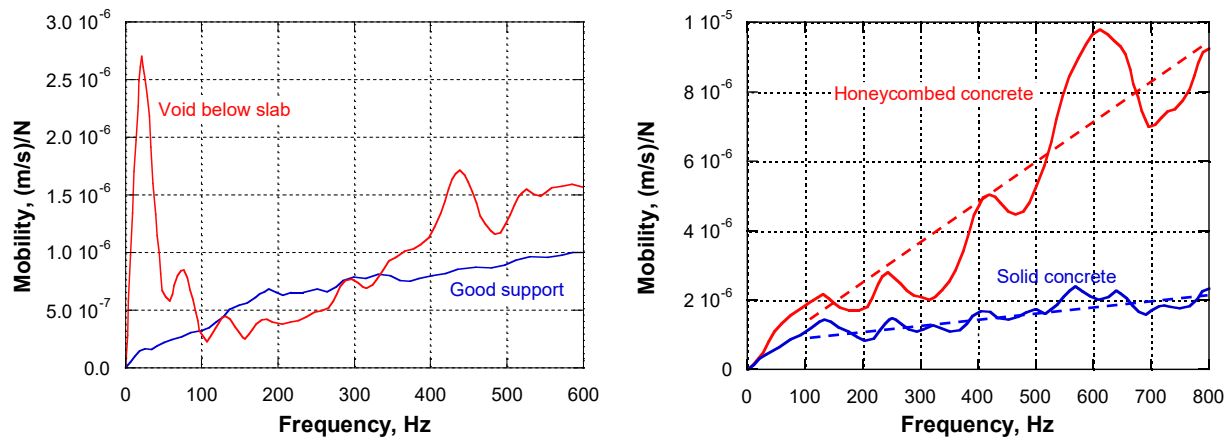
As shown below, the time histories of the hammer force and the measured response velocity are transformed into the frequency domain using the fast Fourier transform (FFT) technique. The resultant velocity spectrum is divided by the force spectrum, to obtain the **mobility** as a function of frequency. An example of a mobility plot for a solid concrete plate-like member is given in the plot on the right.



Mobility is expressed in units of velocity per unit force, such as (m/s)/N, and is an indicator of the relative flexibility of the tested element, which is a function of its thickness, elastic modulus, support conditions, and presence of internal defects.

The parameters from the mobility plot that are used for integrity evaluation are:

- **Average mobility.** The average value between 100 to 800 Hz on the mobility spectrum (dotted blue line in previous figure).
- **Dynamic stiffness.** The inverse of the initial slope of the mobility plot from 0 to 40 Hz (the blue line in previous figure). This value is also an indicator of the relative quality of the concrete, the relative thickness of the member, the relative quality of the subgrade support for slabs-on-ground, and of the support conditions for suspended structural slabs and walls.
- **Mobility slope.** The slope of the fitted straight line between 100 to 800 Hz. A high mobility slope has been found to correlate with locations of poorly consolidated or honeycombed concrete in plate-like structures (right image below).
- **Voids ratio.** The ratio of the amplitude of the low frequency peak to the average mobility. A high ratio has been found to correlate with poor support conditions or voids that may exist beneath concrete slabs bearing on ground (left image below).

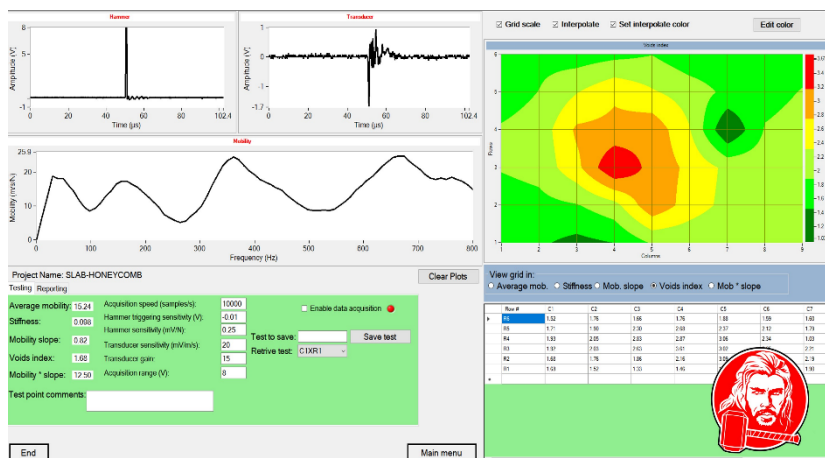


Testing is performed on a grid of points marked on the surface. The **s'MASH** software constructs color contour plots of the various parameters, from which it is easy to identify anomalous regions of the structure that merit further investigation. This is done on-site after the testing has been completed, producing immediate information on the presence of anomalies.

## Test Examples

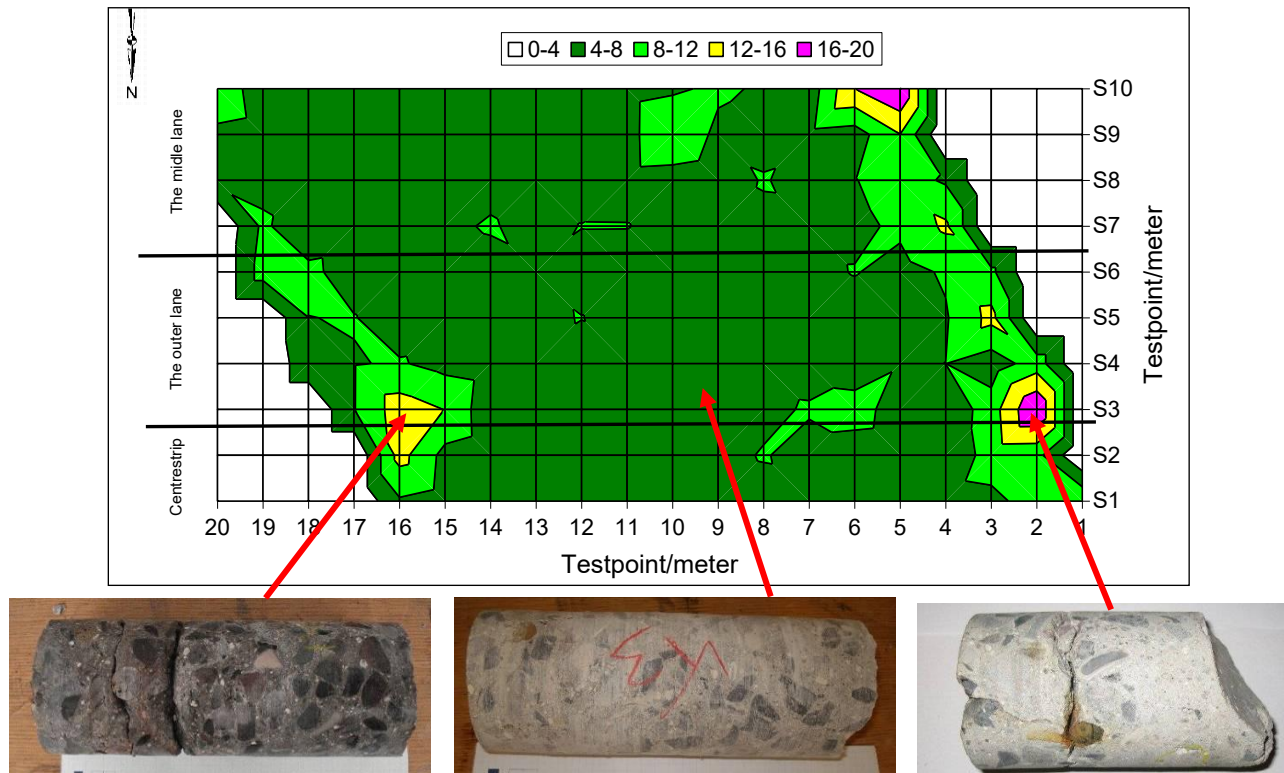
Shown on the right is the result of one test as displayed on the computer with the **s'MASH Thor** software. The top left window is the force-time curve obtained from the impact of the instrumented hammer. The top right window shows the velocity-time curve obtained from the geophone in contact with the concrete surface. The plot in the middle window is the mobility spectrum obtained from the previous two waveforms. The

lower left quadrant shows the various parameters calculated from the mobility plot. The top right window shows the contour plot obtained on the defined testing grid and below, the table shows the individual values of the different parameters at each test point.





The data can also be exported for a more detailed analysis (e.g., to MS Excel). Below is the contour plot in Excel of the average mobility from **s'MASH** tests performed on the soffit of a bridge slab that was suspected of containing delaminations. Tests were performed on a 1 × 1 m grid. Based on the contour plot, cores were drilled at three locations: (1) a region of low mobility, (2) a region of intermediate mobility, and (3) a region of high mobility. The cores confirmed that low mobility (rigid response) corresponded to a sound slab and higher mobility (flexible response) corresponded to the presence of delaminations.



### Application examples



*Testing for voids behind tunnel lining*



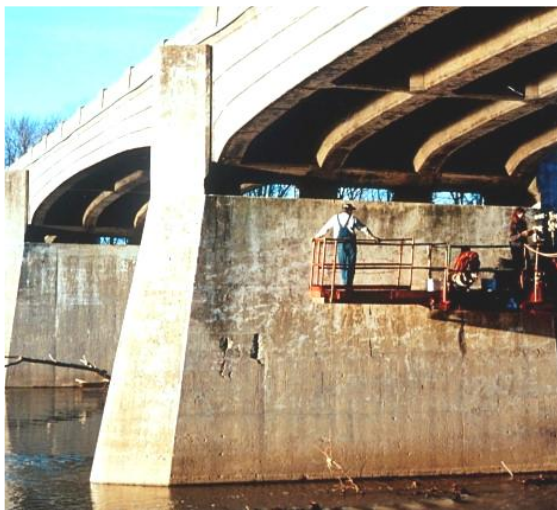
*Testing for delaminations in bridge deck*



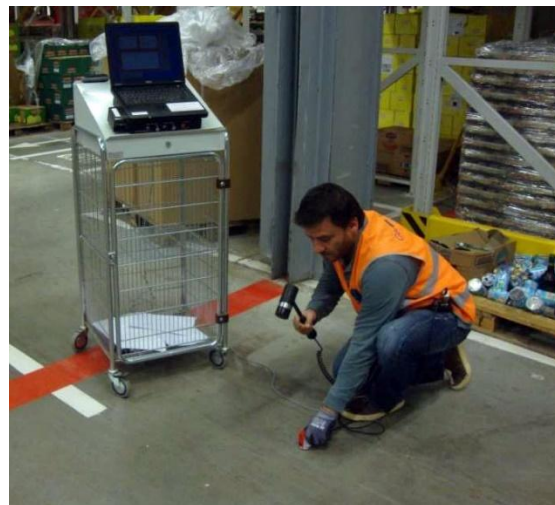
*Testing for delaminations in dam spillway*



*Testing for tightness of joints of concrete tank*



*Testing for honeycombing and delaminations in bridge piers*



*Testing for voids below industrial floor*



*Testing for anchor integrity for granite panels in high-rise building*



*Testing for delaminations in asphalt covered concrete pavement*



## s'MASH Specifications

- Data Acquisition System:
  - 2 channels, 4 MB/channel
  - 8 bits resolution, 50 MHz bandwidth
  - -5V to 5V Input Voltage Range
  - USB interface
- Omni-directional (360°) dry contact geophone transducer
- Electronic impact hammer with external force sensor
- Windows OS based **s'MASH Thor** software for real-time waveform displaying and creation of contour plots for visual representation of average mobility, mobility slope, dynamic stiffness and voids ratio
- Operating conditions: Temperature: -10 to 50 °C, RH ≤ 95 %

## s'MASH Ordering Numbers

### s'MASH-4000 Kit

Item	Order #
Instrumented impact hammer with certificate	SMASH-4000-10
360° transducer with certificate	SMASH-4000-50
Belt box extension with 3 m cable	SMASH-4000-90
User Manual	SMASH-4000-100
Laptop computer with <b>s'MASH</b> software installed	s'MASH-4000-200
USB flash drive with <b>s'MASH</b> software	s'MASH-4000-210
Data acquisition box	s'MASH-4000-220
110-220V AC adaptor	s'MASH-4000-240
Attaché case	s'MASH-4000-110



The acquisition box can also be used for **DOCter** impact-echo testing as a combined system.

A training course is offered separately, covering the theoretical background of impulse-response testing, testing methodology, testing cases from a variety of structures and hands-on training on testing with the **s'MASH**.



## Purpose

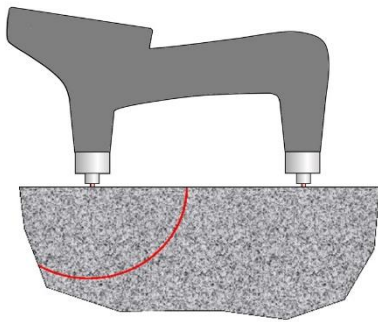
**Surfer** is a compact hand-held instrument for measuring the speed of a pulse of ultrasonic longitudinal stress waves propagating within the near surface concrete; that is, it measures the ultrasonic pulse velocity (UPV). The instrument incorporates two dry-point-contact (DPC) transducers that are brought into contact with the surface of the test object. Thus ultrasonic pulse velocity can be measured without having access to opposite sides of the test object. **Surfer** can be used for the following applications:

- Assessment of concrete uniformity
- Estimation of the extent and severity of deterioration of near-surface concrete
- Evaluate flexural strength of stone panels using correlations
- Evaluation of damage to test specimens during durability testing (freezing and thawing, sulfate attack, alkali-silica reaction)
- Estimation of depth of surface-opening cracks
- Estimation of early-age strength development (with project/mixture specific correlation)



## Principle

**Surfer** is based on measuring the time it takes for a pulse of longitudinal stress waves (P-waves) to travel from one transducer to another on the same surface. Because point transducers are used, the wave pulse travels away from the transmitting transducer along a spherical wavefront. When the wavefront arrives at the receiving transducer, a signal is generated. The instrument measures the pulse transit time from transmitter to receiver and computes the pulse velocity using the known distance between transducers. The transducers are designed to work without a coupling material (grease or gel). In contrast with traditional pulse velocity instruments, which are based on through transmission, **Surfer** measures the wave speed in the near-surface concrete. Thus it is not necessary to have access to opposite sides of the test object. Because there is no cabling, no coupling fluid, and no need to measure the distance between transducers, measurements can be made rapidly within 2 to 3 seconds.



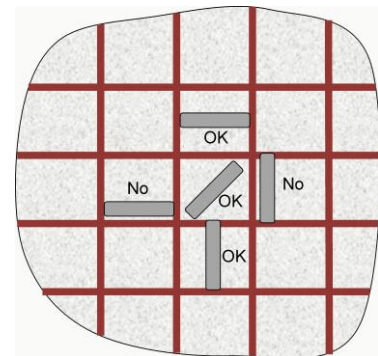
## Method of Operation

There are two main modes of operation:

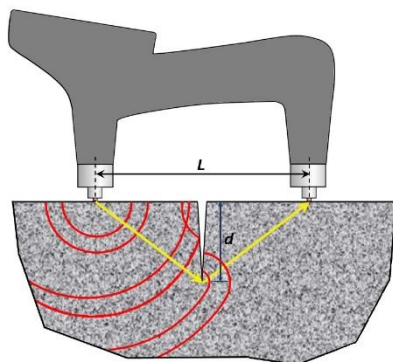
- Measurement of transit time and pulse velocity
- Measurement of depths of surface-opening cracks

Before making transit time measurements, the menu system and keypad are used to set up the instrument. The instrument includes a liquid crystal display (LCD) that can be set up to display transit time or pulse velocity. After the set-up parameters have been entered, the transducers are pressed firmly against the concrete surface. The device will self-activate and begin taking measurements. The transducers need to be perpendicular to the surface and a steady pressure needs to be maintained to obtain accurate and consistent measurements.

Before making measurements in reinforced concrete, a reinforcement locator (**Conquest™ GPR** for instance) should be used locate the reinforcing bars. Orient the **Surfer** so that the effects of the reinforcement are minimized. The above sketch shows acceptable and unacceptable positioning of the **Surfer**. If the device is aligned close to



and parallel to the reinforcement, the stress pulse will refract into the reinforcement and a short transit time will be measured.



**Surfer** can also be used to measure the depths of surface-opening cracks. When the stress pulse reaches the tip of a surface-opening crack, the pulse is diffracted by the crack tip. The diffracted pulse travels away from the crack tip and is detected by the receiver. Because the crack increases the length of the travel path from transmitter to receiver, the transmit time will be greater than if no crack were present. Crack depth is determined by making two transit time measurements. The first one is made with the transducers aligned parallel to the crack, and the second one is made with the transducers perpendicular to the crack. For the second measurement, the crack should be at the midpoint between the transducers. **Surfer** uses these transit times and the distance between the transducers to calculate the crack depth:

$$d = \frac{L}{2} \sqrt{\left(\frac{t_c}{t_p}\right)^2 - 1}$$

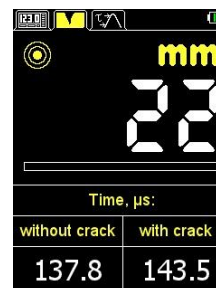
Where  $L$  is the distance between the transducers,  $t_p$  is the transit time measured with the transducers parallel to the crack, and  $t_c$  is the transit time with transducers perpendicular to the crack. The LCD will indicate the two transit times and the calculated crack depth. The following summarizes the process:



Measure transit time ( $t_p$ ) parallel to crack



Measure transit time ( $t_c$ ) across crack



Display of transit times and crack depth

## Estimating In-place Strength

To use **Surfer** to estimate early-age strength development of concrete, a relationship needs to be established between concrete strength and pulse velocity. Such a relationship can be established by making pulse velocity measurements on standard strength test specimens and then measuring their compressive strength. The resulting data can be used to develop a regression equation to represent the relationship between concrete strength and pulse velocity. Refer to ACI 228.1R (In-Place Methods to Estimate Concrete Strength) for guidance on developing and using the strength relationship. The relationship that is developed is applicable only to that specific concrete mixture.



## Elastic Modulus Degradation

Because the modulus of elasticity is proportional to the square of the pulse velocity, **Surfer** can be used as an alternative to resonant frequency testing to monitor deterioration of specimens used in standard durability tests, such as freezing and thawing. In such tests, the decrease in the dynamic modulus of elasticity is used as an indicator of deterioration. The elastic modulus ratio is equal to the square of the pulse velocity ratio:

$$\frac{E_n}{E_i} = \left( \frac{V_n}{V_i} \right)^2$$

Where  $V_i$  and  $E_i$  are the initial values of pulse velocity and modulus of elasticity; and  $V_n$  and  $E_n$  are the values of pulse velocity and modulus of elasticity after exposure to the test conditions.

## Surfer Specifications

- Dry point contact, longitudinal-wave transducers with ceramic wearing tips.
- Distance between transducers: 150 mm.
- 50 kHz center frequency.
- Nominal voltage: 3.3 V.
- Rechargeable battery with 16 hours life.
- LCD screen.
- Data transfer to computer via USB.
- Transit time range: 12.5 to 150  $\mu$ s.
- Transit time (t) measurement accuracy:  $\pm (0.01 \cdot t + 0.1) \mu$ s.
- Crack depth measurement range: 10 to 60 mm.
- Pulse repetition frequency: 2 to 25 Hz.
- Automatic Gain Control (AGC) function.
- Storage capacity: 50,000 results.
- Metric and inch-pound units.
- Instrument's weight: 450 g.
- Instrument's dimensions: 235 x 155 x 65 mm.
- Operating conditions: Temperature: -20 to 50 °C, RH  $\leq$  95 %.

## Surfer (SURF-1000) Ordering Numbers

Item	Order #
Hand-held unit with carrying case	SURF-1001
Plexiglas plate for operational check	SURF-1002
Charger and USB cable for connection to PC	SURF-1003
User manual	SURF-1005

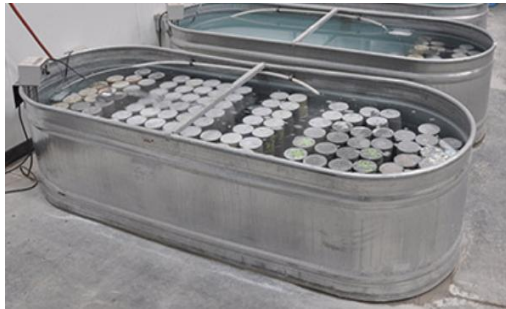




## Purpose

The **VAKKA** sensors are durable and waterproof wireless monitoring devices used to measure the internal temperature and relative humidity of newly cast concrete up to a depth of 3 meters for the following purposes:

- Estimating the compressive strength at an early age using a user defined strength-maturity relationship.
- Timing of pullout testing with **LOK-TEST** for early-age strength measurement.
- Evaluating the effective in-place curing temperature
- Timing the surface treatment on floor slabs.
- Monitoring water penetration in concrete



Proper curing of concrete is essential as it allows the cement particles to effectively hydrate, ensuring the desired concrete strength and durability. It is current practice to make concrete cylinders during concrete placement. These cylinders are left on site to allow the concrete to set and then transported to the laboratory, capped, and then tested in a compression machine to determine the compressive strength.

However, this practice does not measure the actual field curing conditions or the temperature history of the structure because unlike the cast concrete elements, cylinders have small volume and large surface areas which makes them retain much less heat and moisture. This causes a significant difference in the rate of strength gain that does not allow to have real-time information of the strength development of the structure.

Additionally, this method is also very labor-intensive and costly, as the practice is repeated throughout the project and is highly subject to operator errors and frequent delays.

With the **VAKKA** sensors, the traditional method is improved in accuracy and project cost savings by reflecting better the concrete strength gain in real-time. On the other hand, by knowing the up-to-date level of relative humidity of in-place concrete, the timing in which floor coverings are installed, such as resilient flooring, wood, epoxy or polymer-based coatings, can be optimized.

## Maturity Method

The maturity method is a technique to estimate in-place strength after casting by accounting for the effects of temperature and time on the strength gain of concrete. It is described in ASTM C1074 "Practice for Estimating Concrete Strength by the Maturity Method."

The temperature history of the concrete and a maturity function are used to calculate a maturity index that quantifies the combined effects of time and temperature. The strength of a particular concrete mixture is expressed as a function of its maturity index by means of a **strength-maturity relationship**. If portions of the same concrete are subjected to different conditions, the strength-maturity relationship for that concrete and the temperature histories measured at the different locations in the structures can be used to estimate in-place strengths at those locations.

Various maturity functions have been proposed to convert the measured temperature history to a maturity value. The one that has proven to be most accurate in accounting for the combined effects of time and temperature over wide temperature ranges is based on the Arrhenius equation.

$$t_e = \sum_0^t e^{\frac{-E}{R} \left( \frac{1}{T} - \frac{1}{T_r} \right)} \Delta t$$

where:

$\Delta t$  = time interval at actual concrete temperature

$t_e$  = the equivalent age at the reference temperature,

$E$  = apparent activation energy, J/mol,

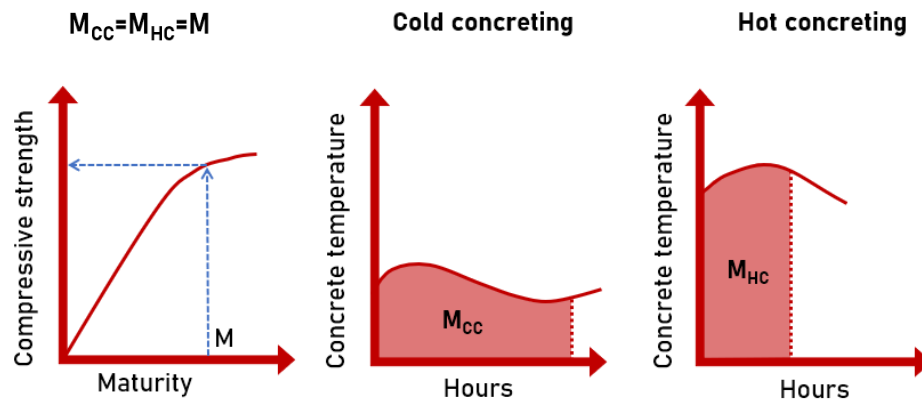
$R$  = universal gas constant, 8.314 J/mol-K,

$T$  = average absolute temperature of the concrete during interval  $\Delta t$ , Kelvin, and

$T_r$  = absolute reference temperature, Kelvin.

The exponential function is an age conversion factor that converts a time interval at the actual concrete temperature to an equivalent time interval, in terms of strength gain, at the reference temperature. The reference temperature is usually taken as the standard-curing temperature for concrete specimens, typically 20 °C (293 K) or 23 °C (296 K).

The activation energy represents the temperature sensitivity of the rate of strength gain during the acceleratory period following final setting and it depends on the cementitious materials in the concrete. For ordinary Portland cement, it has a value of about 40 kJ/mol, and it is greater for mixtures with slag cement and smaller for mixtures with fly ash (1, 2). ASTM C1074 provides strength-testing procedures for estimating the activation energy for a specific cementitious system. Others have used isothermal calorimetry (2) and setting time tests to evaluate activation energy (3).



To use the maturity method for estimating in-place strength, it is necessary to develop the strength-maturity relationship for the particular concrete mixture. As described in ASTM C1074, this can be done by measuring the strength of specimens of the concrete mixture at different values of maturity. The strength-maturity data can thus be used for estimating the strength as a function of age at the locations of the **VAKKA** sensors.

### The **VAKKA**-Sensors

**VAKKA** is a durable, waterproof concrete sensor that wirelessly monitors the environmental conditions within the concrete as it hardens. The patent-pending environmental chamber is unique to the **VAKKA** system and allows for faster and more accurate readings. It quickly equalizes the surrounding environment allowing precise measurements to be recorded within minutes of pouring your concrete.



The free mobile app and cloud service empowers the user's team to make faster and more confident decisions. The data can be downloaded to the app at any time when a connected device is within the 3-4 m range of the sensor and is instantly uploaded to the cloud where it is shared with the team. The app estimates the compressive strength by using the user defined maturity curve and allows instant access to the temperature and relative humidity readings, plotting data, and reports.

## Application



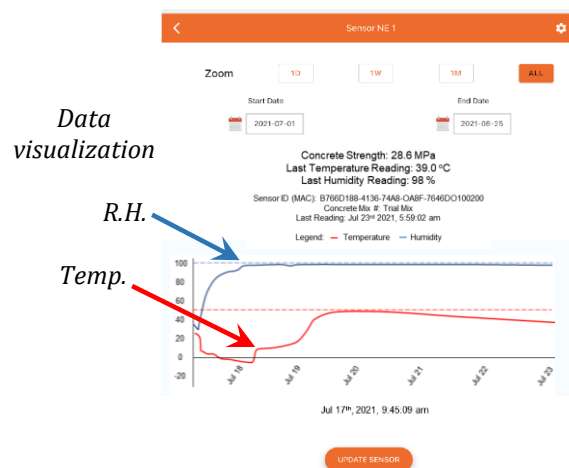
a) Install sensor



b) Synchronize sensor with app



c) Cast concrete



d) Record data

## VAKKA Features and Specifications:

- Free mobile App for Android and IOS devices
- Wireless technology
- Easy installation and activation
- Accurate real-time data display of relative humidity and temperature
- Normalizes to ambient conditions within minutes of placement
- Long storage life with external magnetic activation
- Rugged, crush proof and waterproof design
- Full reporting
- Cloud data storage for team access to projects from any location
- Maturity methods: ASTM C1074 Nurse/Saul and Arrhenius
- Measurement interval: 30 min (fixed)
- Maximum data collection: 4,000 data points (60 days)
- Operational battery life: > 4 months (active)
- Storage battery life: 10 years (unactive)



- Temperature accuracy:  $\pm 0.3^{\circ}\text{C}$
- R.H. accuracy:  $\pm 2\%$
- Embedment depth: 1 m or 3 m probe available for VAKKA-Tx/HTx sensors
- Attachment: Galvanized tie-wires

## VAKKA Ordering Numbers

Item	Order #
Sensor for temperature at the depth of the reinforcement	VAKKA-T
Sensor for temperature with a 1-meter extension probe.	VAKKA-T1
Sensor for temperature with a 3-meter extension probe.	VAKKA-T3
Sensor for temperature and relative humidity at the depth of the reinforcement	VAKKA-HT
Sensor for temperature and relative humidity with a 1-meter extension probe.	VAKKA-HT1
Sensor for temperature and relative humidity with a 3-meter extension probe.	VAKKA-HT3
Sensor for relative humidity with an extended battery life	VAKKA-RHmax



## Test Methods

**ASTM C1074** -Standard Practice for Estimating Concrete Strength by the Maturity Method.

**ASTM F2170** -Standard Test Method for Determining Relative Humidity in Concrete Floor Slabs Using in situ Probes.

## References

1. Carino, N.J. and Lew, H.S., "The Maturity Method: From Theory to Application" <http://fire.nist.gov/bfrlpubs/build01/PDF/b01006.pdf>
2. . Schindler, A.K., "Effect of Temperature on Hydration of Cementitious Materials," *ACI Materials Journal*, Vo. 101, No1, Jan-Feb 2004, pp. 72-81.
3. Pinto, R.C.A. and Schindler, A.K., "Unified modeling of setting and strength development," *Cement and Concrete Research*, Vol. 40, 2010, pp. 58-65.



**[www.germanninstruments.com](http://www.germanninstruments.com)**



## **GERMANN INSTRUMENTS A/S**

Emdrupvej 102, DK-2400 Copenhagen, Denmark

Phone: +45 39 67 71 17

E-mail: [germann-eu@germann.org](mailto:germann-eu@germann.org)

*Claus Germann Petersen, President*

## **GERMANN INSTRUMENTS, Inc.**

8845 Forest View Road, Evanston, Illinois 60203, USA

Phone: (847) 329-9999

E-mail: [germann@germann.org](mailto:germann@germann.org)

*Mariana Lara, Vice-President*



***Test right - Sleep tight***